

**NON-POINT SOURCE POLLUTION PROCESSES AND
CONNECTIVITY MODELLING IN THE MKABELA
CATCHMENT, SOUTH AFRICA**

Kipkemboi Julius Kollongei

Thesis

Submitted in fulfilment of the academic requirements for the degree of
Doctor of Philosophy (PhD)

School of Engineering
University of KwaZulu-Natal

March, 2015

PREFACE

DECLARATION 1- PLAGIARISM

I, **Kipkemboi J. Kollongei**, declare that:

1. The research reported in this thesis, except where otherwise indicated, is my original work.
2. This thesis has not been submitted for any degree or examination at any other university.
3. This thesis does not contain other persons' data, pictures, graphs or other information, unless specifically acknowledged as being sourced from other persons.
4. This thesis does not contain other persons' writing, unless specifically acknowledged as being sourced from other researchers. Where other written sources have been quoted, then:
 - a. their words have been re-written, but the general information attributed to them has been referenced;
 - b. where their exact words have been used, their writing has been placed inside quotation marks, and referenced.
5. Where I have reproduced a publication of which I am an author, co-author or editor, I have indicated, in detail, which part of the publication was actually written by myself alone and have fully referenced such publications.
6. This thesis does not contain text, graphics or tables copied and pasted from the Internet, unless specifically acknowledged, and the source being detailed in the thesis and in the Reference section.

.....
Kipkemboi J. Kollongei

.....
Date

SUPERVISOR'S CONSENT

As the candidate's Supervisor I agree/do not agree to the submission of this thesis

.....
Prof Simon A. Lorentz

.....
Date

DECLARATION 2- PUBLICATIONS

1. K.J. Kollongei, S.A. Lorentz/ *Physics and Chemistry of the Earth* 67-69 (2014) 12-22. Connectivity influences on nutrient and sediment migration in the Wartburg catchment, KwaZulu-Natal Province, South Africa. (*Available Online: 17th February 2014*)

Contributions (mainly based on results and discussions in Chapter 8)

K.J. Kollongei Formulated and wrote the paper, analysed the data, discussed the results and corresponded with the journal editor. All figures, data tables and graphs were produced by the same, unless otherwise referenced in the text of the paper.

S.A. Lorentz Assisted in provision of technical advice, materials and instruments. The co-author also made comments in the manuscript and granted access to field database as well as advised regarding data interpretation.

2. K.J. Kollongei and Lorentz S.A. (under 1st review), *Modelling Hydrological Processes, Crop Yields and NPS Pollution in a Small Sub-tropical Catchment in South Africa Using ACURU-NPS*. *Hydrological Sciences Journal* (*Manuscript ID: HSJ-2014-0188, Date Submitted: 25th April 2014*)

Contributions (mainly based on results and discussions in Chapter 8)

K.J. Kollongei Formulated and wrote the paper; performed data collection, analysed the data, discussed the results and corresponding with the journal editor.

S.A. Lorentz Assisted in provision of technical advice, materials and instruments and made comments in the manuscript.

ACKNOWLEDGEMENT

First of all, glory is to God for His grace was sufficient throughout this study. Secondly, I would like to express my sincere gratitude and appreciation to my supervisor, **Prof. Simon A. Lorentz**, for his constructive criticism, consistent guidance, innovative suggestions, patience, and kindness, and some financial support, which contributed to the success of this PhD thesis. It was a fruitful and enriching experience for me in my life. Thank you very much.

I wish to acknowledge guidance and support of **Prof. G.W.P. Jewitt**, Head of Centre for Water Resources Research (CWRR), **Prof. R.E. Schulze**, Emeritus Professor and **Prof. J.F. Smithers**, School of Engineering, at the various stages of my studies. I am thankful to the Chief Technician CWRR, **Cobus Pretorius**, who made me have hands-on experience of field instrumentation and for his valuable suggestions throughout my field work. Thanks to **David Clark** for introducing me to JAVA programming and troubleshooting many of *ACRU-NPS* model problems. Thanks to **Alistair D Clulow** for configuring ISCO-Water Quality Sampler in Flume 1 at the Wartburg research site within the Mkabela Catchment. I would also like to appreciate comradeship of **Kalala Ngaleka**, **Wayne Jackson**, **Siphiwe Mfeka**, **Nhlakanipho Zondi** and **Patrick Adadzi** while helping me out with field work.

I wish to thank **Fiona Higginson**, postgraduate administrator at the School of Engineering, who was readily available to assist students, **Kim Henry** and **Mpho Mkhwanazi**, both the academic administrative officers – Higher Degrees College of Agriculture, Engineering and Science, for coordinating the registration process and executing PhD submission process.

I also take this opportunity to thank the tax payers of South Africa through **Water Research Commission (WRC)** for funding the projects that supported my studies, **University of KwaZulu-Natal (UKZN)** for providing enabling environment for research and **Masinde Muliro University of Science and Technology (MMUST)** for granting me leave from work to take up this study. I would also like to thank **The School of Engineering (SE)**, University of KwaZulu-Natal (UKZN), for the JW Nelson Fund Award, which assisted me to attend academic meetings, notably the 13th WaterNet Symposium (2012) in Johannesburg.

I am grateful to my wife **Agnes**, daughter **Alexandra** and son **Xavier**. Thanks for your love, steadfast support, encouragement and for your perseverance in loneliness for years for the

sake of this study. Thanks to my mother **Jane**, brothers, sisters and in-laws for your prayers, support and bearing all my responsibilities.

I would like to remember the staff at the School of Engineering and the Centre for Water Resources Research (CWRR): **Prof Cristina Trois** (Dean and Head of the School of Engineering), **Prof Tilahun S Workneh**, **Tinisha Chetty**, **Prof Carel N Bezuidenhout**, **Dr Aidan Senzanje**, **Dr Gikuru Mwithiga**, **Prof Vincent Chaplot**, **Trevor Lumsden**, **Louis Lagrange**, **Mark Horan**, **Richard Kunz**, **Sean Thornton-Dibb**, **Suzanne Kunz** and **Natasha Moneyvalu** for their assistance in their various capacities.

Finally, I wish to recognise my colleagues **George Waswa**, **Benon Zaake**, **Thawani Sanjika**, **Pshesheya Dlamini**, **Carl Freese**, **Kipchumba Cheron** and **Charles Otunga** for the assistance extended to me during my stay in South Africa. I pray that may God almighty grant you peace and best of luck in your daily endeavours.

DEDICATION

This thesis is dedicated to the memory of
My late father Samuel Kiprop Kollongei and late brother Stephen Kipruto Kollongei
Who both loved education so much but were not able to see
My dreams come true.

ABSTRACT

In South Africa water resources and water quality issues are becoming increasingly important as the country manages its scarce water resources. The National Water Act of South Africa Act 36 (1998) stipulates that water resources must be shared in a sustainable fashion among humans, environment and economic land uses. Deterioration of water qualities in rivers are not only unique problems to South Africa. Indeed the degradation of water quality by nutrients originating from agriculture through excessive use of fertilizers (NO_3 and P) and erosion (sediments) is an international environmental concern. Rivers passing through agricultural areas experience high pollution levels from non-point sources resulting from these agricultural activities. Dealing with this issue is not straight forward because the agricultural contribution to diffuse pollution varies widely as a complex function of soil type, climate, topography, hydrological connectivity, land use and management. This creates widespread, intermittent, and poorly defined contaminant sources that degrade water quality in a way that makes their control difficult. In recognition of the accelerated degradation of water bodies from agricultural Non-Point Source (NPS) pollutants, watershed models have evolved from traditional hydrology models to more comprehensive water quality models.

Diminished use or even loss of the water resource for other beneficial uses has resulted from over burdening of the receiving waters with waste fertilizers from agriculture. For example, many surface and groundwater bodies used as a water supply have lost their utility due to agricultural pollution. Upstream users of land do not feel the economic impact of their action on the downstream users who must use water from other sources because the water quality of their source was rendered unusable. Farmers respond to their economic realities, i.e. they want to make at least some profit or at least survive during harsh economic situations, both of which can be accomplished by increased crop yields. Without some intervention in the farmers' economic reasoning, the potential water quality problems far downstream is not a part of the farmers' decision making process with regards to how much fertilizers they will use on their land or how to dispose of their animal waste.

The new *ACRU-NPS* (Agricultural Catchment Research Unit- Nitrogen, Phosphorous and Sediments) model was developed to try to address these challenges. The model was configured using a nested approach, which requires an effective description of all relevant components of the system and an understanding of the processes and feedbacks taking place

within and between different scales and hydrological processes response zones. The concept of connectivity in the model was introduced to improve simulations. Connectivity defines the physical coupling of landforms (e.g. hillslope to channel) within a catchment where the passage of water from one part of the landscape to another is expected to generate a catchment runoff response that may carry along with it dissolved pollutants, sediments and any contaminants that they may carry through the drainage basin.

The connectivity of the river (drainage) network in the Mkabela Catchment (near Wartburg, KwaZulu-Natal) was assessed on a sub-catchment basis and was linked to in-stream controls that included farm dams, wetlands and buffer zones where the fate and transport of dissolved N and P, sediment and associated adsorbed P were studied. A new method of calculating crop yield, different from that used in the *SWAT* (Soil and Water Assessment Tool) model, was developed and incorporated in the *ACRU-NPS* model. In the new method water and nitrogen stresses were used to limit crop growth on a daily time step. This enabled consequences of subsequent nutrient and sediment loads in streams to be studied. The major limitation to long-term use of *SWAT* in South Africa is the lack of long-term nutrient and suspended solids data for calibration and validation.

This study utilized the new *ACRU-NPS* modelling approach to study pollutants emanating from the Mkabela Catchment in South Africa. The developed *ACRU-NPS* model included sufficient process details to allow for the implementation of controls such as wetlands, dams and buffer strips. Successful simulation of crop yields, nutrient and sediment production, together with the fate of NPS pollutants, for various land uses was thus achieved. The major contribution of this study however was to link hydrology and NPS pollution processes by describing and defining pathways through which pollutants moved in the catchment. This was achieved through studying the dynamics and connectivity of water, sediments and nutrient fluxes by combining hydrometric, hydrogeological, geophysics and stable water isotope techniques to interpret the field and laboratory data. Suggestions for future improvements on the *ACRU-NPS* model were given based on the understandings gained from the different observations and sampling done in the Mkabela Catchment.

TABLE OF CONTENTS

PREFACE	ii
SUPERVISOR’S CONSENT	iii
DECLARATION 2- PUBLICATIONS.....	iv
ACKNOWLEDGEMENT	v
DEDICATION	vii
ABSTRACT	viii
TABLE OF CONTENTS	x
LIST OF FIGURES.....	xiv
LIST OF TABLES	xviii
LIST OF ABBREVIATIONS	xix
CHAPTER ONE	1
INTRODUCTION.....	1
1.1 Rationale.....	1
1.2 Hypothesis and Objectives of the Study.....	5
1.3 Contributions of the Thesis to the Knowledge Base	5
1.4 Outline of the Thesis.....	7
CHAPTER TWO.....	9
DESCRIPTION OF THE STUDY SITE	9
2.1 Mkabela Catchment Location.....	9
2.1.1 Climate.....	10
2.1.2 Geology and soils.....	10
2.1.3 Vegetation and land use	12
CHAPTER THREE.....	14
LITERATURE REVIEW: WATER QUALITY MODELLING OF AN AGRICULTURAL CATCHMENT, ADOPTING CONNECTIVITY CONCEPT.....	14
3.1 Hydrological Processes and Scale Issues	15
3.1.1 Plot or local scale simulations.....	17
3.1.2 Field scale simulations.....	17
3.1.3 Catchment scale simulations.....	18
3.2 Effect of Scale on NPS Processes: Small Plot to Catchment-scale.....	18
3.3 Connectivity Concept	19
3.3.1 Landform connectivity.....	19

3.3.2	Hydrological connectivity.....	22
3.3.3	Controls and thresholds.....	24
CHAPTER FOUR.....		28
METHODOLOGY.....		28
4.1	Nested Catchment Monitoring, Materials and Methods.....	28
4.1.1	Local scale.....	30
4.1.2	Field scale	32
4.1.3	Catchment scale	34
4.2	Laboratory Procedures and Analysis	35
4.2.1	Field sampling and analyses for nutrients and sediments.....	35
4.2.2	Field sampling and analyses for stable water isotopes	36
4.3	Development of the modified <i>ACRU-NPS</i> model	38
CHAPTER FIVE.....		40
CONNECTIVITY INFLUENCES ON NUTRIENT AND SEDIMENT MIGRATION IN THE MKABELA CATCHMENT		40
5.1	Mkabela Hydrological Processes Response Zones and Connectivity Processes.....	40
5.1.1	Hydrological processes response zones and connectivity.....	40
5.1.2	Hillslope hydrogeological transects.....	43
5.1.2.1	Transects on Avalon hillslopes (A1-A2 and B1-B2).....	45
5.1.2.2	Transects on Glencoe hillslopes (C1- C2)	46
5.1.2.3	Transects on Cartref hillslopes (D1- D2).....	47
5.1.2.4	Transects on Hutton hillslopes (E1-E2).....	48
5.1.2.5	Longitudinal transects along the river reaches.....	49
5.1.3	Nutrient and sediment source connectivity and controls	50
5.2	Plot Scale Geophysics, Soil Water and Nutrient Dynamics	53
5.2.1	Geophysics.....	53
5.2.2	Soil water and nutrient dynamics.....	58
CHAPTER SIX.....		65
DEVELOPMENT OF THE <i>ACRU-NPS</i> MODEL		65
6.1	<i>ACRU-NPS</i> Model Processes	65
6.1.1	Nutrient processes.....	66
6.1.1.1	Nitrogen processes	67
6.1.1.2	Phosphorus processes.....	75
6.1.2	Sediment processes	81

6.1.3	Crop growth, water and nitrogen stress processes	83
6.2	<i>ACRU-NPS</i> Crop BaseLAI Values	84
6.2.1	Length of crop growth stages.....	85
6.2.2	Numerical determination of crop BaseLAI values	88
6.3	<i>ACRU-NPS</i> Processes at Control Structures and Connectivity Modelling	90
6.3.1	Processes at control structures	90
6.3.1.1	Farm dams and wetlands.....	91
6.3.1.2	Riparian buffer strips	92
6.3.2	Connectivity aspects in NPS pollution migration in the Mkabela Catchment	93
CHAPTER SEVEN.....		99
ACRU-NPS MODEL SIMULATIONS IN THE MKABELA CATCHMENT		99
7.1	Model Input Parameters.....	99
7.1.1	Climatic data	100
7.1.2	Initial soil and nutrient parameters.....	102
7.1.3	Fertilizer and manure applications.....	103
7.1.4	Other agricultural practices.....	105
7.2	Model Calibration and Validation	105
7.2.1	Model evaluation criteria	106
7.2.2	Calibration of runoff, nutrient and sediment yields	108
7.2.2.1	Runoff and root zone water balance	108
7.2.2.2	Nitrate (NO ₃).....	112
7.2.2.3	Phosphorous (Soluble-P)	113
7.2.2.4	Sediments	115
7.2.3	Calibration of sugarcane yields.....	117
7.2.4	Validation of sugarcane yields.....	122
CHAPTER EIGHT.....		124
RESULTS AND DISCUSSION		124
8.1	Connectivity Influences on Nutrient and Sediment Migration.....	124
8.1.1	Field and catchment scale nutrient and isotope events	125
8.1.1.1	Field nutrient and isotope events results	125
8.1.1.2	Catchment nutrient and isotope transect results.....	137
8.1.1.2 (a)	Seasonal nutrients (NO ₃ & P), SS and isotope processes through dams	139

8.1.1.2 (b)	Seasonal nutrients (NO ₃ & P), SS and isotope processes through bridges.....	140
8.1.2	Mass balance mixing model.....	142
8.2	<i>ACRU-NPS</i> Crop Yields and Pollutant Loads Simulations.....	144
8.2.1	Simulation scenarios in the Mkabela Catchment.....	144
8.2.2	Sugarcane crop yields from sub-catchments.....	146
8.2.2.1	Crop yields from zero, quarterbase and halfbase fertilizer application rates.....	146
8.2.2.2	Crop yields from base and doublebase fertilizer application rates.....	147
8.2.2.3	Crop yields from variable irrigation rates with base fertilizer application.....	147
8.2.3	Movement of water, nutrient and sediment loads through control features.....	149
8.2.3.1	Discharge through control features.....	151
8.2.3.2	Transport of nutrient and sediment loads through control features.....	155
8.2.3.2 (a)	NPS pollutant loads through control features with different fertilizer application rates.....	157
8.2.3.2 (b)	NPS pollutant loads through control features with different management scenarios.....	159
CHAPTER NINE.....		165
CONCLUSIONS AND RECOMMENDATIONS.....		165
REFERENCES.....		168
APPENDICES.....		180

LIST OF FIGURES

Figure 2.1:	The location (left) and land-use types (right) of the Mkabela Catchment, near Wartburg, KwaZulu-Natal Province in South Africa (after Miller et al., 2013 and Le Roux et al., 2006).	9
Figure 2.2:	Mkabela Catchment showing 6 dominant soil types with additional detailed soil types in the upper sub-catchment (after Le Roux et al., 2006).	11
Figure 2.3:	Land uses and sub-catchments in the Mkabela Catchment.	12
Figure 3.1:	Hydrological processes and scale issues (Hewett et al., 2009).	16
Figure 3.2:	Spatial and temporal conceptual framework of connectivity associated with notion of “switches” in catchments (after Brierley et al., 2006).	21
Figure 3.3:	Nutrients in water: A schematic diagram of pathways from agricultural use (OECD, 2012).	23
Figure 3.4:	The components that control catchment connectivity (Bracken and Croke, 2007).	24
Figure 4.1:	The nested Mkabela Catchment showing instrumentation and sampling points at the Wartburg research site (Lorentz et al., 2011).	29
Figure 4.2:	Downloading weather data from the automatic weather station located near Wartburg, Mkabela Catchment, KwaZulu-Natal.	30
Figure 4.3:	Downloading data from runoff plot (left) and drawing groundwater from borehole using a bailer (right).	31
Figure 4.4:	ABEM Terrameter used for 2-D Electrical Resistivity Tomography (ERT)	31
Figure 4.5:	Taking in-situ readings using Manta-2 WQ instrument (left) and downloading data from CR 200 data logger (right) at the Lower H-flume.	32
Figure 4.6:	Dam 1 (left) and Bridge 1 (right) located at the middle sub-catchment of Mkabela where grab sampling was done.	34
Figure 4.7:	Taking readings using Manta2 (left) and HACH DR/2000 field test kit (right) at a field station.	35
Figure 4.8:	DLT-100 Liquid-Water Isotope Laser Analyser (LGR, 2007)	36
Figure 4.9:	Examples of object classes in ACRU2000 (after Kiker and Clark, 2001)	39
Figure 5.1:	Classification of reach process zones in the Mkabela Catchment (Lorentz et al., 2011; Miller et al., 2013).	41
Figure 5.2:	Reach process zones and sub-catchment areas within the upper and middle sub-catchments showing the locations of stream and hydrogeological transects in the Mkabela Catchment (after Miller et al., 2013).	43
Figure 5.3:	Upper sub-catchment transects showing the soil profile in the Avalon hillslope. ...	45
Figure 5.4:	Middle sub-catchment transects C1-C2 showing the soil profile in the Glencoe hillslope.	47
Figure 5.5:	Middle sub-catchment transects D1-D2 showing the soil profile in Cartref hillslope.	48
Figure 5.6:	Lower Sub-catchment transects E1-E2 showing soil profile in Hutton hillslope. ...	49
Figure 5.7:	River Reach 1 longitudinal profile.	50
Figure 5.8:	River Reach 2 longitudinal profile.	50
Figure 5.9:	Schematic diagram of the primary processes occurring in each of the three delineated sub-catchments, and the variations in sediment size and source from varying runoff magnitudes (Miller et al., 2013).	51

Figure 5.10: Sedimentological or geomorphic connectivity and sediment storage between sub-catchment zones of the Mkabela Catchment (Lorentz et al., 2011; Miller et al., 2013).....	52
Figure 5.11: ERT transect locations in the upper Mkabela sub-catchment (Lorentz et al., 2011).....	53
Figure 5.12: Transect W1 located between the Runoff Plots and Flume 1 (Lorentz et al., 2011).....	54
Figure 5.13: Transect W2 located adjacent to upstream Flume 1 (Lorentz et al., 2011).....	55
Figure 5.14: Transect W3 adjacent to the nests of soil moisture sensors (Lorentz et al., 2011).	56
Figure 5.15: Transect W4 located between W5 and the upstream Flume 1 (Lorentz et al., 2011).....	57
Figure 5.16: Transect W5 located immediately upstream of Flume 2 (Lorentz et al., 2011).....	58
Figure 5.17: Soil water tension variation: Watermark Nest 1, from 17th – 25th Nov’11.....	59
Figure 5.18: Soil water tension variation: Nest 3 & 4, 9Feb-17 Mar’09 (summer).	61
Figure 5.19: Soil water tension variation: Nest 5 & 6, 25-28 Jul’11(winter).	61
Figure 5.20: Nest 2 (closer to waterway and presence of clay soils) and Nest 4 (furthest from the waterway and presence of sandy soils, but adjacent to the impermeable bitumen road).	64
Figure 6.1: ACRU-NPS soil layers used to model nutrient processes where RFL = rainfall, EFRL = effective rainfall and NetRFL = net rainfall.....	67
Figure 6.2: Nitrate processes included in ACRU-NPS where AM = ammonification, NI = nitrification, DN = denitrification, VL = volatilization, IM = immobilization, UP = uptake and FX = fixation (Campbell et al., 2001).	68
Figure 6.3: P processes included in ACRU-NPS where MN = mineralization, UP = uptake, IM = immobilization, RO = runoff, SED = sedimentation, PERC = percolation. (Campbell et al., 2001).	76
Figure 6.4: Crop growth, water and nitrogen stress processes (Lorentz et al., 2012).	83
Figure 6.5: Typical presentation of the variation in the active (green) LAI over the growing season for a maize crop (Allen et al., 1998).....	85
Figure 6.6: Crop coefficients for maize as related to accumulated growing degree days, Tt, but under water stress in the ACRU maize yield model (Schulze, 1995).....	86
Figure 6.7: The 3-degree Polynomial equation to derive the daily base LAI values for the entire sugarcane (top) and cabbage (bottom) growth periods.	89
Figure 6.8: Sub-catchment boundaries, outlets, river channel locations, farm dams and wetlands (Le Roux et al., 2013) (Left); simplified connectivity network of land segments with control structures in the Mkabela Catchment (Lorentz et al., 2012) (Right).	95
Figure 7.1: Daily weather station data for the Mkabela Catchment for the period 2007 – 2012.	101
Figure 7.2: Hydrologic calibration of ACRU-NPS model for daily runoff for the period October 2007 and March 2008.....	109
Figure 7.3: Cumulative runoff for observed and simulated runoff (left) and 1:1 comparison between observed and simulated runoff (right).....	109
Figure 7.4: Saturated drainage and base flow storage.	110
Figure 7.5: Root zone water balance for simulation period 2008 -2012.	111
Figure 7.6: Hydrologic calibration of ACRU-NPS model for daily NO ₃ yield (kg/ha) for the period October 2007 and March 2008 and validation for the period Jan 2009 and March 2012.	112

Figure 7.7	Comparison of observed and simulated NO ₃ yield (kg/ha) (left) and their scatter comparison (right) generated by the ACRU-NPS model for events occurring between Sep. 2007 and Feb. 2012.....	113
Figure 7.8:	Hydrologic calibration of ACRU-NPS model for daily P yield (kg/ha) for the period October 2007 and March 2008 and validation for the period Jan 2009 and March 2012.	114
Figure 7.9:	Comparison of observed and simulated P yield (kg/ha) (left) and their scatter comparison (right) for the ACRU-NPS model.....	115
Figure 7.10:	Hydrologic calibration of ACRU-NPS model for daily Sediment yield (kg/ha) for the period October 2007 and March 2008 and validation for the period Jan 2009 and March 2012.....	116
Figure 7.11:	Comparison of observed and simulated sediment yield (kg/ha) (left) and their scatter comparison (right) for the ACRU-NPS model.	116
Figure 7.12:	Demand nitrogen concentration as a function of growth ratio for sugarcane. Solid line from original data base; dashed lines for the increased nitrogen demands.....	118
Figure 7.13:	Comparison of sugar cane yield for various N fertilizer applications and potential yields, using values of c1 = 0.17 (initial), 0.325 (final) and 0.525. The dotted lines indicate the incremental crop yield for the different fertilizer applications compared to the use of no fertilizer.	118
Figure 7.14:	Comparison of sugar cane yield for various N fertilizer applications using values of c1 =0.17 (initial), 0.325 (final) and 0.525. The dotted lines indicate the incremental crop yield for the different fertilizer applications against zero fertilizer.	120
Figure 7.15:	Ratoon cane responses to applied N in relation to soil form (Moberly and Meyer, 1984).	121
Figure 7.16:	Comparison of sugar cane yields from 3 no., 18 months crops for 2006-2011 simulations (CANESIM, ACRU-NPS c1=0.17 and ACRU-NPS c1=0.325) and published observed yields for the South African Sugar Industry (SASRI).....	123
Figure 8.1:	H-Flumes rainfall/runoff, nitrates (NO ₃) and soluble-P concentrations and mass loadings for 12 events (Jan '09 - Jan '12).	127
Figure 8.2:	H- Flumes rainfall/runoff, suspended solids (SS) concentrations and mass loading for 12 events (Jan '09 - Jan '12).....	128
Figure 8.3:	Discharge, NO ₃ , P and SS responses for Flume 1 (left) and Flume 2 (right) for a 51 mm summer event of 28 February 2009.	129
Figure 8.4:	Cumulative rainfall, discharge and isotope responses at Flume1 (left) and Flume 2 (right) for the 51 mm summer event of 28th February 2009.	130
Figure 8.5:	Depth below ground level (m), δ ¹⁸ O and δ ² H isotope values (‰) for the period 2008- 2012 at a borehole (BH) in Mkabela Catchment.	131
Figure 8.6:	Discharge, nutrient and isotope responses for Flume 2 for 53 mm, 42 mm and 3 mm winter events of 25th, 26th and 27th July 2011 respectively.....	132
Figure 8.7:	Discharge, rainfall and groundwater δ ¹⁸ O concentrations for Flume 2 flow in winter event of 25th-27th July 2011.	134
Figure 8.8:	Rainfall, discharge and isotope responses at Flume 2 for 34 mm event of 10th November 2010.	135
Figure 8.9:	Concentrations of nutrients from headwater to outlet for the event of 7th January 2011.....	137
Figure 8.10:	Isotope transects from the headwater flumes to the outlet at Bridge 2 for the event of 7 January 2011.	138

Figure 8.11: Isotope $\delta^{18}\text{O}$ / for $\delta^2\text{H}$ ratios for the transect results for the event of 7th January 2011.....	143
Figure 8.12: Percent contribution of the sub-catchment between the impounded tributaries and the bridge stations to total discharge.....	144
Figure 8.13: Modelled sugarcane crop yields from the different sub-catchments with varying fertilizer application rates under rainfall and a base fertilizer application scenario with irrigation applied.....	148
Figure 8.14: Discharges entering and leaving wetland1, buffer1 and dam1 for the simulation period 2006-2012.....	153
Figure 8.15: Discharges entering and leaving buffer2, dam2 and wetlands2 & 3 for the simulation period 2006-2012.....	154
Figure 8.16: Total nutrient (NO_3 and P) and sediment loads from different fertilizer application rates routed out of wetlands, buffers and dams for the entire simulation period (2006-2012).....	158
Figure 8.17: Total nutrient (NO_3 and P) and sediment loads for zero fertilizer routed out of wetlands, buffers and dams for the entire simulation period (2006-2012).	159
Figure 8.18: Total nutrient (NO_3 and P) and sediment loads for different management scenarios routed out of wetlands, buffers and dams for the entire simulation period (2006-2012).....	162

LIST OF TABLES

Table 2.1:	Brief description of the primary soil types found in the study area (Le Roux et al., 2006).....	10
Table 2.2:	Areas of sub-catchments and land use in the Mkabela Catchment.	13
Table 3.1:	Definition of spatial hydrological modelling scales after (Refsgaard and Butts, 1999).....	15
Table 4.1:	Conditional parameters for the CR 200 data logger at the Mkabela H-Flumes.....	33
Table 5.1:	Summary of reach process zones and their general characteristics (Lorentz et al., 2011; Miller et al., 2013).....	42
Table 5.2:	Criteria for choosing cross-sectional and longitudinal transect points.	44
Table 6.1:	Typical values of phenological states of maize related to accumulated growing degree days (Tt) after planting in South Africa (Schulze, 1995)	85
Table 6.2:	Single (time-averaged) crop coefficients, Kc, and mean maximum plant heights for non-stressed, well-managed crops in subhumid climates (RHmin \approx 45%, u2 \approx 2 m/s) for use with the FAO Penman-Monteith ETo.....	87
Table 6.3:	Lengths of crop development stages for various planting periods and climatic regions (days).	87
Table 6.4:	ACRU-NPS model parameters for wetlands, dams and buffer controls.....	93
Table 6.5:	Wetland, buffer and dam controls as influenced by connectivity within the different land uses and soil types.	96
Table 6.6:	Locations and sizes of wetlands and dams within the Mkabela sub-catchments....	97
Table 7.1:	Depths (m) of soil horizons and initial soil water content for different soil forms.	102
Table 7.2:	Average rates (kg/ha) of fertilizer use in KwaZulu-Natal Province (FAO, 2005)	103
Table 7.3:	Manure rates and nutrient composition (Ministry of Agric. KZN, 2005).....	103
Table 7.4:	Fertilizer rates for sugarcane (Source: farmer interviews).....	103
Table 7.5:	Percentage of nutrients present in sugarcane press mud (SPM).	104
Table 7.6:	Statistical ACRU-NPS model performance.	107
Table 7.7:	Nitrogen recommendations for sugarcane based on soil forms (Moberly and Meyer, 1984).	121
Table 7.8:	Rainfall and observed sugarcane yields (SASA, 2012)	122
Table 8.1:	Wet events selection criteria	125

LIST OF ABBREVIATIONS

ACRU	Agricultural Catchment Research Unit Model
ACRU-NP	ACRU– Nitrate and Phosphorous Model
ACRU-NPS	ACRU– Nitrate, Phosphorous and Sediments Model
C: N	Carbon Nitrogen Ratio
GLEAMS	Groundwater Loading Effects of Agricultural Management Systems
HPO_4^{2-}	Hydrogen Phosphate
H_2PO_4^-	Di-hydrogen Phosphate
K_2O	Potassium Oxide
KCL	Potassium Chloride
KHPO_4	Potassium Hydrogen Phosphate
KNO_3	Potassium Nitrate
LAI	Leaf Area Index
LAN	Lime of Ammonium Nitrate
MUSLE	Modified Universal Soil Loss Equation
N	Nitrogen
N_2	Nitrogen gas
NH_3	Ammonia gas
NH_4^+	Ammonium ion
$\text{NH}_4\text{-N}$	Ammonium Nitrogen
NO_2^-	Nitrite ion
NO_3^-	Nitrate ion
NO_3	Nitrate
$\text{NO}_3\text{-N}$	Nitrate Nitrogen
NPS	Non -Point Source
P	Phosphorous
P_2O_5	Phosphorous Pentoxide
SCS-CN	Soil Conservation Service-Curve Number
SPOT	Satellite for Observation of Earth (In French)
SS	Suspended Solids
SWAT	Soil and Water Assessment Tool
UKZN	University of KwaZulu-Natal

CHAPTER ONE

1 INTRODUCTION

Chapter 1 provides background information on the identified problem and the rationale for its study. Hypothesis and objectives of the study are presented. The overview of the contributions of the thesis to the knowledge base (section 1.3) together with the thesis outline (section 1.4) is also included in Chapter 1.

1.1 Rationale

In South Africa, like many other parts of the world facing scarcity of water resources, stringent measures are being taken to ensure that the limited water in rivers is conserved and used in a more sustainable way. Water quality studies on river pollution at both the catchment and urban scales have increased, and consequently several water quality models have been developed in an attempt to alleviate the problem. Depending on the natural and anthropogenic induced processes taking place in a catchment, nutrients and/or other agricultural NPS pollutants enter rivers through several hydrological, geological and biological pathways (McClain *et al.*, 1998; Wassmann and Olli, 2004). These processes generally are known from the numerous studies of small catchments, and are extrapolated to assess nutrient sources at global and continental-scales (Howarth *et al.*, 1996; Jordan and Weller, 1996; Carpenter *et al.*, 1998). Agricultural production has been identified as a major source of non-point source pollution, and sediments typically form the largest single type of NPS-pollutant, followed by nutrients (NRC, 1993). Much of the nitrogen that enters lakes and rivers is associated with eroding sediments and occurs in the form of (i) NH_4^+ , (ii) eroding soil organic matter in the form of organic N and NH_4^+ and (iii) surface runoff in the form of dissolved NO_3^- . Phosphorus on the other hand is normally the limiting nutrient in freshwater eutrophication; thus, additions of phosphorus to the system are more likely to lead to accelerated growth where physical factors are conducive to the growth of algae under typical freshwater conditions as compared to the additions of other nutrients. Studies have been done to try and understand the movement of these non-point source pollutants along with the sediments in the catchment areas with an aim of controlling them.

Prediction of water quality requires an understanding of the hydrologic, physical, chemical, and biological processes both in the landscape and water bodies (Linsley *et al.*, 1988). Accelerated eutrophication and stress on the aquatic water system has led to the “death” of some of our rivers. This is evidenced by general absence of aquatic life, macrophytes and other forms of life. It is exacerbated by anthropogenic activities that may be ascribed to high turbidity, physical action of sediments, periodic spates and instability of the river bed. Some rivers experience high pollution levels from municipal and industrial point sources besides that from non-point sources resulting from agriculture and other commercial activities. Thus rivers have progressively shown signs of deterioration in their quality. This phenomenon affects the downstream use of river water as it contributes to pollution of the receiving impoundments.

Simulation models require better quantification of source zone contributions of sediments and nutrients as well as better understanding of water, nutrient and sediment connectivity both in the landscape and in water bodies (Howe and Lorentz, 1995; Newham and Drewry, 2006). This will allow for more effective land use change impact assessment and evaluation of reduction in loads due to targeted remediation within catchments. The *concept of connectivity* in NPS processes is of increasing interest to a range of disciplines such as landscape ecology, hydrology and geomorphology (Turner *et al.*, 1993; Western *et al.*, 2001; Brierley *et al.*, 2006). *Landscape connectivity* defines the physical coupling of landforms (e.g. hillslope to channel) within a catchment whereas *hydrological connectivity* refers to the passage of water from one part of the landscape to another and is expected to generate a catchment runoff response (Bracken and Croke, 2007). *Sedimentological connectivity* relates to the physical transfer of sediments and attached pollutants throughout the drainage area and may depend on sediment particle size, among other factors. The use of connectivity in NPS catchment models developed to date is limited. Nonetheless, it has the potential to correctly represent complex systems as they occur in the natural system. Thus opportunities for an integrated approach in the study of runoff, nutrient and sediment transfer in the catchments, which provide better understanding of these processes has been missed.

Establishing the hydrological connectivity between the upland and riparian zones in a hydrological system leads to a better opportunity for modelling of runoff generation and nutrient export within a catchment (Ocampo *et al.*, 2006). Identification of the water flow paths between each land segment and the outlet is a prerequisite to hydrological connectivity

analysis (Bracken and Croke, 2007). It is also important to identify the key landscape and land management controls driving nutrient mobilization e.g. road crossings, connected slopes, bedrock controls, farm dams and wetland zones. These water flow paths vary according to the hierarchical organization of the main hydrological processes, i.e. runoff, sub-surface flows or drainage in the riparian buffers, wetlands and dams (Frey *et al.*, 2009). Connectivity varies and evolves through both time and space hence constituting a challenging problem in hillslope and catchment hydrology. A land segment needs to be active in term of water transfer without disconnection, up to the outlet, for hydrologic connectivity to be realized (Ambroise, 2004). This is because with the same rainfall, two catchments can respond differently due to their difference in runoff-generating areas and the nature and degree of their connectivity. Areas in the catchment characterized by runoff generation, but which are not hydrologically connected to the outlet may show no runoff response at the outlet.

Many models that have been developed to simulate NPS pollutant transport at different scales, such as point, field and catchment, treat entire sub-catchments as runoff-contributing areas (Campbell *et al.*, 2001). These models are often applied at a resolution at which it is impossible to determine (i) areas within a sub-catchment that generate runoff and (ii) whether these areas are connected to the outlet of the sub-catchment. Although some models are capable of identifying runoff-generating areas within a sub-catchment, they implicitly assume that infiltration excess is the runoff generating mechanism. The *ACRU* model uses the SCS-CN equation (Schulze, 1995) to predict runoff based on land use and soil type. Although the SCS-CN runoff equation was originally developed to estimate design storm flows for flood forecasting where the location of runoff production was not important, it is increasingly being used for NPS pollution management where identifying the correct location of runoff generation is critical.

The Mgeni Catchment in South Africa is a region of widely varying land use ranging from areas of intense agricultural, to industrial and urban development to conserved natural lands. It is a region with major economic, ecological and cultural importance and careful planning is essential if all these needs and activities are to be sustainable. Large scale sugarcane farming in the Mkabela Catchment in particular, involves use of large quantities of fertilizers, herbicides and pesticides. The current ecological state of the rivers within this catchment and their responses to the natural as well as human induced disturbances must be understood clearly. Because of limited water resource availability in South Africa and continued

deterioration of water qualities in the Mgeni river system, the local research in the Mkabela Catchment must focus on results that could be used to guide the sustainable use of soil and water resources. The need to be able to capture sediment and nutrient pollutant responses from the source to catchment outlet is urgent because river catchments are continuously being threatened from NPS pollution and communities living along them are vulnerable. This study provides a good foundation for understanding the water quality conditions of these rivers to enhance future planning and management schemes and, more significantly, to prevent pollution.

SWAT which was developed to continuously simulate hydrological processes over long periods (Neitsch *et al.*, 2005), and *ACRU-NP* (Campbell *et al.*, 2001) are mixtures of physically and conceptually based models which can be used to predict the degree of NPS nitrate and phosphorous pollution from agriculture. The use of these models to mitigate sediment and nutrient pollution at catchment level has been done with varying degrees of success. The original *ACRU-NP* model is not very effective as it is hindered by a lack of consideration of connectivity. *SWAT* can be used to model connectivity effectively because it captures controls of land surface and sub-surface characteristics (Feng *et al.*, 2013). Its ability to replicate hydrologic and/or pollutant loads at a variety of spatial scales on an annual or monthly basis has similarly been confirmed in numerous studies (Chaplot *et al.*, 2004; Pohlert *et al.*, 2005; Mishra and Kar, 2012; Le Roux *et al.*, 2013). However, the model performance has been inadequate in some studies, especially when predicted output was compared to time series of measured daily flow and/or pollutant loss data (Gassman *et al.*, 2007). The other major limitation to long-term use of *SWAT* in South Africa is the lack of long-term nutrient and suspended solids data for calibration and validation.

This study is designed to develop and apply modelling and observatory techniques to identify and quantify nutrient and sediment source zones, quantify the translation of these pollutants through the landscape and quantify the impact of control features on the transfer of the pollutants through the stream system in the Mkabela Catchment.

1.2 Hypothesis and Objectives of the Study

The premise of this research is that the modelling of NPS pollution and connectivity is effective in determining the spatial and causal linkages between agricultural activities and catchment-scale processes, and can be used to predict nutrient and sediment export in catchments.

The specific objectives are to:

- define the dynamics and connectivity of the hydrological processes response zones of contributing landforms by observing water, sediment and nutrient fluxes using hydrometric, hydrogeological and geophysics surveys as well as stable water isotope responses;
- define and quantify hydrological and dissolved nutrient sources and transport mechanisms within the hydrological processes response zones;
- define and quantify the impact of NPS pollution controls such as riparian buffer zones, wetlands and reservoirs on the migration of sediments and solutes through the catchment;
- simulate crop yield, nutrient and sediment production for various land uses and NPS pollutants at controls and buffers in the stream network within the Mkabela Catchment.

1.3 Contributions of the Thesis to the Knowledge Base

The contribution of this thesis to scientific knowledge base is culminated with the writing of two manuscripts. The first manuscript has been published in the Physics and Chemistry of the Earth Journal. The second manuscript was submitted to the Hydrological Sciences Journal and is under review. The names appearing on the manuscripts are Kipkemboi J. Kollongei and Simon A. Lorentz.

The author hereby referred to Kipkemboi J. Kollongei in this section entirely composed and wrote this thesis which included analysing and evaluating data obtained from the field observations and the laboratory against published data contained in journal articles and text books. Prof Simon A. Lorentz, the author's PhD supervisor, was the principal researcher in the projects that funded the study and the general subject presented in this thesis.

Highlighted below are the specific details of the contributions of the thesis to the scientific knowledge base:

- The *ACRU-NPS* model was configured based on a nested approach which required an effective description of all relevant components of the system and an understanding of the processes and feedbacks taking place within and between different scales and hydrological processes response zones.
- The concept of connectivity in the model was introduced to improve simulations. Connectivity defines the physical coupling of landforms (e.g. hillslope to channel) within a catchment where the passage of water from one part of the landscape to another is expected to generate a catchment runoff response that may carry along with it dissolved pollutants as well as sediments and adsorbed pollutants through the drainage area. The connectivity aspect within the river network in the Mkabela Catchment was achieved by means of sub-catchments that were linked to in-stream controls that included farm dams and wetlands plus buffer zones where the fate and transport of dissolved N and P, sediment and associated adsorbed P were studied.
- A new method of calculating crop yield that was different from that used in the *SWAT* model was developed and incorporated in the *ACRU-NPS* model. Water and nitrogen stresses were used to limit the crop growth on a daily time step. This enabled consequences of subsequent nutrient and sediment loads in streams to be studied on a daily time step. The major limitation to long-term use of *SWAT* in South Africa is the lack of long-term nutrient and suspended solids data for calibration and validation.
- Formulation of a new NPS modelling approach that was used for the first time to study pollutants emanating from the Mkabela Catchment in South Africa. The developed *ACRU-NPS* model included sufficient process details to allow for the implementation of controls such as wetlands, dams and buffer strips. Successful simulation of crop yields, nutrient and sediment production, and fate of NPS pollutants was thus achieved.
- The main contribution of this study was to link hydrology and NPS processes by describing and defining pathways through which pollutants moved in the catchment. This was achieved through studying the dynamics and connectivity of water, sediments and nutrient fluxes by combining hydrometric, hydrogeological, geophysics and stable water isotope techniques to interpret the field and laboratory data. Suggestions for future improvements on the *ACRU-NPS* model were given based on the understandings gained from the different observations and sampling done in the Mkabela Catchment.

1.4 Outline of the Thesis

This thesis is comprised of nine integrated chapters, starting with the introduction of the thesis in Chapter 1 and ending with conclusions and recommendations for future research in Chapter 9. Cited references are listed in section 10 and the appendices appear in section 11. Chapter 1 introduces the study. It gives the background information on the identified problem and the rationale for its study. Hypothesis and objectives of the study are presented. The overview of the contributions of the thesis to the knowledge base (section 1.3) together with the thesis outline (section 1.4) is also included in Chapter 1.

In Chapter 2, the description of the Mkabela Catchment research site is given in detail. Its location, climate, geology and soils, including vegetation and land use type in existence are discussed. Chapter 3 presents a literature review on hydrological processes and scale issues together with up-scaling effects on NPS processes when modelling from field to the catchment level. The connectivity concept which forms the basis of this research is introduced in Chapter 3.

Chapter 4 reports on the methodologies used to achieve the set objectives of the study. Initially a nested catchment monitoring layout is given which takes into consideration scale issues from local, field to catchment levels. Materials and methods used to aid in collection of observed data at plot, field and catchment scales are also provided. The various laboratory procedures and analysis that were used on sampled nutrients, sediments and isotopes is specified. Introduction to *ACRU-NPS* development is also given.

Chapter 5 discusses the connectivity influences on nutrient and sediment migration in the Mkabela Catchment. The Mkabela Catchment hydrological processes response zones and connectivity processes exhibited are described in detail including the study of transects of hillslopes hydrogeology that are important in understanding nutrient and sediment migration in the sub-surface. Plot scale geophysics, soil water and nutrient dynamics in Mkabela are also discussed. From the plot scale geophysics studies, it was possible to link hydrological connectivity with the various sub-surface materials that influences soil water movement alongside dissolved nutrient pollutants.

Detailed *ACRU-NPS* model development is presented in Chapter 6 with the envisioned incorporation of connectivity concepts into the model. This made it possible to study hydrological connectivity between land segments and the linked control structures i.e. buffers, wetlands and dams. This approach took into account runoff, NO₃, P and SS (suspended solids) exchanges between the land segments and river channel together with their fate on entering and leaving buffers, wetlands and dams.

The *ACRU-NPS* simulations in the Mkabela Catchment are presented in Chapter 7. Also reported in this Chapter were the model input parameters, model calibration and validation and the chosen simulation scenarios. Results and discussions are deliberated in Chapter 8 from two perspectives. The first perspective discusses the connectivity influences on nutrient and sediment migration in the Mkabela Catchment based on field and catchment observations. This was achieved by observing discharge, nutrients, sediments and isotope responses using instruments set up at the field and catchment scales. The results from stable $\delta^{18}\text{O}$ and $\delta^2\text{H}$ isotope responses show the influence of impoundments and contributing hillslopes on nutrient and sediment migration in the catchment using a simple mass balance mixing model.

The second perspective discusses the results from the *ACRU-NPS* modelling where crop yields and pollutant loads are elaborated. The sugarcane crop yields from varying fertilizer application rates at the various sub-catchments were considered. Along with this were the discharges, nutrient and sediments loads that were generated in the catchment and eventually passed through buffers, wetlands and dam controls. Using the simulated discharge, the hydrological connectivity between catchment drainage areas and control features was established. Buffer, wetland and dam hydrological responses were investigated in relation to catchment hydrological and NPS pollution processes. The impacts of buffers, wetlands and dams on nutrient and sediment migration in the catchment were clearly seen from the simulation results. A summary of the conclusions and recommendations for future research, arising from the present study, are presented in Chapter 9.

CHAPTER TWO

2 DESCRIPTION OF THE STUDY SITE

2.1 Mkabela Catchment Location

The Mkabela Catchment lies between 29°21'12" and 29°27'16" South and 30°36'20" and 30°41'46" East in the KwaZulu-Natal province of South Africa (Figure 2.1). It is located in the sugarcane growing region next to Wartburg town within the KwaZulu-Natal midlands.

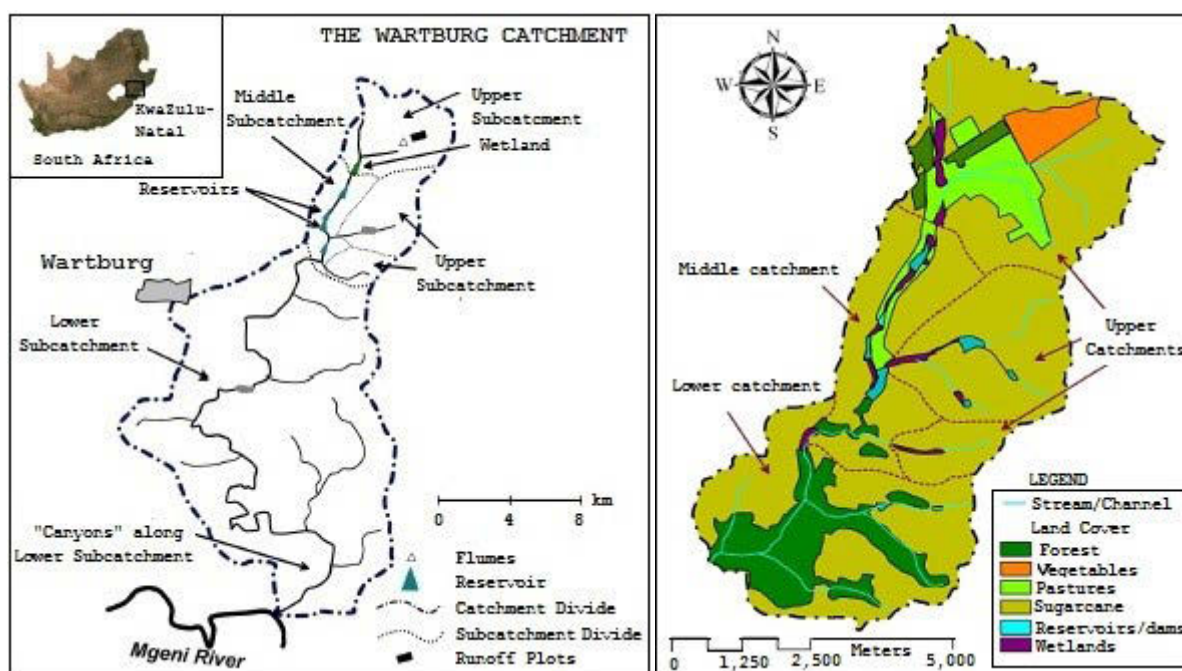


Figure 2.1: The location (left) and land-use types (right) of the Mkabela Catchment, near Wartburg, KwaZulu-Natal Province in South Africa (after Miller *et al.*, 2013 and Le Roux *et al.*, 2006).

Elevation ranges from 880 m at the catchment outlet in the southwest to 1057 m upstream in the northeast of the catchment. The catchment area of 4154 ha is drained by a tributary of the Mgeni River that exhibits a flow length of 12.6 km from its source to the catchment outlet (Le Roux *et al.*, 2013). Land forms are complex, ranging from gently undulating footslopes and valley floors to steep midslopes exceeding 20 %.

2.1.1 Climate

The area experiences the following climatic conditions: a mean annual precipitation (MAP) of 410-1450 mm, mean annual runoff (MAR) of 72-680 mm and mean annual evaporation (MAE) of 1360-2040 mm. The rainfall is strongly seasonal with > 80% falling between October and March (WRC, 2002). July is the coolest month whereas February is the warmest month with mean minimum and maximum temperatures ranging from 6 to 21° C and 17 to 28° C, respectively.

2.1.2 Geology and soils

The geology consists of the Cambrian age sandstone of the Natal Group and relatively small pockets of Dwyka and Ecca sedimentary rocks in the north (Le Roux *et al.*, 2006; Fey, 2010). According to Le Roux *et al.*, (2006) the Westleigh and Longlands soil types are underlain by the Natal Group sandstone while the Avalon soil type is underlain by sedimentary rocks of the Dwyka Group and sandstone of the Natal Group.

Table 2.1: Brief description of the primary soil types found in the study area (Le Roux *et al.*, 2006).

Soil Type	General Characteristics
Avalon (Av)	The Avalon soil type was surveyed up to 120 cm depth and consists for its largest part of soft plinthic B horizons which is a sandy yellow-brown apedal B horizon underlain by hard plinthic horizons.
Cartref (Cf)	Shallow, sandy soils with very little water holding capacity found on steep, short, convex hillslopes.
Clovelly (Cv)	Associated with, and similar to, Longlands soil type.
Glencoe (Gc)	Similar to Avalon soil type, but are dominated by hard plinthic subhorizon, and are found on steeper slopes of higher relief. Parent material is thought to be the Natal Group Sandstone.
Hutton (Hu)	Found near crest and midslopes of high relief, steep hillslopes. Moderately drained and underlain by Natal Group Sandstone.
Katspruit (Ka)	Clayey, strongly gleyed soils found on low-relief (10-15 m) terrain, particular valley bottoms.
Longlands (Lo)	The Longlands soil type was surveyed up to 120 cm depth and consists of soils that are sandier than the Avalon soils with similar profile of soft plinthic B horizons well developed underlain by hard plinthic horizons.
Westleigh (We)	The Westleigh soil type was surveyed up to 110 cm depth and consists of a poorly drained hydrosequence dominated by clayey soils with prominent mottling and deep, clayed subsoils.

The dominant soil types in the Mkabela Catchment are shown in Figure 2.2. These soils vary from poorly drained clays predominately in the northern part of the catchment and areas with low relief (e.g. Westleigh form) to well drained sandy soils mainly in the southern part of the catchment in areas with high relief and steep slopes (e.g. Hutton form) (Le Roux *et al.*, 2006). Table 2.1 provides a brief summary of the soils within the Mkabela Catchment as provided by Le Roux *et al.*, (2006). Nine soil types are present including the Avalon (Av), Cartref (Cf), Clovelly (Cv), Glencoe (Gc), Hutton (Hu), Katspruit (Ka), Longlands (Lo), Glenrosa (Gs) and Westleigh (We).

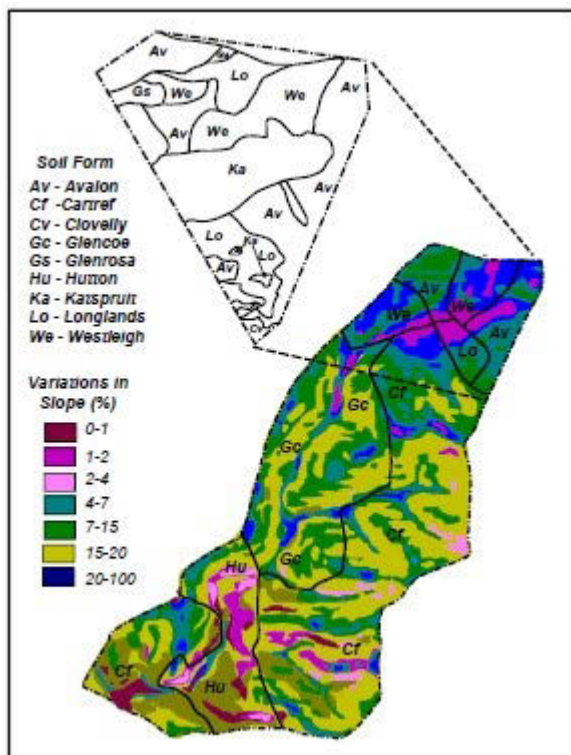


Figure 2.2: Mkabela Catchment showing 6 dominant soil types with additional detailed soil types in the upper sub-catchment (after Le Roux *et al.*, 2006).

The major soil types include the Cartref, Glencoe and Avalon soils. The Cartref soil occupies approximately 36 % of the catchment and primarily occurs in the central part of the catchment. It is a shallow sandy soil located on steep and convex hillslopes with little water holding capacity. Glencoe and Avalon soil forms are deeper sandy soils located on midslopes. They are characterized by soft or hard plinthic sub-horizons that are permeable to water and occupy approximately 20 % of the catchment (Figure 2.2).

2.1.3 Vegetation and land use

The catchment falls within the Savanna Biome (Mucina and Rutherford, 2006) but natural vegetation in the catchment was replaced or modified by agricultural activities several decades ago (Figure 2.3). The catchment is divided into homogenous sections called sub-catchments. These sub-catchments exhibit more or less homogeneous hydrological characteristics that include land cover and soil types (Table 2.2).

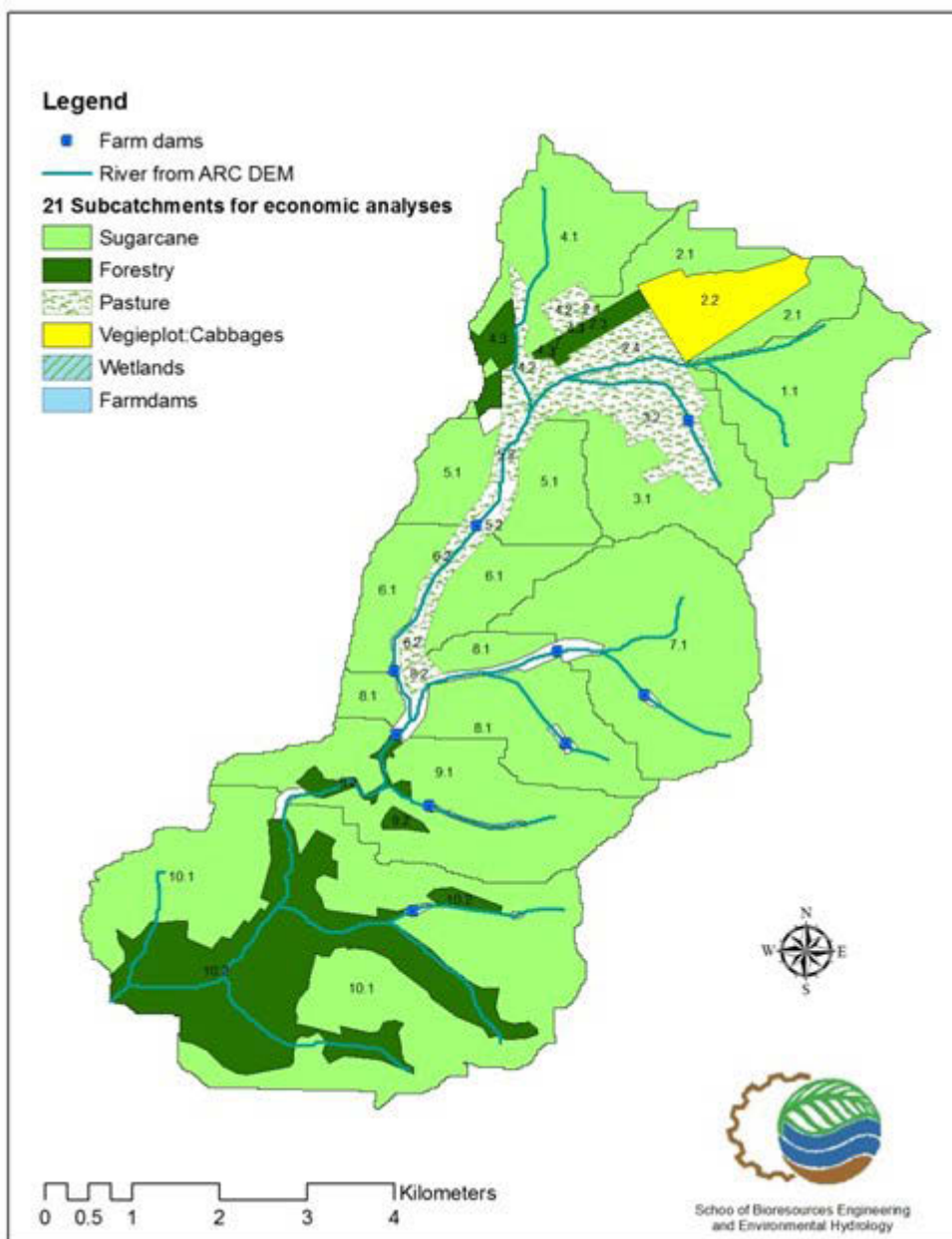


Figure 2.3: Land uses and sub-catchments in the Mkabela Catchment.

Most of the catchment is currently under sugarcane cultivation (76 %) with minority land uses including forestry (13 %), pasture (8 %) and a cabbage plot (3 %) (Figure 2.3).

Table 2.2: Areas of sub-catchments and land use in the Mkabela Catchment.

Land cover	Soil types	Sub-catchment numbers	Areas (km ²)
Sugarcane	Avalon	1.1	2.58
Sugarcane	Avalon	2.1	1.52
Veggie plot: Cabbages	Westleigh	2.2	1.06
Forest : Wattle	Westleigh	2.3	0.25
Pasture	Westleigh	2.4	0.67
Sugarcane	Cartref	3.1	1.91
Pasture	Cartref	3.2	1.24
Sugarcane	Avalon	4.1	2.21
Pasture	Westleigh	4.2	0.49
Forestry: Wattle	Glencoe	4.3	0.36
Sugarcane	Glencoe	5.1	1.83
Pasture	Glencoe	5.2	0.37
Sugarcane	Glencoe	6.1	1.93
Pasture	Glencoe	6.2	0.34
Sugarcane	Cartref	7.1	4.55
Sugarcane	Cartref	8.1	2.77
Pasture	Glencoe	8.2	0.09
Sugarcane	Cartref	9.1	3.84
Forestry: Pine	Hutton	9.2	0.3
Sugarcane	Cartref	10.1	7.85
Forestry: Pine	Hutton	10.2	4.50
Total:			40.66

Table 2.2, Figures 2.2 and 2.3 show the various soil types under which different land-use types in the sub-catchments fall. Sugarcane, with an area of ~31 km², occupies the largest part in the catchment. Forest cover is mostly made up of wattle and pinus plantations.

CHAPTER THREE

3 LITERATURE REVIEW: WATER QUALITY MODELLING OF AN AGRICULTURAL CATCHMENT, ADOPTING CONNECTIVITY CONCEPT

The wish to explore scenarios beyond observable conditions, and the expense of monitoring programs, calls for modelling approaches to assess sediment and catchment-scale nutrient generation in complex catchment systems (Newham and Drewry, 2006). According to Molloy and Ellis (2002), models “play potentially important roles in evaluating changes in land use and management, and their use can assist evaluation of water quality trends and overcome difficulties presented by high temporal variability and limited water quality measurements”. Improved representation of key nutrient and sediment generation processes, however, is needed to advance the utility of NPS modelling outputs and confidence in ensuing management recommendations. Many of the existing NPS models have been developed without consideration of connectivity which can be used to improve prediction of sediment and nutrients yields from the hydrological processes response zones to the catchment outlet. A process zone represents a fundamental unit of watershed management that allows distinct strategies to be developed for specific parts of the drainage network (Miller *et al.*, 2013). They differ in their ability to produce, transport, and store sediment. Certain areas are diffuse pollution hotspots, where high nutrient inputs and inappropriate land use generate a significant nutrient source that is also connected with a hydrological flow path to the drainage networks, hence, there is a need to identify and prioritize these landscapes (Lane *et al.*, 2006).

To develop NPS models that can effectively predict sediment and nutrient yields in catchments, the influence of scale on hydrological processes cannot be ignored. This is because the processes dominating hydrological responses differ as a function of spatial scale. Hydrologists should be able to consider NPS processes at various scales in line with the concept of connectivity whereby interaction of hydrological processes at different time and spatial scales can be studied and linked in agricultural catchments.

“Environmental measurements cannot be scaled-up directly and this presents one of the major challenges in integrating field and modelling approaches to diffuse pollution research” (Beven, 1989). The kind of measurements obtained from a point (1 m²) could differ radically

from measurements made at the hillslope scale (1 ha) in small catchments (1 km²) or in large catchments (1000 km²) (Heathwaite, 2003). New strategies, however, of combining monitoring and modelling are possible through increasingly making environmental measurements accurate at a range of scales and frequencies. By linking plot scale and catchment scale processes through connectivity, it would be possible to improve prediction of downstream impacts of current and future land uses effectively.

3.1 Hydrological Processes and Scale Issues

One of the major goals of hydrological research is to extend the understanding of the impact of changing scales on hydrological processes. Table 3.1 shows the scale definitions usually used in hydrological modelling with spatial scales ranging from point to global (Refsgaard and Butts, 1999).

Table 3.1: Definition of spatial hydrological modelling scales after (Refsgaard and Butts, 1999).

Spatial scale	Characteristics	
	Length	Area
Point scale	< 100 cm	<1 m ²
Field or hillslope scale	100 m	1 ha
Catchment scale	3 – 100 km	10 – 10 ⁴ km ²
Regional scale	100 – 1000 km	10 ⁴ – 10 ⁶ km ²
Continental or global scale	> 1000 km	> 10 ⁶ km ²

Since the interests of an individual farmer, a community, a region or a nation may differ significantly, the range of processes and activities that take place at different scales (Figure 3.1) have significant implications for effective land use planning (Hewett *et al.*, 2009).

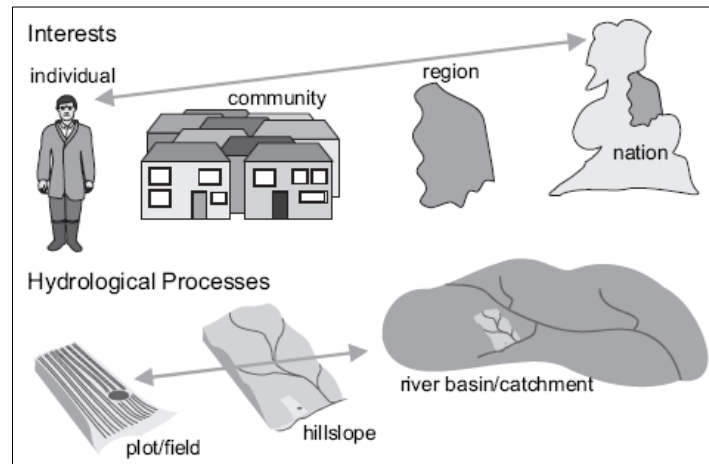


Figure 3.1: Hydrological processes and scale issues (Hewett et al., 2009).

Understanding of upscaling issues is paramount, since hydrological processes inherent at the local (point) scale also impact on the catchment scale (Beven, 1993; Bloeschl, 1997). The individual activities of a farmer at a field scale will eventually have impacts in water courses at the larger catchment scale. The agricultural activities at the plot scale yield sediments and nutrients which may accumulate downstream because the hydrological processes are connected throughout the whole catchment. This will impact negatively on water quality standards within a catchment, if good farming practises were not observed at the field scale.

Local impacts in local streams and aquifers are generated from local hillslope runoff processes. Because of the different contributions from sub-catchments, downstream impacts are cascaded through the hydrological cycle with both the water quantity and quality changing radically dependent on management, soils, geology and climate (Hewett *et al.*, 2009). Thus, ideally a set of scale-appropriate modelling and management tools are needed for each catchment. By this I mean a variety of tools used at different scales within a catchment. Upscaling (the transfer of knowledge obtained at a smaller scale to a larger scale) often requires identifying dominant processes evident at the catchment scale rather than attempting to capture all small-scale variability and complexity (Bloeschl, 2001; Sivapalan, 2003).

Complex or lumped equations can be used to upscale the outflow discharge and nutrient load from field to catchment scale. One example where lumped equations are used is when the model simply assumes that the decrease in N loads, as water moves from the field edge to the catchment outlet, is exponentially dependent on time in transient and can be described with a

single attenuation coefficient (Amatya *et al.*, 1999). The complex method is an integrated model approach that involves use of a combination of models to upscale the nutrient load from individual fields to the nutrient load at catchment outlet. In this research the interest is to develop tools for evaluating non-point source pollution migration in a typical catchment where hydrological processes response zones and connectivity cannot be effectively represented by lumped parameter models.

3.1.1 Plot or local scale simulations

The models applicable in these simulations are employed to address local impacts of various management, soil and climate scenarios. Research plots or soils within a field are the spatial units of interest here. Most nutrient loss models in general have been designed to address this range of local scales. Geographical Information Systems (GIS) technology can provide an overlay of the catchment after spatially referencing individual soil simulation analyses within a field (Shaffer, 1995). To help calculate soil nutrient budgets and make fertilizer recommendations to farmers, models require soil NO₃-N, phosphorous and organic matter levels obtained from field trials. Other essential data are manure and legume credits, crop types and crop yields. Nutrient models of this type are normally applied at the local scale and are limited to the crop root zone.

3.1.2 Field scale simulations

This involves field scale models that consider multiple plots and management enterprises in a simultaneous way. The models that are designed to make fertilizer recommendations (or predict NO₃-N leaching or phosphorous loss at the plot or local scale), may also be applied at the whole farm (or field-scale by aggregating results obtained from plots or smaller areas) through the use of spatially referenced databases and GIS technology (Shaffer, 1995). These groups of models include soil process mechanisms at varying degrees of complexity for computing soil water and nutrient budgets, and transport of nitrate-N or phosphorous through and out of the root zone. Most of these models are site-specific and use lumped parameters. Since lumped-parameter models depend on the averaged conditions of model parameters over the given spatial unit, they may not represent landform and channel connectivity effectively.

3.1.3 Catchment scale simulations

GIS, remote sensing, and simulation technologies are combined to address large scale spatial and temporal impacts of soil, climate and management. The models utilized here are either two or three dimensional models designed primarily for surface runoff calculations with some provision for subsurface flow, or field scale models that have been adapted for use at larger scales (Shaffer, 1995).

3.2 Effect of Scale on NPS Processes: Small Plot to Catchment-scale

The ability of models to predict total or dissolved nutrients is often related to the conditions under which measurements were made, the application and the scale of model development (Newham and Drewry, 2006). “Much of the available nutrient export data has been derived from plot or small-scale field trials and do not always retain the pathway linkages to water, particularly at catchment-scales” (Heathwaite, 2003). According to Di and Cameron (2000) “very few studies have attempted to link transport factors from lysimeter-based experiments to streams though lysimeter-based processes have been incorporated into larger-scale nitrogen models”.

At the plot scale, soil and crop type, nutrient cycling and leaching dominate (Quinn, 2004), while hydrological processes like runoff generation, nutrient and sediment yields dominate at the hillslope scale, with nutrient mobilisation related to connectivity between the source areas and the receiving water (Nash *et al.*, 2002; Quinn, 2002; McDowell *et al.*, 2004). Key influences at a large catchment-scale include variability of land use, rainfall and topography (Quinn, 2004).

Internationally “scaling-up techniques have been noted as an important area of further research” (Quinn, 2002), although it is “associated with considerable uncertainty” (Heathwaite, 2003). Linking of watershed nutrient export with water quality, particularly processes at the edge-of-field remains under-researched (Heathwaite, 2003). “Connectivity issues have been noted as important but requiring research, which could be potentially achieved by models such as modified P and N index models,” (Heathwaite *et al.*, 2000). Here a range of index-based modelling approaches have been used to address nutrient-related water quality issues by identifying areas of greatest nutrient export or so called critical source

areas (Heathwaite *et al.*, 2000). Index-based approaches are used to rank site vulnerability of nutrient loss through accounting for source and transport factors with modifications designed for local conditions (Newham and Drewry, 2006). Source factors could include fertilizer, soil nutrient levels and effluent management where appropriate. Transport factors include leaching, erosion, runoff and the ‘connectivity’ or land connection to the waterway.

3.3 Connectivity Concept

The concept of connectivity in NPS processes is of increasing interest to a range of disciplines such as landscape ecology (Turner *et al.*, 1993), hydrology (Western *et al.*, 2001; Bracken and Croke, 2007) and geomorphology (Brierley *et al.*, 2006; Müller *et al.*, 2007). This is mainly because the transient connection of hillslopes to channel networks is at the centre of important issues such as flood and sediment yield generation, diffuse pollutant fluxes and the trigger of many important ecological events. In order to understand catchment sciences, much of the research has focused on the dynamic role of connectivity in explaining nonlinearities in catchment hydrological response and pollutant fluxes.

In hydrology and geomorphology, three ‘types’ of connectivity are discernable: (1) *landscape connectivity*, that defines the physical coupling of landforms (e.g. hillslope to channel) within a basin; (2) *hydrological connectivity*, that refers to the passage of water from one part of the landscape to another and is expected to generate a catchment runoff response; and (3) *sedimentological connectivity*, that relates to the physical transfer of sediments and attached pollutants throughout the drainage area and may depend on among other factors, the particle size. The concept of connectivity has proved valuable in understanding catchment function, and can be conceptualized in different ways in hydrological models (Tetzlaff *et al.*, 2010).

3.3.1 Landform connectivity

The “character and behaviour of landscape compartments, how they fit together (their assemblage and pattern) and the connectivity between them, provides a platform to interpret the operation of geomorphic processes in any given system” (Brierley *et al.*, 2006). Fryirs *et al.* (2006) introduced the concept of landform impediments termed *buffers*, *barriers* and *blankets* that limit the connectivity between landscape compartments by impeding sediment conveyance. According to the study, the operation of sediment cascades and geomorphic

responses to disturbance events of differing magnitude and frequency is affected by catchment configuration and the nature of connectivity within and between landscape compartments. They defined *buffers* as impediments, which limit sediment delivery to channels, *blankets* as wrappers of channel or floodplain surfaces affecting accessibility of sediments to be reworked, and *barriers* as inhibitors of sediment movement along channels.

The conveyance of water and matter longitudinally, laterally, vertically and temporally is affected by the connectivity between landscape elements (Ward *et al.*, 2002). Longitudinal linkages may include upstream-downstream and tributary-trunk relationships which drive the flow transfer through a system and reflect the capacity of channels to transfer or accumulate sediments of variable amount on the valley floor. Lateral linkages such as slope-channel and channel-floodplain relationships drive the supply of materials to a channel network. Vertical linkages refer to surface-subsurface interactions of water, nutrients and sediments.

Landscape connectivity can be considered within a nested hierarchy at a local scale (i.e. within a landform such as a hillslope), zonal scale between landforms (e.g. slopes and channel), and system scale at a catchment level (Brierley *et al.*, 2006).

System scale changes in connectivity are related to:

1. Position of buffers, barriers and blankets which in turn dictates how effects of geomorphic changes are propagated through the catchment,
2. The nature of their interaction (e.g. in highly connected systems alterations in upper parts of the catchment are manifested relatively quickly),
3. Lag time for change to be manifested in the system e.g. the effective time scale for connectivity may even be 100 or 1000 years.

The spatial pattern of buffers, barriers and blankets characterized in Figure 3.2, influence the time frame over which sediments are reworked in different landscape compartments. Effective catchment area reflects the degree to which the catchment is longitudinally, laterally and vertically connected. At low flow stages associated with frequent, low magnitude energy inputs, landscape disconnectivity is significant. The buffers, barriers and blankets are not breached and sediment cascading is limited. This is because the capacity for slope erosion and fluvial sediment reworking is limited. This results in a low effective catchment area for sediment yield.

As flow stage increases within the channel network, more readily reworked in-stream barriers and blankets are broken. This happens less frequently because of moderate energy input just sufficient to initiate reworking of interstitial fines that form in-stream sediments. It results in connectivity between upstream channel network and lowland plains. The effective catchment area also increases with increasing connectivity.

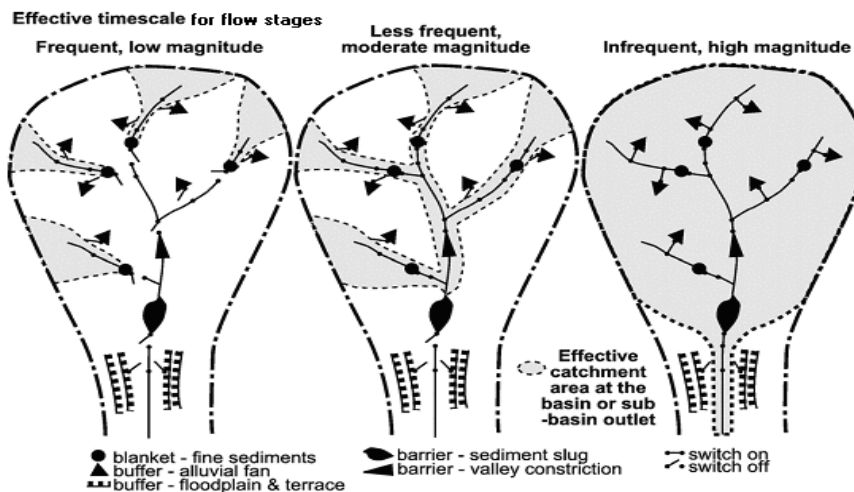


Figure 3.2: Spatial and temporal conceptual framework of connectivity associated with notion of “switches” in catchments (after Brierley *et al.*, 2006).

Infrequent, but high magnitude energy inputs experienced at high flow stages result in more buffers and barriers being breached. Reworking of alluvial fans (buffers) connects the hillslope to the channel network. The sediment slug (barrier) along the lowland plain is also reworked, contributing sediment to the river mouth. Buffering is maintained at floodplains and terraces unless an extreme event occurs. Effective catchment area is the highest under these conditions.

Though an exhaustive list of buffers, barriers and blankets is not presented, these examples provide sufficient guidance on the types of impediments that might occur in any fluvial landscape, which may influence landform connectivity. Catchment-specific variants can be readily added without changing the way in which the approach is applied. For example, analogous to this can be the *riparian buffer strips* (grasses at the edges of the field) that limit sediment delivery to rivers, which will act as buffers, *wetlands* will act as blankets which wrap channels and prevent sediments from being reworked and finally the *dams* that inhibit sediment movement along channels acting as barriers.

According to Brierley *et al.* (2006) there is significant variability in sediment cascading processes and system response times in arid and humid settings. In humid systems, where more seasonal and consistent discharge regimes occur, the movement of bed sediment is recurrent and consistent. Re-storage or slow removal of sediments in a downstream direction is common, resulting in lower sediment yields. Arid and semi-arid systems are characterized by movement of large quantities of bed sediments during infrequent, episodic scour periods. This results in less sediment storage and high sediment yields.

3.3.2 Hydrological connectivity

Pringle (2001) and Freeman *et al.* (2007) defined hydrological connectivity “as water mediated transfer of matter, energy and organisms within and between elements of the hydrologic cycle”. It has important implications for modelling of runoff generation and chemical transport. Dissimilar regions on the hillslope are connected via subsurface water flow and is key in determining the movement of nutrients down a hillslope (Hornberger *et al.*, 1994; Creed and Band, 1998). Stieglitz *et al.* (2003) provided preliminary evidence in a study done in Idaho that the seasonal timing of hydrologic connectivity can affect a range of ecological processes that include biological productivity along the toposequence, C:N cycling downslope and nutrient transport.

Hydrological processes control the recharge of sub-surface water stores, and the pathways and residence times of water throughout landscapes. In-stream connectivity is represented by the pathways and controls of fluxes of human-derived nutrients and toxic wastes in the landscape that reaches water bodies downstream (Figure 3.3). Not all locations in the landscape, even if they have the same land use, contribute equally to in-stream water quality degradation. Identifying the spatial and temporal hydrologic connectivity of runoff source areas within a catchment is therefore a significant step in understanding how landscape hydrologic dynamics lead to hydrologic and solute response in the catchment. This hydrologic connectivity is a “requisite for the flushing of solutes and nutrients downslope through the riparian zone to the stream” (Stieglitz *et al.*, 2003).

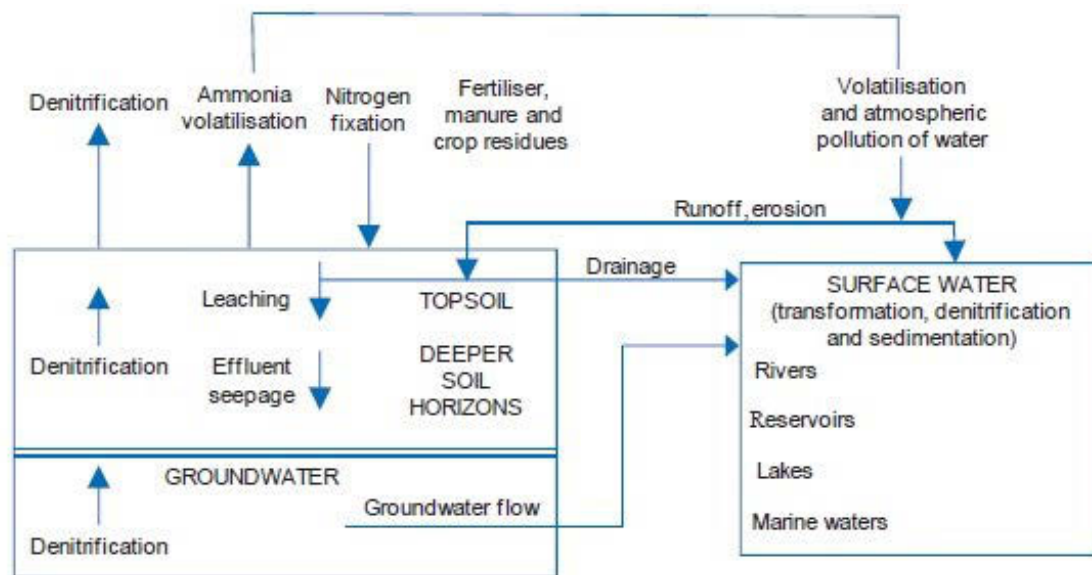


Figure 3.3: Nutrients in water: A schematic diagram of pathways from agricultural use (OECD, 2012).

Depending on location riparian zones may remain at or near saturation with minor to modest water table fluctuations in the upper soil profile and are positioned between the hillslope and stream interfaces often at the base of hillslope drainages (Jencso *et al.*, 2009). Channel characteristics may often include anoxic conditions, high organic matter content, and low hydraulic conductivity associated with the predominance of organic, silt and clay sized particles. According to Jencso *et al.* (2009) “these characteristics lead to potential buffering of hillslope inputs of water and nutrients streams”.

Hydrologic connections between hillslope-riparian-stream (HRS) zones occur when water table continuity builds up across their interfaces and streamflow is present. Ocampo *et al.* (2006) has shown that at the plot scale, riparian and hillslope elements can display independent water table dynamics which is characteristic of each landscape element. These investigations show that the steady state assumption of uniform groundwater rise and fall across the landscape is not realistic. Timing differences between hillslope and riparian water table dynamics were due to the different antecedent soil moisture deficits and drainage characteristics. Research at the catchment scale also mentions water table connectivity between riparian and hillslope landscape elements as a first-order control on solute and runoff response.

McGlynn *et al.* (2004) linked hillslope runoff contributions, total runoff and riparian water table dynamics in five nested catchments to landscape topography and the organization of hillslope and riparian landscape elements. Increasing synchronicity of runoff and solute response across scales was attributed to increasing antecedent wetness, event size, and the resulting increased riparian-hillslope-landscape hydrologic connectivity. These studies highlight the importance of hillslope-riparian-stream connectivity for the explanation and prediction of hydrologic response and the in-stream water quality degradation.

3.3.3 Controls and thresholds

Bracken and Croke (2007) proposed a framework of hydrological connectivity that included the five major components that control hydrological connectivity: *climate*, *hillslope runoff potential*, *landscape position*, *delivery pathway* and *lateral buffering* (Figure 3.4). Within each of these components there are a number of factors that may influence the extent to which a catchment may be regarded as connected.

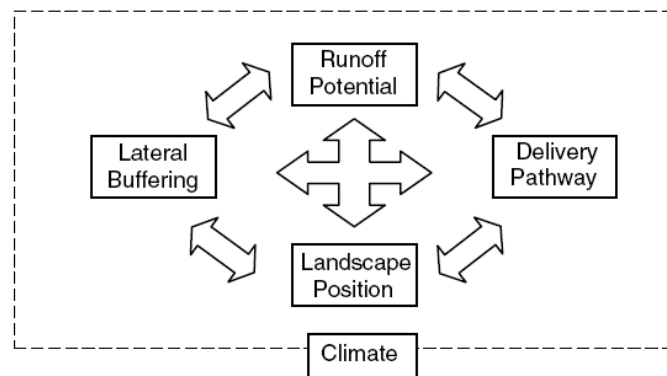


Figure 3.4: The components that control catchment connectivity (Bracken and Croke, 2007).

Climate: climate is a key control on the pattern and distribution of runoff within a catchment, specifically the runoff regime as determined largely by the nature and distribution of rainfall. The response to rainfall and hydrological connectivity is dynamic and will change depending on the nature of rainfall input, antecedent conditions and catchment characteristics.

Hillslope runoff potential: the hillslope is the major landscape unit and is the scale at which most research on runoff generation takes place. There are many factors that influence hillslope runoff, including crusting and surface roughness, heterogeneity within the soil, the

impact of variable density and type of vegetation, changing catchment morphometry, transmission losses in tributaries and main channels, and the impact of land use.

Delivery pathway: each runoff source has its own specific delivery pattern that is dependent upon its landscape position within the catchment and, in many instances, the management practices employed. The delivery of this water downslope involves flow pathways of variable width, depth and velocity. Dominant controls on the type of runoff pathway include such factors as topography, especially the effects of steepest slope, convergent hillslopes and hillslope hollows. Increasingly the effects of anthropogenic structures are emphasized.

Slope length influences connectivity at the hillslope and catchment scales, and is relatively unimportant at the plot scale. On longer slopes it is more likely that the slope will cease to generate runoff before runoff reaches the slope base or channel. The relationship between slope length, rainfall duration and intensity that produces connected flow at the outlet is complex. At the hillslope scale, a range of investigations have proposed a decrease in runoff per unit area with increasing slope length due to increased opportunity for infiltration (Van de Giesen *et al.*, 2000).

Landscape position: landscape position reflects the relationship between runoff source and distance to the outlet-hillslope or catchment. Intuitively, the probability of hydrological connectivity will be enhanced if the transport distance for water is short relative to the effective contributing area (Bracken and Croke, 2007). In its simplest sense, this can be expressed as distance to stream or outlet.

Lateral buffering: lateral buffering defines lateral connectivity in ecological studies, or the nature of flood inundation between a channel and the adjacent floodplain (Pringle, 2001). It has been recognized as a fundamental control on nutrient and organic matter transfer between the main channel and adjacent areas of the floodplain. Hydrological connectivity will be significantly influenced by the degree to which (a) hillslopes are physically connected to channels and (b) the degree to which lateral buffering acts to limit runoff and sediment delivery to the channel.

Bracken and Croke (2007) proposed thresholds called “*volume to breakthrough*” to quantify changing connectivity between different environments and catchments”. This defined the accumulated runoff volume per unit width to be applied to a point before flow appears at a

downslope point. This approach is one possible concept of runoff generation and flood production that moves beyond the traditional view that runoff is generated by either the variable source area (VSA) or Hortonian infiltration excess. The framework is best viewed as a structure for exploring potential gaps in the process understanding and, importantly, data necessary to quantify connectivity.

A study done by Ocampo *et al.* (2006) in Susannah Brook Catchment, Australia showed that “upland and riparian zones responded to rainfall events almost independently and differently”. The riparian zone responded faster to rainfall events due to its high antecedent wetness and shallow soils. The upland zone, due to the drier antecedent wetness and deep soils, experienced a significant delay in the generation of a saturated zone. The shallow groundwater systems along the hillslope enabled down-slope transport of fresh water and NO₃ that had previously accumulated in the upland zone because of the direct hydrological connection between the two zones. Related to this connectivity was a sharp increase in hydraulic gradient that drove shallow subsurface flow in the stream. These results are vital for the modelling of runoff generation and nutrient export at the catchment scale.

Many hydrological models presume that the groundwater table is connected all the way up the hillslope and that the hydraulic gradient is the same as the local gradient of the land surface. This assumption is not correct; to adequately model the development and persistence of the shallow groundwater system we need to explicitly track the time varying hydraulic gradient. A consistent model should show how the hydrological connectivity is established and how it changes in time. It must not only acknowledge the presence of the upland and riparian zones as sources and sinks of NO₃ respectively, but illustrate the key role of antecedent conditions and the thresholds needed to exceed before hydraulic connection can be established.

Detty and McGuire (2010) employed a spatially distributed instrument network designed to represent several topographically defined landform features of a glaciated till mantled catchment and monitored shallow water tables and soil volumetric water content for three seasons. The research was intended to investigate how, when, and where shallow water tables develop and describe the resulting hydrologic connectivity between the various components of the catchment. The hydrologic connectivity between riparian and hillslope areas displayed a strong seasonal signature. The results suggested that much of the catchment was hydrologically disconnected from the channel network during the growing season, while most

of the catchment was continuously connected to the channel network during the dormant season. The largest events in the dormant season allowed shallow transient water tables to develop even at the driest sites and hence nearly the entire catchment could be briefly connected to the stream channel during these events. The seasonal variations in hydrologic connectivity reflected the effects of climate and evapotranspiration on soil moisture storages and shallow groundwater development. These results have implications in modelling sub-surface stormflow, runoff generation and the seasonal or event-based transport of solutes from uplands to streams.

CHAPTER FOUR

4 METHODOLOGY

Chapter 4 reports on the methodologies used to achieve the objectives of the study. Initially a nested catchment monitoring layout is specified which takes into consideration scale issues from local, field to catchment levels. Materials and methods used to aid in collection of observed data at plot, field and catchment scales are also given. The various laboratory procedures and analysis that were used to sample nutrients, sediments and isotopes is elaborated. The development of a modified *ACRU-NPS* model is presented with the envisioned incorporation of the connectivity concept into the model. This makes it possible to study hydrological connectivity between land segments and the linked control structures (in this case buffers, wetlands and dams). This approach takes into account the runoff, NO₃, P and SS exchanges between the land segments and river channel together with their fate on entering and leaving buffers, wetlands and dams.

4.1 Nested Catchment Monitoring, Materials and Methods

A sampling and survey strategy was developed in the Mkabela Catchment where key features of the strategy included automatic sampling during rainfall events which occurred often in summer (October to March) and occasionally in winter (April to August) from field to large catchment scale in a nested system of sub-catchments (Figure 4.1). Storm events were defined as periods of major rainfall separated by at least 24 h of rainfall intensities averaging less than 0.1 mm/h (Wenninger *et al.*, 2008). The automatic samplers were programmed such that more samples were collected at the flumes during high flows and fewer samples during low flows (Kollongei and Lorentz, 2014).

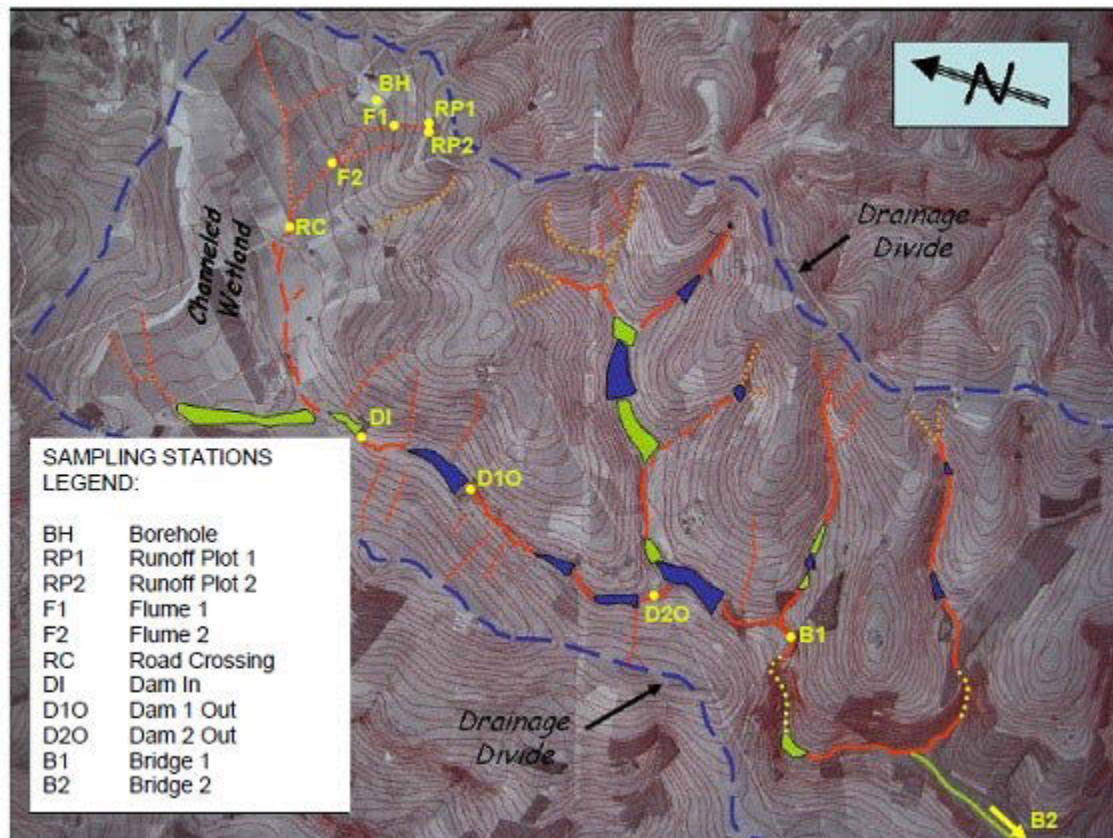


Figure 4.1: The nested Mkabela Catchment showing instrumentation and sampling points at the Wartburg research site (Lorentz et al., 2011).

The automatic recording meteorological weather station installed in the headwaters of Mkabela research catchment shown in Figure 4.2 comprises the following instruments:

- CR 200 Campbell Scientific data logger
- RM Young wind sentry anemometer - model 03101
- Vaisala Temperature/ RH probe - HMP 50-L
- Texas Electronic Rain gauge - TES25 mm-L
- Apogee Silicon Pyranometer sensor.

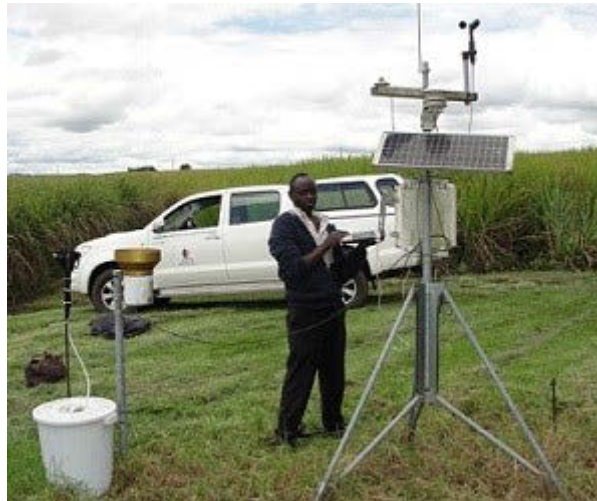


Figure 4.2: Downloading weather data from the automatic weather station located near Wartburg, Mkabela Catchment, KwaZulu-Natal.

Other additional materials and methods used to aid in the collection of observed data at plot, field and catchment scales included:

- Metallic flow isolators, collector troughs and baffle tanks for runoff plots.
- Tipping buckets, event data loggers and manual counters used in runoff plots.
- Watermark sensors for automatic recording of soil water tensions at various depths in soil horizons.
- Pressure transducers for river gauging.
- Constructed H-Flumes and ISCO samplers for discharge measurement and WQ sampling, respectively.
- Liquid-Water Isotope Laser Analyser for determination of $\delta^{18}\text{O}$ and $\delta^2\text{H}$ isotopes in water samples collected from various locations in the catchment.
- Manta-2 WQ (water quality) instrument with ion, pH and EC probes for in-situ water quality detection.
- Geophysical surveys using ERT (Electrical Resistivity Tomography) techniques.
- Laboratory methods for sediment and water quality analysis.

4.1.1 Local scale

Local scale monitoring was conducted on two runoff plots (RP1 and RP2) and included the measurement of discharge rates of overland flow on an event basis in the sugar cane fields located in the upper part of the catchment. 1/10th of the overland flow from each plot was

routed into a container for subsequent sampling of sediments and nutrients (Figure 4.3 *left*). Borehole samples were also collected and tested for nutrients (NO_3 and P) and suspended solids (SS) (Figure 4.3 *right*).



Figure 4.3: Downloading data from runoff plot (left) and drawing groundwater from borehole using a bailer (right).

Two-D surveys conducted using ERT equipment were also obtained to assist in the hydrological characterization of the catchment and were used in a reconnaissance fashion to assist in the interpretation of hydrological processes (Figure 4.4). The surveys were performed during late winter (dry season, March–October/November) period of 2009/2010 as soil moisture contents were at their minimum and therefore variability in electrical resistivity measurements were assumed to have been minimally affected.



Figure 4.4: ABEM Terrameter used for 2-D Electrical Resistivity Tomography (ERT) (ABEM, 2005)

4.1.2 Field scale

Field scale observations were made at an H-flume where discharge was measured and samples automatically extracted for sediment and nutrient analysis. The upper flume consists of a constructed H-Flume with an ISCO sampler triggered by a specified flow volume, recorded by measuring the depth of flow using a pressure transducer. Multiple field or small catchment monitoring was accomplished downstream in a similar H-flume with the exception that the depth of flow in a stilling basin was measured via a float and pulley apparatus (Figure 4.5).



Figure 4.5: Taking in-situ readings using Manta-2 WQ instrument (left) and downloading data from CR 200 data logger (right) at the Lower H-flume.

Monitoring of the water levels and subsequent discharge was based on the principle of a piezometer, where the water level in interconnected columns would always be the same thus making it possible to monitor the water levels in the approach channel by recording the water levels in the stilling well through the use of a pressure transducer (Flume 1), float (Flume 2) and data logger mechanism (both). In Flume 2, the floater in the stilling well oscillates with the rise and fall of the water level in the approach channel and such movements are translated into rotational movements through a pulley system in a shaft encoder, which is linked to a CR 200 data logger. In Flume 1, the height recorded (m) by the pressure transducer results from dividing the pressure measured by the transducer (N/m^2) with specific weight of water (N/m^3) through equations entered into CR 200 data logger, hence converting pressure (N/m^2) into height (m).

The Mkabela Catchment H-flumes were equipped with ISCO samplers, with capacities of 24 sampling bottles of 500 ml each, and controlled by a CR 200 data logger. The number of samples and the sampling rate of the ISCO sampler were varied by the conditional parameters in the CR 200 data logger shown in Table 4.1. The sampling strategy in the Mkabela Catchment was to take infrequent samples during steady flows (low flows) and frequent samples during rapidly changing flows (events).

Table 4.1: Conditional parameters for the CR 200 data logger at the Mkabela H-Flumes

Parameter	Flume 1	Flume 2	Description
Vhf	100	1000	Cumulative flow volume for changing flow i.e. high flow volume threshold (m^3)
Vlf	300	6000	Cumulative flow volume for constant flow i.e. low flow volume threshold (m^3)
Delta <i>HR</i>	0.002	0.01	Elevation change (mm) for recording Q
Delta <i>HS</i>	0.10	0.10	Depth (m) for change in sampling flow volume calculation.
Delta <i>T</i>	5	5	Time interval for depth of flow recording (s)
Maximum samples	24	24	Maximum number of samples to be taken
Sampling head	3	3	Suction head (m)
Suction line	7	7	Total length of the suction line (m)
A1(0)	0	0	Polynomial variable
A1(1)	0.004	0.0013	Polynomial variable
A1(2)	0.59	1.747	Polynomial variable
A1(3)	0.012	0.062	Polynomial variable
A1(4)	0.71	0.2996	Polynomial variable

With reference to Table 4.1, Delta *HS* is used to establish if the flow is constant (low flows) or changing (high flows). If the change in flow rate is such that Delta *HS* is less than 0.10 m, then a sample will be taken after Vlf m^3 of flow has passed the H-flume. Alternatively, if the change in flow is such that Delta *HS* is greater than 0.10 m, as in runoff events, then the samples will be taken after Vhf m^3 of flow. The parameters Vhf, Vlf and Delta *HS* were derived through a calibration process, by simulating observed flow data while checking the sampling scheme of the data logger before adjusting the appropriate variables (Vhf, Vlf and

Delta *HS*). An example of the computer program written for the ISCO sampler that was used at Flume 1 is presented in Appendix A.

4.1.3 Catchment scale

Manual sampling and flow depth observations were periodically made at selected flow controls such as road crossings, wetlands, dams and bridges (Figure 4.6). These grab sampling stations were located at different positions in the catchment. This was done after every week during summer events (frequently) and less frequently after every fortnight during winter.



Figure 4.6: Dam 1 (left) and Bridge 1 (right) located at the middle sub-catchment of Mkabela where grab sampling was done.

In order to get an indication of the sources of water, sediments and nutrients from the headwaters to the catchment outlet, sampling events were conducted such that the complete stream network was sampled within a 2 hour period in certain instances. This sampling campaign called for comprehensive sampling throughout the catchment and during times when negligible precipitation had occurred in the preceding several days.

4.2 Laboratory Procedures and Analysis

Water quality parameters and stable isotopes of water, ^{18}O and ^2H , were determined for all the samples collected from the catchment headwaters to the outlet some 12 km downstream. Samples were collected from overland flow runoff plots (RP1 and RP2), from the flumes (Flume1 and Flume 2) located in the waterways in the sugarcane fields and at the grab sample sites named road crossing, Dam in, Dam1 Out, Dam2 Out, Bridge 1 and Bridge 2. All the collected water samples were analysed in the laboratory for NO_3 , soluble-P, suspended solids (SS) and isotopic composition of Oxygen-18 ($\delta^{18}\text{O}$) and Deuterium-2 ($\delta^2\text{H}$) within 1 day of collection from the field.

4.2.1 Field sampling and analyses for nutrients and sediments

Analyses of NO_3 and soluble-P were done with a HACH DR/2000 Direct Reading Spectrophotometer (Figure 4.7 *right*). The Spectrophotometer was calibrated against known solutions of KHPO_4 and KNO_3 and values for field concentrations of soluble-P and NO_3 read directly (Lorentz *et al.*, 2012). A Manta-2 WQ instrument with specific ion probes was used for in-situ detection of water quality parameters that included turbidity, $\text{NO}_3\text{-N}$, $\text{NH}_4\text{-N}$, specific conductivity, pH, ORP, temperature and chlorides during every site visits (Figure 4.7 *left*).



Figure 4.7: Taking readings using Manta2 (left) and HACH DR/2000 field test kit (right) at a field station.

In the laboratory, 200ml or 100ml of sample was shaken thoroughly and 5ml of hydrochloric acid added to promote the flocculation of the suspended solids. To allow complete settlement

of suspended solids, the mixtures were left overnight. After the sediments settled, the supernatant water was discarded carefully. The remaining wet sediments were oven dried overnight at 105°C. The sediment concentration was then determined as the dry mass of sediments divided by the volume of sample (Lorentz *et al.*, 2012).

4.2.2 Field sampling and analyses for stable water isotopes

The water samples collected from sampling stations were analysed for stable $\delta^{18}\text{O}$ and $\delta^2\text{H}$ isotopes of water using the Liquid-Water Isotope Laser Analyser (LGR, 2007) at the former School of Bio-resources Engineering and Environmental Hydrology (SBEEH) of the University of KwaZulu-Natal (UKZN) (Figure 4.8).



Figure 4.8: DLT-100 Liquid-Water Isotope Laser Analyser (LGR, 2007)

Isotope data were post-processed using LGR LWIA Post Analysis Software and were reported as per mil (‰) $\delta^{18}\text{O}/\delta^{16}\text{O}$ relative to Vienna Standard Mean Ocean Water (VSMOW). Isotope values were compared across sites, water storage impoundments and with the Global Meteoric Water Line (GMWL). The co-variance between $\delta^{18}\text{O}$ and $\delta^{16}\text{O}$ given as GMWL was defined as by Craig (1961).

The mass balance (Equation 4.1) and mixing equations (Equation 4.2) can be used to separate the storm hydrograph into event (rainfall/surface runoff) and pre-event (subsurface water) components (Buttle, 1998):

$$Q_t = Q_o + Q_e \quad (4.1)$$

$$Q_t.C_t = Q_o.C_o + Q_e.C_e \quad (4.2)$$

where: Q is discharge rate,
C is the isotopic ratio,
suffix *t*, *o* and *e* are the total runoff water, the pre-event water and the event water components, respectively.

By combining Equations 4.1 and 4.2, then Equation 4.3 is given below:

$$\frac{Q_o}{Q_t} = \frac{C_t - C_e}{C_p - C_e} \quad (4.3)$$

Therefore, the ratio of pre-event water component to the total runoff rate is estimated by observing runoff rate, and isotopic compositions of stream water, rainfall water and subsurface water. To use this method, the following conditions should be satisfied (Sklash and Farvolden, 1979):

1. The isotopic ratio of the event component is significantly different from that of the pre-event component.
2. The event component maintains a consistent isotopic ratio.
3. The groundwater and soil water are isotopically equivalent or soil water contributions to runoff are negligible due to hydrogeologic constraints.
4. Surface storage contributes minimally to the runoff event.

A simple mass balance mixing model was developed using the $\delta^{18}\text{O}$ values with the end members as the combined discharge from the impounded tributaries (Q_{DO}); the contribution to stream flow of the land unit between the impoundments and the Bridge stations (Q_{LUi}) and the Bridge station discharge (Q_{B1} and Q_{B2}).

For the discharge at the first bridge station, this takes the form given in Equation 4.4 below:

$$Q_{B1} \cdot \delta_{B1} = Q_{DO} \cdot \delta_{DO} + Q_{LU1} \cdot \delta_{LU1} \quad (4.4)$$

where: δ_{B1} = $\delta^{18}\text{O}$ value at the Bridge 1 station (Figure 4.1),
 δ_{DO} = $\delta^{18}\text{O}$ value for discharge from both impounded tributaries and
 δ_{LU1} = $\delta^{18}\text{O}$ value for discharge from the sub-catchment (3.6 km²) between the
most downstream reservoir and the Bridge 1 station.

Recognizing that $Q_{B1} = Q_{DO} + Q_{LU1}$, the ratio of discharge from the contributing sub-catchment to the total discharge at the Bridge station, can be expressed as a function of the isotope ratios as in Equation 4.5:

$$\frac{Q_{LU1}}{Q_{B1}} = \frac{\delta_{B1} - \delta_{DO}}{\delta_{LU1} - \delta_{DO}} \quad (4.5)$$

It was assumed that the eastern, impounded tributary, upstream of Bridge 1, yielded a similar evaporated isotope signal as that in the discharge from the Dam Out stations. The isotope values of the contributing land units between the reservoir outlets and the Bridge stations were also assumed to be similar to the Flume 2 values.

4.3 Development of the modified *ACRU-NPS* model

The research involved the development of algorithms for inclusion in simulation models to allow for the NPS pollution dynamics in hydrological processes response zones and control features. The *ACRU-NPS* model was modified to simulate source-pathway-fate of nutrients and sediments from land segments for various land uses (hydrological processes response zones) to include travel pathways and the effects of control features such as wetlands, riparian buffer zones and impoundments. Schulze (1975) developed the *ACRU* model to simulate hydrological processes in the early 1970's at the University of Natal in South Africa. The model was based on FORTRAN 77 but was later updated to *ACRU2000*, an object-oriented JAVA based model where new processes could be easily added and documented in an organized manner (Kiker and Clark, 2001). *ACRU2000* has since advanced in hydrological, ecological, environmental and agricultural scope. The model simulates both field and catchment scale processes by either a cell-based or lumped parameter model. Figure

4.9 shows several process objects that describe water flows occurring at the surface (PSurfaceFlow), the subsurface (PSubSurfaceFlow), and at the groundwater (PGroundWaterFlow) level.

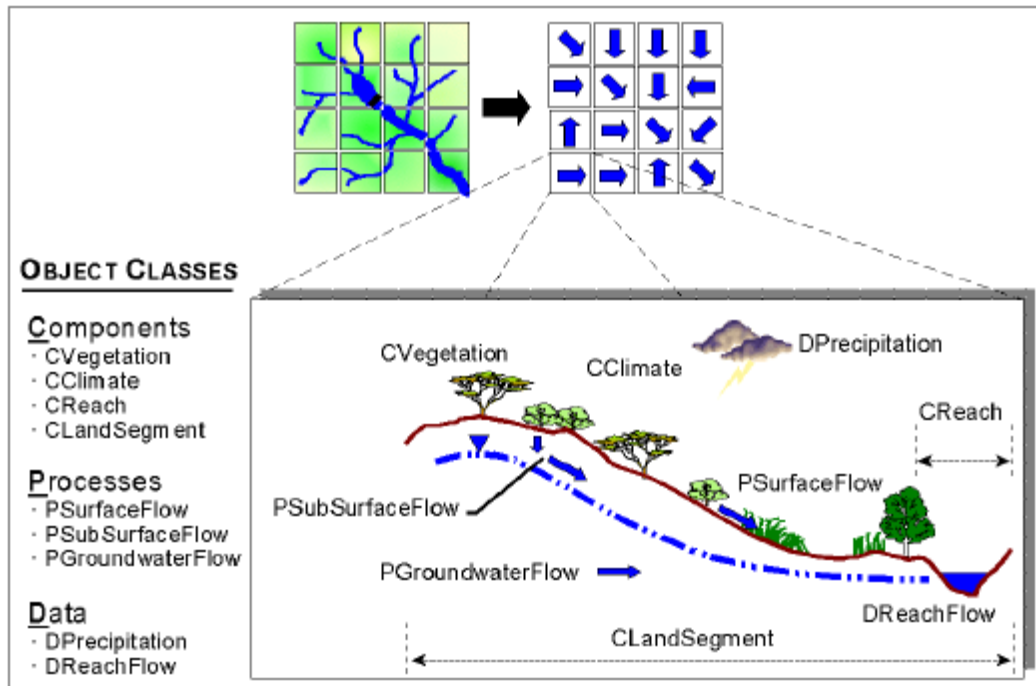


Figure 4.9: Examples of object classes in ACRU2000 (after Kiker and Clark, 2001)

Catchments are split into sub-catchments depending on spatial variability of land use, topography, precipitation or soil characteristics (Schulze, 1995). A sub-catchment area can range from 0.01 to 50 km² and can be easily connected to other sub-catchment objects via streamflow (Smithers and Schulze, 1995). The creation of the new Water Act (NWA, 1998) by the South African government motivated the addition of a water quality component into ACRU2000. The ACRU2000 already had a sediment yield component; hence the new nutrient yield component that was developed, *ACRU-NPS*, focused on nitrogen and phosphorous dynamics.

CHAPTER FIVE

5 CONNECTIVITY INFLUENCES ON NUTRIENT AND SEDIMENT MIGRATION IN THE MKABELA CATCHMENT

The Mkabela Catchment hydrological processes response zones and connectivity processes exhibited are discussed. This includes among others delineation, characterization and mapping of hydrological processes response zones. To understand nutrient and sediment migration in the sub-surface, hillslopes hydrogeology transects were conceptualised and geophysical techniques used to grasp soil water dynamics and nutrient processes.

5.1 Mkabela Hydrological Processes Response Zones and Connectivity Processes

Hydrological processes response zones are areas identified within the catchment that mostly influence pollutant load contribution to both surface and sub-surface water. This includes the hillslopes, valleys, ditches and channels, wetlands etc. They are important when proposing relevant sediment and nutrient loss mitigation strategies within agro-systems. The hydrological processes response zones exhibit specific traits with regards to geomorphic processes (including erosion and deposition) and its hydrologic roles as sources or sinks to pollutant movement. At the agricultural catchment scale, a hydrological processes response zone requires assessing the hydrological connectivity between contributing landforms and the stream network. Landforms can be disconnected from the hydrological network if landscape controls such as hedges block or limit the runoff generated. On the contrary hydraulic controls such as ditches or road network can facilitate the runoff from upstream to downstream areas and hence increase the potential of pollution downstream (Payraudeau *et al.*, 2009).

5.1.1 Hydrological processes response zones and connectivity

The connectivity of the river (drainage) network in the Mkabela Catchment was assessed on a sub-catchment basis and was linked to in-stream controls that included farm dams, wetlands and buffer zones where the fate and transport of dissolved N and P, sediment and associated adsorbed P were studied. The term connectivity in this context is used to describe the extent to which sediments, adsorbed and dissolved pollutants generated on hillslopes (i.e. in the sub-

catchments) is connected to a channel by overland and subsurface flow, as well as the linkage of streamflow and sediment within a channel network (Hooke, 2003; Lesschen *et al.*, 2009; Medeiros *et al.*, 2010). Good vegetation cover in most cases reduces connectivity from hillslopes to channels (Hooke, 2003), whereas different sinks reduce connectivity within channels ranging from partial retention in small wetlands (Hatterman *et al.*, 2006) to even full blocking in large reservoirs (Medeiros *et al.*, 2010).

At the catchment-scale, connectivity aspects are driven by complex physical processes that involve interaction of a large number of spatial and temporal factors that are difficult to monitor directly and model (Bracken and Croke, 2007). An example is modelling changes in channel characteristics and catchment morphology as a single unit. Miller *et al.* (2013) subdivided the Mkabela Catchment into three distinct sub-catchments that differed in their ability to transport and store sediment along the axial valley (Figure 5.1). The current study however defines connective units differently by considering many sub-catchments that differ in land-use, soil type and slope. These sub-catchments are also linked differently to wetlands, buffers and dam controls hence influencing the connectivity of the NPS pollutants and their movement within the Mkabela Catchment. The reach process zones (Figure 5.1 and Table 5.1) defined by Miller *et al.* (2013), to some degree, describes basic hydrologic functions that include 1) magnitude, spatial and temporal continuity of surface water flow, and 2) surface water interaction with subsurface water.

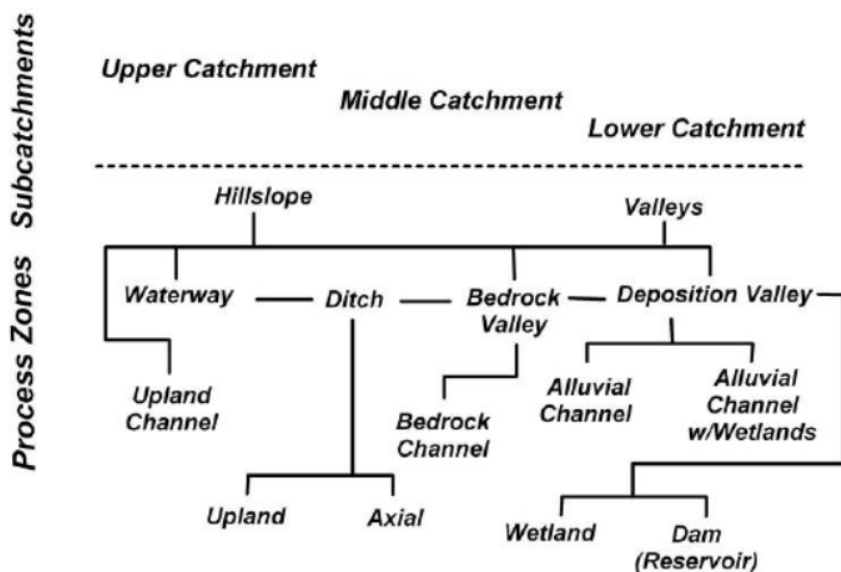


Figure 5.1: Classification of reach process zones in the Mkabela Catchment (Lorentz *et al.*, 2011; Miller *et al.*, 2013).

The general characteristics of the reach process zones in the Mkabela Catchment are presented in Table 5.1.

Table 5.1: Summary of reach process zones and their general characteristics (Lorentz et al., 2011; Miller et al., 2013).

Reach Zones	Process	Character	Dominant Process
Waterways		<ul style="list-style-type: none"> • Man-made, typically in upland areas • Slope parallel • Wide, shallow channel • V. little sediment storage • Grass covered channel bed 	<ul style="list-style-type: none"> • Sediment transport over “rough” bed • Predominantly a zone of recharge
Ditch		<ul style="list-style-type: none"> • Man-made, trapezoidal channel • Valley parallel, slope perpendicular (axial), slope Parallel (upland) • Relatively low gradient • Channel bed - sediment 	<ul style="list-style-type: none"> • Sediment transport through low gradient, but efficient channel • Recharge zone
Wetland Valley (with channel)		<ul style="list-style-type: none"> • Natural, flat-lying alluvial & lacustrine fill • Wide valley • May or may not exhibit through flowing channel 	<ul style="list-style-type: none"> • Sediment deposition & storage • Groundwater discharge
Alluviated Valley (with riparian wetlands)		<ul style="list-style-type: none"> • “Natural” flat, alluvial valley floor of varying width • Narrow, deep channel form • May or may not be bordered by riparian wetlands 	<ul style="list-style-type: none"> • Sediment transport through channel • Sediment storage on floodplain • Dominated by groundwater discharge
Bedrock Channel		<ul style="list-style-type: none"> • Narrow, bedrock controlled valley • Steep channel, with multiple knick-points present • V. little sediment storage 	<ul style="list-style-type: none"> • Sediment transport through highly competent channel

Figure 5.2 shows that the natural drainage density, calculated at 1.05 km/km², is extremely low, and is rivalled by the density of roads within the catchment. Stream lengths are frequently expressed as km of channel per km² of drainage area. This ratio is termed as the drainage density of a catchment. It is computed by extending the drainage network on shown topographic sheet to the termination of V-shaped crenulations in contours.

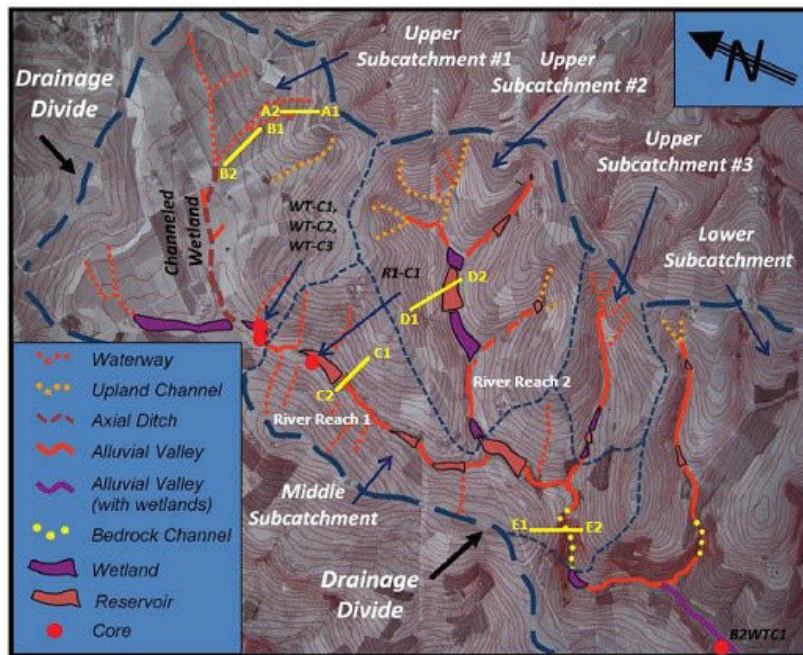


Figure 5.2: Reach process zones and sub-catchment areas within the upper and middle sub-catchments showing the locations of stream and hydro-pedological transects in the Mkabela Catchment (after Miller *et al.*, 2013).

The drainage network in Mkabela Catchment is characterized by a common downstream sequence of hydrological processes response zones. Headwater areas, particularly within the sugarcane fields, typically possess waterways that deliver water and sediment to upland channels. The drainage density in the sugarcane fields is approximately 2.5 km/km². The upland channels then feed water, sediment (and associated nutrients) to alluvial valley segments, or axial ditches. Many of the upland channels along the south side of the catchment are short, draining relatively small areas, and are disconnected geomorphically from the axial valley, suggesting that they deliver relatively minor amounts of sediment to the axial channel in comparison to northern and headwater drainages.

5.1.2 Hillslope hydro-pedological transects

Hydro-pedology relates soils to hydrology. It is an emerging field formed from intertwining branches of soil science and hydrology where focus is on the interface between hydrosphere and pedosphere. Bouma *et al.* (2011) explored the potential of hydro-pedology in characterizing the dynamic behaviour of soil water regimes at different scales in space and time in context of catchment hydrology. Since specific soil properties are captured in different genetic soil horizons, soil properties and their spatial distribution can serve as indications of hydrological behaviour (Van Tol *et al.*, 2012). Consequently, hydro-pedological

classification transforms pedogenetic knowledge of geochemical and hydrological relationships, embedded in soil properties, to hydrological information that is useful for classifying soils. The pedological classification of horizons with their hydrological behaviour can be converted to hydrological functional units based on their hydrological responses (Van Tol *et al.*, 2012). These functional units therefore describe the hydrological behaviour of a specific soil horizon. Van Tol *et al.* (2013) grouped hillslopes from all over South Africa into five hydrological soil types based on the interpretation of the dominant hydrological pathway. The results from the study can be used to select on-site sanitation limiting water pollution.

To comprehend water generating mechanisms based on hydropedological evidence, some cross-sectional and longitudinal transects were made from topographical and soil descriptions data for the various hillslope sections in the Mkabela Catchment. These sections were chosen from the cross-sectional transects of the different hillslope types. The longitudinal transects were extracted for the two main river reaches that meet at a junction and continue as an outlet reach. Table 5.2 shows the criteria for choosing the transect locations.

Table 5.2: Criteria for choosing cross-sectional and longitudinal transect points.

Transects	Hillslope Soil Type	Remarks
A1 – A2	Avalon	Runoff plots/Flume 1 waterway
B1 - B2	Avalon	Flume 2 waterway
C1 – C2	Glencoe	Alluvial valley
D1 – D2	Cartref	Wetland
E1 – E2	Hutton	Bedrock channel
River Reach 1	Glencoe, Hutton	Longitudinal profile
River Reach 2	Cartref , Hutton	Longitudinal profile

The hillslope soil types in Table 5.2 were obtained after surveying with a hydropedological survey technique as presented in Le Roux *et. al.* (2011). The technique involved the identification of representative hillslopes in the study area, augering observations along transects perpendicular to the slope, detailed descriptions, identification of horizons, taxonomic classification of the soil profiles, and recording of all soil features related to hydrology. The soil information gathered during the survey phase was interpreted and related to associate hydrological behaviour.

Transects in Table 5.2 were used to describe Mkabela hydropedology with an aim of estimating near surface discharges that would influence sub-surface migration of dissolved

nutrients in the sugarcane fields. The interpreted hydrogeological surveys were used to generate the figures in the sections below. Though the figures were not drawn to scale, the variations in their layering were based on available information from the extensive soil survey done in the Mkabela Catchment (Le Roux et al., 2006). The surface topographies were however accurate as they were based on distinct contours that were mapped on 2007 georectified SPOT images, with the aid of stereoscopic viewing of 2004, 1 : 10 000 aerial photographs (Miller et al., 2013).

5.1.2.1 Transects on Avalon hillslopes (A1-A2 and B1-B2)

Transects A1-B2 occur along hillslopes northeast and northwest of the catchment. They are characterised by the Avalon soil form characterized by an orthic A horizon over a yellow-brown apedal B horizon over a soft plinthic B horizon (Figure 5.3). The sandy nature of the soils allows for the easy infiltration of rain water, while the soft plinthic horizon acts as the aquitard supporting the perched water table. This is a typical plinthic hydrosequence with a decreasing degree of drainage downslope. For the largest part of the hillslopes, soft plinthic B horizons are underlain by hard plinthic horizons and the hard plinthic horizons have large pipes of soil material connecting the solum with the saprolite (Le Roux *et al.*, 2006).

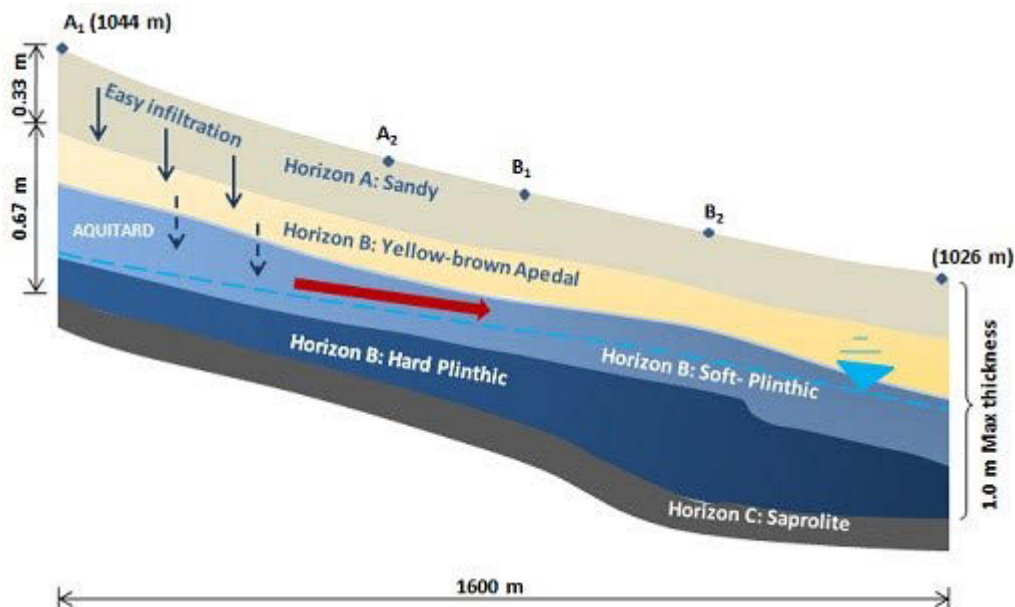


Figure 5.3: Upper sub-catchment transects showing the soil profile in the Avalon hillslope.

The Avalon soils are moderately drained with slopes ranging from 2-7 %. The relative flat slope supports a low interflow component of which most of the water moves in the intermediate vadose zone. According to Le Roux *et al.* (2006), the morphological character of these soils implies that the material underlying this hillslope is impermeable. Drainage is therefore dependent on lateral movement only. The perched water table forms in the subsoil when the rainfall exceeds evapotranspiration on a daily basis and the hydrological behaviour of this hillslope is expected to result in accumulation of water during the rainy season followed by lateral drainage in the saprolite and soft plinthic horizons. The water table sits below and in the soft plinthic B horizon of the Avalon soils for significant periods during the peak rainy season. Increase in wetness is expected as water moves downslope towards the Avalon B area.

During very wet spells lateral drainage is also expected to occur in the sandy yellow-brown apedal B horizon. The time it takes to form a water table will depend on the rainfall. The soil profile can hold a large amount of water before water tables forms. The water table periodically rises into the yellow-brown apedal B horizon and may occur there for one to four months on average in the rainy season. The water draining from the Avalon soils feeds the water table of the Katspruit soils lying down slope.

5.1.2.2 Transects on Glencoe hillslopes (C1- C2)

The Glencoe hillslope is steeper than the Avalon hillslope with slopes ranging from 4-15 % (Figure 5.4). Its soil horizons can extend to maximum depths of 0.9 m. According to Le Roux *et al.* (2006) the hydrological behaviour of the Glencoe hillslope is expected to be similar to that of the Avalon hillslope except for the effect of the steeper slope and higher relief.

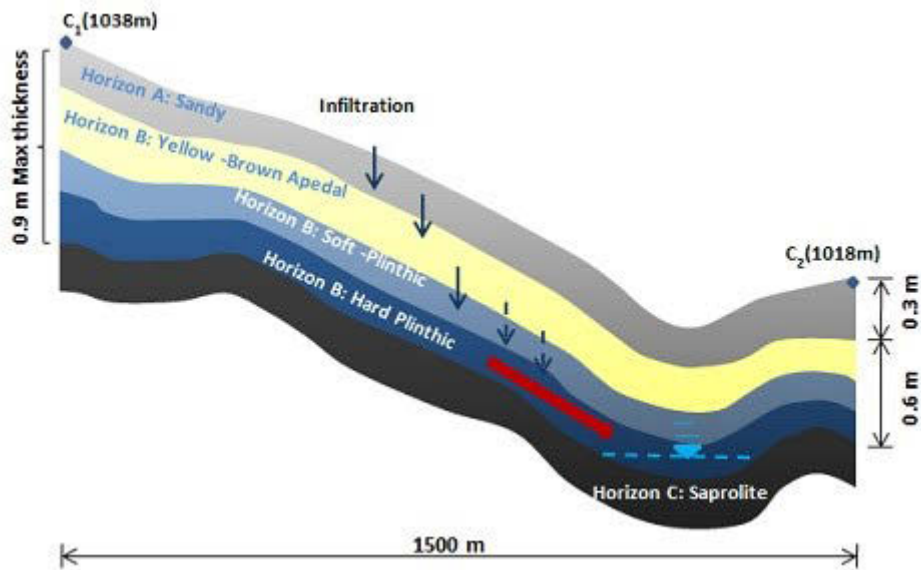


Figure 5.4: Middle sub-catchment transects C1-C2 showing the soil profile in the Glencoe hillslope.

The occurrence of a hard plinthic horizon on steep slopes requires a special environmental setup and iron rich parent material or special hydrology can explain it. The hard plinthic subsoils are matured plinthic horizons and may be an indication that the redox process is more intense compared to the Avalon hillslope. Significant water supplied by the crest feeding the Glencoe soils in the hillslopes create a water table under the hard plinthic B horizon (Figure 5.4) which may occur for some significant duration in the rainy season.

5.1.2.3 Transects on Cartref hillslopes (D1- D2)

Cartref hillslopes exhibit steep, short, convex slopes near the ridges that are combined with an undulating planform shape (Figure 5.5). The slope ranges from 4-15 %. The underlying material is Natal Group sandstone while the soils under these transects are shallow and sandy with very low water holding capacity (Le Roux *et al.*, 2006). It has a relief of 60 m.

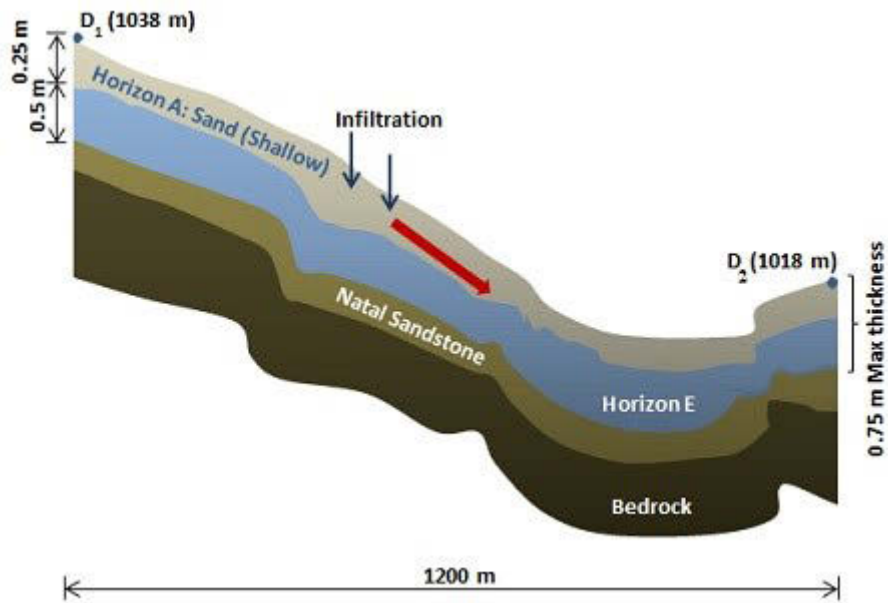


Figure 5.5: Middle sub-catchment transects D1-D2 showing the soil profile in Cartref hillslope.

The hydrology of the Cartref area (D) is characterized by an infiltration excess component as the shallow soils saturate quickly. The E horizon indicates a significant interflow component although for relative short periods.

5.1.2.4 Transects on Hutton hillslopes (E1-E2)

The Hutton hillslope has the highest relief (120 m) and occurs in the steepest sloping area with some parts of the slope exceeding 20 % (Figure 5.6). Transect E1 –E2 has a slope ranging between 7-20 %. According to Le Roux *et al.* (2006) shallow Glenrosa soils occur on steep slopes, whereas deep well drained Hutton soils occur on the more gentle slopes of the crest and midslope.

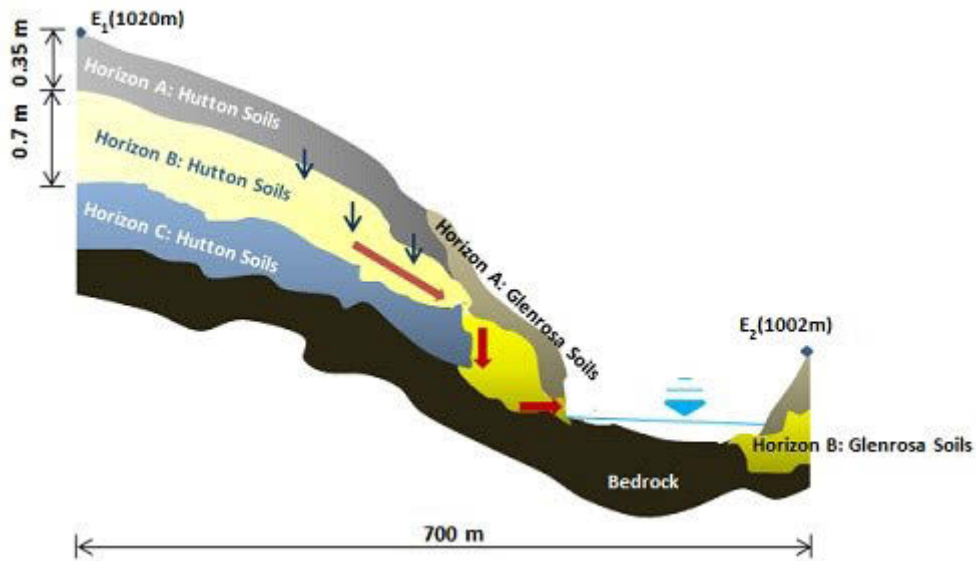


Figure 5.6: Lower Sub-catchment transects E1-E2 showing soil profile in Hutton hillslope.

The underlying material is Natal Group sandstone. The Hutton soils are deep and well drained with moderate water holding capacity while Glenrosa soils have very low water holding capacity.

5.1.2.5 Longitudinal transects along the river reaches

Longitudinal profiles record downstream changes in elevation, and hence slope, along a river course. Overlaying longitudinal profiles from different sub-catchments can be used to assess the topographic nature of area draining into each section of the river course and to compare downstream changes in slope and discharge. It also defines the relative contributions from different parts of the catchment, and provides a quick, visual overview of changes in catchment area (and hence discharges) at tributary confluences.

Figures 5.7 and 5.8 show longitudinal transects performed in the catchment. River reach 1 is longer and steeper than river reach 2. River reach 1 is on a slope with a relative straight planform curvature and little redistribution of water would occur. The main flux in River reach 1 is to the river (Figure 5.7). River reach 2 has convex planform curvature with the main flux to the tributaries (Figure 5.8).

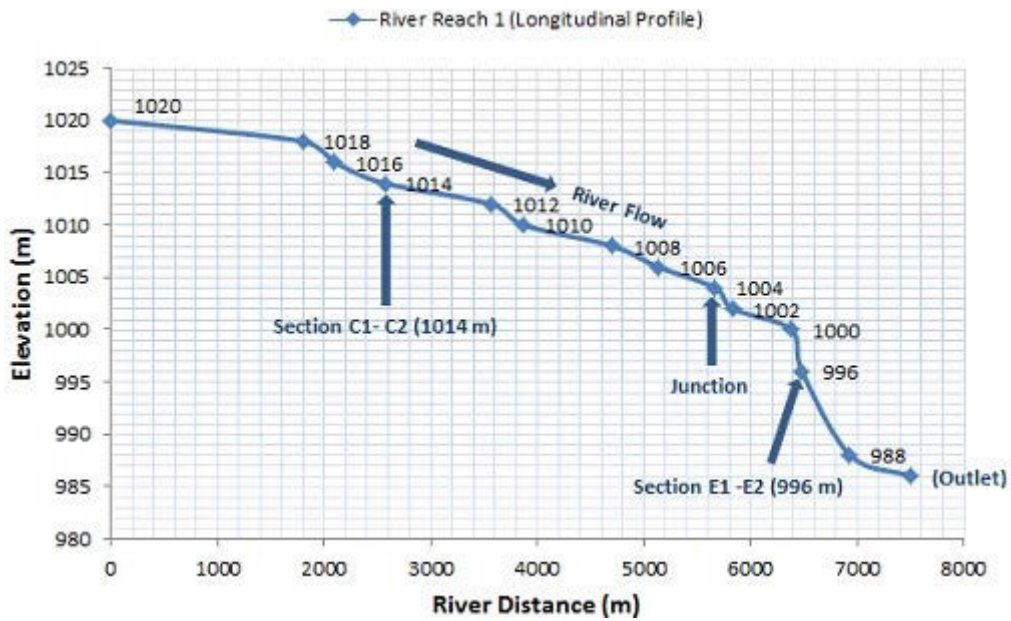


Figure 5.7: River Reach 1 longitudinal profile.

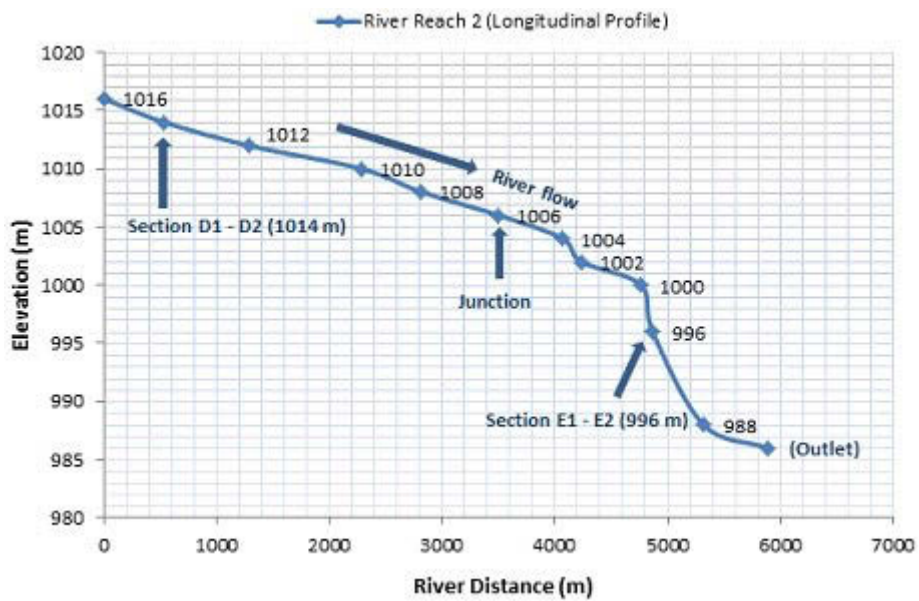


Figure 5.8: River Reach 2 longitudinal profile.

The location of transects C1-C2, D1-D2 and E1-E2 and river Reaches 1 and 2 is shown in Figure 5.2 (section 5.1.1).

5.1.3 Nutrient and sediment source connectivity and controls

Miller *et al.* (2013) combined provenance studies with data from geomorphic investigations to show that the Mkabela Catchment within the KwaZulu–Natal midlands could be

subdivided into three geomorphologically distinct sub-catchments. These sub-catchments vary in relief, the nature of their drainage network (or reach process zones) and their ability to store and transport sediment. Consequently, sediment transport and storage are characterized by spatially abrupt changes in their nature and magnitudes, but do not systematically vary along the axial drainage system (Miller *et al.*, 2013).

The capability of the hydrological processes response zones to transfer sediment and adsorbed nutrients, and their spatial distribution at the catchment scale indicates that the movement of material through the Mkabela Catchment is limited and discontinuous except, perhaps, during high magnitude runoff events (Lorentz *et al.*, 2011; Miller *et al.*, 2013). Sediment which is delivered to and transferred through waterways and upland channels on hillslopes will primarily be deposited downstream within wetlands and dams (reservoirs) during low- to moderate-floods. Thus, the upper catchment areas are characterized by a highly disconnected sediment transport system (Figure 5.9).

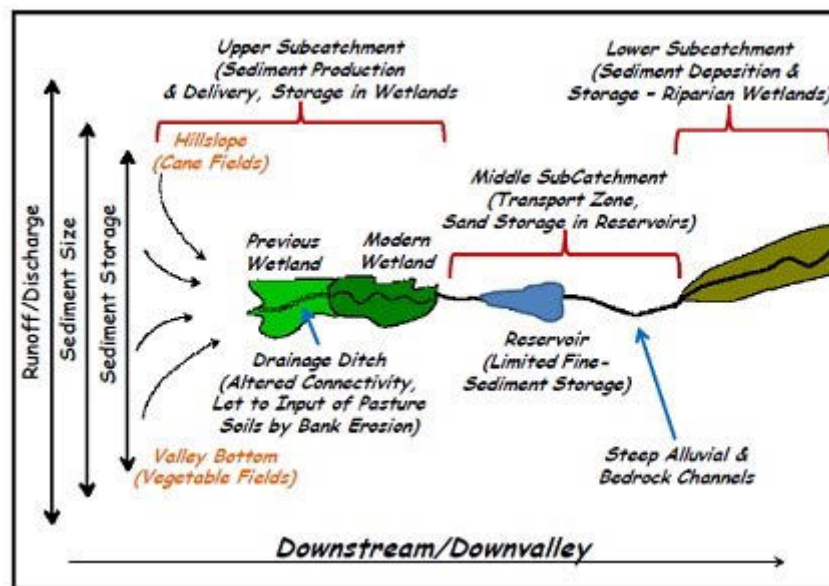


Figure 5.9: Schematic diagram of the primary processes occurring in each of the three delineated sub-catchments, and the variations in sediment size and source from varying runoff magnitudes (Miller *et al.*, 2013).

In headwater areas with intact valley floors, sediment eroded predominantly from low-lying areas during low-magnitude events are largely deposited within wetlands that comprise large segments of the valley floor (Miller *et al.*, 2013). The construction of the drainage ditch through the wetland appears to have negated some of the effectiveness of best management practices that are used on the cane fields to limit sediment and nutrient losses from the

hillslopes (Lorentz *et al.*, 2011; Miller *et al.*, 2013). Before valley modification there was a lack of fine sediment within the reservoir in general, suggesting that while the axial drainage network may be integrated during large floods, during low to moderate events, the upper catchment areas were disconnected from downstream sections of the catchment (Figure 5.10). Thus, the wetlands in their natural state serve as long-term sinks of sediment and associated nutrients.

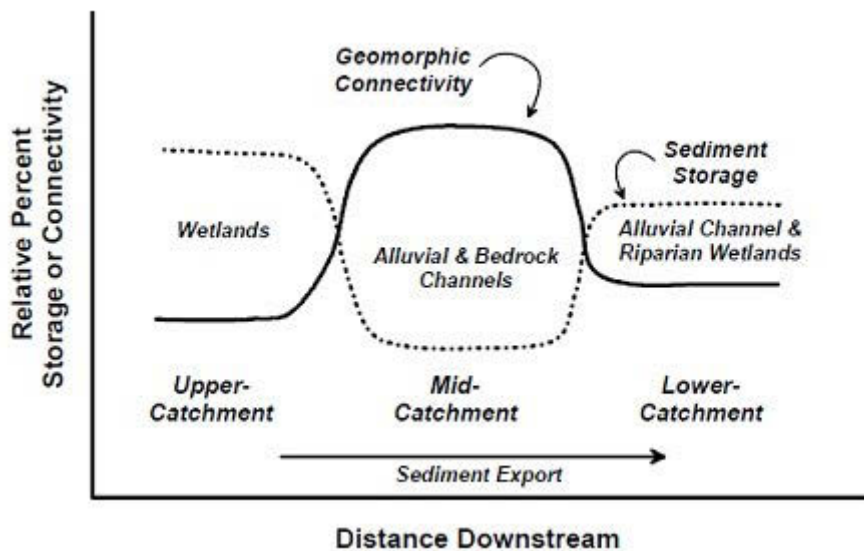


Figure 5.10: Sedimentological or geomorphic connectivity and sediment storage between sub-catchment zones of the Mkabela Catchment (Lorentz *et al.*, 2011; Miller *et al.*, 2013).

The mid-catchment areas are dominated by relatively high gradient alluvial and bedrock channels, with fewer, natural depositional zones (although dams now exist). Hence, the mid-catchment area possesses a greater ability to effectively transport sediment and adsorbed nutrients downstream, although a larger percentage of the transported sediment is likely to be stored along the more extensive valley bottoms (floodplains). The lower catchment is dominated by a low gradient, alluvial channel bordered by extensive riparian wetlands (Figure 5.10). The storage of sediment within this zone is extensive, once again limiting the downstream translation of sediment and nutrients that they may carry. The general lack of fine sediment within the reservoirs indicates that once silt- and clay-sized sediment is entrained, it is transported through this section of the catchment, although at least some of the transported material may be stored on or within floodplains that are more extensive than they are upstream (Miller *et al.*, 2013).

5.2 Plot Scale Geophysics, Soil Water and Nutrient Dynamics

The section below identifies the trends measured at the plot scale in greater detail. It attempts to identify the dominant processes and trends shown between different rainfall events. This was done through support of geophysics techniques and studying soil water dynamics and nutrient processes.

5.2.1 Geophysics

To characterize the hillslopes or hydrological processes response zones, Electrical Resistivity Tomography (ERT) studies resulted in five transects being done in the Mkabela headwater sub-catchment (Figure 5.11). According to Miller *et al.* (2013) reach process zones are reach-scale units representing a fundamental unit of watershed management. The ERT technique is a 2D electrical imaging system which is carried out using a large number of electrodes connected to a multi-core cable (Griffiths and Barker, 1993). In order to obtain a 2D electrical image, horizontal and vertical data coverage is achieved by automatic sequential measurements of current and potential locations.

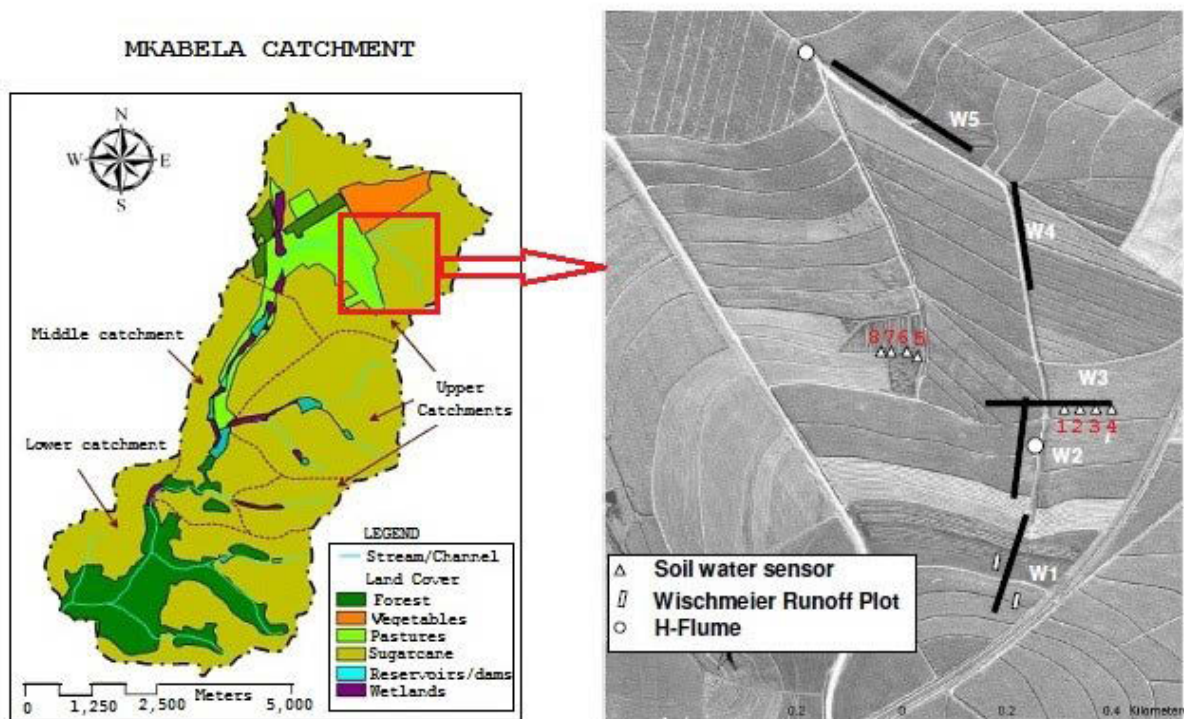


Figure 5.11: ERT transect locations in the upper Mkabela sub-catchment (Lorentz *et al.*, 2011).

ERT measurement is a geophysical method used to characterize the subsurface material (ABEM, 2005) and has gained popularity in hydrological sciences in the past decade due to its ability to profile the properties of the subsurface material and underlying features which influence subsurface hydrology, something which is quite challenging to achieve with classical catchment monitoring networks. Marti and Sabater (1996) identified that parent geology is related to the nutrient uptake within the riverine systems. In particular, Munn and Meyer (1990) found that the ratio of N to P largely determined the uptake of one or other nutrient: streams with a lower N: P ratio (e.g. volcanic parent geology) would have a higher uptake rate of N than P, while those of lower P availability (e.g. granitic parent geology) would show higher uptake of P than N. In other words limitation of a given nutrient would increase its uptake (Valett *et al.*, 1996).

Figure 5.12 displays the subsurface resistivity distribution in a NS direction obtained along the ERT survey W1. Presence of high soil moisture in the top layer that probably connects with a perched aquifer with very conductive material ($<100 \Omega\text{m}$) exists near the northern edge of the ERT transect at 6 m below ground level. Compared with hillslope hydrogeology transects shown in Section 5.1.2 above, the sandy nature of the soils allowed easy infiltration of rain water, while the soft plinthic horizon acted as the aquitard supporting the perched water table. Drainage was dependent on lateral movement only where an increase in wetness was expected as water moved downslope in a SN direction.

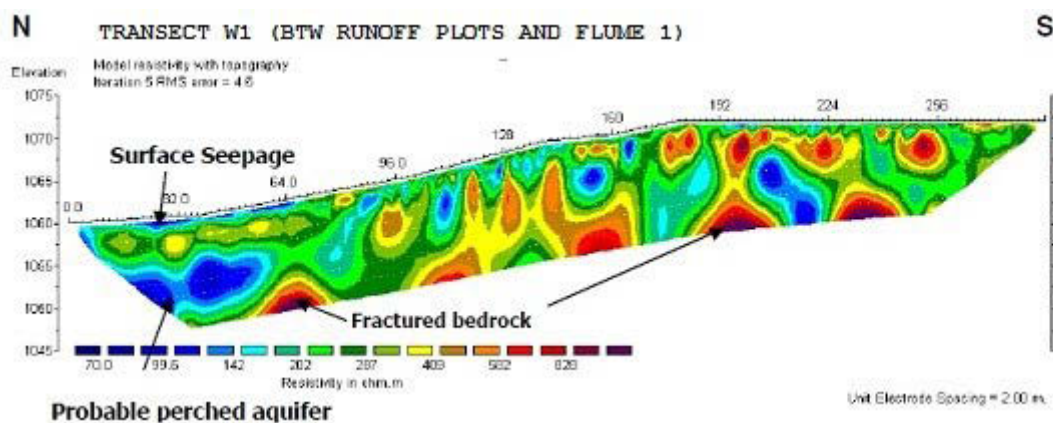


Figure 5.12: Transect W1 located between the Runoff Plots and Flume 1 (Lorentz *et al.*, 2011).

A shallow resistant unit (200-300 Ωm) overlies the perched aquifer and on the downstream end of the field water seepage can be seen on the ground surface. There appears to be a near surface water supply to the waterway as well as a deeper water body, which is likely the same

as that observed in the borehole (BH), located in the upper headwater catchment of Mkabela. This creates hydrologic connectivity where surface-subsurface water interaction occurs resulting in nutrients and sediment loads being exchanged. This is corroborated from isotope analyses of runoff water collected from runoff plots (RP1 and RP2) where similar isotope values to those obtained from the borehole (BH) occurred (Appendix K).

Resistivity measurements along transect W2 indicates a ~3m deep sandy and resistive layer (400–900 Ωm) at the middle of the transect overlying a weathered zone comprised of two shallow, perched water bodies (<100 Ωm), one along the northern side that is about 36 m long and 10 m thick and another south of the transect (Figure 5.13).

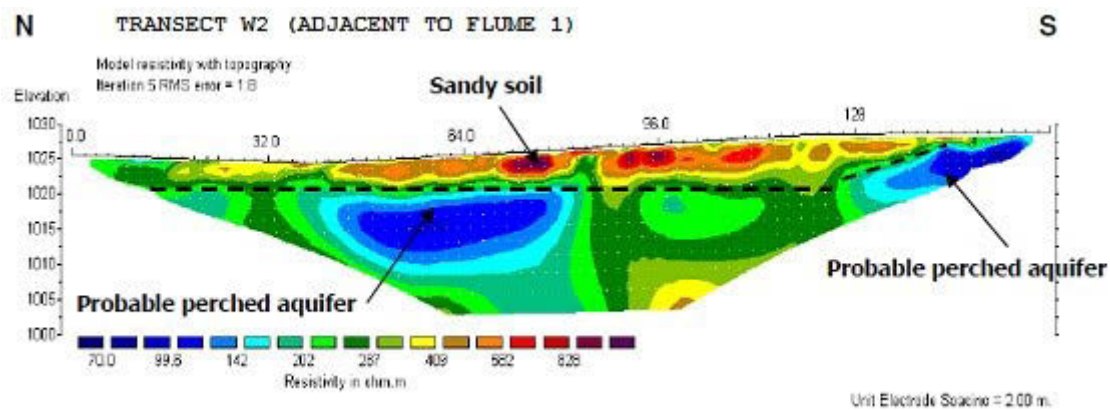


Figure 5.13: Transect W2 located adjacent to upstream Flume 1 (Lorentz et al., 2011).

These perched water bodies are responsible for holding pre-event water and allow nutrient loads to migrate from the subsurface to the surface where it becomes runoff on the waterway. This occurs during rainfall events and is demonstrated by a similarity in the analysed isotopes collected at Flume 1, specifically the isotope values in rainfall and borehole water. The hydrological behaviour of this hillslope as explained in Section 5.1.2 is expected to result in the accumulation of water during the rainy season followed by lateral drainage in the saprolite and soft plinthic horizons.

Transect W3 was located along watermarks 1, 2, 3 and 4 in the upper sub-catchment (Figure 5.11). The section traverses the waterway as indicated in Figure 5.14. A sandy layer (200-600 Ωm) covers both sides of the stream. It is underlain toward the west by a perched aquifer (<100 Ωm) at about 4 m depth. Immediately below surface of the waterway there exists unconsolidated and transported sediments (sands) (~290-300 Ωm) that overly deeper leached

fine clay deposits that have a lower resistivity (~140-200). At the eastern end of the transect, a very dry portion (>500 Ωm) is revealed.

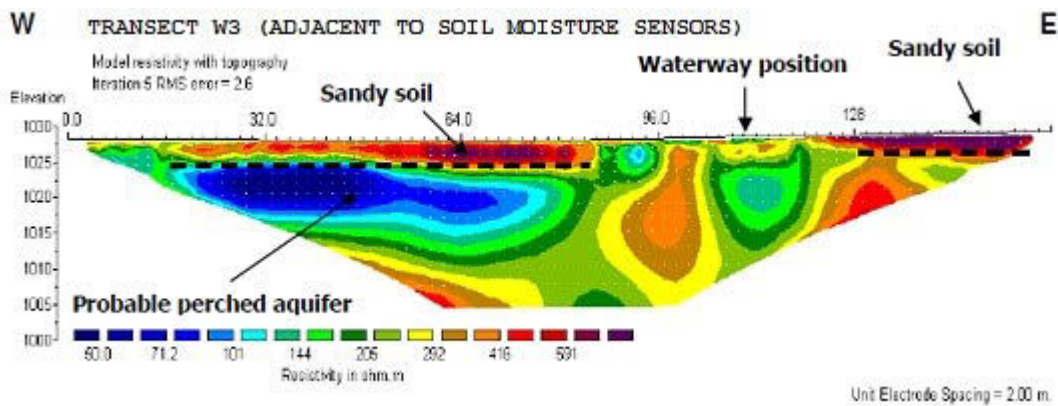


Figure 5.14: Transect W3 adjacent to the nests of soil moisture sensors (Lorentz et al., 2011).

From a hydrologic connectivity point of view, the unconsolidated sand layer on the surface of the waterway has less water retention capacity than the consolidated very fine clay deposit below it (waterway position, Figure 5.14). This means that during a rainfall event, even of low intensity, the thin sand layer on top of the waterway would be easily saturated as it is connected to the clay deposits below. Thus, runoff results much faster on the surface of the waterway than it would upslope of its traverse to the channel (Figure 5.14). At this juncture, much of the water contributed to the stream would be from the sub-surface (pre-event water). This is probably the reason why the seasonal time series data show that water samples collected from Flume 1 exhibit stable isotopic values similar to those in water from the borehole at the early stages of winter events (July-November). In contrast, isotope values in surface waters differ significantly from those in the borehole later in the year (November-March) as some values began to be similar to those from rainfall (Appendix K).

The resistivity section obtained along transect W4 exhibits three major layers including 3.7 m of sandy soil (200-600 Ωm), followed by groundwater bearing saprolite (<100 Ωm) with a water table located at approximately 4 m depth. Sandstone is located at a depth of 20 m depth (Figure 5.15).

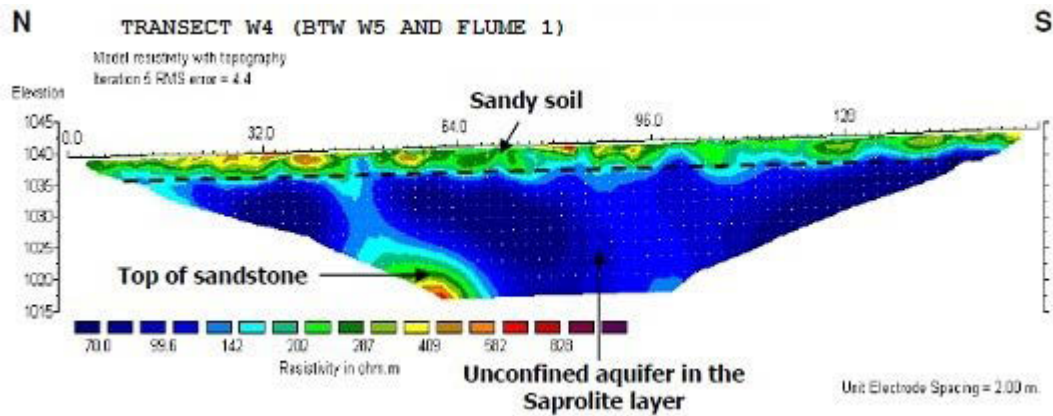


Figure 5.15: Transect W4 located between W5 and the upstream Flume 1 (Lorentz *et al.*, 2011).

The unconfined aquifer in the saprolite layer shown in Figure 5.15 can hold a large amount of water before a water table forms and may occur for one to four months on average during the rainy season (see Section 5.1.2 above). The ramification of this is that leached nutrients from excessive fertilizer applications may find their way to this groundwater source. Once in the groundwater the fertilizer may be hazardous to the environment for a long period because of the vast quantities of water present. It is difficult to clean-up a contaminated groundwater source once pollution occurs.

Transect W5, which is located adjacent to Flume 2, exhibits a conductive thin layer of soil (<70 Ωm) followed by a sandy soil horizon which thickens upslope. A perched aquifer (<100 Ωm) is located in the weathered zone as indicated on Figure 5.16. The bedrock which is fractured sandstone forms a resistive bottom layer (> 200 Ωm). It is located from 2 m to 12 m deep, increasing upslope. This interplay of geologies has important implications for the hydrological processes operating within this catchment, particularly since soil hydraulics will be influenced by the different soil textures and porosities associated with these different geologies (Riddell *et al.*, 2010). Transect W5 reveals the nature of sandy soils which overly deep leached fine clay deposits, which are confined by vertical weathered saprolitic protrusions from the underlying fractured Natal sandstone or bedrock. The significance of this observation is particularly important in the way the aquifer retains water. Further isotope analysis will reveal the nature of the groundwater recharge processes that these weathered zones facilitate within the confines of bedrock controls or fractured Natal sandstone.

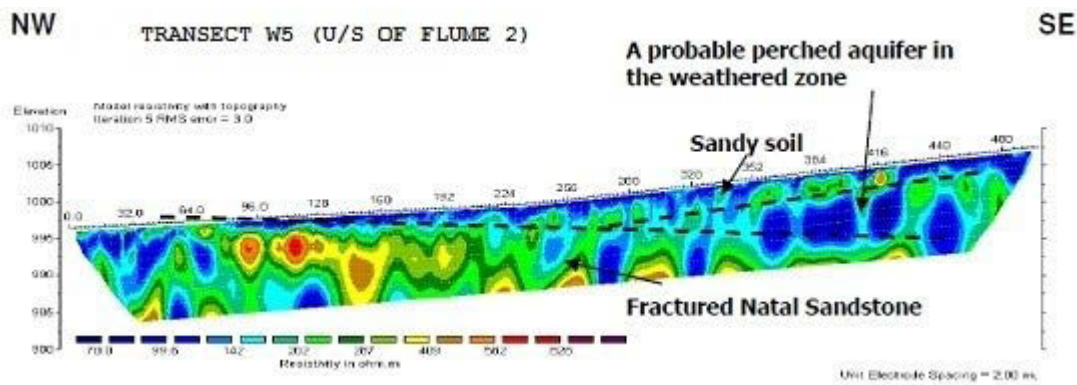


Figure 5.16: Transect W5 located immediately upstream of Flume 2 (Lorentz *et al.*, 2011).

5.2.2 Soil water and nutrient dynamics

Figure 5.17 shows rainfall events that occurred during the early summer (17th- 25th November 2011) in the Mkabela Catchment. Watermark Nest 1 (a soil water sensor) was located close to the waterway where 3 watermarks were positioned at different depths of 250 mm, 400 mm and 1000 mm below the ground surface. Before the rainfall events, the watermark at a depth of 1000 mm was the wettest of the three as indicated by a soil water tension of ~0 mm. The 250 mm-depth watermark exhibited a soil water tension of 1750 mm and was the driest, while the 400 mm-depth watermark had an intermediate soil water tension of ~500 mm. Upon an initial rainfall of 7.8 mm on the 19th November 2011, only the shallowest watermark (250 mm-depth) responded to a change in soil moisture; soil water tension was reduced from 1750 mm to ~750 mm (Figure 5.17). The 400 mm-depth watermark responded on 20th November 2011 (a day later), while the deepest watermark (1000 mm-depth) responded on 21st November 2011 after a 14.4 mm rainfall event.

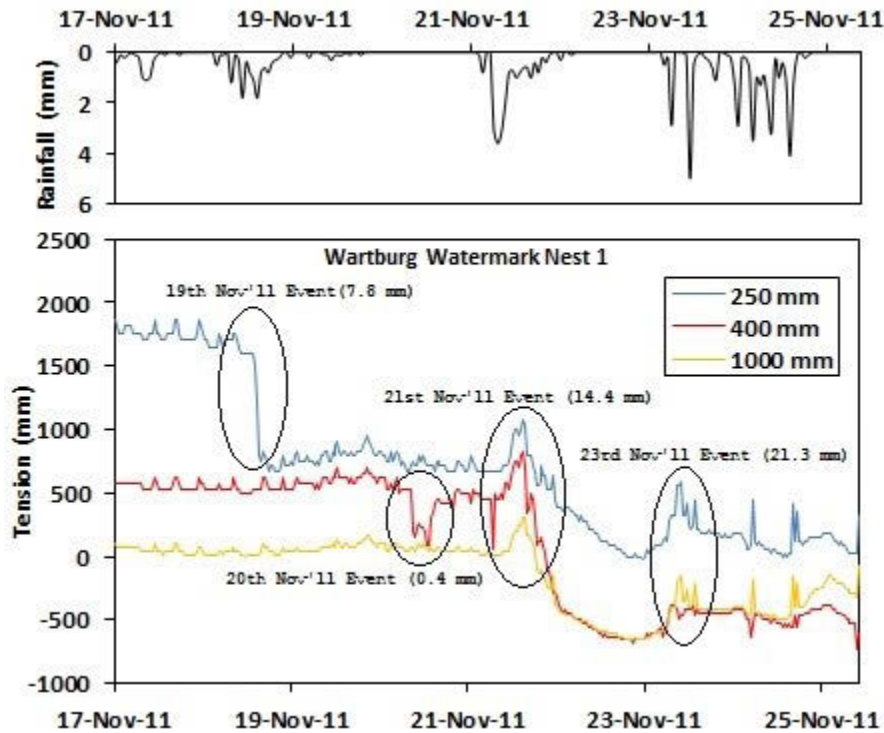


Figure 5.17: Soil water tension variation: Watermark Nest 1, from 17th – 25th Nov’11.

Interestingly all 3 watermarks responded at the same time on 21st November after an additional rainfall of 14.4 mm was added to the antecedent moisture content (AMC) in the soil. This meant that hydrological connectivity was complete all the way from the shallowest watermark (250 mm-depth) to the deepest watermark (1000 mm-depth). Soil moisture had infiltrated completely through the soil layers and connected the shallowest to the deepest watermark. A further 21.3 mm rainfall was added to the soil column after the event of 23rd November 2011, resulting in watermarks 2 (400 mm-depth) and 3 (1000 mm-depth) being fully saturated (negative soil tension). Watermark 1 (250 mm-depth) was just below the water table and exhibited a soil tension of 0.

Similarly dissolved nutrient migration in the soil column (i.e. NO_3 and soluble-P movement) is expected to follow the same trend as soil water. Initially the leached NO_3 and soluble-P should percolate through fissures or preferential flow lines in the soil, and would be expected to reach the shallowest watermark first and the deepest watermark last. Soil moisture and nutrient dynamics would be expected to behave in the same manner when discharge is observed at the flumes. It is only when complete connectivity of soil moisture has been achieved within the catchment that the flow volumes in the flume would be expected to

increase. It is also expected at this juncture that there would be elevated NO_3 and soluble-P loads when higher peak discharges are observed at the flumes.

Figure 5.18 shows the hydrologic responses to the additional soil water moisture during the summer rainfall events of 9th Feb- 17th Mar 2009 at Nest 3 and Nest 4. Only two watermarks at Nest 3 were operational; they were positioned at a depth of 250 mm and 1000 mm. At Nest 4, three watermarks were located at depths of 200 mm, 400 mm and 1000 mm. From the ERT survey, these two nests were located away from the waterway with watermark Nest 4 being the furthest, where sandy soils were present. ERT images in Figure 5.14 had shown these sandy soils to be very dry. The thin layer of sand in Nest 3 holds very little water which is reflected by very high soil water tensions of up to 30000 mm (Figure 5.18 *top*). The deepest watermark at 1000 mm-depth was a bit wet with soil water tensions as low as ~5000 mm.

Watermark Nest 4 is located adjacent to the bitumen road where it receives runoff from the impervious surface of the road during rainfall events. Figure 5.18 *bottom* shows lower soil water tensions of up to ~4000 mm. Unlike the previous case, all the watermarks in Nest 4 responded at the same time to rainfall events of 18.6 mm and 51 mm on the 11th and 28th February 2009, respectively. This could be attributed to the ease with which sandy soils saturate allowing water to infiltrate quickly because of the bigger pore sizes in the soil particles.

Immediately after the rainfall event of 28th February 2009, the sandy soils began to dry up at a faster rate resulting in increased soil water tensions (Figure 5.18 *bottom*). All the watermarks in Nest 4 started drying immediately after the rains stopped. The shallowest watermark in Nest 3 (200 mm-depth) however did not dry up. Such behaviour has implications for the migration of NO_3 and soluble-P in the catchment. This illustrates that with heavy rains sustained for longer periods such soils will allow for the movement of pollutants dissolved in surface water to the sub-surface since hydrological connectivity will be much facilitated.

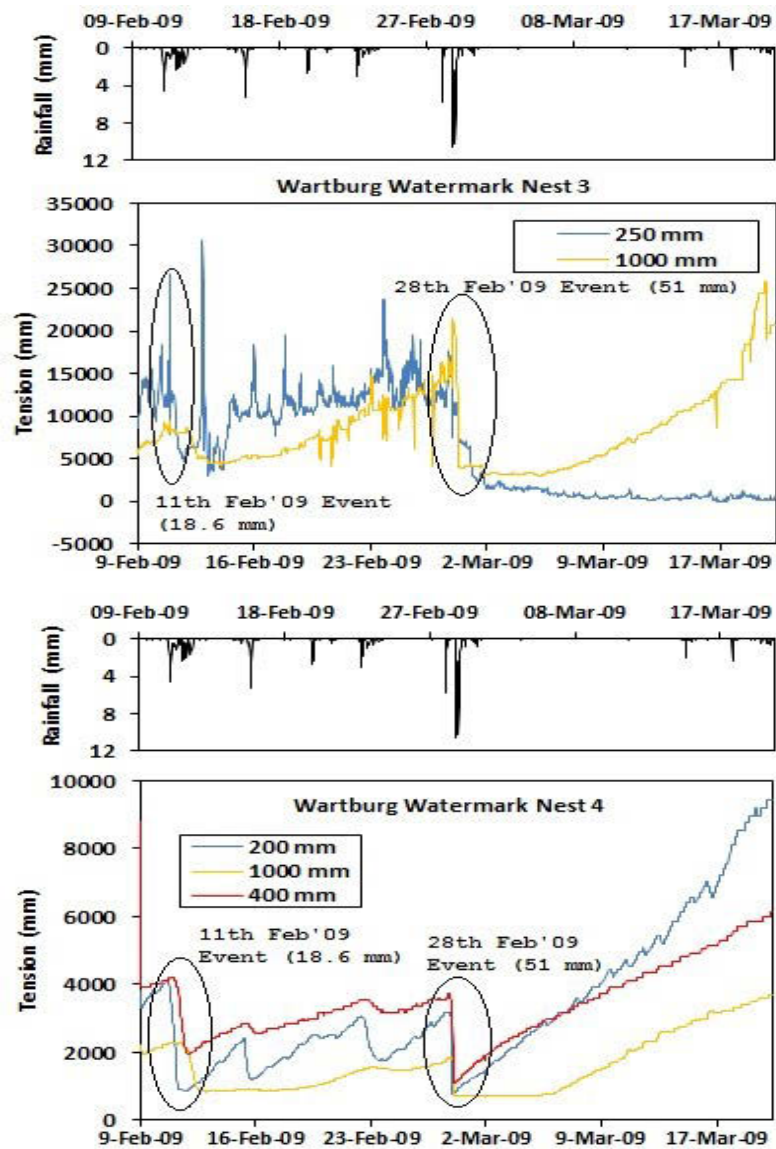


Figure 5.18: Soil water tension variation: Nest 3 & 4, 9Feb-17 Mar'09 (summer).

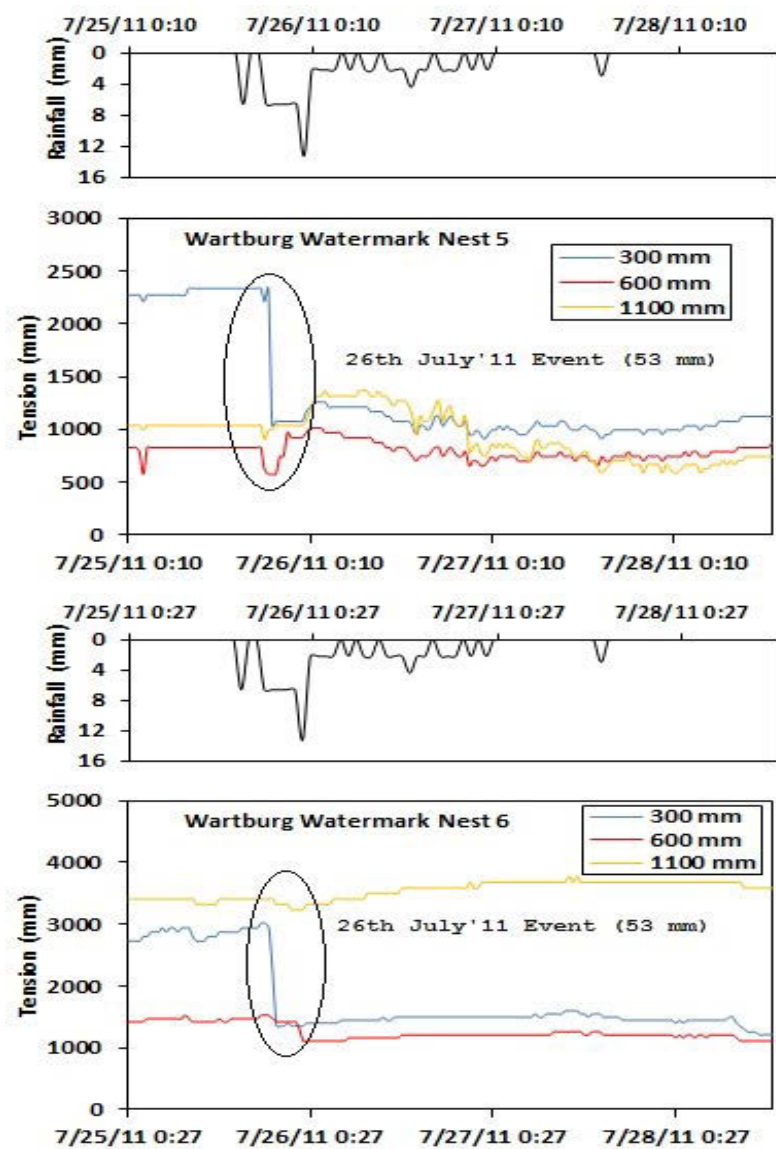


Figure 5.19: Soil water tension variation: Nest 5 & 6, 25-28 Jul'11(winter).

The 53 mm rainfall event of 26th July 2011 occurring in winter showed watermarks at Nest 5 were more responsive than those at Nest 6 to the movement of moisture in the soil column. Since the watermark at Nest 5 was closer to the waterway than that at Nest 6, the soil water tension was lower at Nest 5 (>500 mm) than at Nest 6 (>1000 mm) before the rainfall event (Figure 5.19). This means that it was drier at Nest 6 than at Nest 5.

After the rainfall event, all the three watermarks at Nest 5 were responsive to the infiltrated rain water in the soil column. It was however different at Nest 6 where only watermarks at depths of 300 mm and 600 mm responded to the rainfall event. The deepest watermark (1000 mm-depth) at Nest 6 did not respond to the 53 mm rainfall event as it remained dry. This could be attributed to its distant location from the waterway compared to that at Nest 5. If additional soil moisture was added during a rainfall event, it would be much easier for runoff to occur at Nest 5 than it would at Nest 6. The riparian zone responded much faster to rainfall events due to its high antecedent wetness and presence of shallow soils. The occurrence of this hydrologic connectivity is essential before flushing of solutes and nutrients downslope through the riparian zone to the stream.

Figure 5.20 shows the soil water tension dynamics obtained from the installed watermarks for Nest 2 (closer to a waterway and the presence of clay soils) and Nest 4 (furthest from the waterway and presence of sandy soils, but adjacent to the impermeable bitumen road) for the period of 23rd -26th January 2010. Initially soil water responses from all the watermarks at both of these stations showed the intermediate soil layer (400 mm-depth) to be the driest. It was also noted that the upper soil layer (200 mm-depth) at both nests was the wettest, confirming the presence of antecedent soil moisture from previous rainfall events. Between 23rd and 25th January 2010, the upper soil layer for both nests began to steadily dry with the layer at Nest 4 drying at a faster rate because of its sandy nature. The intermediate (400 mm-depth) and deepest (800 mm-depth) soil layers at Nest 4 were kept at lower soil water tensions (~2000 mm) compared to Nest 2 (~3000 mm) at the start. This can be explained by the presence of sandy soils at Nest 4 and it being closer to the bitumen road where even lower rainfall intensities and runoff would be directed to this area.

Nest 2 was located at a place of consolidated clay with lower electrical resistivity as earlier confirmed from the ERT survey. There were responses to a 40 mm rainfall event in the soil profile on 26th January 2010 at all three depths. The shallowest (200 mm-depth) and the

intermediate (400 mm-depth) watermarks responded instantly to the rainfall event and approached the soil saturation point. The deepest watermark (1000 mm-depth) responded later but was far from reaching the soil saturation point as much of the rainfall did not percolate to this depth. Hence, most of the water that was available at this instant in the nearby Flume 1 together with the dissolved NPS pollutants, would most probably originate from the subsurface at depths of 200 mm and 400 mm.

The ERT survey shown in Section 5.2.1 above confirmed the existence of a very dry area containing sandy soils where watermark Nest 4 was located. Because of this sandy soil type, there were instantaneous soil moisture responses at the watermarks from the 40 mm rainfall event of 26th January 2010 for all the soil profiles (i.e. 200 mm, 400 mm and 800 mm-depths) as shown in (Figure 5.20). The soil moisture at these depths however did not approach the soil saturation point and probably no surface or subsurface runoff was generated immediately. In fact, after this rainfall event, there was immediate drying of the shallowest soil layer. The intermediate soil layer dried up gradually but the deepest soil layer remained relatively wet. This further confirms the presence of sandy soils at this particular location.

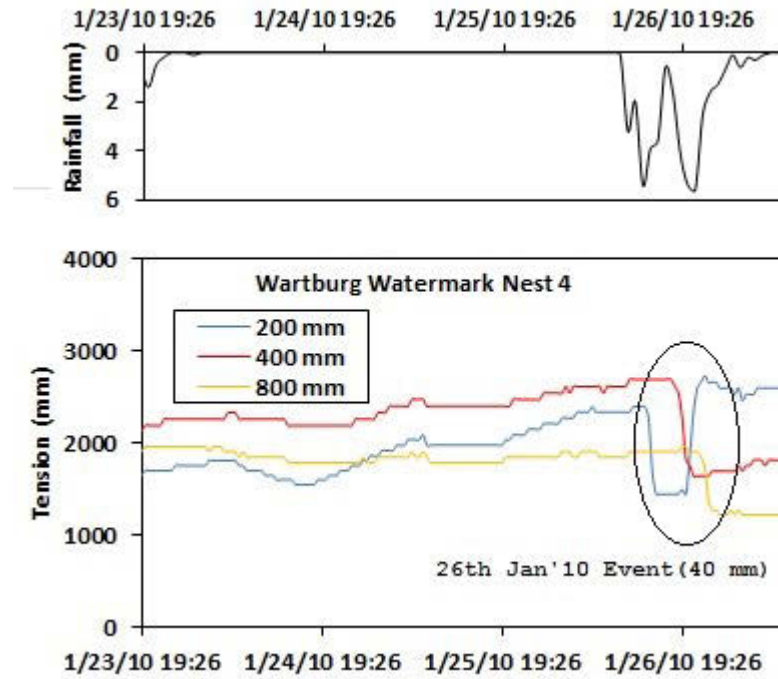
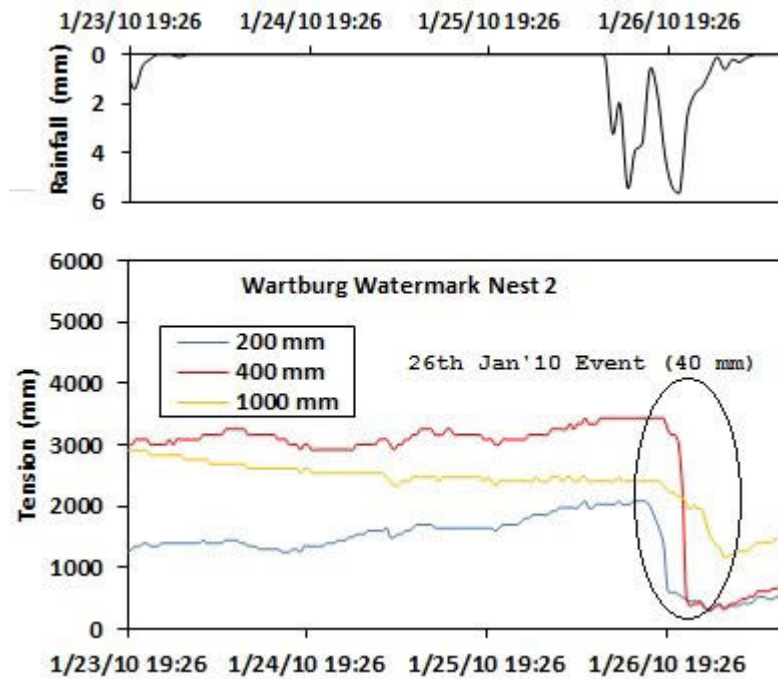


Figure 5.20: Nest 2 (closer to waterway and presence of clay soils) and Nest 4 (furthest from the waterway and presence of sandy soils, but adjacent to the impermeable bitumen road).

CHAPTER SIX

6 DEVELOPMENT OF THE ACRU-NPS MODEL

During this research modifications were made to the *ACRU-NPS* model on the basis of knowledge gained from studying the connectivity influences on nutrient and sediment migration in the Mkabela Catchment. These modifications enhanced the model's ability to not only simulate N and P dynamics in a catchment but also the pathways and fate of nutrients (N and P) and sediments through farm dams, wetlands and riparian buffer strips.

6.1 *ACRU-NPS* Model Processes

Campbell *et al.* (2001) incorporated a nutrient module into *ACRU-NP* creating what is now referred to as *ACRU-NPS*. The module was applied in the Java language as an extension to the *ACRU2000* modelling system. The N and P component, process and data objects applied in *ACRU-NPS* were patterned after transformation and transport concepts used in the *GLEAMS* model (Knisel and Davis, 1999). Possible nutrient sources in the model include rainfall, irrigation, fertilizer, and plant/animal waste.

The main goals of Campbell's work were to add capabilities to *ACRU2000* to simulate;

- N and P losses in surface runoff, sediment transport and leaching,
- N and P cycling in the soil-water-plant-animal system, and
- N and P mass balances in the watershed system.

Lorentz *et al.* (2012) has highlighted the importance of evaluating the economic impacts of NPS pollution in agriculture to compare the benefits of specific land use practices on crop yield against the costs of deteriorated water quality. Consequently the water quality impact may be assessed at the outlet of a farm unit/source area or at some position in the stream network downstream of multiple source contributions. The prediction of water quality impacts immediately downstream of a source can be used to evaluate load reductions due to remediation at each source, while predictions in the stream network can be used to determine

the relative contribution from each source and, in so doing, to direct remedial measures and assess their net effects.

For this purpose the resulting *ACRU-NPS* model apart from simulating nutrient (N and P) and sediment production in agricultural catchments was modified to include:

- algorithms to simulate nutrient and sediment production from land segments for various land uses,
- a crop growth algorithm in which the crop yield is influenced by water and nitrogen stress and
- algorithms to simulate nutrient and sediment fate at controls and buffers in the stream network. These included provision for farm dams, wetlands and riparian buffer strips.

6.1.1 Nutrient processes

The *ACRU-NPS* processes modelled in the soil layers represented in Figure 6.1 include:

- Unsaturated upward movement of water from the A-horizon to the soil surface layer driven by the hydraulic gradient induced by evaporation in the soil surface layer;
- Evaporation of water on the soil surface layer;
- Transpiration of water from the soil layers A and B through the plant roots;
- Solution of NO_3^- and soluble-P in stormflow during a rainfall event controlled by rain water/soil water contact time and soil properties;
- Mixing of NO_3^- and soluble-P with rainfall in the soil surface layer during an event;
- Movement of NO_3^- and soluble-P in stormflow, proportioned on a daily runoff basis;
- Redistribution of NO_3^- and soluble-P from surface layer into A-Horizon after event;
- Movement of NO_3^- and soluble-P in baseflow after percolation into the bedrock aquifer store, proportioned on a daily basis.

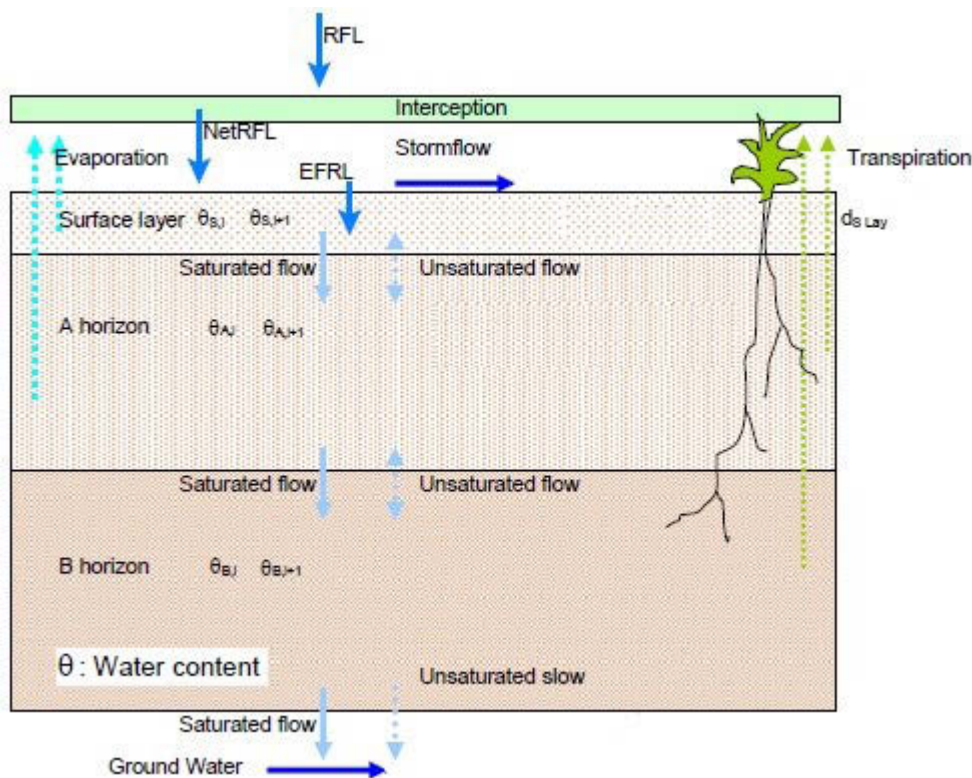


Figure 6.1: *ACRU-NPS* soil layers used to model nutrient processes where RFL = rainfall, EFRL = effective rainfall and NetRFL = net rainfall.

Each sub-catchment includes a surface layer, soil A and B horizon and groundwater store. A series of interlinked sub-catchments could then be used to characterise the dynamics of water and NPS pollutant transfer in a catchment. This is obviously a simplification of the observations made in hydrological process studies but was pursued to develop simple algorithms for larger scale catchment modelling. This modelling approach took into consideration the different hillslopes present in Mkabela Catchment characterised by dissimilar land use, soil type and slope.

6.1.1.1 Nitrogen processes

Figure 6.2 depicts a conceptual model of the Nitrogen Cycle in the soil-plant-atmosphere that includes the primary nutrient processes that are essential for maximizing agricultural productivity and profitability, whilst reducing the impacts of N fertilization on the environment (Rossouw and Gorgens, 2005). The cycling of N involves several chemical forms: Organic N, Ammonium (NH_4^+), Ammonia (NH_3), Nitrite (NO_2^-), Nitrate ion (NO_3^-), and N_2 (gas). The transformation in *ACRU-NPS* between these different forms occurs by different processes including ammonification, immobilization, nitrification, denitrification, fixation, volatilization, and adsorption (Campbell *et al.*, 2001).

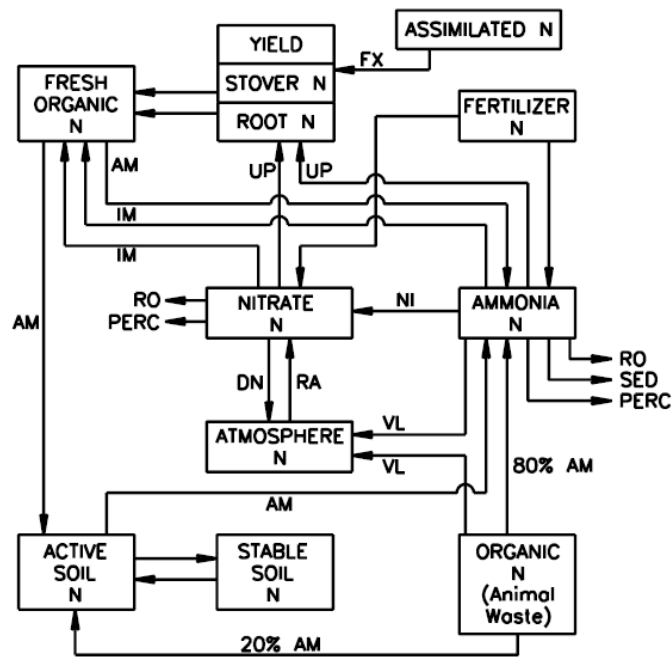


Figure 6.2: Nitrate processes included in *ACRU-NPS* where AM = ammonification, NI = nitrification, DN = denitrification, VL = volatilization, IM = immobilization, UP = uptake and FX = fixation (Campbell et al., 2001).

Mineralization: mineralization occurs from active soil N, fresh organic N, and organic N from animal wastes in two stages: a first-order ammonification process followed by a zero-order nitrification process. Organic N in the residues of plants and animals is mineralised to NH_4^+ by heterotrophic soil organisms. Some mineralised and fertilized NH_4^+ is absorbed by plant roots, volatilised as NH_3 to the atmosphere, or adsorbed on the cation exchange complex of soils. The adsorbed NH_4^+ is not susceptible to leaching, and some of it may even be fixed when soils have 2:1 clays (Rossouw and Gorgens, 2005). Some of the NH_4^+ can also be immobilised as organic N by heterotrophic soil organisms. Both mineralization and immobilization can occur simultaneously. However, one process usually dominates the other depending on the carbon to nitrogen (C:N) ratio in the soil (Rossouw and Gorgens, 2005).

In the *ACRU-NPS* model ammonification of organic N from animal waste on the surface add to a soluble surface NH_4^+ pool in the surface soil layer. Nitrification of the soluble surface NH_4^+ is assumed to occur on the soil surface and at the same maximum rate (100 mg $\text{NO}_3\text{-N/kg}$ of soil/wk). The produced NO_3 is then added to a soluble NO_3 pool. Both the soluble NO_3 pool and the soluble surface NH_4^+ pool are accumulated and immobilized onto residue until rain or tillage occurs. Rain or tillage events cause them to return to the surface layer where they are again added to the NO_3 and NH_4^+ pools (Knisel and Davis, 1999).

The active mineralizable N pool is defined using C:N ratios from 12-25. The long-term stable N pool (no mineralization occurs) has a C:N ratio less than 12. There is also a N flux between the two pools, which is governed by their relative sizes.

Equation 6.1 is used in the *ACRU-NPS* model to estimate N mineralization (MN) (kg/ha/day) in soil layer i from the active N pool (Knisel and Davis, 1999) as:

$$MN_i = (CMN)(POTMN_i)[(SWFA_i)(TFA_i)]^{0.5} \quad (6.1)$$

where: CMN is the mineralization constant (0.003 kg/ha/day)
 TFA is the temperature factor for ammonification
 SWFA is the soil water factor for ammonification
 POTMN is the active N pool

During the nitrification process most of the NH_4^+ that resulted from either fertilization or mineralization is oxidized via NO_2^- to NO_3^- by a small group of chemoautotrophic nitrifying bacteria. These bacteria keep concentrations of exchangeable NH_4^+ relatively low in aerobic soils, but their activity is inhibited by lack of O_2 in anaerobic soils (Rossouw and Gorgens, 2005). This nitrification process does not result in losses of N from soils, but alters the susceptibility of N to loss through various processes, such as plant uptake, leaching and denitrification. The NO_3^- that results from either fertilization or nitrification can also be immobilized into organic N by heterotrophic soil organisms.

The zero-order nitrification process is independent of the amount of NH_3 in the soil layer, i. This process occurs when the soil water content is above the immobile water content, and below saturation with optimum at field capacity.

Nitrification in *ACRU-NPS* is expressed as in Equation 6.2 (Knisel and Davis, 1999):

$$NIT_i = (TFN_i)(SWFN_i)/(SOILMS_i) \quad (6.2)$$

where: NIT is nitrification (kg/ha/day), max of 100 mg NO_3 -N/kg soil/week
 TFN is the temperature factor for nitrification

SWFN is the soil water factor for nitrification

SOILMS is the soil mass (Mg/ha)

Similar equations are also used for mineralization of crop residues on the surface and in the soil, and animal wastes acted upon by soil microbes. An estimate used in *ACRU-NPS* model that originated from *GLEAMS* is that 20% of the mineralized fresh organic N in crop residues goes to mineralizable soil N while the other 80% is transferred to the NO₃-N pool (Sharpley and Williams, 1990). Similarly, Bhat *et al.* (1980) estimated that 80% of the mineralization from organic N in animal waste is added to the NH₃ pool while 20% is added to the active N pool. The only differences in the calculation of ammonification of organic N in animal waste from surface crop residue are that just the top 1 cm of soil is considered for soil water factors and atmospheric temperature replaces soil temperature (Knisel and Davis, 1999).

Immobilization: immobilization is defined as the range of C:N greater than 25 at which microbes assimilate N onto the residues from sources such as soil NO₃ and NH₃ (Rossouw and Gorgens, 2005). In *ACRU-NPS* model immobilization ceases when the C:N ratio reaches approximately 25.

The immobilization rate considers NH₃ and NO₃ in its calculations as given in Equation 6.3 (Knisel and Davis, 1999):

$$WIMN_i = (DCR_i)(FRES_i)(0.016 - Cnfr) \quad (6.3)$$

where: WIMN is the N immobilization rate (kg/ha/day)

Cnfr is the concentration of N in fresh residues

DCR is residue decay rate constant

FRES is fresh residues

If the amounts of nitrate and ammonia available are less than the immobilization estimate, the decay rate is adjusted to let only 95% of the NO₃-N and NH₄-N in layer i be immobilized, and the fresh residue in each layer is reduced (Knisel and Davis, 1999). WIMN, or 95% NO₃-N, is added to the fresh organic N pool on the day of occurrence.

If immobilization is unlimited by NO₃ and NH₄, then the fraction of WIMN as NO₃ and NH₃ are partitioned according to empirical formulas. Surface residue immobilization is simulated in the same manner, with the exception that for surface residues the NH₄ and NO₃ pools are combined with the separate surface pools produced by surface mineralization processes (Knisel and Davis, 1999).

Denitrification: denitrification is a biological process by which denitrifying bacteria reduces NO₃⁻ and sometimes also NO₂⁻ to nitrogen oxides and eventually N₂. Conditions conducive to denitrification include absence of O₂, the presence of NO₃⁻ or NO₂⁻ and an electron-donating substrate like organic residues to support microbial respiration (Rossouw and Gorgens, 2005). Although the absence of one or more of these conditions usually prevents rapid denitrification, a short period of favourable conditions can result in substantial losses of NO₃⁻ from soil.

Soil NO₃⁻ can be denitrified to N₂ (gas) by anaerobic bacteria when soil water content is greater than the soil's field capacity. In the *ACRU-NPS* model denitrification is a first-order reaction process with a rate constant that is a function of organic carbon and modified by soil water content and temperature. Fresh organic residues, organic C in animal waste and organic C in the potential mineralizable N pool are involved in the reaction. Denitrification begins at a moisture content of approximate 10 % above field capacity and increases to a maximum of unity at saturation.

Denitrification is subtracted from soil NO₃ for each layer on each simulated day, and occurs in the upper soil layers on days with rainfall or irrigation (when percolation from the root zone may not occur), and in the lower soil layers (when percolation may occur for an extended period due to perched water table).

Denitrification (DN) (kg/ha) in a given soil layer *i*, is calculated by Equation 6.4 (Knisel and Davis, 1999):

$$DN_i = SNO3_i \left(1 - \exp \left[- (DK_i) (TFDN_i) (SWFD_i) \right] \right) \quad (6.4)$$

where: SNO3 is the NO₃-N mass in the soil (kg/ha)

DK is the active soil C decay rate

TFDN is the temperature factor for denitrification

SWFD is the soil water factor for denitrification

N losses in runoff, sediment and percolation: the form of N most likely to be lost through leaching process is NO_3^- . Leaching refers to the downward movement of N in water through the soil profile and out of the plant rooting zone. Movement of soluble N from the soil surface to depths where plant roots are active in the soil profile increases N availability to the crops and may not be considered as leaching per se. NO_3^- is usually not adsorbed to the soil particles and hence it is the most abundant form of N in the water that moves. The importance of N losses by leaching varies greatly depending on the timing and magnitude of the downward flux of water in the soils (Rossouw and Gorgens, 2005). Losses can be substantial in agricultural systems where fertilizer application or mineralization results in high concentrations of NO_3^- during periods when leaching is likely. Significant N losses from soils are most likely to occur when NH_3 from fertilizers or animal manure remain on the surface. In most soil-plant-atmosphere systems, losses of N by leaching are associated with short-term weather events that can be neither controlled nor predicted. In many highly weathered soils, NO_3^- leaching can be retarded by positively charged particles in acid subsoils, leading to a substantial storage capacity for NO_3^- in such soils (Rossouw and Gorgens, 2005).

During rainfall, an infiltration rate lower than the rainfall rate results in ponding and subsequently runoff. The movement of chemicals with runoff is dependent on the chemical type and the soil characteristics. The *ACRU-NPS* model uses the general equations adopted by *GLEAMS* for determining nitrate, ammonia, phosphorus and pesticides concentrations available for runoff and infiltration in the upper soil layer (Knisel and Davis, 1999). *GLEAMS* allows for incomplete extraction of these chemicals in the surface soil layer into runoff, with an extraction coefficient between 0.05 to 0.5 and a partitioning coefficient, K_d (Knisel and Davis, 1999).

Since NH_4^+ is partially adsorbed to the soil particles, its concentration is dependent on erosion and sediment losses which are a function of sediment yield, solid concentration and enrichment ratios. Percolation of NO_3^- and NH_4^+ in deeper soil layers however is determined as a function of their concentrations in the surface soil layer, which is calculated by their concentration relative to the dry weight of the soil. The percolation component is then found

as a ratio of total available mass and total concentration of available nitrogen (Knisel and Davis, 1999).

N losses to uptake, evaporation and fixation: the overall process of N uptake by plants involves movement to and across the plasma membrane of root cells as separate processes where ammonium moves to the membrane primarily by diffusion and nitrate primarily by mass flow in the transpiration stream (Rossouw and Gorgens, 2005). Rates of N uptake by plants tend to vary greatly with stage of growth. Many annual plants take up most of their N within a few weeks during the growing season. All crops differ in their ammonia and nitrate uptake capabilities; however, the model assumes that uptake is equal to the relative mass of each N-species in the soil layer being considered for transpiration processes. *ACRU-NPS* calculates nitrogen uptake by the concentration of biomass-N expressed as a power function of total dry matter, where relationships estimating nitrogen demand for many different crops are given (Campbell *et al.*, 2001). N concentration in plant biomass is a function of empirical coefficients, Leaf Area Index (LAI), total dry matter and N dry matter.

Ammonia and nitrate uptake are found from a calculation of the concentration of the chemical in the water, and the transpiration calculated for each layer of root growth. Total uptake is found by summing over the number of transpiration layers. It is assumed that an overabundance of nitrate and ammonia does not result in a flush of uptake greater than the demand calculated. Such a flush occurs in nature where plants take up more elements than they need for growth because of excess nutrients. This is evidenced by dark green, almost black, colour of growing crops. It is currently not possible to simulate the flush of nutrients uptake in *ACRU-NPS* model. If soil nitrogen is greater than a threshold value, leguminous plants will take N from the soil. If soil nitrogen is less than the threshold, these plants will fix N₂-N from the atmosphere. The threshold value that determines this process is crop and soil pH specific, among other factors; however it is assumed to be 5 mg/L, combined for nitrate and ammonia, within the *ACRU-NPS* model. Nitrogen demand for a leguminous plant is calculated, and then the ammonia and nitrate concentrations in the solution phase are summed in layers where transpiration occurs.

During evaporation the ammonia and nitrate are moved upward in the soil one computational layer above the one at which evaporation occurs. This upward movement up is caused by an upward water flux, and then by a vapour flux in the near-surface (Campbell *et al.*, 2001).

Ammonia is not volatilized from the surface. The equations governing nitrate and ammonia evaporation from a layer result in an enrichment of these species in the upper 1 cm of soil, for subsequent runoff and percolation processes (Knisel and Davis, 1999).

Nitrogen fixation occurs naturally through biological processes while industrial N fixation occurs when nitrogenous fertilizers are being manufactured. Nitrogen in plant and animal residues and N derived from the atmosphere through industrial electrical and biological fixation is added to soil (Rossouw and Gorgens, 2005). Usually, nitrogenous fertilizers contain N in the form of urea, ammonium or nitrate. Electrical N fixation results through lightning, while biological N fixation is mediated by certain micro-organisms, which can be either free-living or symbiotic in nature. Symbiotic N fixation has a far greater effect on N availability to plants than non-symbiotic N fixation, although the biochemical processes involved with both are similar. Biological N fixation produces the primary flow of N in soil-plant-atmosphere systems with legumes, but is unimportant in the systems without legumes.

In *ACRU-NPS* it is assumed that N fixation does not add N to the soil until harvest or tillage, at which point the appropriate residues are added to the correct nitrogen pools (Campbell *et al.*, 2001). On a daily time step, if the demand exceeds the threshold value, uptake is calculated as for other crops as described earlier. Otherwise, the fixed N mass is equal to the daily optimum N demand for a given crop.

Rainfall and Fertilizer N: in the *ACRU-NPS* model nitrogen can also be instantaneously added to the system via fertilizer and rainfall, the latter of which contains both ammonia and nitrate (Knisel and Davis, 1999). These processes are simplified by assuming that all rainfall nitrogen is as nitrate, the user-input concentration of which remains constant throughout the simulation period. Separate nitrate and ammonia pools are maintained, allowing nitrate and ammonia fertilizers to be considered separately. Fertilizer and animal waste can be applied on the surface, incorporated, injected or fertigated. Application of inorganic fertilizer on the soil surface is assumed to mix with the appropriate species upon tillage or rainfall (Knisel and Davis, 1999).

Ammonia volatilization: ammonium in soil solutions tends to equilibrate with NH_3 in air which often results in losses of N through NH_3 volatilization. This process is favoured by high pH and short distances between the solution and moving air. Volatilization is also

dependent on the storage and handling of the waste, and the environment where the waste is applied. Ammonia losses to volatilization are high from surface-applied animal waste, but drastically reduced when the waste is incorporated post-application (Knisel and Davis, 1999).

Volatilization is considered as a non-point source pollution process in the *ACRU-NPS* model that is related to air temperature. It is calculated daily for one week after application or until rainfall or tillage occurs and it is assumed to occur only for surface applied solid, slurry and liquid animal waste (Knisel and Davis, 1999). Liquid waste or immediate incorporation of solid and slurry wastes are assumed to volatilize for six hours. After rainfall, remaining ammonia in the waste is added to the surface soil layer's soluble ammonia pool, where it is assumed that it cannot be volatilized. In the model, the volatilization of ammonia mineralized from crop residue and animal waste other than soluble ammonia is not considered (Knisel and Davis, 1999).

6.1.1.2 Phosphorus processes

Figure 6.3 illustrates the cycling of P in the soil-plant-atmosphere system as conceptualised in the *ACRU-NPS* model. In the environment, P originates from natural weathering of the phosphate mineral apatite, sewage, phosphate detergents, industrial fertilizers and organic fertilizers (manures). Similar to the N cycle, the P cycle can also be divided into P inputs or gains, P outputs or losses and P cycling within the soil where P is neither gained nor lost by the processes (Rossouw and Gorgens, 2005). The only significant removal of phosphorous from soils is by plant uptake and subsequent harvest of plants from the field. Hence, most agricultural soils exhibit a steady accumulation of phosphorous (Salomons and Stol, 1995).

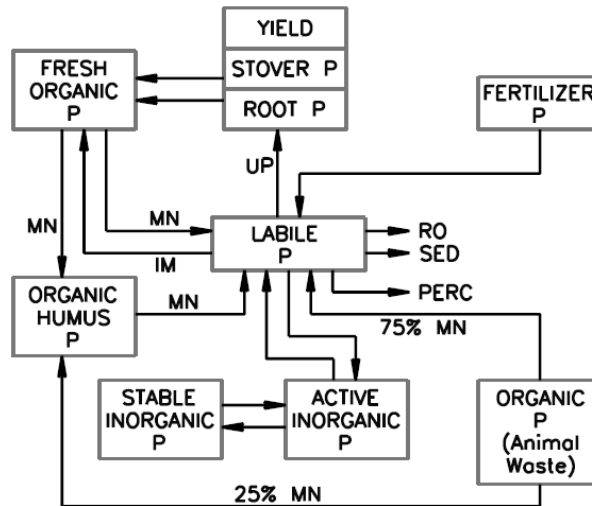


Figure 6.3: P processes included in *ACRU-NPS* where MN = mineralization, UP = uptake, IM = immobilization, RO = runoff, SED = sedimentation, PERC = percolation. (Campbell et al., 2001).

To guarantee a better foundation for management of P for optimum agricultural production with minimal environmental damage, an understanding of the above processes is essential (Figure 6.3). Gains of P in soils are attributed to fertilizers and plant or animal residues. Commercial fertilizers such as super- and ammonium phosphates, contain mainly inorganic P compounds, which are water soluble. However, sometimes water insoluble inorganic P compounds are added to acidic soils as rock phosphate. Mainly organic P compounds occur in either plant or animal residues that have been identified primarily as inositol phosphates, phospholipids and nucleic acids (Rossouw and Gorgens, 2005).

Losses of P from soils are attributed to plant uptake, erosion and leaching (Rossouw and Gorgens, 2005).

- Plant uptake: H_2PO_4^- and HPO_4^{2-} ions are the forms in which plants actively obtain P from the soil solution. Plant uptake of HPO_4^{2-} however seems to be slower than that of H_2PO_4^- due to the use of different carriers. Though both ions move to the roots by diffusion, soils with a pH below 7 are dominated by H_2PO_4^- ions while in those with pH above 7 the dominant ion is HPO_4^{2-} .
- Erosion: water or wind erosion of soil sediments is responsible for large losses of the various P fractions from agricultural fields. Both H_2PO_4^- and HPO_4^{2-} are strongly sorbed to soil particles when incorporated by means of a fertilizer in the topsoil.
- Leaching: for both ionic forms, leaching is limited due to their easy transformation into immobile forms. Therefore H_2PO_4^- and HPO_4^{2-} are unlikely to move into groundwater

except in very sandy soils under excessively high loading rates of P, like is sometimes found with effluent irrigation and waste disposal.

The Phosphorus Cycle is comprised of phosphorus in one of several forms: Organic P, labile P, and inorganic P. Transformation of P between these different forms occurs by different processes: immobilization, fixation, mineralization and adsorption (Figure 6.2). Cycling of P within the soil involves several biological and chemical processes that influence the soil solution P concentration. The biological processes comprise mineralization and immobilization, whilst the chemical processes are adsorption and desorption as well as precipitation and dissolution.

Phosphorus processes included in the *ACRU-NPS* model are;

- Mineralization
- Immobilization
- P losses in runoff, sediment and percolation
- P losses to uptake, evaporation and fixation
- P in fertilizers

Mineralization: these are biological processes that comprise mineralization of organic P to inorganic P and the immobilization of inorganic P to organic P by heterotrophic soil organisms. Several other factors also affect the direction, extent and rate of these processes in soil. According to Knisel and Davis (1999) mineralization and immobilization in general are similar to those for N in that both occur simultaneously with one usually dominating the other depending on the C:N ratio in the soil.

Mineralization of phosphorus is simulated as a single-step first-order process following the same general procedure as nitrogen. Seventy-five percent of the mineralization from fresh organic P is added to the labile pool, while 25% is added to the organic humus pool (Knisel and Davis, 1999). Phosphorus in the surface residue is mineralized to soluble P in the same manner as fresh organic P.

Equation 6.5 defines mineralization from organic humus in layer i ($PMNi$) ($kg/ha/day$) (Knisel and Davis, 1999) as:

$$PMN_i = (CMN)(SORGP_i)(POTMN_i / SOILN_i) [(SWFA_i)(TFA_i)]^{0.5} \quad (6.5)$$

where: CMP is the mineralization constant
 SORGP is soil organic humus P
 POTMN is active soil P pool
 SOILN is stable soil P pool
 SWFA is the soil water factor (same as for N)
 TFA is the temperature factor (same as for N)

In *ACRU-NPS* there are three soil P pools: mineralizable organic humus, active mineral and long term stable mineral. Mineralizable crop residue and surface residue are represented by the fresh organic pool (Figure 6.2). There is also a separate pool for organic phosphorus in animal wastes. The labile P pool represents both plant available and mobile phosphorus. Analogous to the nitrogen component, the P pools are defined by their respective C:P ratios. Fresh organic P generally has a C:P ratio greater than 200, while the mineralizable organic humus P pool has a range from 125-200.

Flows between the stable/active mineral P pools remain constant in the long term system with respect to the stable pool, which is 4 times the size of the active mineral pool at equilibrium (Knisel and Davis, 1999). The flow between the active and stable mineral P pools is defined as a function of soil water, temperature, labile P, the P sorption coefficient and active mineral P. The active mineral P pool aids in immobilization of labile P by sorption. The sorption of phosphorus is a function of soil characteristics.

Immobilization: the general governing processes for P immobilization are the same as those for nitrogen, with the exception that there is only one source of P. Immobilization of plant available labile P occurs when the C:P ratio of crop residues is greater than 200 (Knisel and Davis, 1999).

Immobilized P (WIMP) (kg/ha/day) is therefore defined as in Equation 6.6 (Knisel and Davis, 1999):

$$WIMP_i = (DCR_i)(FRES_i) \left[(0.16PLI_i - (Cpfr)_i) \right] \quad (6.6)$$

where: DCR is the decomposition of crop residue
 FRES is fresh crop residue
 PLI is the labile P immobilization factor
 Cpfr is concentration of P in the fresh residue

The 0.16 in Equation 6.6 is based on the assumption that carbon comprises 40% of the fresh residue, while 40% of the carbon is assimilated by soil microorganisms (Knisel and Davis, 1999). If WIMP is greater than 95% in the labile pool, then the adjusted residue decay rate is calculated differently. Immobilization can be limited by either phosphorus or nitrogen, and immobilized P is subtracted from the labile pool and added to the fresh organic pool. Surface immobilization is calculated using the same method as that for nitrogen. It is subtracted from labile P in the top soil layer and added to P in the surface residue (Knisel and Davis, 1999).

P losses in runoff, sediment and percolation: the soil solution P concentration controls the amount of P sorbed by the soil particles; nonetheless, there is a large difference in the amount of P sorbed by different soils for a given solution P concentration. In addition, P sorption is a function of the amount and type of hydrous oxides of Al and Fe and reactive Ca compounds present, as well as other ions, pH of the system and reaction kinetics (Knisel and Davis, 1999). The release of sorbed P into solution by means of desorption is usually not completely reversible since all that has been sorbed cannot desorb.

Since both ammonia and phosphorus are adsorbed to the soil clay fraction, P adsorption and partitioning follows the same processes as that for ammonia. The *ACRU-NPS* model assumes that the partitioning coefficient for phosphorus is related only to the soil clay content, not the P status, degree of clay surface coverage or the nature of the surface (Knisel and Davis, 1999). This assumption tends to hold for agricultural systems; however, the partitioning coefficient may be overestimated for soils with low adsorptive capacity that receive large P loads (Knisel and Davis, 1999; Kiker and Clark, 2001).

Phosphorus concentration in the top soil layer that can enter percolation or runoff is calculated from the concentration of labile P based upon the dry weight of the soil times an exponential function analogous to ammonium (Knisel and Davis, 1999; Kiker and Clark, 2001). This, and the partition and extraction coefficients, determines the concentration of P in water. The concentration of P in water then enables the calculation of P in runoff, and in the sediment associated labile P. The percolated mass of P is calculated using the soil dry weight P concentration. Total P sediment losses are finally found using sediment P from animal waste, active and stable mineral P and sediment humus P (Knisel and Davis, 1999).

P losses to uptake and evaporation: the solubility product of the least soluble P component in the solid phase controls dissolution and thus solution P concentration. In general, Ca controls these reactions in neutral or calcareous soils, while Al and Fe are the dominant controlling cations in acidic soils. This causes several secondary phosphate minerals to be formed in soils which vary widely in solubility thereby resulting in different dissolution rates (Rossouw and Gorgens, 2005). Apatite is the most common primary P mineral and its dissolution requires a source of H⁺ from soil or biological activity, and a sink for Ca and P. The dissolution of apatite varies with rainfall and temperature and is therefore quite difficult to model. Labile P is the readily available portion of both inorganic and organic fractions that exhibit a high dissociation rate and rapidly replenishes soil solution P. Depletion of labile P causes some non-labile P to become labile, but at a slow rate.

Phosphorus demand and subsequent uptake data of N:P ratios are available for 78 different crop simulations in the *ACRU-NPS* model, although the average N:P ratio is about 7:1 (Knisel and Davis, 1999; Kiker and Clark, 2001). The phosphorus demand is determined as the difference between the total dry matter P (which is in turn a function of the optimum phosphorus content estimated from nitrogen content) on successive days (Knisel and Davis, 1999). Labile P uptake is estimated for each layer in which transpiration occurs, and total uptake is a sum over all transpired layers. Adjusted P demand is subtracted from the labile P pool for each layer. However, growth is not constrained for P deficiency, like it is in the nitrogen component (Lorentz *et al.*, 2012). Phosphorus moves upward with evaporation in the same way as nitrogen including movement within the subsurface soil layers (Knisel and Davis, 1999).

Fertilizer P: labile P is assumed to be instantaneously available from the inorganic P fertilizer applied. If it is applied to the surface, the quantity is added to the soluble P pool, after which it moves into the surface layer with rain or irrigation. The solubility of different forms of P based fertilizers are not considered (Knisel and Davis, 1999).

6.1.2 Sediment processes

Erosion processes take place at different scales i.e. catchment, hillslope and at land facet. The land surface contributes water and sediment to any given stream network at the *catchment scale*. Within this study the relevant erosion processes that occur at the catchment scale are interrill and rill erosion, gully erosion, stream channel erosion and flood plain scour. The *routing of sediment* through the catchment is an important process at the catchment scale. A *hillslope* is an area extending from the watershed divide of a catchment down to the stream channel and represents the spatial variation of topography, soil and land management patterns along the hillslope. A small catchment consists of a stream channel that is linked with *hillslopes*. The erosion processes that occur at the hillslope scale are interrill and rill erosion and gully erosion.

The spatial distribution of hydrological response units and hence the *spatial connectivity* of runoff-producing areas is an important process determining the spatial extent of the erosion processes along the hillslope and the major sediment delivery processes to the stream channel. A hillslope consists of *land facets* along the hillslope. A land facet is an area of homogeneous topography, soil and land management. The land facet scale represents the combined processes of rill and interrill erosion. On the upper parts of hillslopes, particularly on those of convex form, interrill erosion is the dominant erosion process. Rills are initiated at a critical distance downslope where overland flow becomes channelled and experience has shown that in most South African hillslopes 5 m is about the minimum slope length that will adequately represent a rill system (Van Zyl, 2007). This however will vary depending on soils, slope, regional climate etc.

The Modified Universal Soil Loss equation (*MUSLE*) algorithm through which Sediment yield per unit area (SS) from a land unit can be determined is given in Equation 6.7 (Lorentz and Schulze, 1995) as:

$$SS = \alpha_{sy} (Q_v \cdot q_p)^{\beta_{sy}} K.LS.C.P \quad (6.7)$$

where: SS is the sediment yield from an individual event (tonne)
 α_{sy} and β_{sy} are climate and catchment specific constants (dimensionless),
 Q_v is the storm flow volume for the event (m^3),
 q_p is the peak discharge for the event (m^3/s),
K is the soil erodibility factor (tonne.h/N/ha),
LS is the slope length and steepness factor (dimensionless),
C is the cover factor and P is the practice factor (dimensionless).

The MUSLE approach is primarily used in *ACRU-NPS* to estimate sediment yield from individual rainfall events at a catchment scale because it has been developed as a hydrologically driven simulator (Lorentz and Schulze, 1995). The MUSLE method is thus well suited for use with the modified SCS techniques to generate storm flow in an event based *ACRU-NPS* model.

According to Simons and Sentürk (1992) the MUSLE coefficients, α_{sy} and β_{sy} , are location specific and must be determined for specific catchments in specific climatic zones. Though very little research has been undertaken on calibrating these runoff energy factors (Kienzle and Lorentz, 1993) the originally calibrated values, $\alpha_{sy} = 8.934$ and $\beta_{sy} = 0.56$, for catchments in Texas, Oklahoma, Iowa and Nebraska in the USA by Williams (1975) are commonly used when Q_v and q_p are in SI units. These values for α_{sy} and β_{sy} have been adopted extensively with varying degrees of success (Lorentz and Schulze, 1995). The storm volume, Q_v (m^3), for the event is related to the detachment process while peak discharge, q_p (m^3/s), is associated with sediment transport.

The factors K , LS , C and P are determined from empirical equations and experimental observations. In *ACRU-NPS*, various options are offered to estimate these parameters, depending on the level of data and information available. These options have been developed from the USLE and the RUSLE manuals and, for modelling in southern Africa, from local experimental observations (Lorentz and Schulze, 1995).

6.1.3 Crop growth, water and nitrogen stress processes

A crop growth algorithm has been incorporated in the *ACRU-NPS* model so that the economic analysis of fertilizer application and land use practice can include the benefits of improved yield against the costs of possible increases in nutrient release to streams (Lorentz *et al.*, 2012). The daily crop growth is limited by either water or nitrogen stress, whichever is the most severe. On a daily basis, the water stress is determined by comparing actual transpiration against potential transpiration. The nitrogen stress is determined by comparing the nitrogen uptake (driven by transpiration uptake and prevalent soil water nitrogen concentration), against the nitrogen demand (driven by the crop growth). The processes inherent in estimating the nitrogen stress are detailed in Figure 6.4.

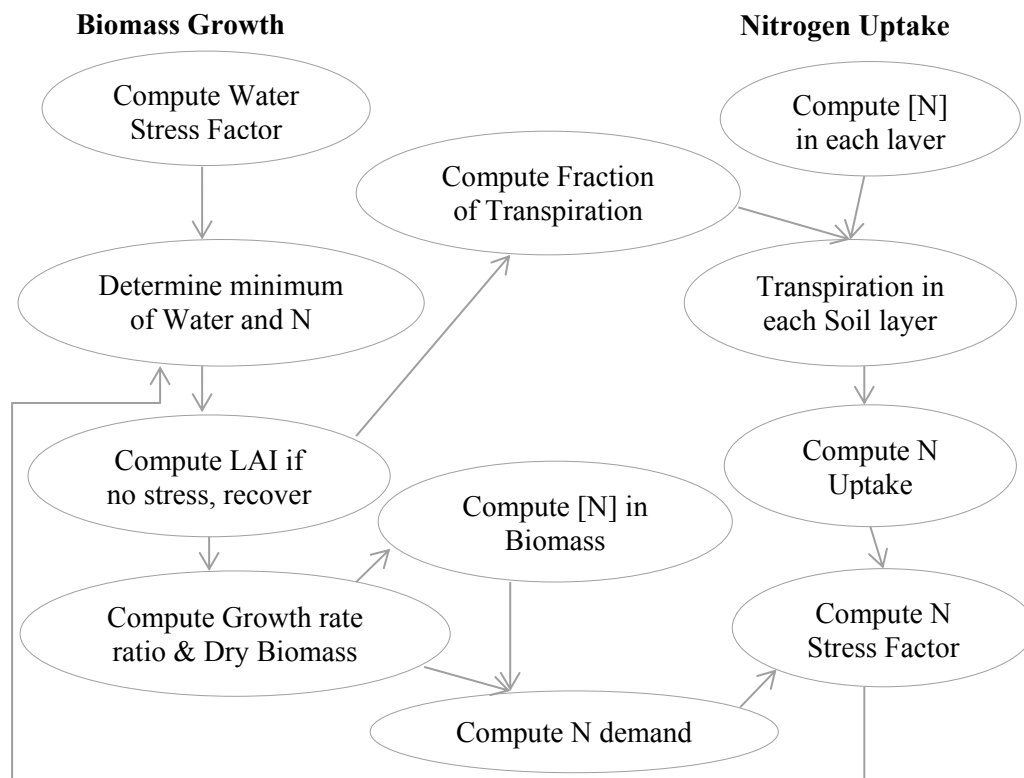


Figure 6.4: Crop growth, water and nitrogen stress processes (Lorentz *et al.*, 2012).

The crop growth is determined by tracking the daily crop Leaf Area Index (LAI), which is calculated relative to a known crop potential LAI (BaseLAI) for each stage of growth. The actual LAI increment is reduced from the potential LAI, on any day in which water or nitrogen stress are experienced. If the LAI is reduced through water or nitrogen stress, the

subsequent permissible transpiration is reduced by a fraction (FractionTranspiration) as determined in Equation 6.8.

$$FractionTranspiration = \frac{1 - e^{-0.5LAI}}{1 - e^{-0.5BaseLAI}} \quad (6.8)$$

If the crop has been previously stressed, and neither water or nitrogen stress conditions exist on a particular day, then the LAI is allowed to recover fractionally towards the potential. The daily crop growth ratio (GRT) is defined as the ratio of LAI to BaseLAI and is used to generate the incremental Dry Matter BioMass, based on a potential crop yield. The GRT is also used to determine the required nitrogen concentration (CN%) for a particular stage of growth from, $CN\% = C1 \cdot GRT^{C2}$, where C1 and C2 are crop specific parameters which regulate the yield response to nitrogen application. The nitrogen demand (DemN) is subsequently determined from CN% and compared to the uptake (UpN) to determine the nitrogen stress factor (StressFacN) for a particular day from Equations 6.9 and 6.10:

$$StressFacN = 1 - \frac{UpFac}{UpFac + e^{3.39 - 10.39UpFac}} \quad (6.9)$$

where:

$$UpFac = 2 \left(1 - \frac{UpN}{DemN} \right) \quad (6.10)$$

This results in a stress factor being applied whenever the demand is greater than the uptake. The stress factor decreases rapidly and is effectively zero (no LAI or growth increment) for any day in which the uptake is less than 60% of the demand (Lorentz *et al.*, 2012).

6.2 ACRU-NPS Crop BaseLAI Values

The Leaf Area Index (LAI), a dimensionless quantity, is the leaf area (upper side only) per unit area of soil below it. It is expressed as m² leaf area per m² ground area. The active LAI is the index of the leaf area that actively contributes to the surface heat and vapour transfer. It is generally the upper, sunlit portion of a dense canopy. The LAI values for various crops differ widely but values of 3-5 are common for mature crops (Allen *et al.*, 1998). For a given crop,

green LAI changes throughout the season and normally reaches its maximum before or at flowering (Figure 6.5). LAI further depends on the plant density and the crop variety.

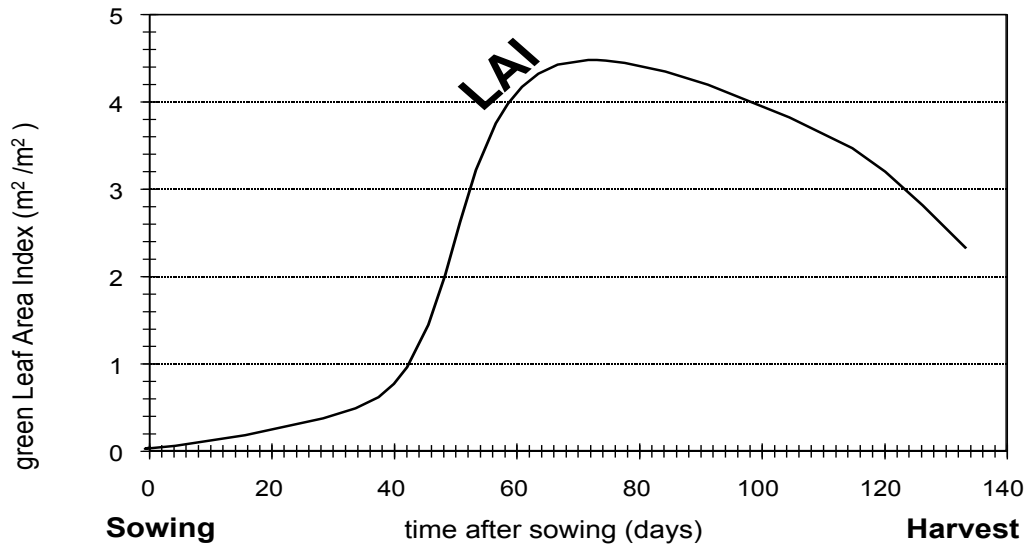


Figure 6.5: Typical presentation of the variation in the active (green) LAI over the growing season for a maize crop (Allen *et al.*, 1998).

6.2.1 Length of crop growth stages

In some situations, the time of emergence of vegetation and the time of effective full cover can be predicted using cumulative degree-based regression equations or by more sophisticated plant growth models (Schulze, 1995; Allen *et al.*, 1998). These types of models should be verified or validated for the local area or for a specific crop variety using local observations. Table 6.1 gives default values of accumulated growing degree days (T_t) for various states of phenological development for an *ACRU maize yield model*.

Table 6.1: Typical values of phenological states of maize related to accumulated growing degree days (T_t) after planting in South Africa (Schulze, 1995)

Phenological State	Accumulated degree days, T_t
Emergence (Ini.)	150
Onset of flowering (Dev.)	700
End of flowering (Mid)	1150
Maturity (Late)	1700

Figure 6.6 illustrates the relationship between crop coefficients at given phenological states (K_{cm}) and accumulated growing degree days (T_t). When accumulated crop ("actual") transpiration (mm) for a given growth stage i , from all soil horizons (E_{t_i}) is equal to accumulated maximum transpiration (mm) for a given growth stage i , from all soil horizons (E_{tm_i}) i.e. $E_{t_i} = E_{tm_i}$, the relationship follows the no stress profile (Schulze, 1995). When, however, the $E_{t_i} : E_{tm_i}$ ratio is less than unity and growth is in the vegetative phase, then the increase in "ideal" K_{cm} is reduced to the fraction E / E_{tm_i} . In other words, the crop coefficient advances at a reduced rate when the plant is under stress. When rainfall or irrigation occurs and soil water deficit stress is relieved, K_{cm} will again resume at the "ideal" rate. When the threshold T_t for the onset of flowering is thus reached, ACRU's maize crop will flower, as it would have under natural conditions, despite the K_{cm} possibly being at a reduced value. It should be noted that in the *ACRU maize yield model* there is no reduction of K_{cm} for stress during flowering, the reduction only being operative in the vegetative phase between plant emergence and the onset of flowering.

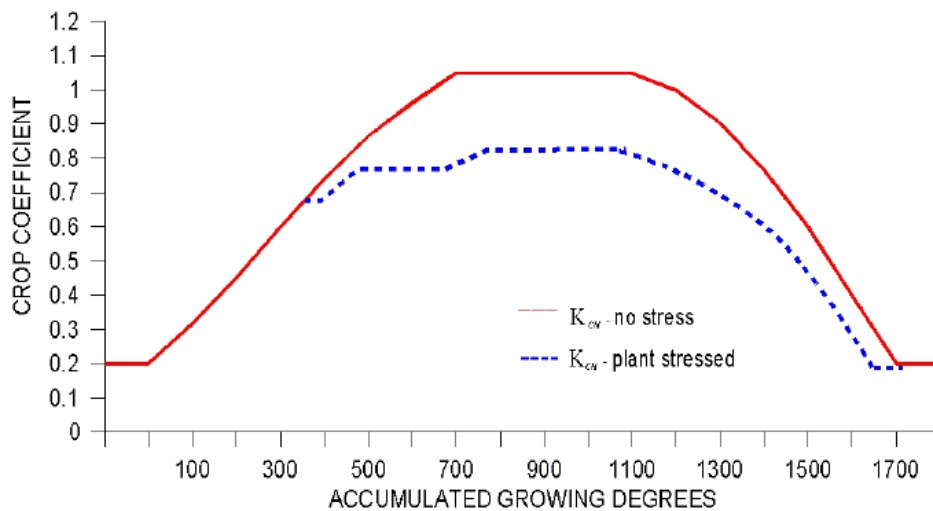


Figure 6.6: Crop coefficients for maize as related to accumulated growing degree days, T_t , but under water stress in the *ACRU maize yield model* (Schulze, 1995).

Typical values for $K_{c_{ini}}$, $K_{c_{mid}}$, and $K_{c_{end}}$ for sugarcane and cabbage are given in Table 6.2. These values were developed for non-stressed crops cultivated under excellent agronomic and water management conditions and achieving maximum crop yield. The coefficients integrate the effects of both transpiration and evaporation over time. The values $K_{c_{mid}}$ and $K_{c_{end}}$ represents those for a sub-humid climate with an average daytime minimum relative humidity (RH_{min}) of about 45% and with calm to moderate wind speeds averaging 2

m/s. For more humid or arid conditions or for more or less windy conditions, the K_c coefficients for the mid-season and end of late season stage should be modified.

Table 6.2: Single (time-averaged) crop coefficients, K_c , and mean maximum plant heights for non-stressed, well-managed crops in subhumid climates ($RH_{\min} \approx 45\%$, $u_2 \approx 2$ m/s) for use with the FAO Penman-Monteith ET_o .

Crop	$K_{c_{ini}}$	$K_{c_{mid}}$	$K_{c_{end}}$	Max. crop height (h) (m)
Sugar Cane	0.40	1.25	0.75	3.0
Cabbages	0.70	1.05	0.95	0.4

Adopted from FAO Irrigation and Drainage Paper 24 (Doorenbos and Pruitt, 1977)

FAO Irrigation and Drainage Paper No. 56 provide general lengths for the four distinct growth stages and the total growing period for various types of climates and locations (Allen et al., 1998). This information has been supplemented from other sources and is summarised in Table 6.3.

Table 6.3: Lengths of crop development stages for various planting periods and climatic regions (days).

Crop	Init. (L_{ini})	Dev. (L_{dev})	Mid (L_{mid})	Late (L_{late})	Total	Plant Date	Region
Sugarcane, virgin	50	70	220	140	480		Tropics
Sugarcane, ratoon	30	50	180	60	320		Tropics
Sugarcane*	65	85	235	155	540	Aug	South Africa
Cabbages	40	60	50	15	165	Aug	South Africa

* *Adjusted K_c factors to represent the growing period of sugarcane in South Africa 540 days (18 months) by distributing the extra 60 days equally among the 4 stages (15 days each).*
Adopted from FAO Irrigation and Drainage Paper 24 (Doorenbos and Pruitt, 1977)

The values in Table 6.3 are useful only as a general guide and for comparison purposes. The listed lengths of growth stages are average lengths for the regions and periods specified, and are intended to serve only as examples (Allen et al., 1998). The specific plant stage development used for South African sugarcane incorporated the effects of plant variety, climate and cultural practices. After interviewing farmers and local researchers in KwaZulu-Natal Province, the total crop growth period of 540 days was given. The extra 60 days were distributed equally among the 4 stages.

6.2.2 Numerical determination of crop BaseLAI values

Allen *et al.* (1998) suggested that the K_c coefficient for any period of the growing season could be derived by considering that during the initial and mid-season stages, K_c is constant and equal to the K_c value of the growth stage under consideration. During the crop development and late season stage however, K_c varied linearly between the K_c at the end of the previous stage ($K_{c_{prev}}$) and the K_c at the beginning of the next stage ($K_{c_{next}}$), which is $K_{c_{end}}$ in the case of the late season stage. Equation 6.11 is used to determine daily K_c values for any crop stage and is given by;

$$K_{c_i} = K_{c_{prev}} + \left[\frac{i - \sum(L_{prev})}{L_{stage}} \right] (K_{c_{next}} - K_{c_{prev}}) \quad (6.11)$$

where i = day number within the growing season [1... length of the growing season];
 K_{c_i} = crop coefficient on day i ;
 L_{stage} = length of the stage under consideration [days];
 $\sum(L_{prev})$ = sum of the lengths of all previous stages [days].

Considering that LAI for the optimal growth curve would have the same shape as that for the optimal values of the K_c curve, for sugarcane,

$K_c = 1.25$ (at Max ETc) and LAI = 6.0 (Max BaseLAI or Potential LAI)

$K_c = 0.40$ (initial stage ETc) and LAI = 1.92 (Initial stage BaseLAI)

$K_c = 0.75$ (Late stage ETc) and LAI = 3.6 (Late stage BaseLAI)

For cabbages the following would be true;

$K_c = 1.05$ (at Max ETc) and LAI = 3.5 (Max BaseLAI/Potential LAI)

$K_c = 0.70$ (initial stage ETc) and LAI = 2.3 (Initial stage BaseLAI)

$K_c = 0.95$ (Late stage ETc) and LAI = 3.2 (Late stage BaseLAI)

It is therefore possible to determine LAI for crop development and mid-season stages to complete the Leaf Area Index (ELAIM) for the whole crop cycle. ELAIM (DLeafAreaIndex) is the standard ACRU module data input (Kiker and Clark, 2001).

Equation 6.12 gives the daily LAI for any crop stage.

$$LAI_i = LAI_{prev} + \left[\frac{i - \sum(L_{prev})}{L_{stage}} \right] (LAI_{next} - LAI_{prev}) \quad (6.12)$$

where i = day number within the growing season [1... length of the growing season];
 K_{ci} = crop coefficient on day i ;
 L_{stage} = length of the stage under consideration [days];
 $\sum(L_{prev})$ = sum of the lengths of all previous stages [days].

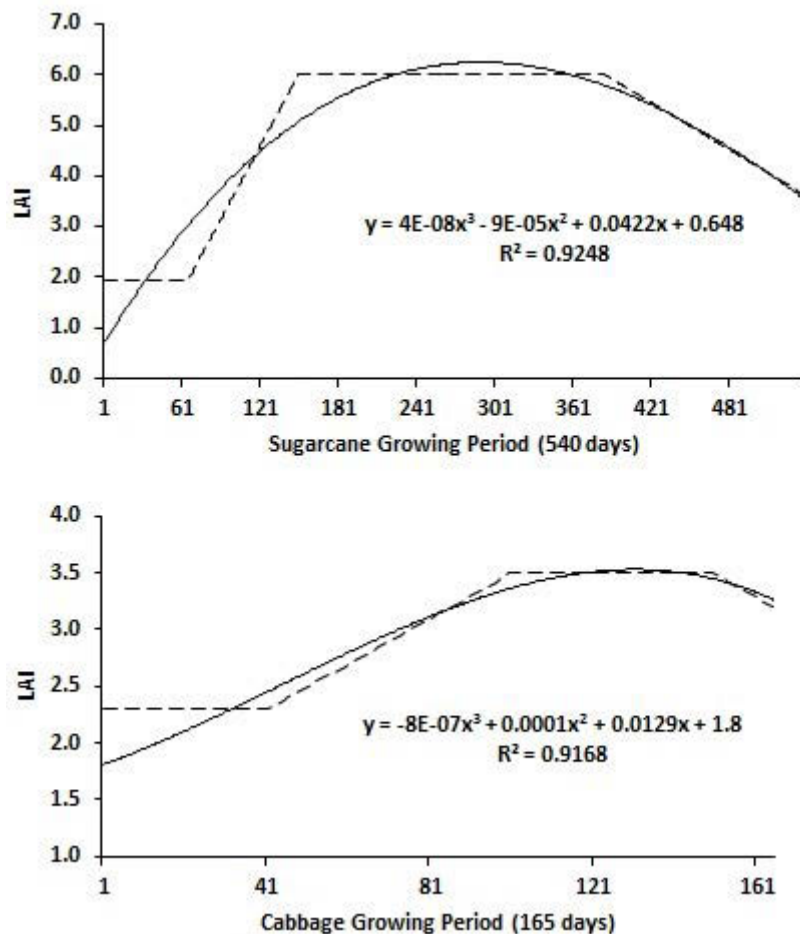


Figure 6.7: The 3-degree Polynomial equation to derive the daily base LAI values for the entire sugarcane (top) and cabbage (bottom) growth periods.

The derived polynomial equations were used to compute daily BaseLAI for sugarcane and vegetables for all of their growth stages (Figure 6.7).

6.3 ACRU-NPS Processes at Control Structures and Connectivity Modelling

Ocampo *et al.* (2006) showed that by considering explicitly the hydrological connectivity of separate units of the landscape and the complex internal dynamics of flow, transport and reaction, predictive models could be developed which remained accurate as well as internally consistent. It is natural in most hydrological models to represent mechanisms through which different sources are transferred from hillslopes to the streams. This is challenging because there are few direct measurements available to quantify how these transfer mechanisms should be characterized. Nevertheless, models have been developed which attempt to differentiate between sources and flow paths of water. The *ACRU-NPS* model inherently uses exponential transfer functions relating the storage state in groundwater and delayed storm flow reservoir to the fluxes from these components.

Detty and McGuire (2010) linked the export of solutes from uplands to streams to hydrologic connectivity which is regarded as one of the key controls in determining catchment rainfall-runoff responses. Incorporating the concept of connectivity into the *ACRU-NPS* model would help in simultaneously improving process representation as well as overall predictive capability of the model. This would however require identifying when, where, and to what extent saturated areas are hydrologically connected to the channel network and are therefore actively contributing to runoff (McDonnell, 2003; Ambroise, 2004; Bracken and Croke, 2007).

6.3.1 Processes at control structures

In the Mkabela Catchment, natural or man-made control structures in the stream network have been shown to retard the migration of sediments and nutrients through agricultural catchments (Lorentz *et al.*, 2012). Algorithms have therefore been developed to route daily water discharge and sediments, nitrogen and phosphorus loads through farm dams, wetlands and riparian buffer strips. For each land segment the simulated daily discharge and sediment, N and P loads are read into a “network” spreadsheet and resultant output discharges and loads are calculated for each control feature in the catchment network (Lorentz *et al.*, 2012).

6.3.1.1 Farm dams and wetlands

A water balance algorithm has been developed for farm dams and wetlands and is given in Equation 6.13 as:

$$V_i = V_{i-1} + V_{in} - V_{evap} - V_{seep} - V_{out} \quad (6.13)$$

where:

- V_i = dam or wetland volume on day, i;
- V_{i-1} = dam or wetland volume on day, i-1;
- V_{in} = inflow volume on day, i;
- V_{evap} = evaporation volume on day i, controlled by area-volume relationship for the impoundment (this can be enhanced for wetland vegetation transpiration);
- V_{seep} = seepage volume from the base of the impoundment on day i, controlled by an effective hydraulic conductivity and the impoundment area;
- V_{out} = outflow volume on day i, controlled by the storage volume in excess of the full volume. A user specified percentage of the seepage volume is added to the outflow volume.

The sediment load stored in the dam or wetland is determined by a mass balance of inflow sediment load and the change in sediment load in the water body due to settling of sediments. The mass of settled sediments is determined in Equations 6.14 and 6.15 by calculating the sediment concentration at the end of each day (C_f) from:

$$C_f = (C_i - \bar{C})e^{-ks.d_{50}} + \bar{C} \quad (6.14)$$

where:

- C_i = sediment concentration and the start of the day,
- \bar{C} = a user specified equilibrium sediment concentration,
- ks = a settling rate constant,
- d_{50} = the 50 percentile particle size of delivered sediment, determined from,

$$d_{50} = e^{0.41Cl + 2.71Si + 5.71Sa} \quad (6.15)$$

Cl, Si and Sa are the catchment parent soil clay, silt and sand textural fractions, respectively.

The initial concentration of nutrients in the water body is calculated by dividing the initial mass of nutrient by the initial volume of water. Nutrient transformation simulated in pond, wetlands and reservoirs are limited to the removal of nutrients by settling. Transformations between nutrient pools (e.g. $\text{NO}_3 \rightleftharpoons \text{NO}_2 \rightleftharpoons \text{NH}_4$) are ignored. Settling losses in the water body can be expressed as a flux of mass across the surface area of the sediment-water interface (i.e. flux = settling velocity \times concentration).

The mass nutrient lost via settling is calculated by multiplying the flux by the area of the sediment-water interface. Equation 6.16 gives the mass balance of N and P loads (M_{sett}) in farm dams or wetlands which is controlled by the inflow and is determined using a user specified settling velocity (V_{sett}) as:

$$M_{\text{sett}} = V_{\text{sett}} \cdot C_i \cdot A_i \quad (6.16)$$

where C_i is the initial concentration of N or P in the impoundment on day, i
 A_i is the area of the sediment-water interface on day, i (Lorentz *et al.*, 2012).

The water body is assumed to have a uniform depth of water and the area of the sediment-water interface is equivalent to the surface area of the water body.

6.3.1.2 Riparian buffer strips

Sediment loss in buffer strips is controlled, in part, by the width (w) of the strip (Neitsch *et al.*, 2005). For strip wider than 29 m, all the input sediment is trapped. The sediment output (Sed_{out}) for strips less than 29m wide is calculated from the inflow sediment (Sed_{in}) as in Equation 6.17 (Neitsch *et al.*, 2005):

$$\text{Sed}_{\text{out}} = \text{Sed}_{\text{in}} - \text{Sed}_{\text{in}} 0.367w^{0.2967} \quad (6.17)$$

N and P losses in buffer strips have been associated with strip width (w), slope towards the channel (Slope) and an empirical vegetation parameter (Veg: 0 for grass and 1 for forest) defined by Bereitschaft (2007) in which the nitrogen output is determined from Equation 6.18.

$$N_{out} = N_{in} - N_{in} \left[\left(24.6 + 55.3 \log(w) - 0.05 \text{Slope}^2 - 14.4 \text{Veg} \right) \right] \quad (6.18)$$

Equation 6.19 shows a similar relationship that is used for P output from a buffer strip (Lorentz *et al.*, 2012).

$$P_{out} = P_{in} - P_{in} \left[\left(24.6 + 55.3 \log(w) - 0.05 \text{Slope}^2 - 14.4 \text{Veg} \right) \right] \quad (6.19)$$

6.3.2 Connectivity aspects in NPS pollution migration in the Mkabela Catchment

Table 6.4 below shows the *ACRU-NPS* model parameters used to simulate the transport and fate of NPS pollutants through the wetlands, dams and buffer strips. The Mkabela Catchment nutrient and sediment migration is impacted by connectivity which is influenced by a series of 9 farm dams and 5 wetlands along the axial valley, ranging between 0.6-10 and 2.6-22 ha respectively, alongside riparian buffer strips in some areas with widths ranging from 10-15 m (Tables 6.4, 6.5 and 6.6).

Table 6.4: *ACRU-NPS* model parameters for wetlands, dams and buffer controls.

Parameters	Wetlands	Dams	Parameters	Buffer 1
alphaA (-)	29	10	Width (m)	10
betaA (-)	0.55	0.42	Slope (%)	10
alphaQ (-)	0.09	1.1	Vegetation (-)	1
betaQ (-)	0.8	0.9	Soil (-)	1
Seepage rate (mm/h)	0.8	1	<hr/> Parameters	<hr/> Buffer 2
Settling velocity (m/y)	50	250	Width (m)	15
Sediment decay (1/day)	0.02	0.184	Slope (%)	10
Initial storage (% full)	10	60	Vegetation (-)	1
Initial conc. Sed. (mg/l)	200	300	Soil (-)	1
Equil. conc. Sed. (mg/l)	20	20		
Initial conc. N (mg/l)	5	2.5		
Initial conc. P (mg/l)	0.5	0.02		
Vegetation (-)	3	-		

Surface area (SA) and volume (Q) of the wetland and dam varies with change in the volume of water stored in reservoir and their daily values are updated according to Equations 6.20 and 6.21:

$$SA = \alpha_A V^{\beta_A} \quad (6.20)$$

$$Q = \alpha_Q V^{\beta_Q} \quad (6.21)$$

where V is the volume of water in the impoundment,
 α_A & α_Q are coefficients and β_A & β_Q are exponents.

For natural lakes, measured phosphorous settling velocities most frequently fall in the range of 5 to 20 m/year although values less than 1 m/year to over 200 m/year have been reported (Chapra, 1997). Panuska and Robertson (1999) noted that the range in apparent settling velocity values for man-made reservoirs tends to be significantly greater than for natural lakes. Higgins and Kim (1981) reported phosphorous apparent settling velocity values from -90 to 269 m/year for 18 reservoirs in Tennessee with a median value of 42.2 m/year. A negative settling rate indicates that the reservoir sediments are a source of N or P; a positive settling rate indicates that the reservoir sediments are a sink for N or P.

Figure 6.8 illustrates the natural or man-made control structures in the stream network that have been shown to retard and attenuate the migration of sediments and nutrients through agricultural catchments (Bereitschaft, 2007; Knox *et al.*, 2008; Weissteiner *et al.*, 2013). Algorithms have therefore been developed that can route daily water discharge and sediments, nitrogen and phosphorus loads through farm dams, wetlands and riparian buffer strips (Lorentz *et al.*, 2012). For each land segment the simulated daily discharge and sediment, N and P loads are read into a “network” spreadsheet and resultant output discharges and loads are calculated for each control feature in the catchment network (Lorentz *et al.*, 2012).

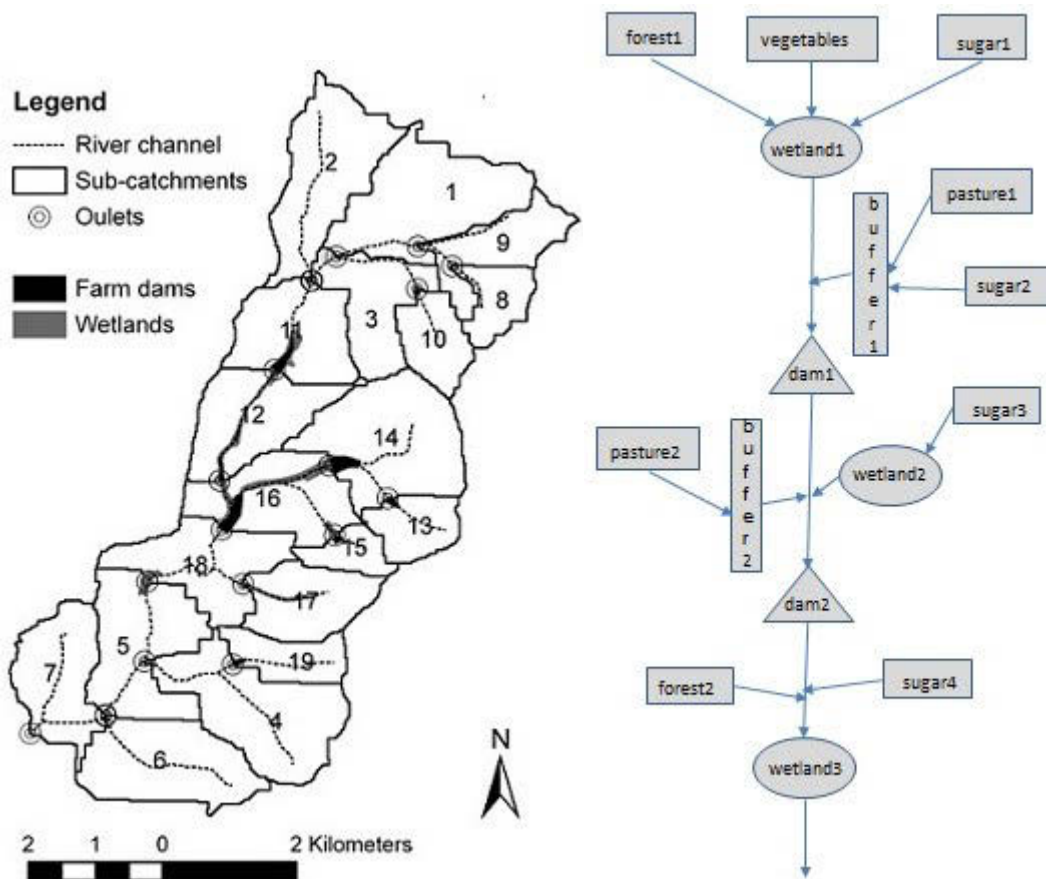


Figure 6.8: Sub-catchment boundaries, outlets, river channel locations, farm dams and wetlands (Le Roux *et al.*, 2013) (Left); simplified connectivity network of land segments with control structures in the Mkabela Catchment (Lorentz *et al.*, 2012) (Right).

Table 6.5 shows the sizes of the different land cover types (i.e. sugarcane 76%, forest 13%, pasture 8% and vegetable 3%) and soil types (i.e. Avalon-*Av*, Glencoe-*Gc*, Westleigh-*We*, Hutton-*Hu* and Cartref-*Cf*) (Le Roux *et al.*, 2006). These land segments have control structures that include wetlands, buffers and dams which influence downstream sediment and nutrient migration through the catchment (Kollongei and Lorentz, 2014). The largest land segment is under sugarcane that has an area of 1169 ha, all of it underlain by the Cartref soil type. The smallest land segment is pasture with an area of 9 ha under Glencoe soil type. The water balance in each farm dam and wetland is controlled by water balance equation that relates dam or wetland volume on a particular day to a previous day (Lorentz *et al.*, 2012). The water volume difference in a particular day is brought about by volume changes due to inflow, evaporation, seepage and outflow.

Table 6.5: Wetland, buffer and dam controls as influenced by connectivity within the different land uses and soil types.

Land use	Soil type	Area (km ²)	Control
Sugar1 (LS1)	Av	6.31	Wetland1 Area = 13.83 ha, Volume = 207,450 m ³
Forest1: Wattle (LF1)	We, Gc	0.61	
Cabbages (LV)	We	1.06	
Pasture1(LP1)	We, Cf, Gc	3.11	Buffer1 Width = 10m, Slope = 10 %
Sugar2 (LS2)	Cf, Gc	5.67	
Pollutant loads from Wetland1 and Buffer1 flow into Dam1			Dam1 Area = 9.5 ha, Volume = 283,200 m ³
Pasture2 (LP2)	Gc	0.09	Buffer2 Width = 15m, Slope = 10 %
Sugar3 (LS3)	Cf	7.32	Wetland2 Area = 22.46 ha, Volume = 336,900 m ³
Pollutant loads from Dam1, Buffer2 and Wetland2 flow into Dam2			Dam2 Area = 24.1 ha, Volume = 721,500 m ³
Forest2: Pinus (LF2)	Hu	4.80	Wetland3 Area = 10.24 ha, Volume = 153,600 m ³
Sugar4 (LS4)	Cf	11.69	
Pollutant loads from Dam2, Forest2 and Sugar4 flow into Wetland3			
Total Catchment Area		40.66	

Table 6.6 shows the sizes of dams and wetlands in the Mkabela Catchment. Wetland2 is the largest with an area of 22.46 ha while wetland3 with an area of 10.24 ha is the smallest. Dam2 with an area of 24.1 ha has the larger volume compared to dam1 with an area of 9.5 ha. The sizes of these controls will influence how NPS pollutants that pass through them will be attenuated. Dams are very effective in settling coarser sediments while wetlands are better in attenuating fine sediments with nutrients attached to them specifically nitrates and phosphorous. Dams can also capture fine-grained sediments in silt and clay dominated soil layers during some low magnitude events, but not as efficiently as it would with sand-sized sediments.

Table 6.6: Locations and sizes of wetlands and dams within the Mkabela sub-catchments

Sub-catchment	Farm dams	Dam area(ha)	Dam volume(m ³)	Wetlands	Wetland area (ha)	Wetland volume(m ³)
10	10	0.6	18600	-	-	-
11	11	5.9	175800	11	4.78	71700
12	12	3.0	88800	12	9.05	135750
	Dam1	9.5	283200	Wetland1	13.83	207450
13, 14	13	1.5	45900	-	-	-
	14	8.5	253500	-	-	-
15,16	15	1.4	40800	-	-	-
	16	10.5	315600	16	22.46	336900
				Wetland2	22.46	336900
17,18	17	0.6	17400	17	4.82	72300
	18	-	-	18	2.63	39450
19,5	19	1.6	48300	5	2.79	41850
	Dam2	24.1	721500	Wetland3	10.24	153600

Sugarcane fields located in the headwater areas of Mkabela Catchment have waterways that deliver water, sediments and associated nutrients to the upland channels. The NPS pollutants emanating from these areas are deposited in dams and wetlands sited within. Some of these upland channels however are short, draining relatively small areas, thus delivering minor amounts of sediment as they are geomorphically disconnected from the axial valley (Miller *et al.*, 2013). Miller *et al.* (2013) studied sediment fingerprints in Mkabela Catchment and suggested that silt- and clay-rich layers found within wetland and reservoir deposits of the upper and upper-mid sub-catchments were derived from the erosion of fine-grained, valley bottom soils frequently utilized as vegetable fields. Coarser-grained deposits within these wetlands and reservoirs resulted from the erosion of sandier hillslope soils extensively utilized for sugarcane, during relatively high magnitude runoff events that were capable of transporting sand-sized sediment off the slopes. Thus, the source of sediment to the axial valley varied as a function of sediment size and runoff magnitude.

Sediment exported from upper to lower catchment areas was limited until the early 1990s, in part because the upper catchment wetlands were hydrologically disconnected from lower parts of the watershed during low to moderate flood events. The construction of a drainage ditch through a previously unchanneled wetland altered the hydrologic connectivity of the catchment, allowing sediment to be transported from the headwaters to the lower basin where much of it was deposited within riparian wetlands. The axial drainage system is now geomorphically and hydrologically connected during events capable of overflowing dams

located throughout the study basin. The study indicated that increased valley connectivity partly negated the positive benefits of controlling sediment/nutrient exports from the catchment by means of upland based, best management practices.

CHAPTER SEVEN

7 ACRU-NPS MODEL SIMULATIONS IN THE MKABELA CATCHMENT

The *ACRU-NPS* model was applied to simulate hydrology and NPS pollution in the Mkabela Catchment. More specifically, it was used to simulate stream runoff, sediment yield and NPS pollutant loads (NO_3 and soluble-P). In most catchments agro-chemical losses are not monitored, whereas their application grows day by day to increase agricultural production. Since hydrology is the most important driver behind these losses, a well calibrated model for catchment hydrologic processes can be used to simulate NPS pollution loadings from a catchment. However, to improve the accuracy of such simulations, more process-oriented model validation is needed. Overall, parameterization of a hydrologic model for an individual catchment under different climatic and land cover conditions is useful to understand the hydrologic and associated processes of the catchments.

The results of simulations reveal that the *ACRU-NPS* model can be successfully utilized in characterising the stream runoff, sediment yield and associated NPS pollution of water and thus it can serve as a decision management tool in solving water quantity and quality problems. The results can be used as a decision support tool by stakeholders for designing an appropriate management strategy to control runoff and sediment from an area. It can also be used in water and fertilizer management in agricultural fields to minimize the NPS pollution losses hence improving nutrient use efficiency of rain fed crops.

7.1 Model Input Parameters

The *ACRU-NPS* model simulates runoff, sediment and nutrient (NO_3 and P) responses for defined land segments. In addition, algorithms have been developed external to the model to allow for connectivity by permitting routing of these responses through control features, which is critical to the fate of sediments and nutrient migration through the catchment. A preliminary parameterisation of *ACRU-NPS* for the Mkabela Catchment is described here.

7.1.1 Climatic data

Daily climatic data were obtained within the Mkabela Catchment from the automatic recording meteorological station for the period 2007-2012. Some of these data are shown in Figure 7.1. The weather variables were recorded on an hourly interval. These variables were later converted to average daily values of ambient maximum (TMAX) and minimum air temperature (TMIN), rainfall (RFL), relative humidity (RH) and potential evapotranspiration (ETo). This was necessary because the *ACRU-NPS* model requires climatic data to be input on a daily basis. The minimum temperatures (TMPCUT) required for leaf and shoot development are 10°C and 16°C (Inman-Bamber, 1994), respectively. For the *ACRU-NPS* model, TMPCUT used was 10°C which represents the mean temperature threshold for active growth to take place. Other important variables for the *ACRU-NPS* model obtained from the weather station but not plotted here include the solar radiation and the wind speed.

Figure 7.1 shows that the climatic data varied depending on the season of the year. During the summer period (October to March), there were a lot of rain events and the temperatures were normally high. This therefore gave rise to high potential evapotranspiration rates and consequently high relative humidity levels. During the winter season events (May to August), temperatures were normally lower as were rainfall events. This eventually caused lower potential evaporation rates that led to lower relative humidity levels.

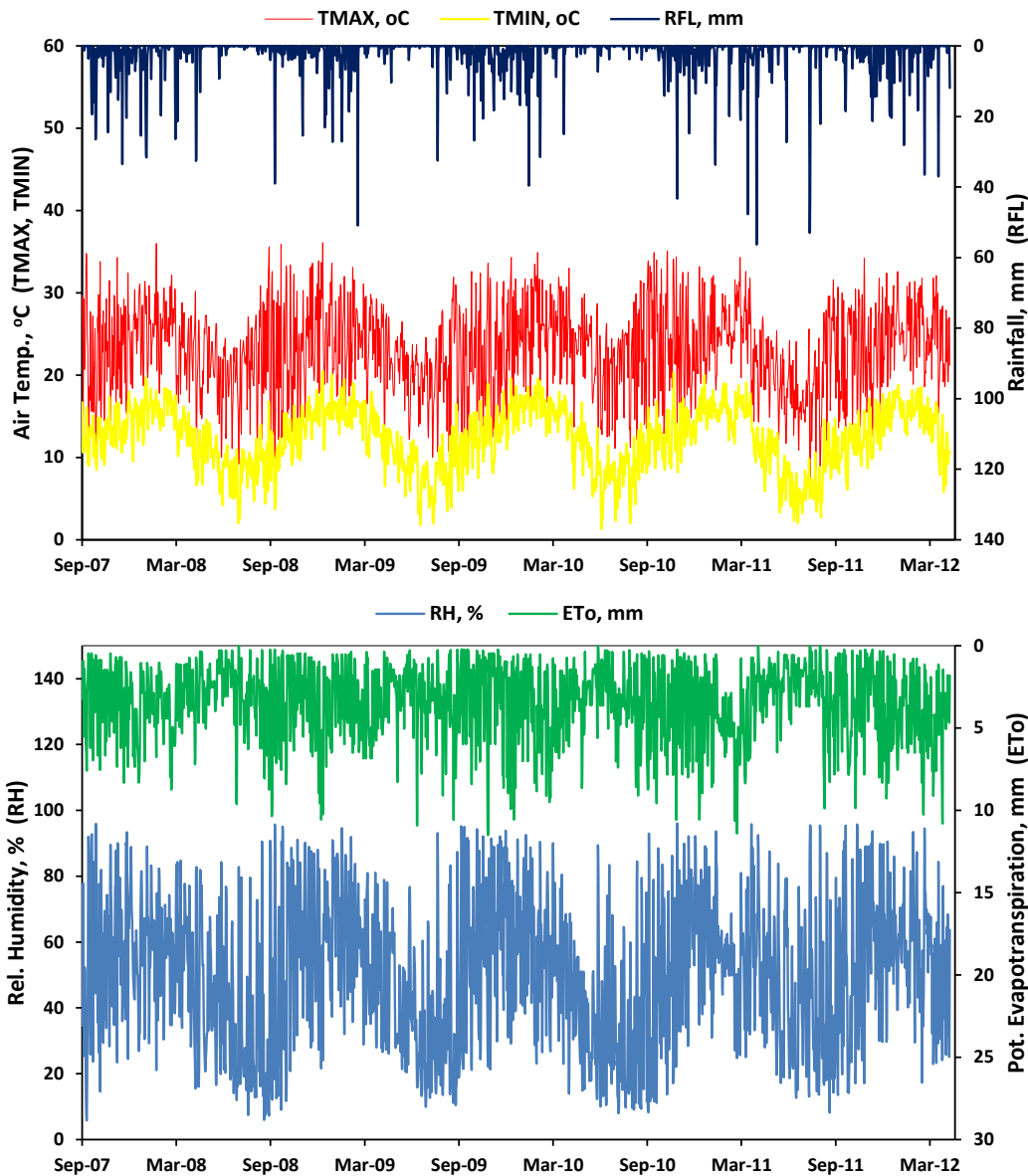


Figure 7.1: Daily weather station data for the Mkabela Catchment for the period 2007 – 2012.

Evaporation in the *ACRU-NPS* model has an important influence on simulations of the water cycle (Lorentz *et al.*, 2012). Specification of a daily time series of the A-pan equivalent evaporation must be chosen with care. For the simulations over the observation period, the potential evapotranspiration (ETo) was determined from the Mkabela research catchment meteorological record. The daily meteorological data series was used in the generation of reference potential evaporation using the FAO approach to the Penman-Monteith equation (Allen *et al.*, 1998). The calculation of soil water evaporation and plant transpiration were separated (EVTR = 2) as required in *ACRU-NPS*. No enhanced wet canopy evaporation and no enhanced CO₂ levels were activated in the simulations (Lorentz *et al.*, 2012).

7.1.2 Initial soil and nutrient parameters

Le Roux *et al.* (2006) surveyed the soils in the catchment on a very fine scale, particularly in the headwaters section of the catchment. The soil parameters extracted include the depths of soil horizons, which were in turn used to calculate the initial soil water content as 50% of the soil horizon, called SMAINI (Initial Soil Moisture -Horizon A) and SMBINI (Initial Soil Moisture -Horizon B) (Table 7.1). *ACRU-NPS* also includes a soil surface layer, which was simulated with a depth of 1cm (Lorentz *et al.*, 2012). Horizon A soil properties were adopted for the soil surface layer properties. Where Le Roux *et al.* (2006) described more than two soil layers, the B1 and B2 soil horizons were combined (using depth-weighting) in the parameterizations to give Horizon B properties.

Table 7.1: Depths (m) of soil horizons and initial soil water content for different soil forms.

Horizon/Soil Type	Avalon (Av)	Westleigh (We)	Cartref (Cf)	Glencoe (Gc)	Hutton (Hu)
A (DEPAHO)	0.30	0.264	0.25	0.297	0.347
B (DEPBHO)	0.55	0.536	0.50	0.603	0.704
A (SMAINI)	0.170	0.068	0.056	0.052	0.113
B (SMBINI)	0.170	0.145	0.131	0.101	0.238

The soil texture of Avalon (Av), Cartref (Cf) and Glencoe (Gc) soil forms were specified as sandy loam soils, Hutton (Hu) soil forms as clay soils and Westleigh (We) soil forms as loam soils. These soil textures were used to parameterize the fractions of saturated soil water to be redistributed daily from the soil horizons to the subsoil (Schulze, 1995). Other soil parameters are specified within the *ACRU-NPS* model along with the nutrient and soil parameter estimations provided in Appendix B where the equations for the calculations of soil and nutrient parameters were obtained from different literature sources. Appendix B lists the calculated values of the nutrient parameters for the different soil types found in the Mkabela Catchment. Appendix C shows the monthly means of crop coefficients, canopy interception losses in mm per rain day, root mass distribution in the topsoil, coefficient of initial abstractions for the different land covers and percentage surface cover.

7.1.3 Fertilizer and manure applications

Estimates for manure and fertilizer applications were obtained from different sources. Tables 7.2 and 7.3 show respectively, the amounts of fertilizer and manure applied to sugarcane in the Mkabela Catchment in KwaZulu-Natal (KZN) Province.

Table 7.2: Average rates (kg/ha) of fertilizer use in KwaZulu-Natal Province (FAO, 2005)

Crop	N	P ₂ O ₅	K ₂ O	P	K
Sugar cane	92	57	133	25	110
Pastures	50	44	7	19	6
Vegetables/cabbages	170	159	120	70	100

Source of conversion equations: $P = 0.44 * P_2O_5$; $K = 0.83 * K_2O$

(<http://www.home-garden-soil-improvement.com/nutrients-in-fertilizer.html>)

Table 7.3: Manure rates and nutrient composition (Ministry of Agric. KZN, 2005).

Type of manure (WASCMP)	Rate (t/ha) (WASAPR)	Nutrients supplied (kg/ha)		
		N	P	K
Cattle	5	10	10	50
	20	40	40	200
Poultry	5	162	54	65
	20	648	216	260

The information obtained after interviewing farmers is given in Table 7.4. Before 2003, the farmers in the Mkabela Catchment used only superphosphates, potassium chlorides and lime of ammonium nitrates as fertilizers in the sugarcane fields. After 2003, however, the farmers started using composted farmyard manure which consisted mainly of cattle, pigs, poultry, etc. manure and sugarcane press mud (SPM). The current practise is to apply compost farmyard manure during planting followed by several top dressings using lime of ammonium nitrate (Table 7.4).

Table 7.4: Fertilizer rates for sugarcane (Source: farmer interviews).

Fertilizer Rates (kg/ha)	Sugarcane
• Manure since 2003 for sugarcane	
• Topdressing LAN (28 % N)	150
At planting	
• N:P:K (3:2:1)	
• KCL (50% K)	

Fertilizer Rates (kg/ha)	Sugarcane
Before 2003	
• Superphosphates (10.5 % P)	200
• KCL (50% K)	150
• LAN (28% N)	400

SPM can be directly transported to the fields from sugarcane mills and applied as an organic enhancement in the field which result in increased sugarcane yield and decrease in demand of inorganic fertilizers (Sardar *et al.*, 2006). Table 7.5 shows the percentage of nutrients present in sugarcane press mud used as bio-fertilizer.

Table 7.5: Percentage of nutrients present in sugarcane press mud (SPM).

Nutrients	%
Moisture	50-65
Fiber	20-30
Crude wax	7-15
Sugar	5-12
Crude protein	5-10
Nitrogen	2-2.5

Source: (Sardar et al., 2006)

During simulations it was assumed that 100 % of the total area under sugarcane and cabbages would have received a full nutrient loading of fertilizer and manure within the first 5 months in every 18 month cropping cycle for sugarcane and within 2 months in every 6 month cropping cycle for cabbages. It was assumed that an equivalent of 20 t/ha cattle manure representing 40 kg/ha of N was added to 42 kg/ha of N from topdressing (28% N of 150 kg/ha of fertilizer) to give 82 kg/ha N for use in sugarcane fields. Similarly, 40 kg/ha of P contained in 20t/ ha of cattle manure was used in sugarcane. This assumption was necessary because the various nutrient contents in the farmyard compost manure used in Mkabela is not known. Simulations excluded fertilizer use in forests and pastures.

The following application rates were determined and used in *ACRU-NPS* simulations:

Sugarcane: for NO₃-N: 16.4 kg/ha/month
for phosphorus (P): 8 kg/ha/month
Cabbages: for NO₃-N: 85 kg/ha/month
for phosphorus (P): 35 kg/ha/month

The parameterization indicates that for sugarcane the fertilizers were applied 5 times in a cropping cycle, beginning on the 1st day of planting and the remaining four subsequent portions equally spaced every month. Fertilizers were applied on cabbages twice every cropping cycle, beginning on the 1st day of planting and the second application after a month.

7.1.4 Other agricultural practices

Several assumptions were made while implementing the simulations of agricultural practices. Actual tilling in the catchment took place before the planting of cabbages, as well as during the fertilizer application on sugarcane with cattle manure (tilling between the sugarcane rows). During simulations it was assumed that all sugarcane fields were tilled on the first planting date along with the application of cattle manure, to a depth of 15cm, using the “disk harrow in tandem” method. Model simulations incorporated tilling of cabbage fields, to a depth of 15cm during planting of cabbages, using the same tilling method. Pastures and forests were not tilled in the simulations.

Cabbages were harvested after every 165 days while sugarcane harvesting took place after every 540 days. Pines were not harvested because it takes place after every 15 years. Wattle trees should be harvested after 5 years. Pasture harvesting took place every 3 months. Sugarcane and forests were simulated as perennial plants (plants which last for several seasons) while cabbages and pastures were classified as non-perennials. The simulation period was between 1st August 2006 and 22nd April 2012.

7.2 Model Calibration and Validation

Calibration was restricted to runoff, nutrients and sediment measurements from the ISCO sampler and H-flume at the outlet of Flume 2 from October 2007 to March 2008, from 6 rainfall events within this period. No downstream calibration was done because instruments were only installed upstream of the catchment. Flume 2 catchment area used for calibration was 58 ha and had sugarcane grown in it. The soils available at this area were Avalon type with the following parameters: organic matter (0.67-1.2 %), bulk density (1.65 %), base saturation (62-83 %), pH (4.5-5.8), clay content (11-18.7 %) and silt content (22.7-24.3 %).

Calibration of the *ACRU-NPS* model mainly focused on the hydrological part of the model adjusting the most sensitive parameters. The *hydrological component* was calibrated by adjusting both the QFRESP (storm flow/quick flow response coefficient) and COFRU (base flow response coefficient). QFRESP represents the fraction of total storm flow that will runoff from the catchment on the same day as rainfall event and was found to be 0.6 during calibration. COFRU represents the fraction of ground flow store that becomes stream flow on a given day which was found to be 0.0012 after calibration.

The *erosion component* was calibrated by adjusting the MUSLE soil erodibility and support management practises. The MUSLE equation allows the prediction of sediment yields for an individual event directly without using sediment delivery ratio. Appendix D shows a summarized table of all parameters required to estimate sediment yield using the MUSLE equation for the different hillslopes in the Mkabela Catchment.

The *ACRU-NPS nutrient components* that were found to be sensitive to the simulated nutrient loads were RD (plant rooting depth), LAI (leaf area index), OM (fresh organic matter) and RNCONC (rainfall NO₃-N concentration). FON (fresh organic nitrogen in crop residue) is represented as 20% mineralizable soil-N (PLRSN) and 80% NO₃-N (SNO3). Adjusting the RNCONC was effective in NO₃-N calibration. The model performance was tested by subjecting the data to statistical tests. The observed H-flume data for selected events from both Flume 1 and Flume 2 between Jan' 09 to Jan' 12 that were used in model validation are given in Appendix E.

7.2.1 Model evaluation criteria

The performance of the model for simulating hydrologic variables was evaluated with the help of graphical comparisons and various statistical tests. The statistical evaluation was performed between daily measured values and model outputs in a similar way as was done by Mishra and Kar (2012) and Mishra *et al.* (2009). The following parameters were determined; the student's *t*-test of significance (two-tailed), linear regression (coefficient of determination, R²), Nash and Sutcliffe coefficient of efficiency (NS_E), Root mean square error (RMSE) and Percent deviation (Dv) tests (Table 7.6). A summary of statistical evaluation output results from the SigmaPlot software is given in Appendix F.

Table 7.6: Statistical *ACRU-NPS* model performance.

Criteria	Runoff (mm)	NO ₃ (kg/ha)	P (kg/ha)	Sed. (kg/ha)	Formula
Coefficient of determination (R ²)	0.94	0.98	0.95	0.98	$R^2 = \frac{\sum_{i=1}^N [O_i - O_{Avg}] [S_i - S_{Avg}]}{\left[\sum_{i=1}^N [(O_i - O_{Avg})^2]^{0.5} \sum_{i=1}^N [(S_i - S_{Avg})^2]^{0.5} \right]}$ <p>Equation 7.1</p>
Nash and Sutcliffe coefficient of efficiency (NS _E)	0.87	0.96	0.90	0.95	$NS_E = 1 - \frac{\sum_{i=1}^N [S_i - O_i]^2}{\sum_{i=1}^N [O_i - O_{Avg}]^2}$ <p>Equation 7.2</p>
Overall % deviation (D _v)	0.01 %	3.82 %	6.21 %	0.66 %	$D_v (\%) = \frac{\sum_{i=1}^N [O_i - S_i]}{\sum_{i=1}^N [O_i]} \times 100$ <p>Equation 7.3</p>
Root mean square error (RMSE)	0.37	0.44	0.006	3.35	$RMSE = \sqrt{\frac{1}{N} \sum_{i=1}^N (O_i - S_i)^2}$ <p>Equation 7.4</p>
Ratio	99.99 %	96.18 %	93.79 %	99.34 %	$Ratio = \frac{Q_{sim}}{Q_{obs}}$ <p>Equation 7.5</p>
Student t- test	-5 × 10 ⁻⁶	-0.005	-0.014	-0.001	(t _c - critical = 1.97)

where $O_i = i_{th}$ observed parameter, O_{Avg} = mean of the observed parameter, $S_i = i_{th}$ simulated parameter, S_{Avg} = mean of model simulated parameter and N = total number of events.

The coefficient of determination (R²) in Equation 7.1 (Table 7.6) describes the proportion of the total variance in the measured data explained by the model and it ranges from 0.0 to 1.0. Higher values indicate better agreement. Equation 7.2 gives the basic goodness-of-fit criterion according to Nash-Sutcliffe (1970) simulation efficiency (NS_E) or modelling efficiency. The NSE values vary from a negative value to 1. A value of 1 indicates a perfect fit whereas a negative value shows that the prediction of the model is worse than the average of the observed data.

Bingner *et al.* (1989) suggested the overall percentage deviation (D_v) in Equation 7.3 as a measure of the accumulation of differences in observed and simulated values for the

particular period of analysis. It predicts performance and the level of acceptance of a model. For a perfect model, D_v is equal to zero. According to Mishra and Kar (2012), the threshold values for underprediction or overprediction were considered low, moderate, and severe, when D_v was $\leq 10\%$, 10-20%, and 20-30% of the measured values respectively. Model simulation accuracy was considered as acceptable when $D_v \leq 20\%$.

Other measures of the model's accuracy used in the study were the root mean square error (RMSE) (Equation 7.4) and ratios of simulated to the observed data shown (Equation 7.5). The RMSE measures how far on average the error is from 0 for the pair of data sets (observed and simulated data) with a value equal to 0 showing a perfect simulation. A ratio of simulated to observed discharge (Equation 7.5) less than 100% indicates parameter uncertainty and model error.

7.2.2 Calibration of runoff, nutrient and sediment yields

The measured daily runoff, nutrient and sediment yield from the catchment during the summer months of 2007 and 2008 have been used for model calibration, whereas, measured NPS pollutant loads during 2009 to 2012 were used to evaluate the model performance. Calibration was restricted to runoff, nutrients and sediment measurements from the ISCO sampler and H-flume at the outlet of Flume 2 (58 ha) from October 2007 to March 2008, from 6 rainfall events within this period (Figure 7.2). It mainly focused on adjusting the most sensitive parameters of the hydrological part of the model. The hydrological component calibration was done by adjusting both the QFRESP (stormflow/quickflow response coefficient) and COFRU (baseflow response coefficient). The erosion component was calibrated by adjusting the MUSLE soil erodibility and support management practises. A total of 12 rainfall events for the period 2009 to 2012 were available for evaluating the model performance in simulation of pollutant loads.

7.2.2.1 Runoff and root zone water balance

The model was run for the period 2006 to 2012 using the measured meteorological data and comparisons were made for the summer period of October 2007 and March 2008.

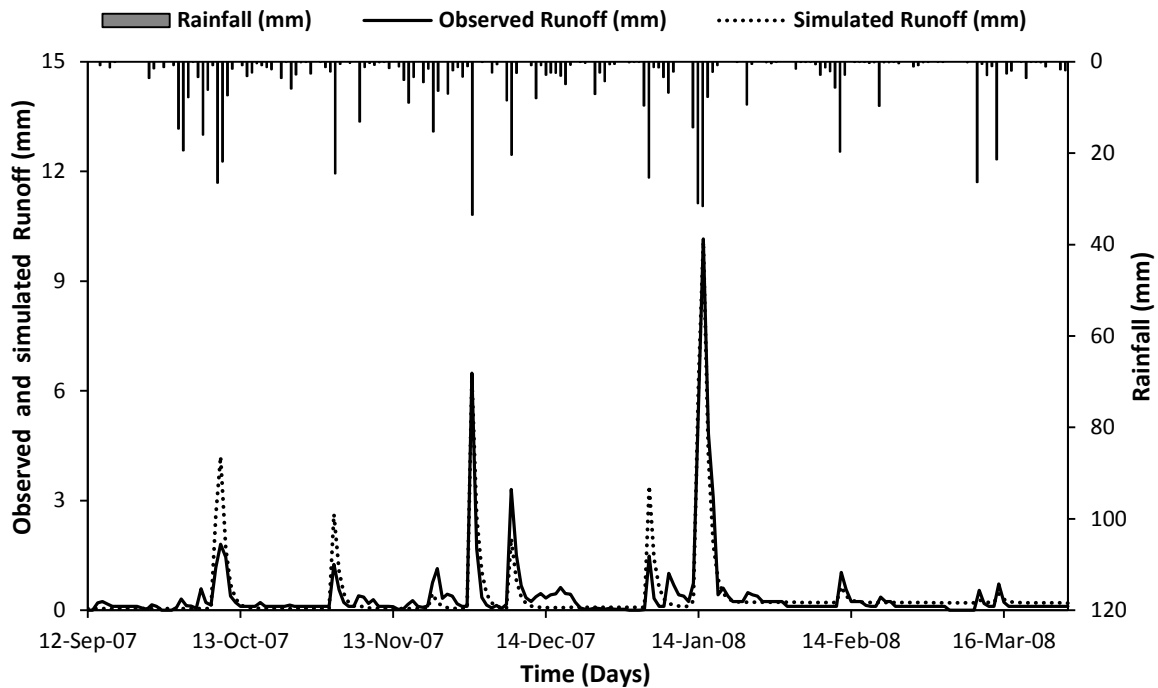


Figure 7.2: Hydrologic calibration of ACRU-NPS model for daily runoff for the period October 2007 and March 2008.

The measured and simulated daily runoff from Flume 2, shown in Figure 7.2, indicates that the simulated runoff follows a similar trend as that of measured runoff. From the graphical comparisons (Figures 7.2 and 7.3) it can be inferred that the calibrated parameters for the studied catchment realistically represent the nature and behaviour of the catchment. The marginal differences may have resulted from inaccuracies associated with input data to the model, specifically, subtle differences in channel, soil and subsurface properties (Van Liew and Garbrecht, 2003).

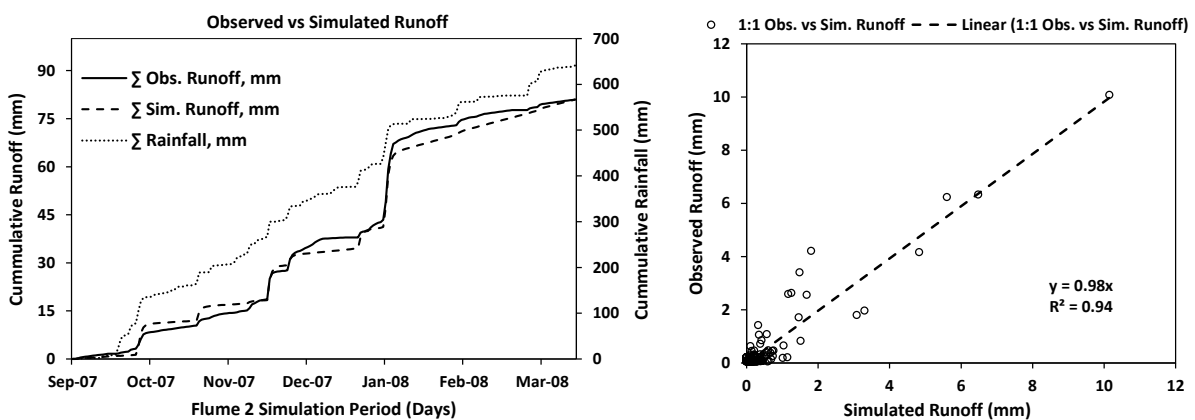


Figure 7.3: Cumulative runoff for observed and simulated runoff (left) and 1:1 comparison between observed and simulated runoff (right).

The results of the statistical tests outlined in Table 7.6 showed that the measured and the simulated mean runoff was not significantly different at the 95% confidence level during hydrologic calibration of the model as the calculated student's t -test value was lower than the critical limits ($-0.000005 < 1.97$). The values of R^2 (0.94) and NS_E (0.87) also indicated agreement between the measured and simulated results. The value of RMSE for daily runoff (0.37mm) showed that the model slightly deviated from the respective measured runoff.

Figure 7.4 shows saturated drainage, baseflow and baseflow storage throughout the *ACRU-NPS* simulation. During calibration the final value of ABRESP (i.e. the fraction of “saturated” soil water to be redistributed daily from the topsoil into the subsoil store when the topsoil is above the drained upper limit) was set to 0.60. Final BFRESP value was 0.75 and it represented the fraction of “saturated” soil water to be redistributed daily from the subsoil into the intermediate/groundwater store when the subsoil is above its drained upper limit. For the whole period of simulation there was more cumulated saturated water draining from the A-Horizon to B-Horizon (SUR1) than that draining from the B-Horizon to groundwater (SUR2).

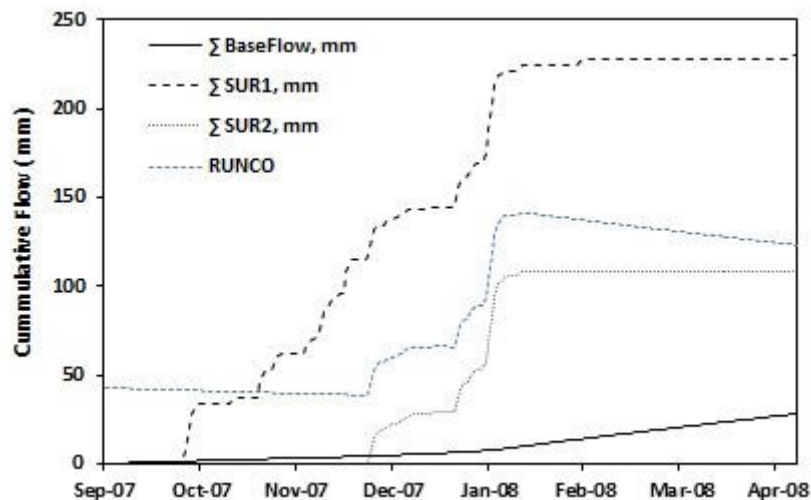


Figure 7.4: Saturated drainage and base flow storage.

At the onset of summer rains in October there was little base flow storage (RUNCO) because saturated drainage was from A-Horizon to B-Horizon only. However, as the rainy season continued (from October towards April) vertical drainage contributions from B-Horizon to the groundwater zone was realised (around December). The increased hydrological connectivity between the two soil horizons (A and B) resulted in more water reaching the

groundwater store and hence the increase in base flow storage. This later culminated in more base flow being constituted in storm flow as opposed to surface runoff as in the beginning. Baseflow can be separated from stormflow using isotope techniques.

The results from the root zone water balance (Figure 7.5) indicates that during the simulation period around 14th January 2008, the soil water contents in horizons A (STO1) and horizon B (STO2) had exceeded the field capacities in both horizons (i.e. FC1 and FC2 = 0.32) thereby resulting in soil surface runoff as confirmed in Figure 7.2. During rainy seasons (October to April), there is more soil water in the A-horizon than in the B-Horizon. Most of the water is transpired from the A- Horizon (ATRAN1) as crop growth proceeds. This in turn results in a more rapid LAI increase (VOGLAI).

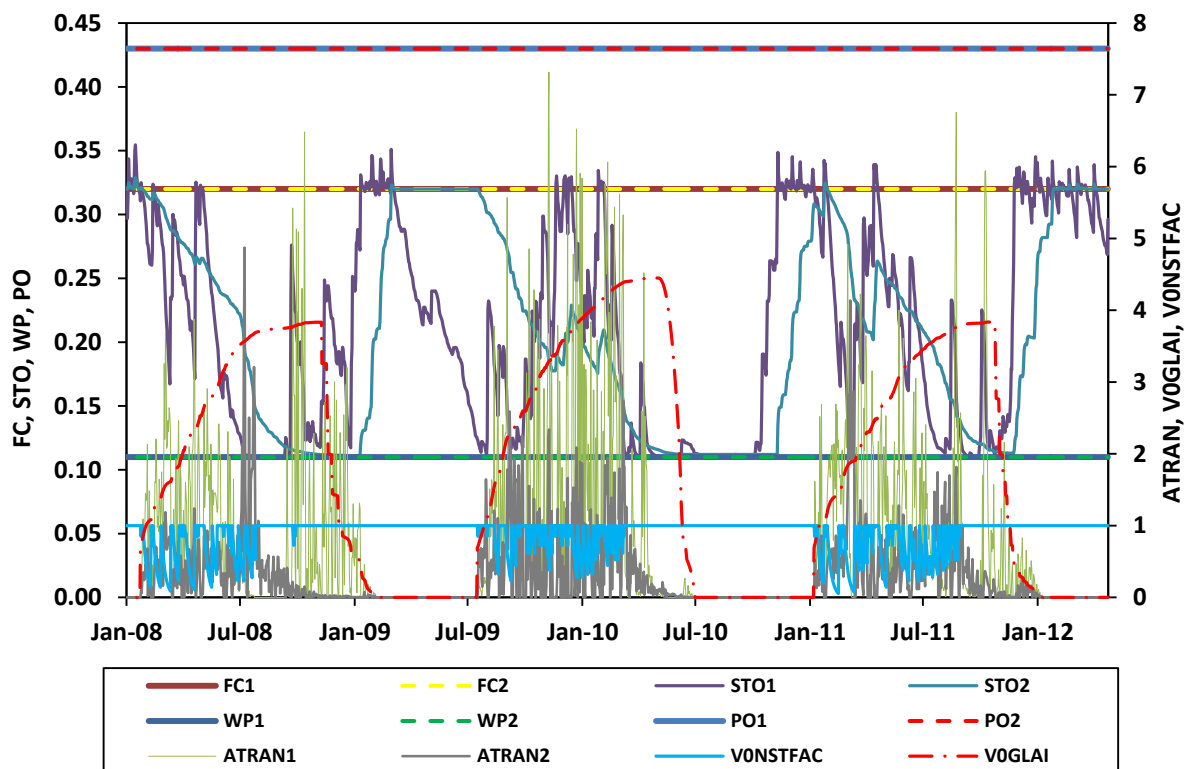


Figure 7.5: Root zone water balance for simulation period 2008 -2012.

The onset of plant water stress is determined by a constant of 0.2 (CONST = 0.2). This constant is the fraction of the plant-available water within the soil horizon at which total evaporation is assumed to drop below the maximum evaporation during drying of the soil. During the early stages of plant growth, sugarcane experiences less water stress because there is an abundance of water. The rapid LAI increase associated with N-uptake from the rapidly growing crop (indicated by a steep slope in VOGLAI) results in more nitrogen stresses

(V0NSTFAC) (Figure 7.5). At later stages of the season, however, rainfall decreases along with the soil water content in the A- Horizon. Since the crop has now developed deeper roots it is forced to transpire more B-Horizon (ATRAN2) water. This eventually results in reduced LAI growth (indicated by flatter slope) and rapid depletion of soil moisture contents in both horizons. The trend is shown in Figure 7.5 as moisture contents STO1 and STO2 approach the wilting points $WP1 = 0.11$ (A-Horizon) and $WP2 = 0.11$ (B-Horizon). The soil porosities for A-Horizon (PO1) and B-Horizon (PO2) were both 0.43 which indicates the soil water content at saturation.

7.2.2.2 Nitrate (NO_3)

The model results were compared with the measured NO_3 loads at the outlet of Flume 2 on different events during the simulation period. The simulated events shown in Figure 7.6 indicate that the NO_3 loads (kg/ha) in the runoff were, in general, reasonably well predicted by ACRU-NPS for most events; for a few events loads were under-estimated.

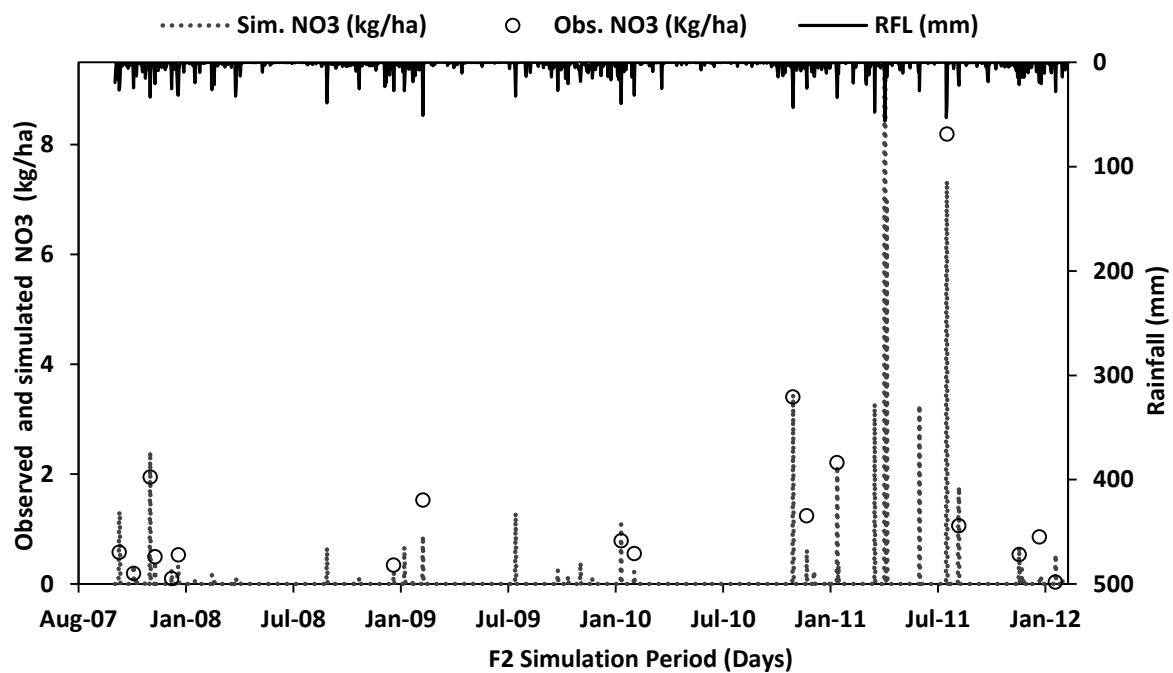


Figure 7.6: Hydrologic calibration of *ACRU-NPS* model for daily NO_3 yield (kg/ha) for the period October 2007 and March 2008 and validation for the period Jan 2009 and March 2012.

The statistical test evaluation of the measured and simulated NO_3 loads revealed a close agreement at the 95% level (t -calculated, -0.005, was less than t -critical, 1.97). A close agreement between the measured and simulated NO_3 was also indicated by the high

coefficients of determination (0.98) and Nash-Sutcliffe simulation efficiencies (0.96) with root mean square errors of 0.44 kg/ha. The percentage deviation (3.82%) indicated low under-prediction. Hence predictions were within the acceptable level of accuracy (96.18%).

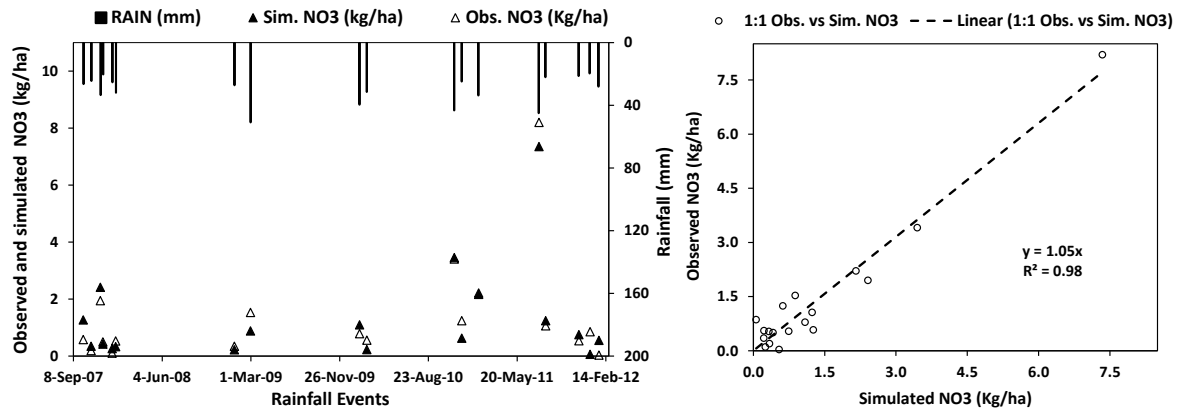


Figure 7.7 Comparison of observed and simulated NO₃ yield (kg/ha) (left) and their scatter comparison (right) generated by the ACRU-NPS model for events occurring between Sep. 2007 and Feb. 2012.

The scatter comparison between measured and simulated NO₃ loads for the rainfall events studied show slight under-prediction for at least some observations. However, the statistical analyses suggest that the predictions were within acceptable accuracies. Figure 7.7 (left) shows some rainfall events where prominent high loads were generated from rainfall events of almost similar magnitudes. One such event occurred on August 2011 (winter season) and this may be attributed to a high concentration of nitrates in the base flow which could probably have its source from the summer events of the previous season that had percolated as groundwater.

7.2.2.3 Phosphorous (Soluble-P)

The comparisons between the measured and simulated values of water soluble-P loads for selected periods between 2007 and 2012 are presented in Figure 7.8. The scattergram comparison of the same are presented in Figure 7.9. The simulated results, shown in Figure 7.8, reveals that soluble-P is under-predicted by the model for at least for some of the observation dates. However, the results of the statistical tests performed on the measured and simulated soluble-P show that the values are not significantly different at the 95% confidence level.

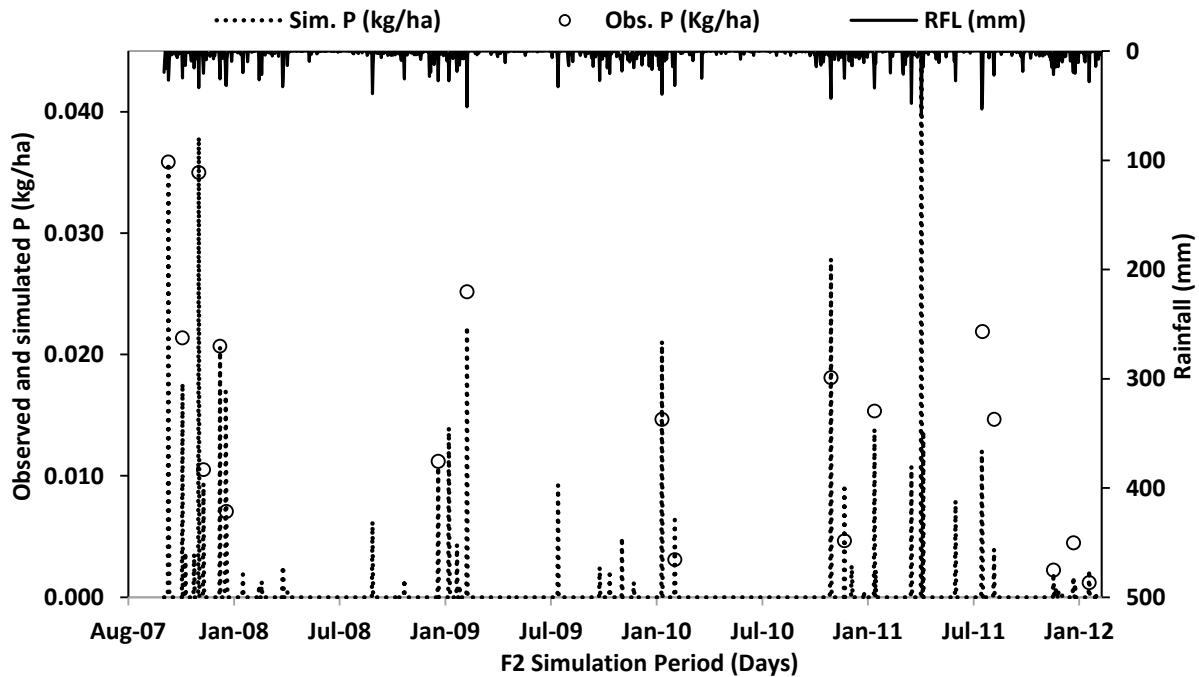


Figure 7.8: Hydrologic calibration of *ACRU-NPS* model for daily P yield (kg/ha) for the period October 2007 and March 2008 and validation for the period Jan 2009 and March 2012.

The R^2 and NS_E for the simulated soluble-P at the 95% confidence level was 0.95 and 0.90, respectively. This indicated a close agreement between the measured and simulated values. The RMSE was 0.006 kg/ha, a value close to 0. The D_v value indicates that soluble-P was under predicted by 6.21%, which was lower than the level of acceptance of 20% (Mishra and Kar, 2012). Moreover, other statistical comparisons, for instance the calculated student t -test showed a value of -0.014 compared to the t -critical value of 1.97. Thus, performance of the model is within the acceptance level for this particular student t -test.

The scatter gram between the measured and simulated soluble-P loads for the rainfall events studied show under-prediction for some of the observations (Figure 7.9). Some of the observed values were on the upper side of the 1:1 line, indicating higher observed soluble-P values than simulated during some peaks. The two outliers of 26th July 2011 shown in Figure 7.9 (*right*) illustrate higher values for observed soluble-P than simulated.

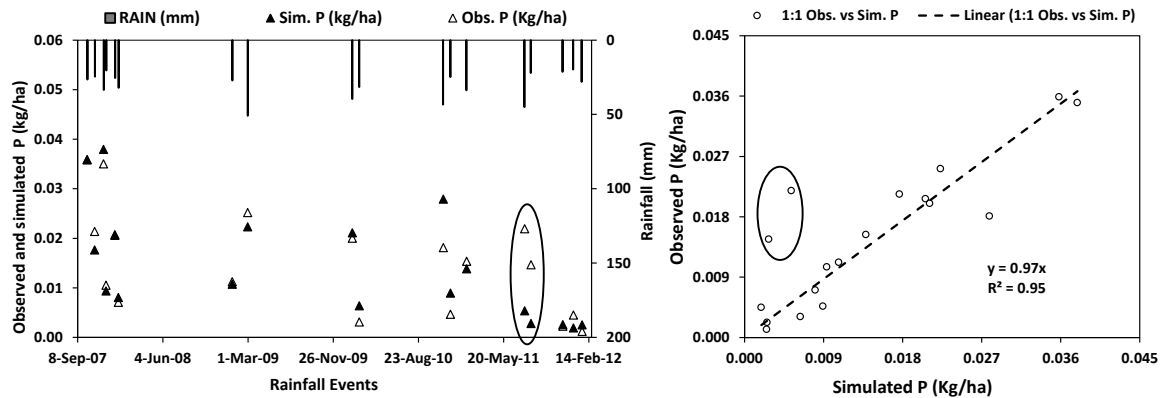


Figure 7.9: Comparison of observed and simulated P yield (kg/ha) (left) and their scatter comparison (right) for the *ACRU-NPS* model.

According to Lorentz *et al.* (2011) much of the P transport in contributing hillslopes in the Mkabela Catchment is in the dissolved phase and is likely to occur in the subsurface during recession and low flow sequences in winter. The *ACRU-NPS* model should be improved to capture this important contribution mechanism for nutrients in the landscape in the subsurface, where lateral discharge occurs in the intermediate layer between the sandy soil and bedrock. This could be the reason for the higher observed value compared to simulated soluble-P values.

7.2.2.4 Sediments

The daily measured and simulated values of sediment yield are presented and compared graphically in Figure 7.10. The predicted daily values matches well with the trend of the measured sediment yield throughout the calibration period. However, the model underestimates the daily sediment peaks in some instances and overestimates them for other events. A high intensity summer rain could generate more measured sediment yield compared with the simulated counterpart, which is estimated on the basis of total quantity of rainfall in a day. Because of this, some peaks of simulated sediment yield were not well matched with their measured counterparts. Nevertheless, the overall prediction of the daily sediment yield during the calibration period showed close agreement with its measured counterpart.

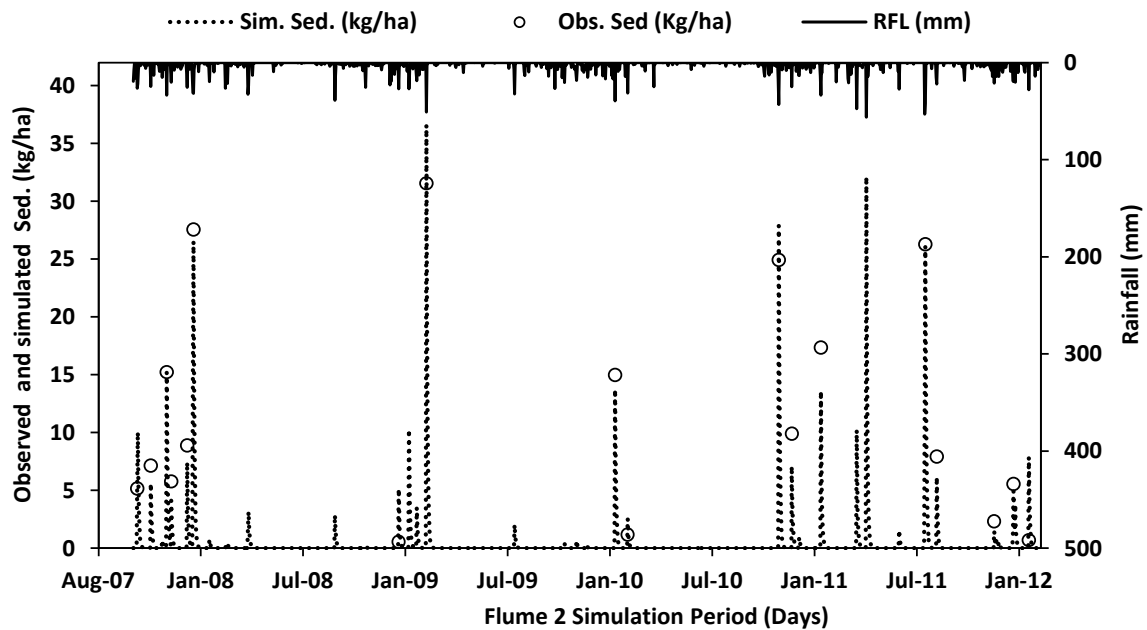


Figure 7.10: Hydrologic calibration of *ACRU-NPS* model for daily Sediment yield (kg/ha) for the period October 2007 and March 2008 and validation for the period Jan 2009 and March 2012.

Figure 7.11 shows the simulated yields were distributed along the 1:1 line for both low and high values of the measured sediment. However, some of the values were on the lower side of the 1:1 line, indicating higher simulated sediment than observed, particularly during low peaks. The results of the statistical analyses performed to compare the simulated daily sediment yield with their measured counterparts are presented in Table 7.6.

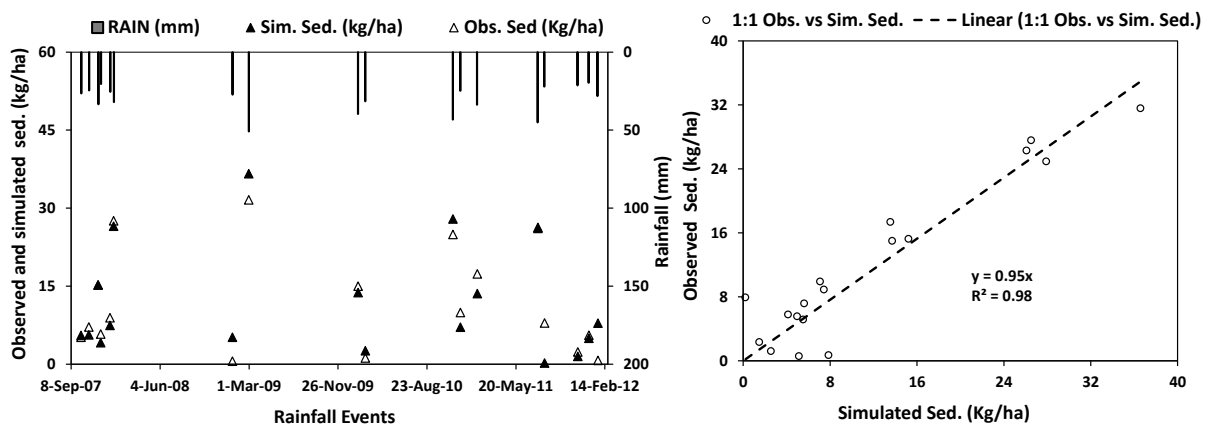


Figure 7.11: Comparison of observed and simulated sediment yield (kg/ha) (left) and their scatter comparison (right) for the *ACRU-NPS* model.

The student's *t*-test mean values of measured and simulated sediments were not significantly different at the 95% level of confidence, because *t*-calculated (-0.001) was less than *t*-critical (1.97). High values R^2 (0.98) and NS_E (0.95) showed that the simulated sediment yields were in close agreement with their measured counterparts. RMSE of 3.35 kg/ha and Dv of 0.66% further indicated that the model predictions were within the acceptable level of accuracy.

7.2.3 Calibration of sugarcane yields

Knisel (1993) determined the per cent nitrogen content of the dry matter (cN) and crop yield (CY) from Equations 7.6 and 7.7 given below:

$$cN = c_1 (GRT)^{c_2} \quad (7.6)$$

$$CY = \frac{TDM}{DMR} = GRT \times PY \quad (7.7)$$

where: cN = Demand nitrogen content of the crop;
 GRT = Growth ratio expressed as a ratio of actual to potential LAI (base LAI);
 c1 = is the Scale factor;
 c2 = is the Shape factor;
 CY = Crop yields;
 TDM = Total Dry Matter;
 DMR = Dry Matter Ratio and
 PY = Potential Yield.

Figure 7.12 shows the N concentration in plants as a function of plant maturity. Equations 7.6 and 7.7 show that the crop yields (CY) can be increased by either increasing the potential yield (PY) or lowering the demand N concentration (cN) through lowering of the scale factor c1.

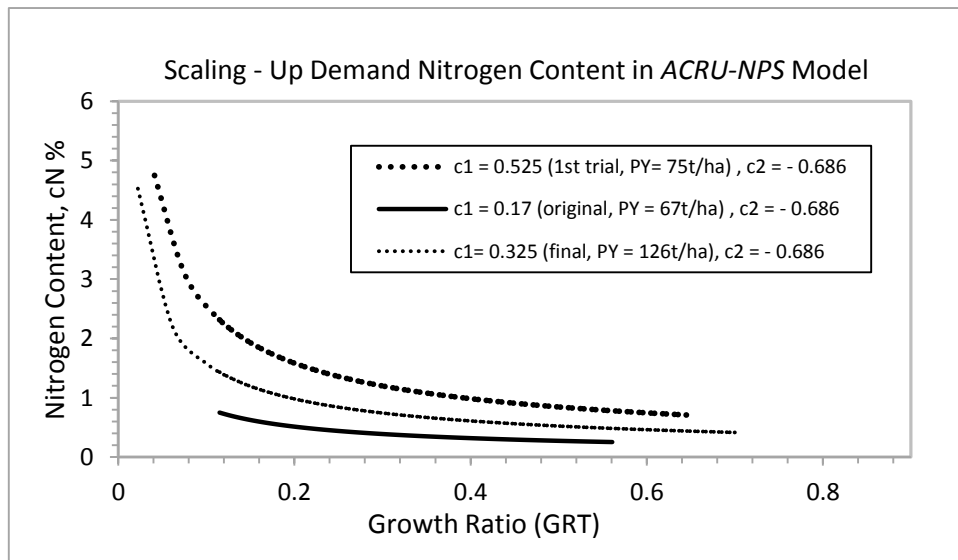


Figure 7.12: Demand nitrogen concentration as a function of growth ratio for sugarcane. Solid line from original data base; dashed lines for the increased nitrogen demands.

From the initial runs the *ACRU-NPS* model was unable to predict sugarcane yields that were similar to the observed (actual) yields from the Mkabela Catchment (SASA, 2012). The simulated sugarcane yields from the model were lower than the observed sugarcane yields. It was also noted that the quarter fertilizer application rate produced similar yields to the base fertilizer application rate (Figure 7.13).

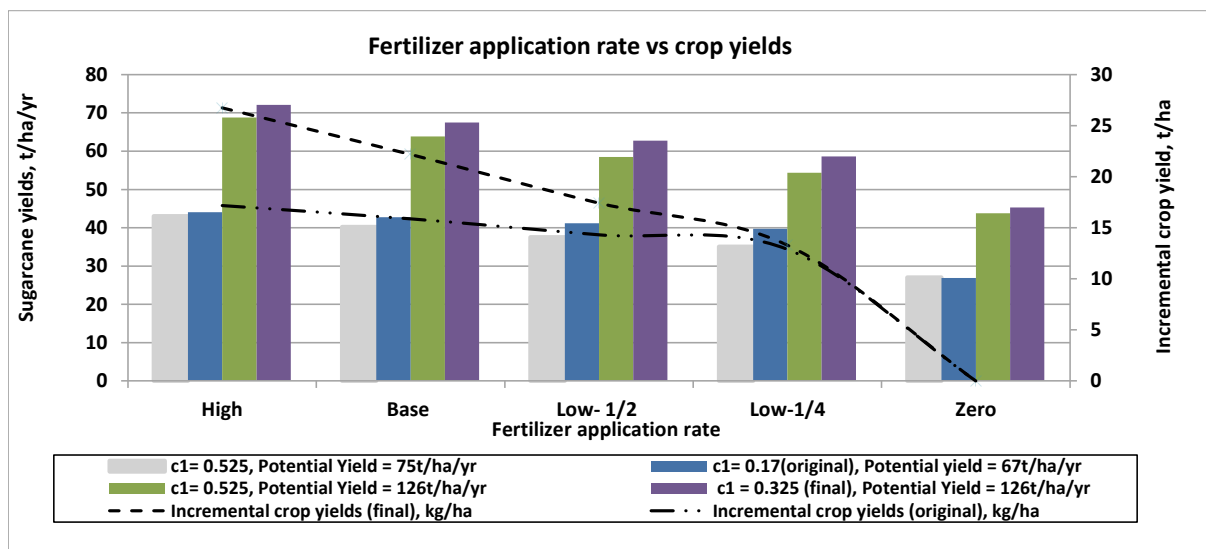


Figure 7.13: Comparison of sugar cane yield for various N fertilizer applications and potential yields, using values of $c1 = 0.17$ (initial), 0.325 (final) and 0.525 . The dotted lines indicate the incremental crop yield for the different fertilizer applications compared to the use of no fertilizer.

The following observations were made during the calibration of the *ACRU-NPS* model for the crop yield component (Figure 7.13):

- Increasing the PY from 75t/ha to 126t/ha while maintaining $c1 = 0.525$ increased the simulated crop yields.
- Lowering $c1 = 0.525$ to $c1 = 0.325$ while maintaining the PY = 126t/ha increased the crop yields slightly.
- The simulated base scenario average sugarcane yields of 67.5t/ha/yr for 50 years (1950-1999) using $c1 = 0.325$ and PY = 126t/ha was comparable to the observed crop yields of 67.7t/ha for the Mkabela Catchment for the period 1997- 2011.
- By comparing the original runs ($c1 = 0.17$, PY = 67t/ha) with the final runs ($c1 = 0.325$, PY = 126t/ha), wider ranges in incremental crop yield is realised in the later as compared to the former when fertilizer rates are increased from low-1/2 towards high.

A sugarcane crop N55/805 on trials at the Agronomy Department in Mt Edgecombe SASA Station on a coastal red sand soil achieved a maximum crop yield of 142 t/ha/yr and the succeeding 12 month ratoon crops gave similar or slightly higher yields (Glover, 1972).

Figure 7.14 shows the *ACRU-NPS* model simulations using PY = 126t/ha and varying $c1$ values (0.17, 0.325, 0.525) for various fertilizer application rates. The simulated sugarcane yields responded in distinct ways:

- $c1 = 0.525$, PY = 126t/ha: represents the highest N-concentration demand in the crop that results in highest N-stresses. This produces the lowest sugarcane yields among the three scenarios.
- $c1 = 0.325$, PY = 126t/ha: represents intermediate N-concentration demand in the crop that results in intermediate N-stress and intermediate sugarcane yields.
- $c1 = 0.17$, PY = 126t/ha: represents the lowest N-concentration demand in the crop which results in the lowest N-Stresses and hence highest sugarcane yields among the three scenarios.

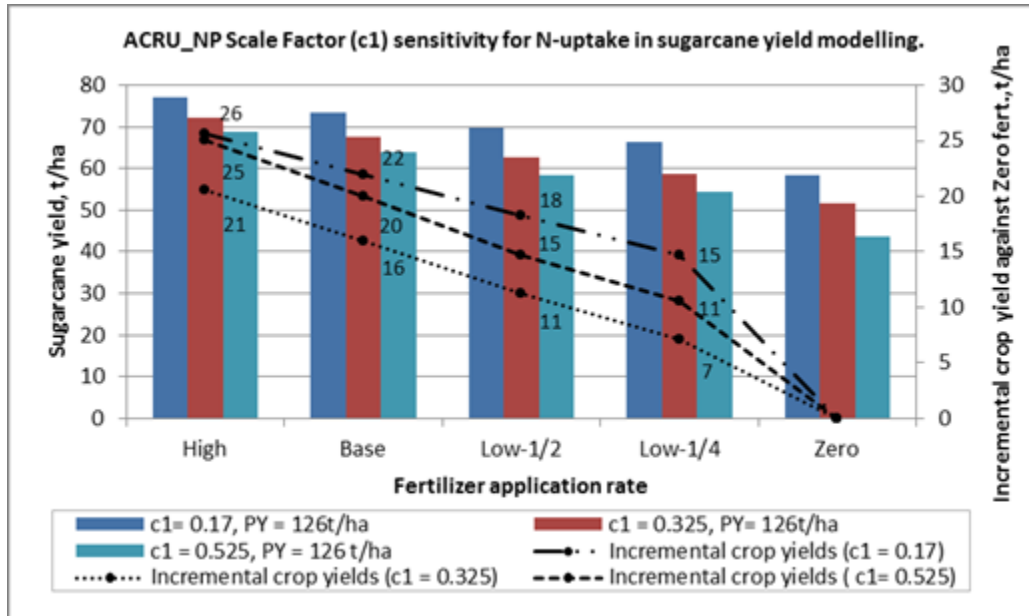


Figure 7.14: Comparison of sugar cane yield for various N fertilizer applications using values of $c1 = 0.17$ (initial), 0.325 (final) and 0.525 . The dotted lines indicate the incremental crop yield for the different fertilizer applications against zero fertilizer.

Using $c1 = 0.17$ in the simulation displays a much higher sensitivity or response to crop yield increase (15t/ha) for the $1/4$ fertilizer application rate, but it may not reflect the reality on the ground (Figure 7.14). Besides this, the incremental sugarcane yields for the base application rate is high (22 tons/ha). The final value of $c1 = 0.325$ proposed rectifies the above anomalies. It allows the difference between incremental sugarcane yields in any two consecutive fertilizer application rates to be within realistic levels, while at the same time maintaining the sensitivity for the $1/4$ fertilizer application rate from zero application to be low (7t/ha).

Field experiments and laboratory studies have shown that “the amount of nitrogen available to the crop differs markedly between soils and is probably influenced by factors such as climate, aeration, moisture availability, organic matter and the depth of the soil” (Moberly and Meyer, 1984). The differences in the response of ratoon cane grown to applied N in the Longlands, Mayo and Inanda form soils are shown in Figure 7.15. Similarly, Cartref soils, which belong to the same Soil Group as Longlands (Table 7.7), would be expected to produce much higher yields in response to applied N as compared to Hutton soils for similar fertilizer application rates.

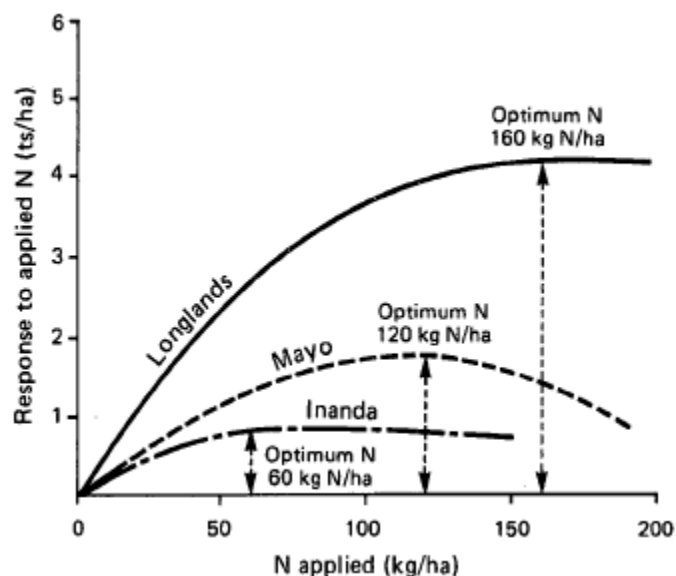


Figure 7.15: Ratoon cane responses to applied N in relation to soil form (Moberly and Meyer, 1984).

Moberly and Meyer (1984) suggested that the recommended amounts of nitrogen should be modified according to soil groups. The ratio of nitrogen (kg) to be used per ton of cane (tc) expected in each of the soil forms is given in Table 7.7. This however should be modified slightly according to factors such as soil depth and moisture availability.

Table 7.7: Nitrogen recommendations for sugarcane based on soil forms (Moberly and Meyer, 1984).

Soil group	1	2	3	4
Soil form	Fernwood Cartref Longlands Westleigh Kroonstad Katspruit Glenrosa (light) Estcourt Sterkspruit Dundee	Glenrosa (heavy) Clovelly (light) Hutton (light) Oakleaf Swartland Bonheim Valsrivier Tambankulu Willowbrook Rensburg	Milkwood Mayo Inhoek Arcadia Hutton (moderate) Shortlands	Champagne Inanda Nomanci Kranbkop Magwa Hutton (humic phase) Clovelly (humic phase) Griffin (humic phase)
Plant, kg N/ha	120	100	80	60
Ratoon, kg/tc	1.6	1.3	1.0	0.8

Testing the resulting model by applying deficit irrigation to sugarcane for the various land segments that have different soil types gave increased crop yields as would be expected

because of reduced water stress. Similarly for the different soil forms present in Mkabela Catchment that were simulated, different sugarcane crop yields were realised. As noted above, this probably results from different moisture availability, organic matter and the depth of the soils that were used as input parameters to the *ACRU-NPS* model.

7.2.4 Validation of sugarcane yields

The results of model validation of the simulated sugarcane yields are presented in Figure 7.16. By changing the scale factor (c1) from 0.17 to 0.325 and adjusting the potential yield (PY) from 67t/ha to 145t/ha, the *ACRU-NPS* simulations of sugarcane yields became comparable to the observed sugarcane yields for the simulation period 2006-2011 consisting of 3 crop cycles each of 18-months (Table 7.8). Results from the *ACRU-NPS* simulations model were also compared to the *CANESIM* model to gauge its nutrient component performance.

Table 7.8: Rainfall and observed sugarcane yields (SASA, 2012)

Year	Rainfall (June to May)	Yields of harvested cane (tons/ha)
1997/1998	1101	74.70
1998/1999	801	72.48
1999/2000	1306	67.74
2000/2001	894	73.95
2001/2002	1001	64.96
2002/2003	850	71.64
2003/2004	792	62.64
2004/2005	898	60.42
2005/2006	921	66.02
2006/2007	982	66.36
2007/2008	1026	64.17
2008/2009	941	68.70
2009/2010	973	67.67
2010/2011	887	66.74
Average		67.72

The following observations were made during the validation process (Figure 7.16);

- *CANESIM* model considers the water stress only and not nitrogen stress; hence, its yields were expected to be higher where rainfall amount was high.
- *ACRU-NPS* model considers both water and nitrogen stress and whichever is severe is used to reduce crop growth. This implies that wherever lower crop yields occur it could be

as a result of nitrogen stress or the rainfall was not sufficient during the critical growing stage of the crop.

- The calibrated value of $c1 = 0.325$ was successfully used to simulate sugarcane yields in the ranges similar to observed yields.

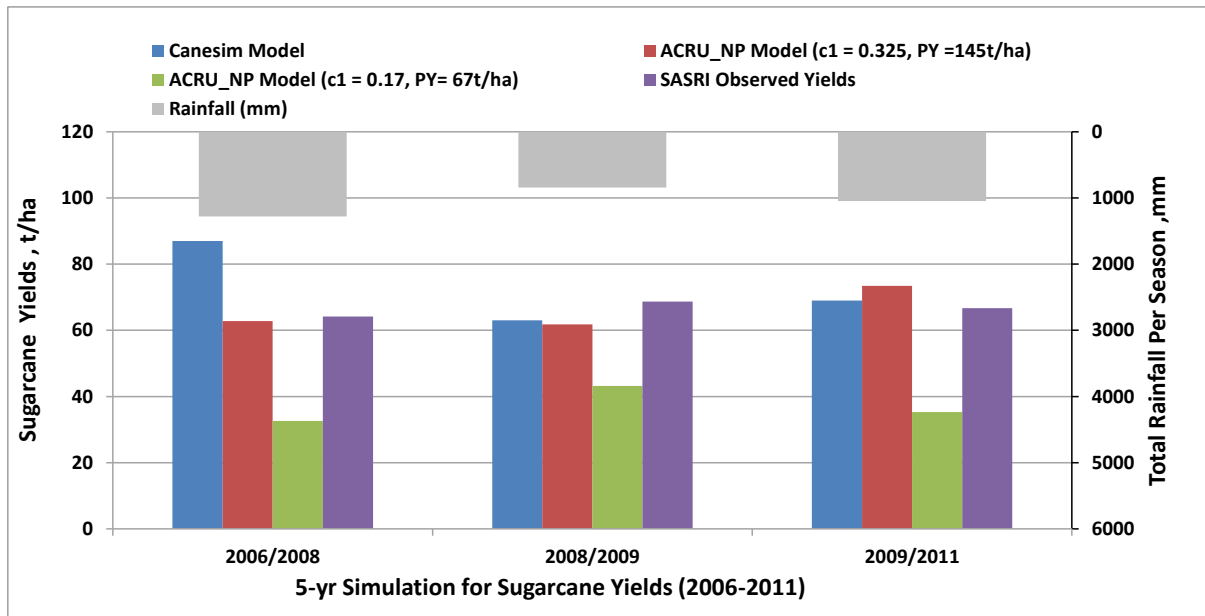


Figure 7.16: Comparison of sugar cane yields from 3 no., 18 months crops for 2006-2011 simulations (*CANESIM*, *ACRU-NPS* $c1=0.17$ and *ACRU-NPS* $c1=0.325$) and published observed yields for the South African Sugar Industry (SASRI).

CHAPTER EIGHT

8 RESULTS AND DISCUSSION

Results and discussions are deliberated from two perspectives. The first perspective discusses the connectivity influences on nutrient and sediment migration in the Mkabela Catchment based on field and catchment scale observations. This was achieved by observing discharge, nutrient, sediment and isotope responses using instruments set up at the field and catchment scales. The second perspective discusses the results from the *ACRU-NPS* modelling where crop yields and pollutant loads from the catchment are studied. The sugarcane crop yields were considered after varying fertilizer application rates at the various sub-catchments. Along with this were the output of discharges, nutrient and sediments loads that were generated in the catchment and eventually passed through buffers, wetlands and dam controls.

8.1 Connectivity Influences on Nutrient and Sediment Migration

Hydrological processes response zones are based on geomorphic parameters of the catchment that include land use, soils, geology, topography, valley width and confinement, terrace frequency, channel morphology and material composition (Montgomery and Buffington, 1998). These zones have similar landforms that reflect comparable hydrologic and erosional processes to water and sediment yields. The connectivity of particle sources becomes crucial to the understanding of suspended load dynamics and the transport of particle-associated pollutants along the catchment.

The application of isotope techniques is an alternative strategy that can be used to define hydrological connectivity between surface water features such as streams and wetlands and the groundwater systems below these features. The age or transit time of water offers a link to water quality since the contact time in the subsurface largely controls the chemical composition of waters from which one can deduce responses in storage, flow pathways and source of water from simple observations (McGuire *et al.*, 2007).

8.1.1 Field and catchment scale nutrient and isotope events

The concept of connectivity has proved invaluable in understanding migration of NPS pollutants in catchments. Observations of sediments or suspended solids (SS), nitrate (NO₃) and phosphorous (P) fluxes alongside stable water isotope sampling were made on a nested basis at field and catchment (41 km²) scales for a series of events in the Mkabela Catchment. The nested catchment scale sampling focused on control features in the stream network, including road crossings, farm dams and wetland zones. The analysed stable water isotopes ($\delta^{18}\text{O}$ and $\delta^2\text{H}$) results were used to interpret the connectivity of the contributing landforms and the stream network.

The results reveal the dominant influences of farm dams and wetlands in limiting the downstream migration of sediment and nutrients for all but the most intense events. Certain events resulted in mixing in the dams and larger resultant outflow than inflow loads. These occurrences appear to be a result of combinations of reservoir status, catchment antecedent conditions, rainfall depth and intensity.

8.1.1.1 Field nutrient and isotope events results

Table 8.1 shows the criteria used to select wet events that were plotted in Figure 8.1 and Figure 8.2. A total of 24 events from both Flume1 and Flume2 were selected based on percent runoff that corresponded to low, intermediate and high flows. It is important to note that the low flows for the determination of runoff events during the hydrological years 2009–2012 were calculated by using daily discharge values. Increases in runoff above the mean daily discharge, MQ, were defined as runoff events. For graphical analysis of precipitation, runoff and pollutant loads relationships, only distinct flood events were considered. These events were defined by a peak runoff value exceeding five times the mean annual discharge ($Q_{\text{threshold}}$) (Wenninger *et al.*, 2008).

Table 8.1: Wet events selection criteria

Selection criteria	Runoff %	No. of events	
		Flume 1	Flume 2
Low flows	3 - 10	7	3
Intermediate flows	10 - 20	3	5
High flows	20 - 50	2	4

High precipitation events in most cases corresponded with higher runoff percentage resulting in increased pollutant loads (Figure 8.1 and Figure 8.2). The pollutant loads at Flume 1 in most instances were always less than those at Flume2 because of the larger drainage catchment for Flume2 (58 ha) as compared to Flume1 (17 ha). This may reflect the increasing contribution to discharge and mass transport at the outlet of Flume2. Runoff ranged between 3.1% and 44.9% at Flume1 and 4.9% to 48.7% at Flume2 (Figure 8.1 and Figure 8.2). It can be noted that soluble-P concentrations for Flume1 are generally higher than those for Flume2 and this probably reflects the existence of soluble-P in the groundwater that permanently oozes upstream of Flume1 from a spring (Lorentz *et al.*, 2011). This soluble-P in the subsurface water from the headwaters of the catchment is later diluted downstream in Flume 2 resulting in low soluble-P concentrations.

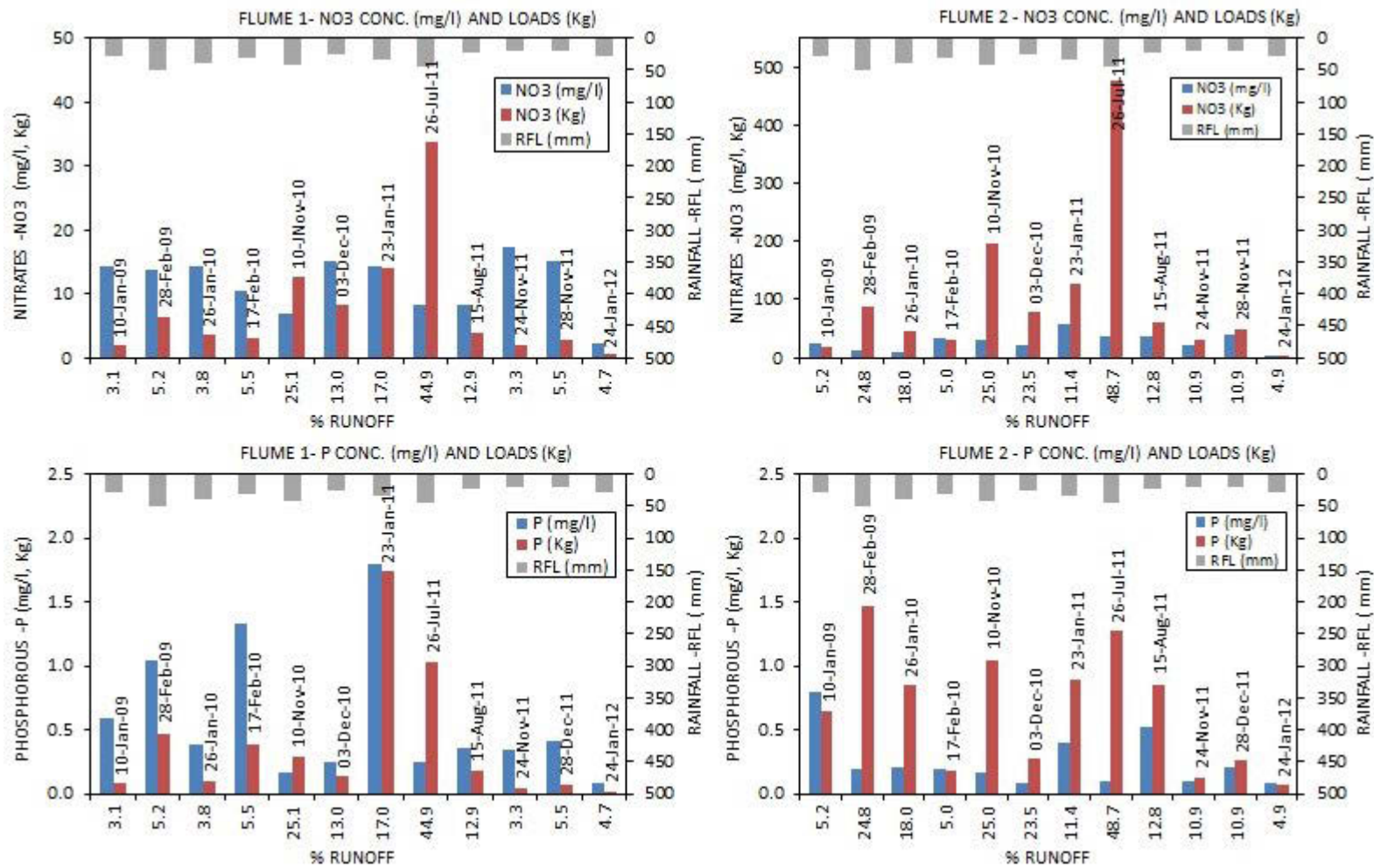


Figure 8.1: H-Flumes rainfall/runoff, nitrates (NO₃) and soluble-P concentrations and mass loadings for 12 events (Jan '09 - Jan '12).

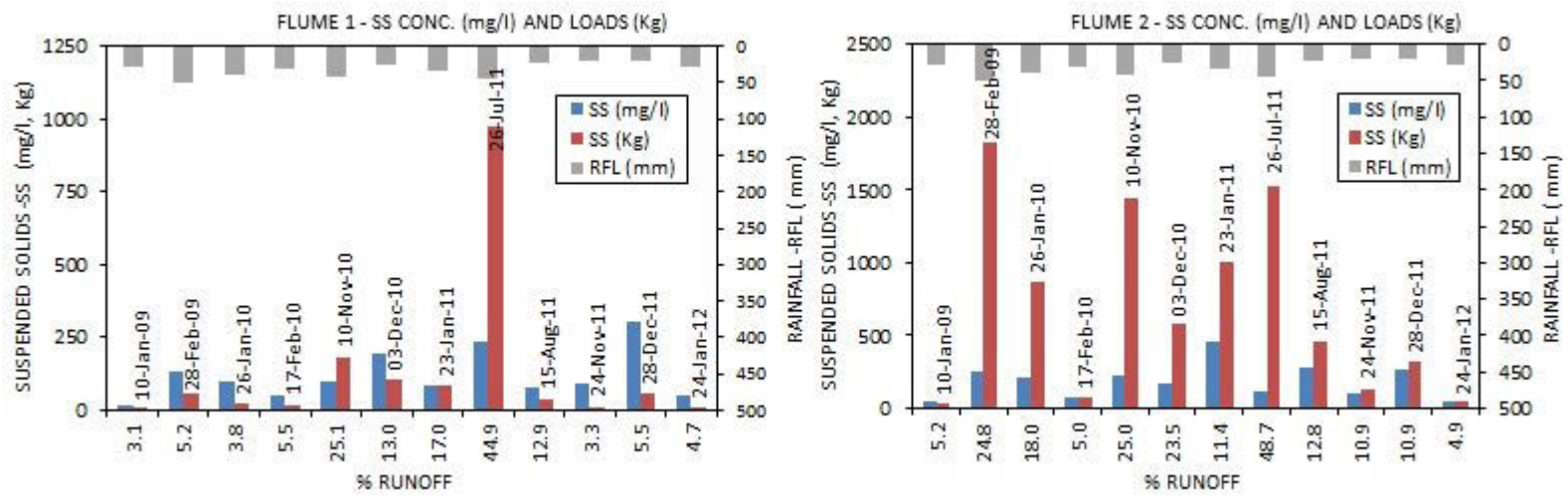


Figure 8.2: H- Flumes rainfall/runoff, suspended solids (SS) concentrations and mass loading for 12 events (Jan '09 - Jan '12).

The summer event of February 28, 2009 shows the NO₃ concentrations in the stream water in Flume1 increasing by ~6 mg/l during peak flow and later dropping during the receding limb (Figure 8.3). P increased by ~2 mg/l during peak flow, and then dropped slowly during flood recession. SS followed a similar trend as in NO₃ concentrations. Though few samples were collected from Flume2, it can be seen from Figure 8.3 that there was a general increase of NO₃, P and SS as the flow increased towards the peak flow. NO₃ increased by ~14 mg/l during peak flow.

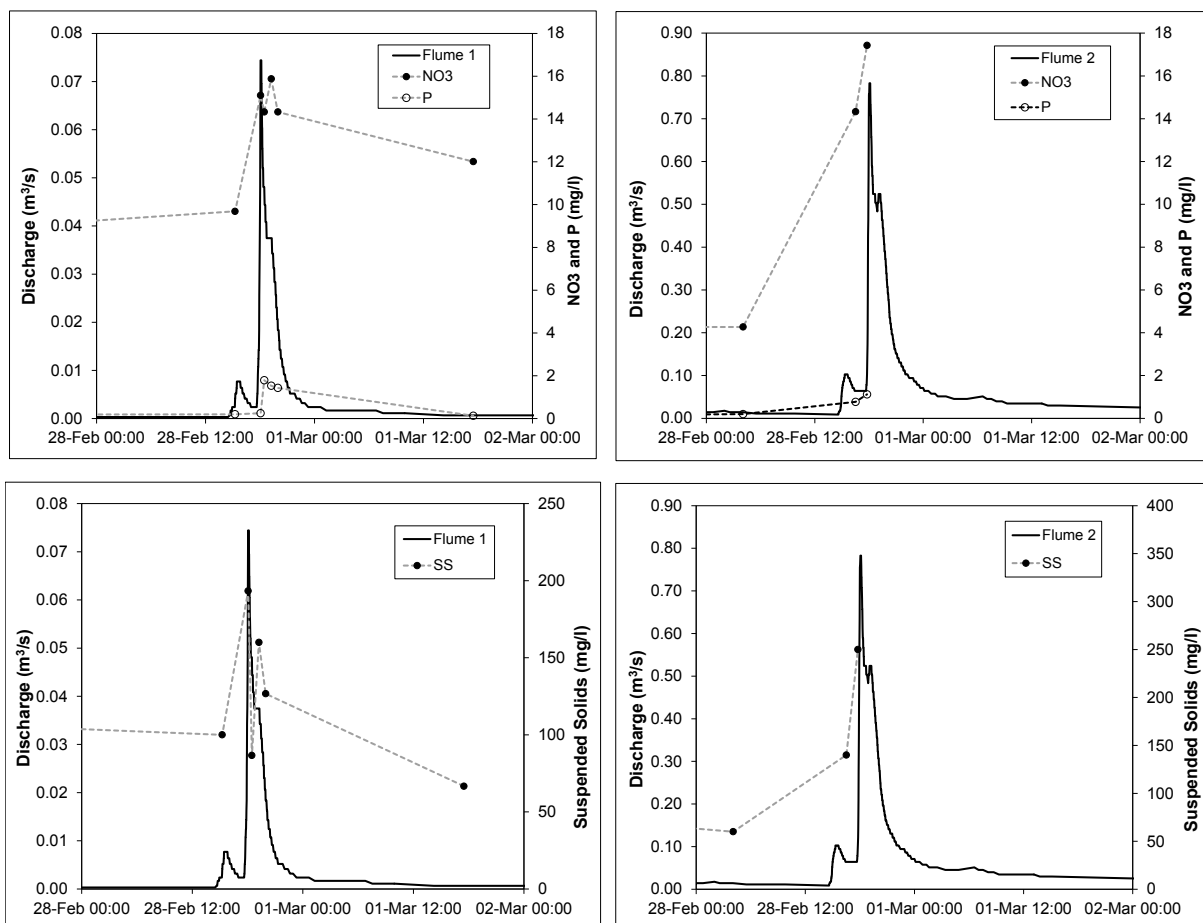


Figure 8.3: Discharge, NO₃, P and SS responses for Flume 1 (left) and Flume 2 (right) for a 51 mm summer event of 28 February 2009.

There is a significant contribution of nutrient and sediment loads resulting from the nutrient (NO₃ and P) and suspended solids responses to the February 28, 2009 high intensity rainfall event (51 mm). It is important to note at Flume1 that there is the double peak in nutrient and suspended solids concentrations during the event, which mimics the double discharge peak (Figure 8.3). These results reflect connectivity thresholds (distinct flood events) for sediments and nutrient delivery which are dependent on event depth and intensity.

The isotope ratios for selected precipitation events analysed for rainfall and runoff at the headwater flume stations include events on February 28, 2009 (51 mm), July 25–27, 2011 (98 mm) and November 10, 2010 (43 mm). In addition, several samples were collected periodically throughout the catchment during the event of November 10, 2010.

The February 28, 2009 results show a distinct drop in isotope ratio during the event. The runoff at Flume1 has an increasing contribution from the event water, indicated by the progressive change in the isotope ratios from the initial value close to the groundwater signal towards the isotope ratio of the event water (Figure 8.4). The contribution from event water (rainfall) peaks about 2 h after the peak of the discharge event, at which time most of the discharge is contributed by event water. After this peak, the runoff contributions are increasingly dominated by subsurface water.

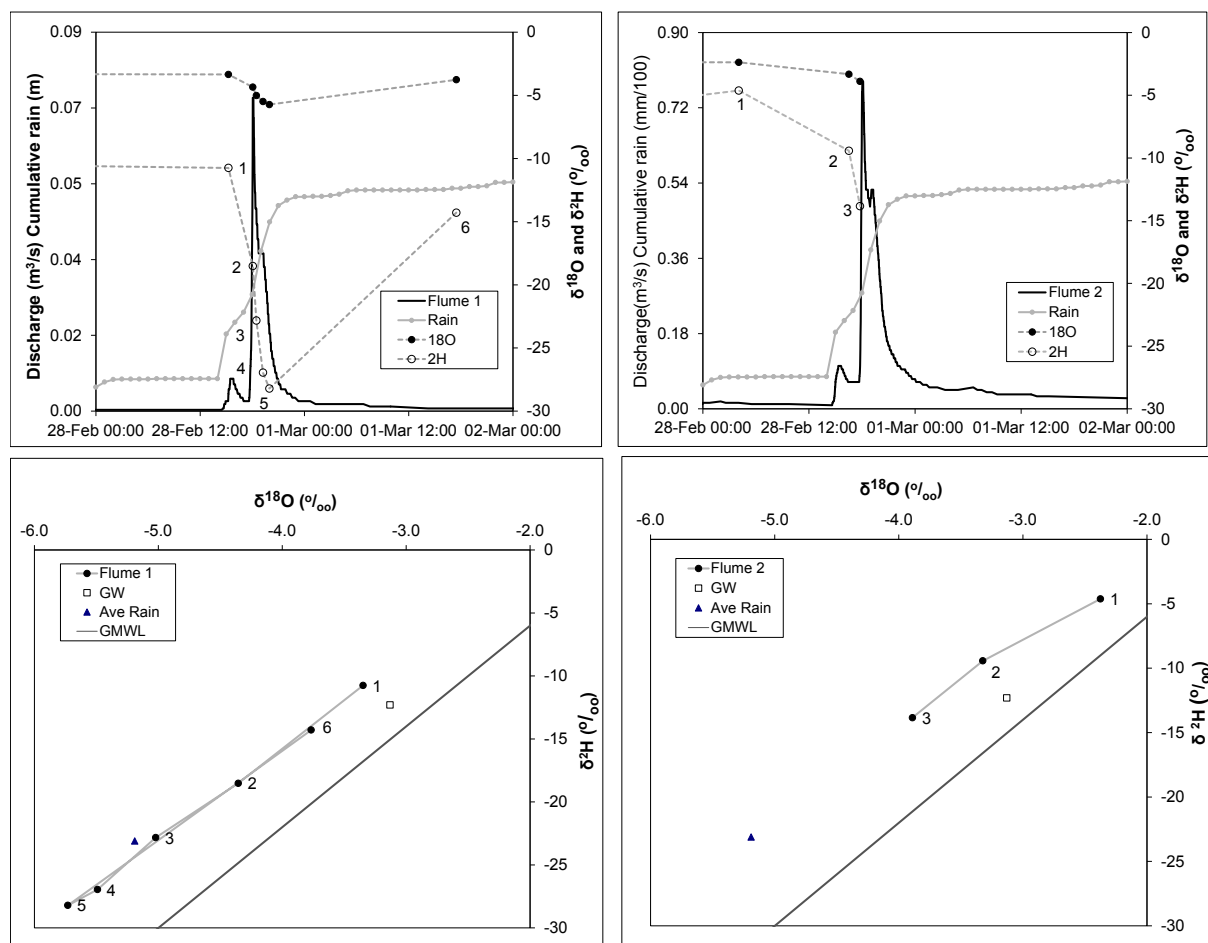


Figure 8.4: Cumulative rainfall, discharge and isotope responses at Flume1 (left) and Flume 2 (right) for the 51 mm summer event of 28th February 2009.

The discharge isotope signal then returns to values representative of the mean groundwater values of -3.4 ‰ for $\delta^{18}\text{O}$ and -12.3 ‰ for $\delta^2\text{H}$ within 24 h of the cessation of the rainfall (Figure 8.5). Thus, there appears to be a threshold of event magnitude and intensity (distinct flood events) which controls the connectivity of overland flow and subsurface event water discharge to the lower slopes in the sugar cane fields. Wenninger *et al.* (2008) from studies in Eastern Cape Province, South Africa, showed values of the shallow subsurface water (groundwater wells) to vary between -3 ‰ and -4.2 ‰ with a mean of -3.5 ‰ for $\delta^{18}\text{O}$, and between -7 ‰ and -18 ‰ with a mean of -11.5 ‰ for $\delta^2\text{H}$.

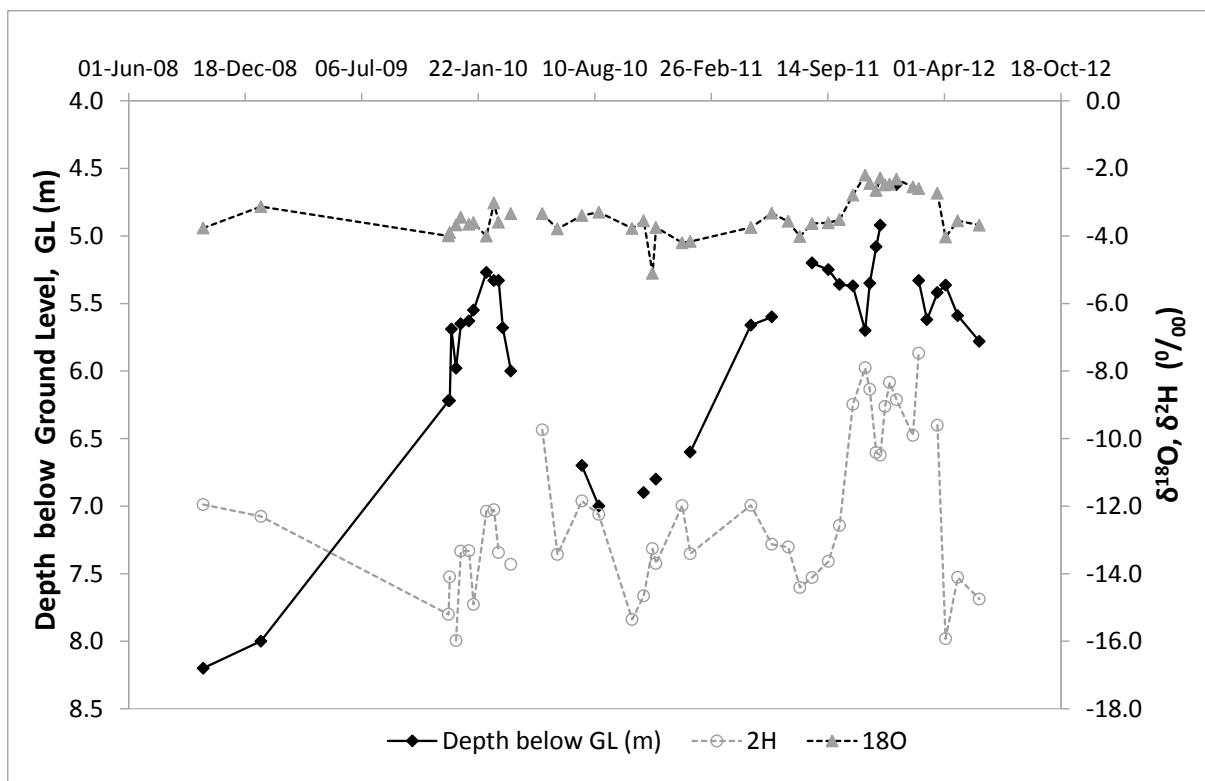


Figure 8.5: Depth below ground level (m), $\delta^{18}\text{O}$ and $\delta^2\text{H}$ isotope values (‰) for the period 2008- 2012 at a borehole (BH) in Mkabela Catchment.

The July 25–27, 2011 winter event behaves in a similar way as the summer event of February 28, 2009. Runoff at Flume2 has an increasing contribution from the event water, indicated by the progressive change in the isotope ratios, from the initial value close to the groundwater signal, towards the isotope ratio of the event water. Wenninger *et al.* (2008) found that surface water isotope values during low flow periods are similar to groundwater isotope values and are close to -3‰ for $\delta^{18}\text{O}$ and -7‰ for $\delta^2\text{H}$. Similar groundwater isotope values were obtained from Mkabela as -4‰ for $\delta^{18}\text{O}$ and -10‰ for $\delta^2\text{H}$ (Figure 8.6). During runoff

events the reactions of these isotopes were consistent for both February 28, 2009 and July 25–27, 2011, with both isotopes getting generally lighter as the runoff period progresses.

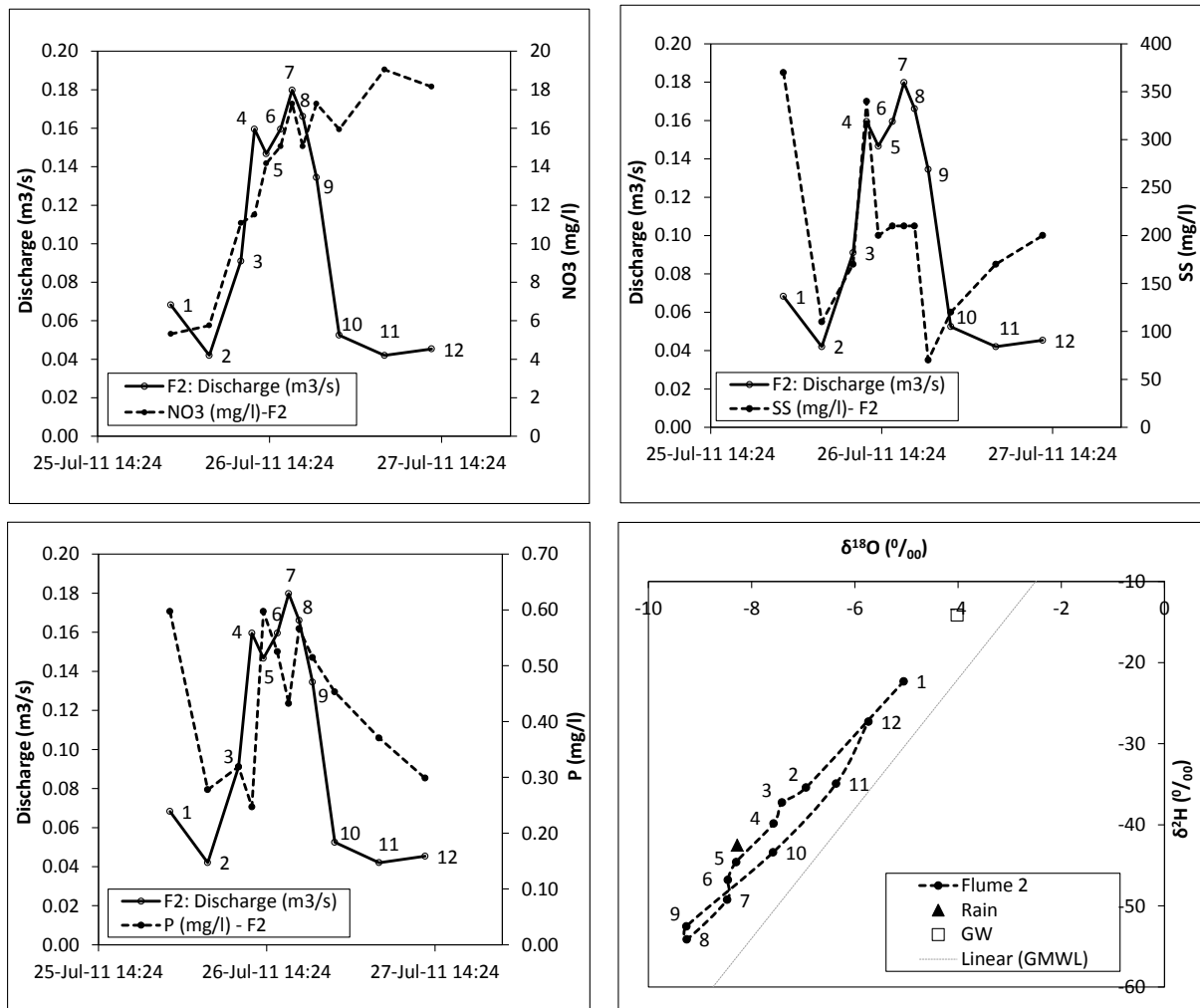


Figure 8.6: Discharge, nutrient and isotope responses for Flume 2 for 53 mm, 42 mm and 3 mm winter events of 25th, 26th and 27th July 2011 respectively.

NO₃ concentrations in the stream water in Flume2 increased by ~13 mg/l during peak flow and remained elevated during the receding limb. The fact that NO₃ concentrations remains elevated after peak flow suggests there could be a continuous release of water from another source after peak flow (Figure 8.6). The presence of groundwater seepage upstream of Flume2 may explain this phenomenon as there is a continuous release of pre-event water and thus runoff contributions are more likely to be increasingly dominated by the subsurface water after the cessation of the rainfall. This seepage water contained NO₃ concentrations > 17 mg/l and had probably been leached to the groundwater during the preceding summer events.

Soluble-P concentrations mimic the discharge pattern where it initially dropped by ~0.3 mg/l before increasing by the same margin during peak flow and finally dropping slowly as with discharge during the flood recession (Figure 8.6). SS concentrations initially followed a similar trend as soluble-P concentrations but their pattern differed at the later stages. Initially SS concentrations dropped by 275 mg/l and increased with the same margin during the peak flow. However after recession limb, SS concentrations started to increase again. The increase in SS concentrations may be due to the presence of fine particle colloids that may have passed through fissures in the ground and now being emitted together with groundwater as preferential flow. These fine colloids mimic discharge patterns just as P ions that are adsorbed to the colloids mimic discharge as well.

Figure 8.7 shows isotope changes from initial values close to the groundwater signal towards the event signal as the discharge peaks, and then back again to groundwater signal during the receding limb. The mixing model was used to assess percent contribution from each discharge component. Initially the baseflow contribution to the total discharge was 86 % while that from surface runoff was 14 %. As the storm event proceeded, the contribution from the baseflow decreased to 61 % while the surface runoff increased to 39 %. In the receding limb, immediately after the discharge peaks, the surface runoff contributed 70 % to the total discharge while baseflow contribution had decreased to 30 %. Towards the end of the rainfall event, the baseflow contribution to the total discharge was 77 % while that of surface runoff was 23 %. By the end of the storm event, baseflow contribution to the total discharge was 92 % while that from the surface runoff was 8 %. The trend on water movement suggested by the isotopes influences the movement of nutrients and sediments in a catchment as surface water gets connected to the subsurface water. It is most likely that NO_3 and P loads before the event peaks are emanating from the dissolved subsurface source. During the event, NO_3 , P and SS loads will most likely be from overland flow or surface runoff. The isotope values can therefore be successfully used to show evidence of surface–subsurface water connectivity and the associated pollutants moved.

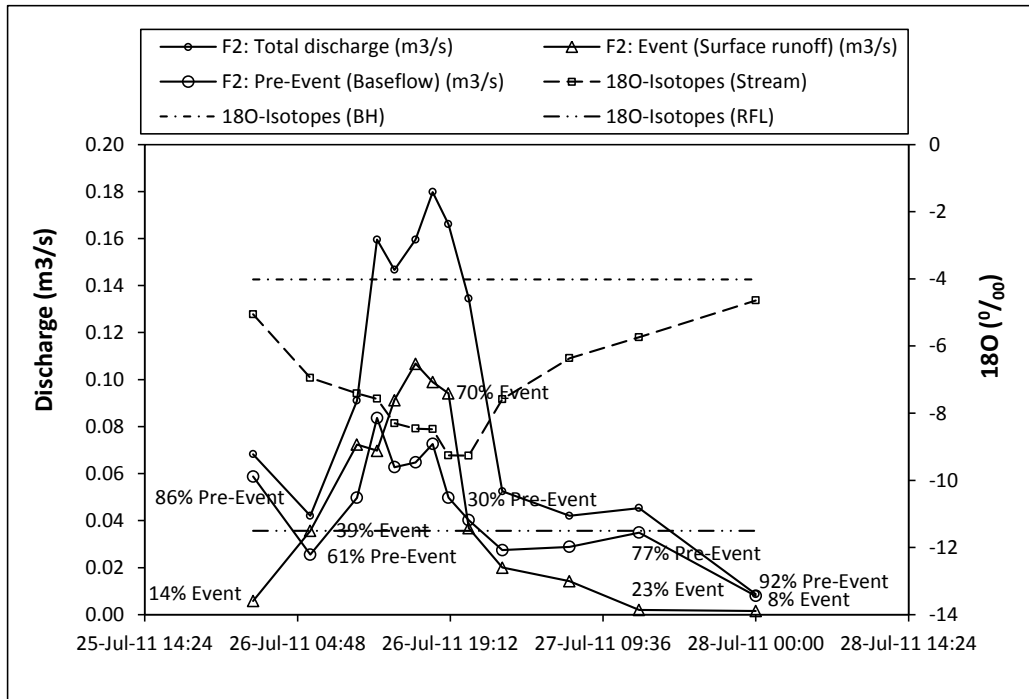


Figure 8.7: Discharge, rainfall and groundwater $\delta^{18}\text{O}$ concentrations for Flume 2 flow in winter event of 25th-27th July 2011.

Analysis of three isotope samples that were collected from Flume2 during the sampling event of November 10, 2010 is shown in Figure 8.8. The resultant isotope values have been used, together with end member values for the groundwater and average rain water, to render the fractional contribution of the subsurface or pre-event water to the total discharge at Flume2. This pre-event contribution comprises 19% of the total discharge at the peak of the event and typically returns to 100% of the contribution within 24 h of the cessation of rain.

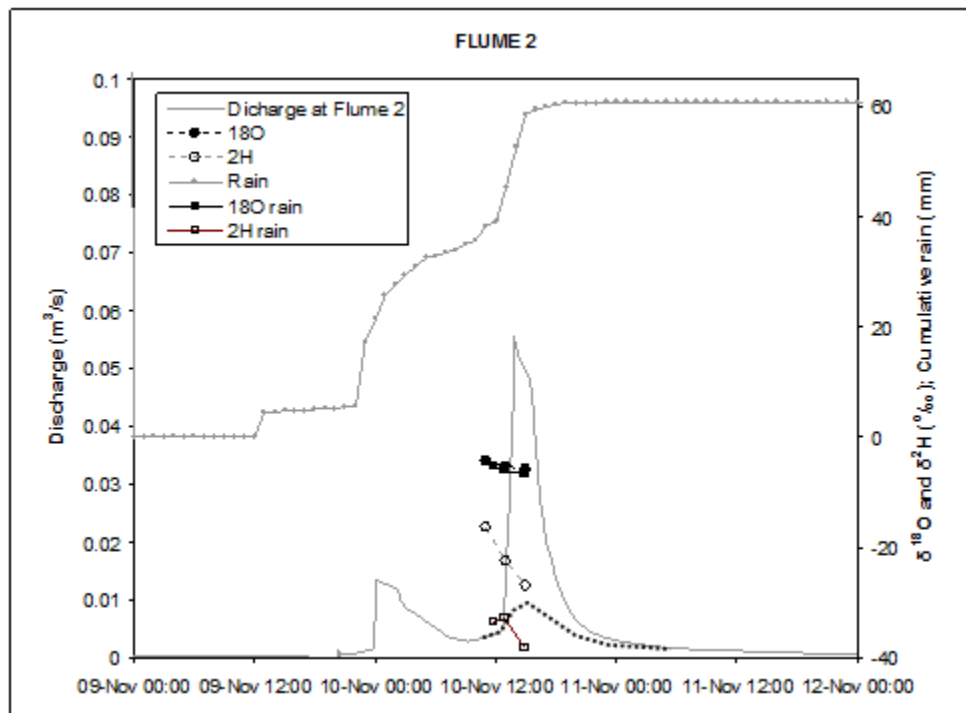


Figure 8.8: Rainfall, discharge and isotope responses at Flume 2 for 34 mm event of 10th November 2010.

Appendix K show analysed isotope results through the seasons from December 2008 to March 2012 for runoff plot and flume rainfall events. There were few events from runoff plots (RP1 and RP2) in general compared to those from flumes (Flumes1 and 2). There were no discharge events from runoff plots during winter period (Jul-Sep) because all the water from winter rainfall infiltrated into the ground due to the inherently dry conditions. From studies conducted by Lorentz *et al.* (2013) in the Potshini catchment in South Africa, a reason for the low initial contribution of soil water to the micro-catchment runoff was that the water from the first rains is stored in the soil profile rather than moving through it. Once the soil moisture deficit is satisfied, soil water contributions increased. NO₃, P and SS concentrations obtained from RP1 and RP2 were similar. This could be associated with the fact that the two runoff plots are located close to each other and have the same Avalon soil type characteristics. The Avalon soils are moderately drained and have a low interflow component of which most of the water moves in the intermediate vadose zone. Except for the occasional differences of these NPS pollutants that may have arisen from the fact that the sugarcane growing on it was staggered during planting resulting in differences in NO₃, P and SS concentrations in the discharges, the values for RP1 and RP2 were within the same range. In general, there were high concentrations of NO₃, P and SS obtained from the runoff plots as they ranged from 10-100 mg/l, 1-12 mg/l and 100-3200 mg/l, respectively. The similar ranges

of isotope values for RP1 and RP2 confirms that the two runoff plots were hydrologically connected through both the surface (event) and sub-surface (pre-event) processes as confirmed from isotope values (Appendix K).

While isotope values for runoff plots consisted of a mixture of isotope values similar to those of both the rainfall (event) and groundwater or borehole (pre-event) water, most of the isotope values from flumes (Flumes1 and 2) mainly exhibited values similar to groundwater (BH) (Appendix K). This means that there was an increasing contribution to discharge and mass transport nearer the lower slopes of the small catchment draining into Flume2 caused by hydrological connectivity of soil moisture content experienced through the sub-surface. This has a consequence of increasing NPS pollutant loads downstream between Flume1 and Flume2 as earlier discussed.

During the winter period (Jul- Sep'11), isotope values in water from both flumes (1 and 2) were similar to those obtained from the borehole. It is most probable that discharge flowing through both the flumes at this period is mainly from groundwater (pre-event water) that was displaced by the infiltrating rainfall (event water). The $\delta^{18}\text{O}$ and $\delta^2\text{H}$ compositions for the flume discharges during the mid to late summer period (Dec'11- Mar'12) are different from the isotopic composition of the groundwater (BH) (Appendix K). Plenty of rains are experienced during summer in comparison to the winter season in Mkabela Catchment and the isotopic values from discharges in both flumes start to deviate away from borehole values. There is, however, a marked difference in the way Flume1 and Flume2 isotope responses behave in summer.

During the mid-summer period, Appendix K shows incessantly more depleted isotopic signatures relative to borehole values (more negative values of ^{18}O), or isotopes getting generally lighter for Flume1 discharge that is further upstream of Flume2. This suggests that this water could be more from recharge following large flood events. Such depleted isotopic signatures due to heavy rains tend to have relatively negative isotopic compositions as there is relatively less evaporation. The downstream discharges from Flume2 have relatively enriched isotopic signatures (less negative values of ^{18}O) or isotope values getting generally heavy. According to Simpson and Herczeg (1991) under low or average flow conditions, river water tends to be isotopically enriched in ^{18}O relative to rainfall values because of

surface water evaporation. Discharge collected from Flume2 has most likely undergone substantial evaporation resulting in less negative values of ^{18}O .

8.1.1.2 Catchment nutrient and isotope transect results

The NO_3 and soluble-P responses for the catchment analysed along transect from the headwater to outlet for a selected January 7, 2011 sampling event are shown in Figure 8.9. The water quality data show a remarkable drop in NO_3 and soluble-P concentrations between the runoff plot and Flume1. This may be associated with the dilution of the pre-event water (groundwater) with event water (rainfall) between the runoff plots on the upper slopes and the Flume 1.

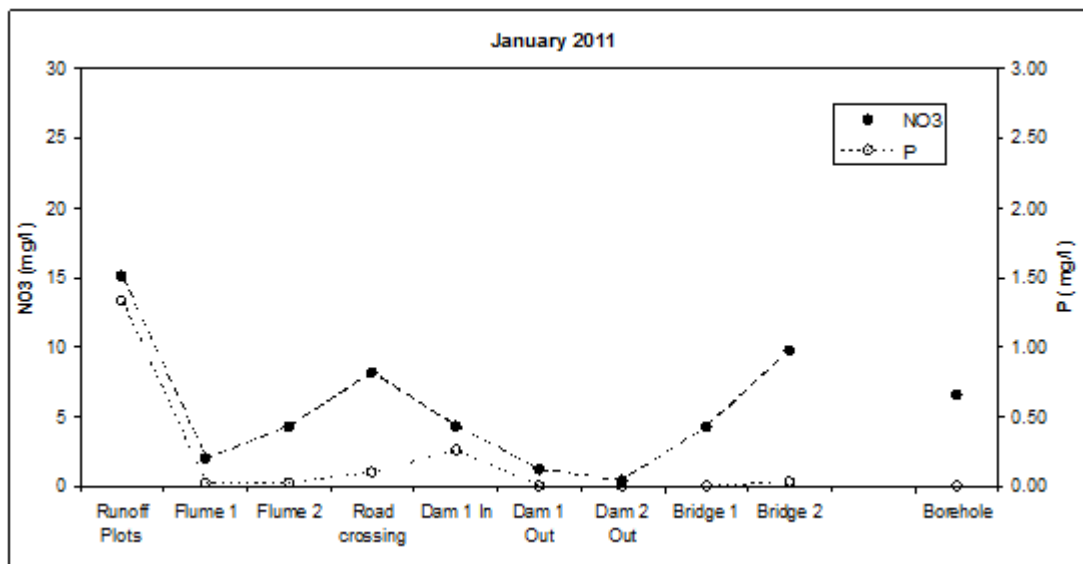


Figure 8.9: Concentrations of nutrients from headwater to outlet for the event of 7th January 2011.

NO_3 concentrations increase between the first and second flume and continues to increase further at the Road crossing. Increase in soluble-P concentrations follows the same trend as in NO_3 but the increase is minor. This increase could be associated with emergence of a subsurface seepage zone between Flume1 and Flume2 resulting in subsurface sources contributing nitrate and phosphate (Deasy *et al.*, 2007). Between the Road crossing and Dam Out stations, there exists a series of wetlands and reservoirs. Soluble-P and NO_3 are clearly retarded in the wetland and reservoir controls. NO_3 loads increases beyond Dam Out, reflecting contributions from the sugarcane land use between the Dam Out station and the

outlet of the catchment. Increase in soluble-P loads between Dam2 Out and Bridge 2 however appears minor.

The stable isotopes signal at the two flumes differ slightly reflecting different mixes of water. The recorded isotope delta values from the Flumes to Dam1 In are similar to that in the groundwater as reflected in the borehole sample (BH) (Figure 8.10). The existence of a spring upslope of the first flume and subsurface seepage zone between Flume1 and Flume2 have resulted in isotope signals close or similar to groundwater isotope signal. The isotope values at Flume2, Road Crossing and Dam In sampling stations are closer to the groundwater signal while Flume1 signal is identical to the groundwater signal. Most of the pollutant loads contained here appear to mostly emanate from the subsurface. However, further downstream, samples at the Dam1 Out and Dam2 Out stations reflect the evaporation from the reservoirs which occur between the Dam In and Dam Out stations. These isotope values are highly enriched and are similar for Dam1 and Dam2 outlets.

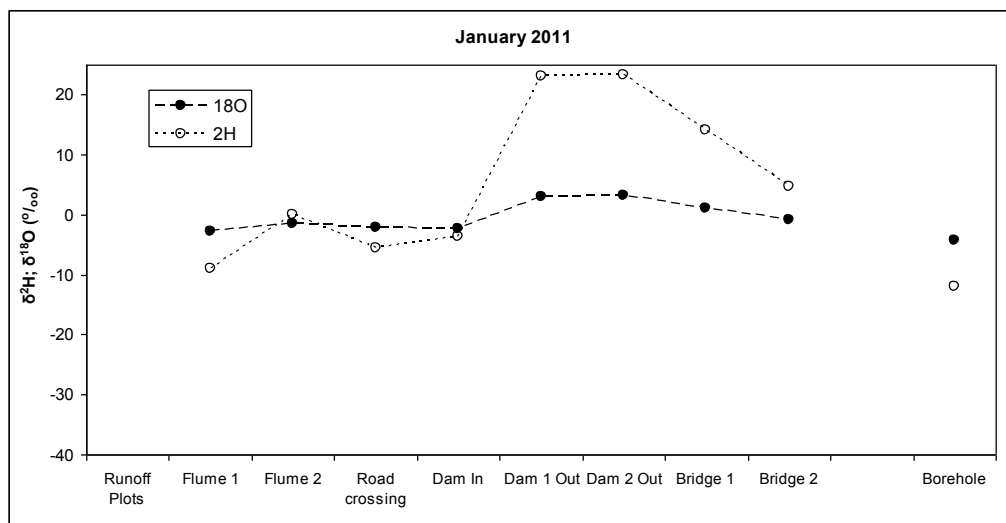


Figure 8.10: Isotope transects from the headwater flumes to the outlet at Bridge 2 for the event of 7 January 2011.

Downstream of the reservoir outlets, the isotope values at the Bridge 1 and Bridge 2 stations reflect a mixture of upstream inflow from the impounded tributaries (Dam1 and Dam2) as well as contributions from the land units between the reservoirs and the Bridge sampling stations (groundwater). The hydrological connectivity experienced here between upstream reservoir sources (water from dams that have undergone substantial evaporation) and subsurface water (groundwater) has influence on the NO_3 and soluble-P pollutant loads

carried along. These pollutant loads reflect a mixture of both upstream reservoir sources and subsurface NO_3 and soluble-P concentrations.

8.1.1.2 (a) Seasonal nutrients (NO_3 & P), SS and isotope processes through dams

Appendix L shows catchment scale nutrient, sediment and isotope time-series in dams and bridges for the period 2011-2012. Dam1 In isotope values were similar to the isotope transect values of 7th January 2011 event for the same station and were comparable to those at the borehole (BH) for both dry-winter (Jul-Sep) and rainy-summer (Oct-Mar) periods. The $\delta^{18}\text{O}$ isotope values of ~ -3.0 ‰ were similar to borehole values of -3.4 ‰ suggesting that most of the sampled water at this station during the entire period was most likely originating from groundwater. Hence most of NPS pollutants emanating at this station for all the samples collected were from the subsurface source, probably that which had percolated in the preceding wet season. Dam2 Out station water samples had more enriched $\delta^{18}\text{O}$ isotopic signatures (~ 1.0 ‰) relative to borehole values during summer period (Oct-Mar) hence reflecting sources that had undergone substantial evaporation, most probably from the upstream reservoirs sources. This means that the NPS pollutants present in collected water samples from this station during this period was mostly likely originating from upstream surface source rather than that emanating from the subsurface.

During the winter period (Jul-Sep), discharge entering Dam1 In and that leaving Dam2 Out showed highest peak in NO_3 concentration of ~ 40 mg/l compared to summer period (Oct-Mar) that had concentrations < 30 mg/l for both stations with values decreasing further as summer rains period proceeded. The highest reductions in NO_3 concentrations during the summer occurred at the Dam 2 Out station. During winter most of the discharge at Dam1 In was originating from the sub-surface as confirmed from the isotopic signature similar to the groundwater signal. The sub-surface source of NO_3 was probably that which had leached and percolated into the groundwater during the previous season. Because of much less rainfall during winter, dilution of NO_3 did not occur and that was why NO_3 that came out in Dam2 Out was still highly concentrated (~ 40 mg/l) during this period. Similar behaviour was seen in Dam2 Out during winter where SS concentrations of slightly < 400 mg/l were maintained at the outlet. Isotope values similar to groundwater signal confirmed that the SS source in the sampled water during winter probably originated from the sub-surface as fine colloids

passing through micro-pores by means of preferential flow. Farmers use manure in sugarcane growing in Mkabela Catchment which is a probable source of colloids. P fate in the dams during the winter season shows little change in peak P concentration from ~0.2 mg/l in Dam1 In to slightly < 0.2 mg/l in Dam2 Out.

In summer (Oct-Mar), the infiltrating rainfall gradually displaced sub-surface groundwater in the adjacent land segment and ended up in Dam1 In carrying along with it dissolved NO₃ but slightly at lower concentrations (< 30 mg/l). As the rainfall was sustained through the summer season, the water in the reservoirs was continually diluted by surface runoff. This resulted in diluted NO₃ concentration values of < 10 mg/l at Dam2 Out. It was however noted that SS concentrations in both Dam1 In and Dam2 Out increased gradually as summer season progressed. The increased runoff due to summer rains carries along with it more sediments and SS. Continued increase in displaced sub-surface water entering Dam1 In and surface water reaching Dam2 Out means that more SS were available as the summer season progressed. This resulted in higher SS concentrations of up to ~300 mg/l in the dams by the end of the summer season. These higher concentrations of SS can also be partly attributed to more rapid algae growth associated with higher summer temperatures. During summer period, Dam1 In source still originated from groundwater while Dam2 Out source was from surface runoff as seen from the isotope signatures. P concentration for both dams increased immediately at the start of summer period. Dam1 In P concentrations increased up to peak values of ~ 0.4 mg/l while in Dam2 Out up to ~ 0.8 mg/l before the concentrations started going down to < 0.2 mg/l. The increase in peak values from 0.4 in Dam1 In to 0.8 mg/l in Dam2 Out means that certain rainfall events resulted in mixing in the dams and hence the larger resultant outflow than inflow concentrations or loads. These P concentrations in both dams were later diluted as the summer season progressed up to concentration values of ~ 0.1 mg/l by the end of the season.

8.1.1.2 (b) Seasonal nutrients (NO₃ & P), SS and isotope processes through bridges

Isotopic $\delta^{18}\text{O}$ signatures for discharge at Bridge 1 (B1) were similar to those at Dam2 Out for both winter and summer periods (Appendix L). Bridge stations B1 and B2 also portrayed more enriched $\delta^{18}\text{O}$ values relative to borehole values during summer period, which means that NPS pollutants in the samples collected at these stations during the rainy summer period

were mostly those which had undergone evaporation, i.e. hydrologically connected through upstream surface source. It is however important to note that during some winter periods, isotopic signatures from the Bridge stations showed $\delta^{18}\text{O}$ isotope values similar to the groundwater signal. This isotopic behaviour at the bridges thus reflected a mixture of upstream inflow from the impounded tributaries (Dam1 and Dam2) as well as contributions from the subsurface from the land units between the reservoirs and the Bridge sampling stations (groundwater). This therefore revealed that discharges at the bridges were hydrologically connected through both upstream reservoir sources (event water) in summer and groundwater source (pre-event water) in winter.

This means that discharges in these locations were hydrologically connected through baseflow in winter and surface runoff in summer. The shapes of the graphs for NO_3 , P and SS for Bridge 1 were similar to those at Dam2 Out. Though this was the case, it was however noted that graphs at Bridge 1 were slightly attenuated for all the nutrient pollutants. This indicated that there was in general slight reduction in pollutants that occurred between Dam2 Out and Bridge 1 as the season progressed. The reduction in these pollutants could be attributed to the riparian vegetation located within the river bed channel along this section. Peak NO_3 and P concentrations decreased from $> 40 \text{ mg/l}$ to $< 40 \text{ mg/l}$ and 0.8 mg/l to 0.5 mg/l respectively as discharge moved from Dam2 Out to Bridge1. The peak SS concentration decreased during winter from 300 mg/l to 250 mg/l for the same stations except for an instance during summer where an increase of concentration from 250 mg/l to 350 mg/l was noted towards the end of the season. The increase in SS concentration between the two stations in this instance was an isolated case because plumes of colloids could have moved in the surface runoff occasionally.

The isotopic $\delta^{18}\text{O}$ signatures displayed during summer (Oct-Mar) at Bridge 2 (B2) were similar to those at Bridge 1 at $\sim 1.0 \text{ ‰}$ (Appendix L). This indicated hydrological connectivity between B1 and B2 through surface water for most of this period. Again it is important to note that at station B2, the isotopic signature of sampled water around the 10th September 2011 showed an evaporated signal. This was not the same with B1 as the sample collected had a similar signal to the BH value. This therefore confirms that for this date the probable source of B1 water samples was from the groundwater while that at B2 was from the surface.

During winter (Jul-Sep) the peak NO₃ concentrations decreased from 40 mg/l to 30 mg/l as discharge moved from stations B1 to B2. For the same scenario, the peak P concentrations during summer (Oct-Mar) decreased from 0.5 mg/l to 0.3 mg/l. Moving from B1 to B2 was however different with peak SS concentrations. There were increases in SS concentrations with peaks that ranged from 250- 350 mg/l during winter and 350- 400 mg/l during summer. It is also important to note that there was a reduction of peak SS concentration from 350 mg/l to 200 mg/l in the late summer. The nutrient loads increase during summer rains (Oct-Mar) where increases in NO₃, P and SS concentrations occurred between B1 and B2 stations, reflected the bedrock control where contributions from the sugarcane hillslopes between these stations were not retained, even in the short wetland upstream of B2. The bedrock channel is highly efficient in NPS pollutant movement downstream. It is narrow and steep with multiple knick-points present which offer very little sediment storage.

8.1.2 Mass balance mixing model

The isotope ratios were used to estimate the proportion of the discharge, at each of the Bridge stations, emanating from local land units, downstream of the reservoirs. For the sampling event of January 7, 2011 the Q_{LUi}/Q_{B1} ratio was 45% (Figure 8.11). This implied that just less than half the discharge at Bridge 1 (B1) was generated from the 3.6 km² (360 ha) sub-catchment between the most downstream reservoir and the B1 station. Similar estimates performed for the Bridge 2 (B2) station showed that for the same sampling event the contribution from the 13 km² (1300ha) sub-catchment between the B1 and B2 stations comprised 71% of the total discharge at B2. Analysis of the remaining selected sampling events yielded the contributions shown in Figure 8.11 below.

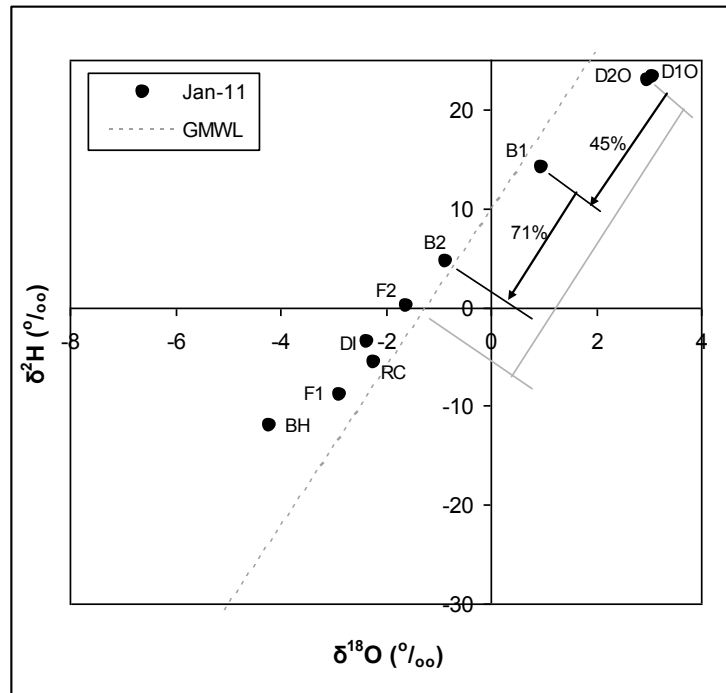


Figure 8.11: Isotope $\delta^{18}\text{O}$ / $\delta^2\text{H}$ ratios for the transect results for the event of 7th January 2011.

The isotope values consistently show decreased evaporated signals at the B1 and B2 stations, reflecting the significant contribution from non-impounded sources between the dams and the downstream reaches (Figure 8.11). This progressive return of the isotope signal to the MWL indicates increased hydrological connectivity between the contributing hillslopes and stream in the landscape between the Dam Out and Bridge stations. This connectivity continues through the base flow period, as reflected by the analyses for June 2010 where 49% of the discharge at B1 and 34% of that at B2 are contributed by the relatively small connected sub-catchments immediately upstream of the Bridge stations (Figure 8.12).

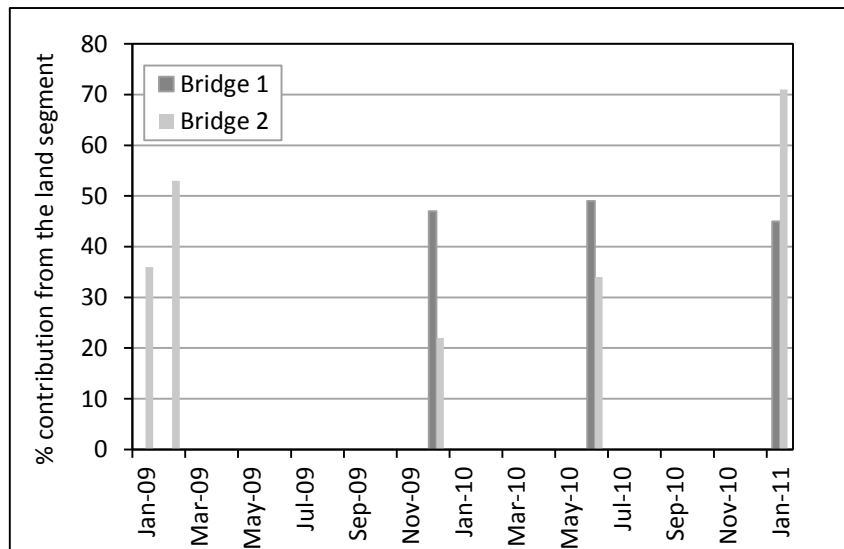


Figure 8.12: Percent contribution of the sub-catchment between the impounded tributaries and the bridge stations to total discharge.

Isotope analyses revealed that the headwaters, comprising 70 % of the catchment area, contributed as little as 29 % of the total catchment discharge, due to impoundments in this area. However, this contribution varied significantly for different events, reaching a maximum of 78 % of the catchment discharge. Studies done in Potshini catchment in South Africa gave an indication and insight of the spatial variations of the runoff generation at 3 different scales of 23ha, 100ha and 1000ha (Lorentz *et al.*, 2013). The mean contribution of the three selected water sources i.e. overland flow, soil water and groundwater were determined using end-member mixing analysis. The results showed that there was a general trend for soil water contributions to increase with the increase in catchment size during baseflow. Groundwater was estimated to contribute the most to the total runoff at all the three nested catchments. The mean groundwater contribution was 63 % at 23 ha, 50 % at 100 ha and 55 % at 1000 ha. The mean soil water contribution to catchment runoff increased from 15 % at 23 ha to 28 % at 100 ha and to 37 % at 1000 ha. Overland flow or event water contribution was almost stable at 22 % at 23 ha and 22 % at 100 ha but highly decreased to 8 % at the 1000 ha catchment outlet.

8.2 *ACRU-NPS* Crop Yields and Pollutant Loads Simulations

8.2.1 Simulation scenarios in the Mkabela Catchment

With the newly modified and calibrated *ACRU-NPS* model a series of scenarios were tested based on the catchment configuration and observations made in the Mkabela research

catchment. Large scale sugarcane farming in the Mkabela Catchment in particular, involves use of large quantities of fertilizers, herbicides and pesticides. The current ecological state of the rivers within this catchment and their responses to the natural as well as human induced disturbances must be understood clearly. The *ACRU-NPS* model, which simulates nutrient (NO_3 and P) and sediment production in agricultural catchments, was used to evaluate by modelling, the impact of farming practices and land-use changes on crop yields, water discharge, and nutrient and sediment loads in the 41 km² Mkabela Catchment in the KwaZulu-Natal midlands, South Africa.

Five scenarios of management practices were simulated: (1) *Base case*: simulation of the catchment under current land use; (2) *No contours*: current land use, assuming no contours are used in the sugarcane estates; (3) *All sugar*: assuming all land area comprises sugarcane; (4) *Irrigation*: current land use, but with deficit irrigation applied to the sugarcane; (5) *No control features*: the base scenario with both artificial and natural structures (farm dams, buffers and wetlands) removed. These scenarios were run with a series of fertilizer management applications, comprising current fertilization practice, twice, half and a quarter of the base fertilizer applications and finally, no fertilizer (zero) application. The resulting crop yields, water discharges, nutrient and sediment loadings are analysed.

The simulation period consisted of an 18 month crop cycle. The 1st crop (1/8/2006-23/1/2008) had 1280 mm of rainfall for the season, 2nd crop (24/1/2008-15/7/2009) had 842 mm of rainfall for the season and the 3rd crop (16/7/2009-6/1/2011) had 1046 mm of rainfall for the season. The resulting crop yields, water discharges, nutrient and sediment loadings are given below. Doubling fertilizer application from base rates resulted in 5 t/ha as the highest sugarcane yield increase on average. Zero fertilizer application resulted in the highest sugarcane yield reduction (11 t/ha on average). When a base fertilizer application rate was retained while applying deficit irrigation, 16 t/ha was the highest sugarcane yield increase on average. The *ACRU-NPS* model retention capacities of wetlands, dams and buffers of the total loads for the base case scenario for the period 2006-2012 are discussed below.

8.2.2 Sugarcane crop yields from sub-catchments

Appendix G gives tabular analysis of simulated average crop yields for all the crop seasons for different land segments in the catchment with different fertilizer application rates and soil types. LS3 and LS4 containing Cartref soils (100 % Cf) produced on average the highest crop yields for the entire crop seasons for zero, quarterbase and halfbase fertilizer applications with 57, 61 and 63 t/ha, respectively. LS2 (34 % Cf and 66 % Gc) on average produced lower crop yields for the same fertilizer applications with 54, 58 and 61 t/ha respectively. LS1 containing Avalon soils (100 % Av) produced on average intermediate crop yields for similar fertilizer applications with 55, 60 and 62 t/ha, respectively. LS1, however, produced the highest crop yields with 66 t/ha for base and 71 t/ha for doublebase fertilizer applications. LS2 produced on average the least yields for base and doublebase fertilizer applications, 63 t/ha and 68 t/ha, respectively. LS3 and LS4 on average produced intermediate crop yields for base and doublebase fertilizer applications (65 and 69 t/ha respectively). LS1 produced the highest crop yields of 82 t/ha during irrigation with base fertilizer application. LS2, LS3 and LS4 on the other hand produced the least crop yield of 79 t/ha during irrigation with base fertilizer application. The observed catchment average crop yields for South African sugarcane grown in KwaZulu-Natal province is 67.7 t/ha (SASA, 2012).

8.2.2.1 Crop yields from zero, quarterbase and halfbase fertilizer application rates

Cartref soils (LS3 and LS4) are shallow sandy soils with very little water holding capacity while Avalon soils (LS1) are deeper sandy soils with soft or hard plinthic sub-horizons that are permeable to water. Growing season 2008/2009 had the least amount of total rainfall available in the catchment with 842 mm/season. During the season 2008/2009 Cartref soils produced on average much higher crop yields than Avalon soils for quarter, half and zero fertilizer application rates (Figure 8.13). This may be attributed to the ease with which water in the Cartref soils dissolve the little available soil nutrients or fertilizer on saturation which then becomes more readily available to the sugarcane crop. The deeper Avalon soil-horizons cannot be easily saturated with the low rainfall available; hence the limited available nutrients cannot be easily accessed by the plant roots leading to slightly lower crop yields than in Cartref soils. Crop yields from LS2 (34 % Cf and 66 % Gc) were not as good as those from areas composed purely of Cartref or Avalon soils. This is probably because Glencoe soils have similar characteristics as Avalon soils. The only difference is that Glencoe soils were

located in steeper slopes making it even more difficult compared to Avalon soils to be saturated during periods of low rainfall. This then leads to the least available nutrients to the sugarcane crop resulting in the lowest crop yields (Figure 8.13).

Abandoning fertilizer application completely would not be viable economically given that on average there would be a loss in crop yields of between 8-11 t/ha for all soil types. Reducing fertilizer application by half may be a viable option in some instances especially in landsegments LS2, LS3 and LS4 where there only would be a 2 t/ha loss on average in crop yields with an advantage of lesser nutrient loads emanating from these fields.

8.2.2.2 Crop yields from base and doublebase fertilizer application rates

Avalon soil types (LS1) performed much better than Cartref and Glencoe soil types (LS2, LS3 and LS4) for base and doublebase fertilizer applications with a minimum of 66 t/ha and maximum of 71 t/ha respectively on average (Appendix G). This is probably due to the fact that good crop cover associated with adequate nutrients and deeper soils on less steep slopes would retain more soil moisture compared to shallow soils on very steep slopes. In essence there would be less nutrient and moisture stresses in Avalon soils and more stresses for shallow Cartref and steeper Glencoe soils. Doubling fertilizer applications from base rate increased crop yields on average by 5 t/ha for LS1 and LS2 and 4 t/ha for LS3 and LS4.

8.2.2.3 Crop yields from variable irrigation rates with base fertilizer application

During deficit irrigation base fertilizer application rates was maintained and only the amount of moisture added varied. The amount of irrigation water supplied depends on effective rainfall, the crop water consumption at different stages of crop growth and soil water holding capacity (soil type). This eventually results in less moisture stress to sugarcane crops. Given that adequate fertilizer rates were applied already (less nutrient stress) this means that more crop yields would be realised. This is reflected by crop yield increase in most of the land segments. The highest increase in crop yields with irrigation occurred in both LS1 and LS2 with 16 t/ha increases from base crop yields. LS3 and LS4 had 14 t/ha increase with irrigation from base crop yields. The 16 t/ha increase in crop yields probably is related to deeper soils (LS1 and LS2) that hold more moisture compared to 14 t/ha from shallower soils (LS3 and LS4) that were easily saturated and encouraged runoff.

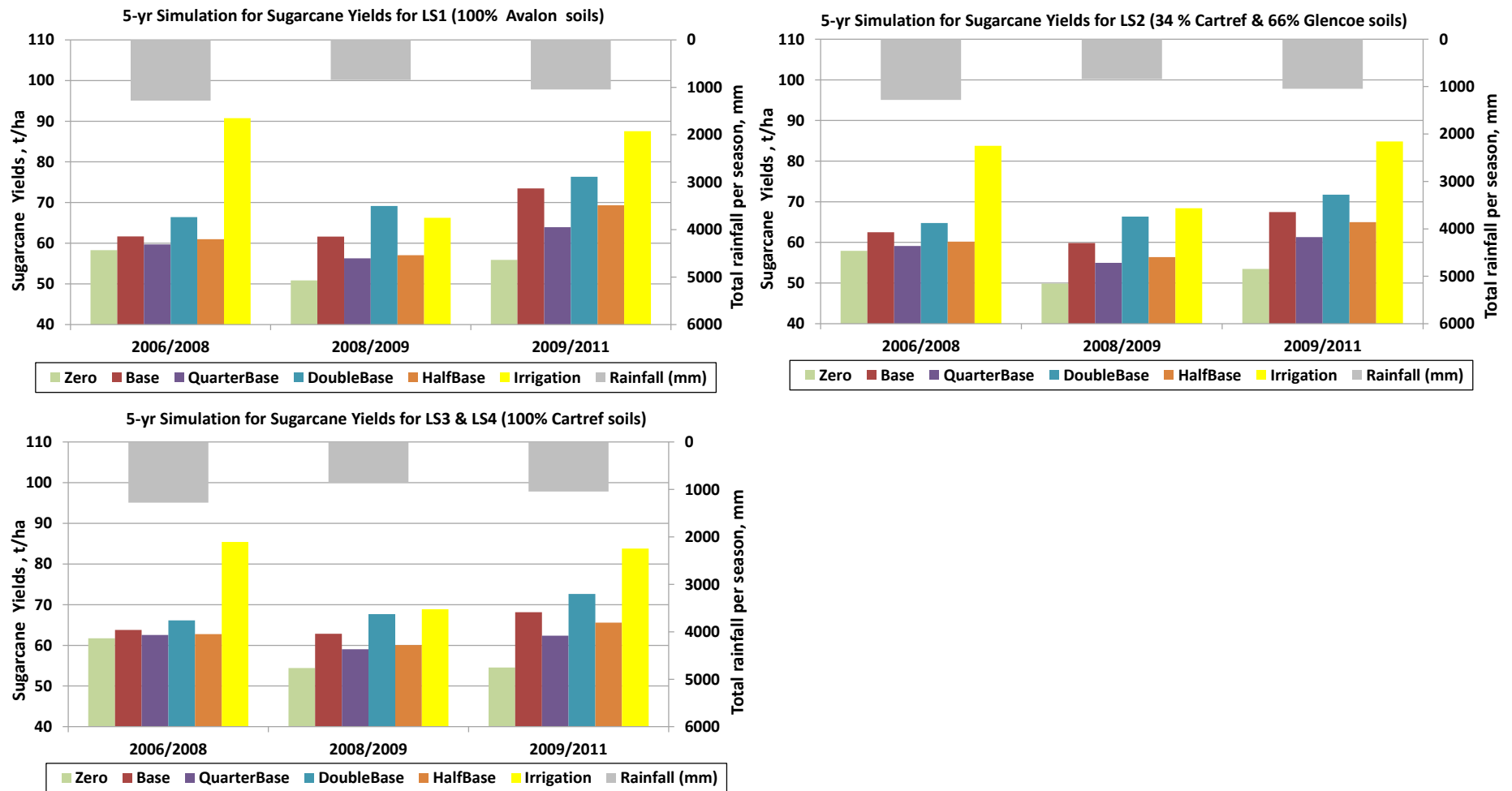


Figure 8.13: Modelled sugarcane crop yields from the different sub-catchments with varying fertilizer application rates under rainfall and a base fertilizer application scenario with irrigation applied.

It is, however, interesting to note that during the 2008/2009 crop season sugarcane crop yields under irrigation did not perform well for most sub-catchments and it was worse in LS1 where Avalon soil type existed (Figure 8.13). The lower yields are probably related to the climatic conditions and planting dates. The 24th January 2008 planting date for 2008/2009 crop season was towards the end of summer. This means that the first 6 months of crop growth would occur during the winter season where low temperatures are experienced. With lower temperatures, less evapotranspiration would occur and this would not favour rapid crop growth. The effect is much worse in deeper soils like Avalon that would remain mostly saturated. In essence the deficit water supplied through irrigation would not be very effective in increasing crop yields. 1st August 2006 and 16th July 2009 planting dates for the 2006/2008 and 2009/2011 crop seasons, respectively, were towards the end of winter. This means that for these seasons the first 6 months of crop growth occurred during summer where temperatures were higher. The provision of supplemental water to replace water lost through evapotranspiration would favour rapid crop growth that was eventually revealed in higher crop yields at the end of the season (Figure 8.13).

Irrigation with base fertilizer application rate resulted in increased crop yields and therefore would be the best alternative considering the extra fertilizer costs to be incurred and excess nutrient loads generated with doubling of fertilizer applications. This however must be done with appropriate timing of planting date being considered.

8.2.3 Movement of water, nutrient and sediment loads through control features

Based on the simulations performed using observed climate input data, the influence of the riparian buffers, wetlands and dams on runoff and on the downstream transfer of nutrients and sediments was assessed by estimating the changes between the amounts entering these control features and the amounts exiting them.

The *ACRU-NPS* model has sufficient process details to allow for the implementation of control features such as wetlands, dams and buffer strips. The retention capacities were generated in the *ACRU-NPS* model as an output after considering peak discharge, sediments and nutrient (NO_3 and P) loads reaching these control features and subtracting them from those exiting these systems. The amounts retained are given as a percentage of NPS pollutants that had originally reached the control features.

The retention capacities for the base scenario (see Appendix H for details) obtained from the *ACRU-NPS* model simulations in the Mkabela Catchment are summarized below;

Buffers: Sediments (72.7-82 %), NO₃ (60.5-70.2 %) and P (60.5-70.6 %)

Wetlands: Sediments (88.4-94.7 %), NO₃ (62.4-69.4 %) and P (60.7-68.8 %)

Dams: Sediments (17.8-80.0 %), NO₃ (27.7-33.1 %) and P (32.2-38.2%)

Peak discharge attenuation: Dams (28.9-54.1%), buffers (0-0.1%) and wetlands (95.2-97.5 %)

The total loads outputs from *ACRU-NPS* simulations for 2006-2012 period are given for different fertilizer application rates in Appendix I and different management scenarios in Appendix J. Retention capacities for these scenarios were, however, not calculated because the controls (i.e. buffers, wetlands and dams) were expected to behave in the same manner as for the base scenario. Hence, the expected retention capacities for the different NPS pollutants and the peak discharges attenuated for these controls would be in the same % ranges, similar to those obtained from the base scenario.

The daily *ACRU-NPS* model output for NO₃, P and sediments entering and leaving wetlands, buffers and dams for the base scenario are shown in the graphs in Appendix M. It can be seen from these graphs that in general there were significant reduction in daily NPS pollutants leaving most of these controls. All the NO₃, P and sediment loads leaving buffers, wetlands and dams were mostly attenuated. Dams in general are expected to perform well in attenuating sediments as compared to attenuating NO₃ and P loads at the outlet (Appendix M). Dam2 however performed poorly in attenuating sediments. The probable reason for this behaviour is discussed below in section 8.2.3.2.

Wetlands can provide important benefits to water quality by retaining or transforming pollutants such as nutrients, sediments, pathogens, pesticides and trace metals (Knox *et al.*, 2008). Riparian buffer zones on the other hand play an important role as nutrient pollution controls for rivers and have been accepted as important management practices to improve the quality of rangeland runoff before it enters streams or rivers (Knox *et al.*, 2008; Weissteiner *et al.*, 2013). Dams have been known to be effective in attenuating peak floods and have also acted as sinks for suspended sediments generated from the catchments as it allows mostly coarser sediments to settle (Verstraeten and Poesen, 2000).

Studies done by Knox *et al.* (2008) in the US showed that natural wetlands were able to retain 48-91 % of TSS, 32-95 % of NO₃ and 5-50 % of ortho-PO₄⁻. In addition, retention capacities for constructed wetlands for municipal wastes were 68 % TSS, 51 % NO₃, 55 % TN, 41 % ortho-PO₄⁻ and 34 % TP. Mburu *et al.* (2013) showed that constructed wetlands in Kenya reduced 84 % of TSS, 8 % of NH₄⁺ and 26 % of TP for municipal wastes. In Nigerian, Adelegan and Agbede (2011) achieved removal efficiencies of 88.4 %, 26.6 % and 25.0 % for TSS, NO₃ and TP respectively from food processing waste in a subsurface flow constructed wetland. Weissteiner *et al.* (2013) estimated retention in surface runoff emissions of 33 % for N and 65 % for P for buffer attenuation in studies done in Europe. In Australia a grass buffer reduced TP, filterable reactive P, TN and SS loads from surface runoff by 50 to 60 % (McKergow *et al.*, 2006).

8.2.3.1 Discharge through control features

Wetlands were more effective in attenuating peak discharges than dams and buffers for most frequencies and magnitudes of flood events. This could be directly related to the higher volumes of water that wetlands can store given that they were only 10 % full at the beginning of simulation compared to 60 % full for dams. It is important however to note that the sizes of the dams and wetlands varied. The geographical distribution and extent of the farm dams and wetlands were digitized from SPOT 5 panchromatic sharpened images at 2.5 m resolution acquired in soil survey done in 2006 (Le Roux *et al.*, 2006). The areas of dam1 and dam2 were 9.5 ha and 24.1 ha, respectively. The sizes of wetland1, wetland2 and wetland3 were 13.83 ha, 22.46 ha and 10.24 ha, respectively. Appendix H corroborates the above argument in that there is 95.2-97.5 % reduction in peak discharge coming out of wetlands and 28.9-54.1 % for the dams. Figure 8.14 shows the peak discharges coming out of wetland1 and dam1 to be significantly attenuated.

All the runoff reaching the buffers will ultimately leave the buffer area into the stream. A decrease in runoff volume and velocity as water moves through the buffer allows for sediment and associated pollutants to deposit in the buffer and increases the time of contact for adsorption onto soil and vegetation (Fajardo *et al.*, 2001; Rankinen *et al.*, 2001). This results in a reduction in surface runoff and associated pollutants to down-slope riparian systems (Hayes *et al.*, 1979; Rankinen *et al.*, 2001). As water moves through the buffers their ability to attenuating peak discharges through reduced surface runoff is negligible and buffers

may not be as effective as dams and wetlands in attenuating flood peaks.

There is higher peak discharge coming out of wetland3 compared to that coming out of wetland1 and wetland2 (Figures 8.14 and 8.15). This is possibly due to the lower area (10.24 ha) and volume capacity (153,600 m³) of wetland3 and that wetland3 receives more runoff from the larger upstream catchment area (16.49 km²) that includes discharge out of dam2. Peak discharges coming out of wetland2 are the least perhaps because of its highest area (22.46 ha) and volume capacity (336,900 m³) and less runoff received from smaller upstream catchment area (7.32 km²). The wetland1 peak discharge at the outlet lies in between that which comes out of wetland2 and wetland3. This is probably due to its intermediate area (13.83 ha) and volume capacity (207,450 m³) with an upstream catchment area of 7.98 km².

Though peak discharge is not attenuated at either buffer more runoff is received in buffer1 than buffer2. This is reflected in a higher peak discharge coming out of buffer1 than buffer2. Buffer1 has a higher upstream catchment area of 9.78 km² and a width of 10 m while buffer2 has 0.09 km² and is 15 m wide. Hence, buffer2 managed to attenuate peak discharge by a negligible 0.1 %. Dam1 with upstream catchment area of 17.76 km² received almost double the amount of runoff compared to that which was received at dam2 with an upstream catchment area of 7.41 km². Both of them, however, had similar quantities of runoff released at the outlet. Both dams were 60 % full at the beginning of simulation but dam1 managed to retain most of the water flowing into it. Hence dam1 with a lesser capacity (283,200 m³) received more runoff than dam2 (721,500 m³) and could be said to have been the most effective in attenuating the peak discharges (54.1 % as compared to dam2 with 28.9 %).

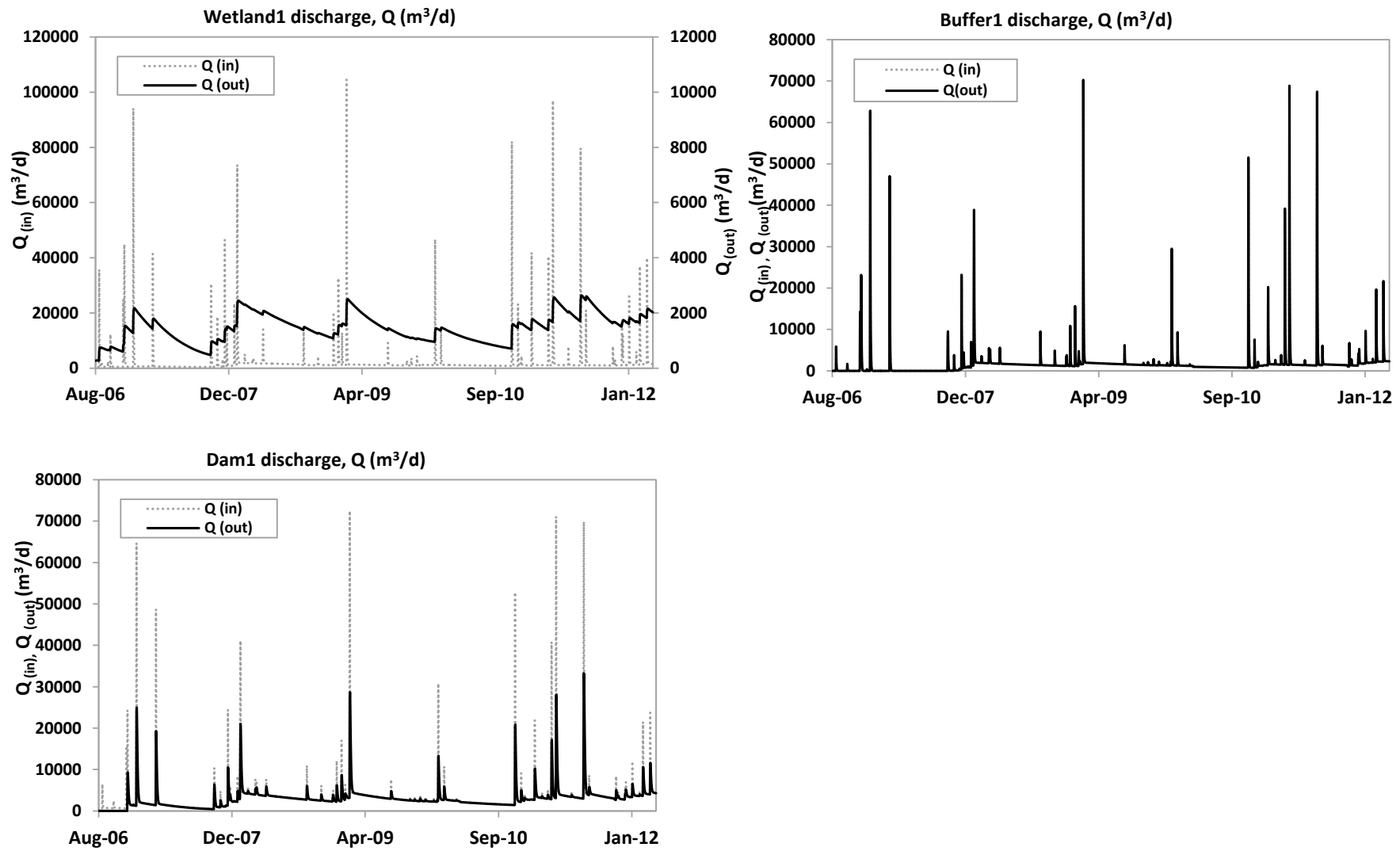


Figure 8.14: Discharges entering and leaving wetland1, buffer1 and dam1 for the simulation period 2006-2012.

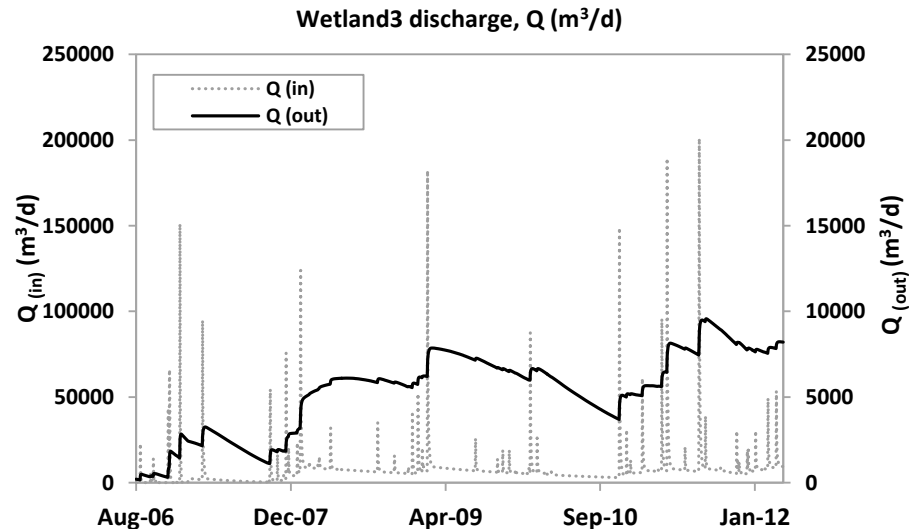
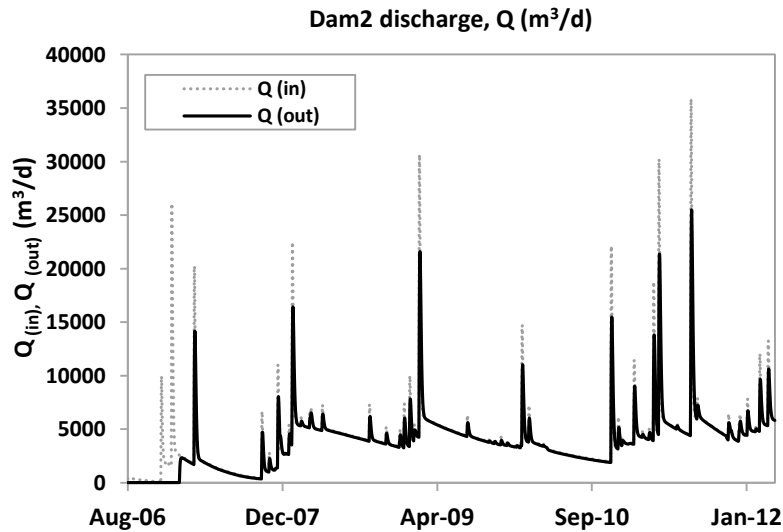
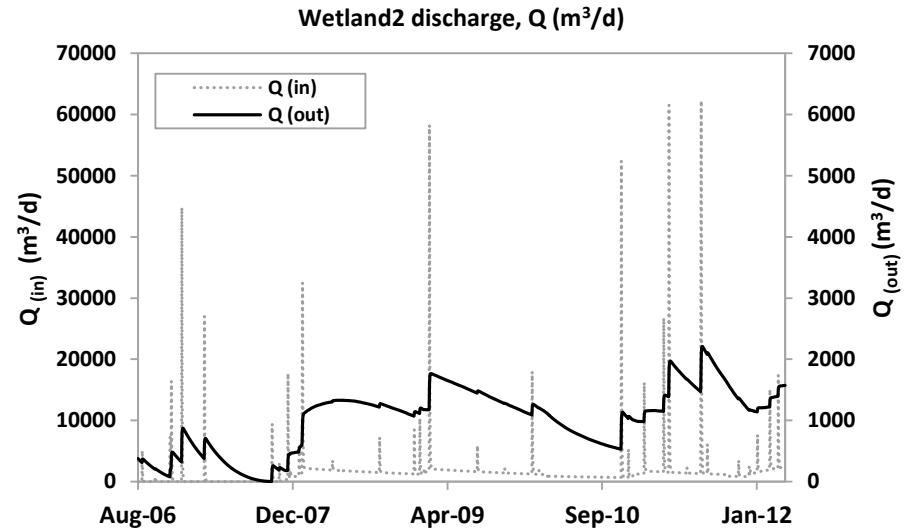
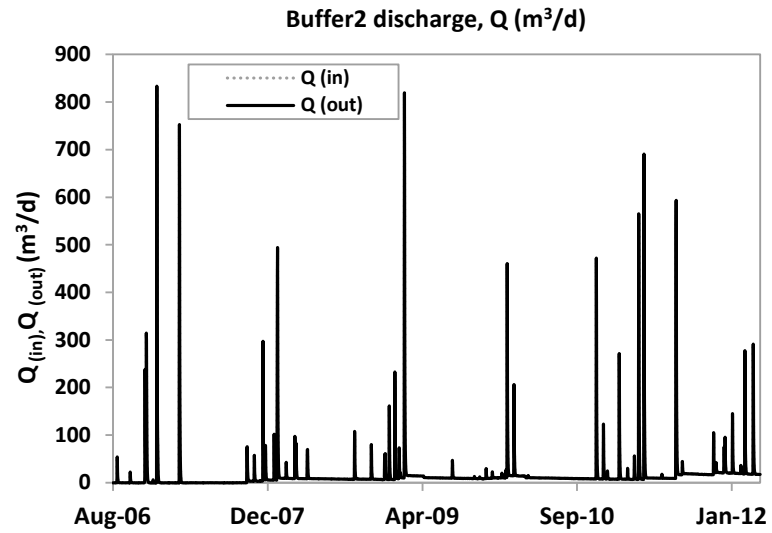


Figure 8.15: Discharges entering and leaving buffer2, dam2 and wetlands2 & 3 for the simulation period 2006-2012.

8.2.3.2 Transport of nutrient and sediment loads through control features

Wetlands, buffers and dams all possess capabilities for attenuating NPS pollutant loads. It is the degree to which each attenuate or reduce NPS pollutant loads as they pass through them that differs. Apart from reducing NO₃ and P significantly, wetlands and buffers performed even better in attenuating sediments (Figure 8.16). It was however noted that dams registered low retention capacities for NO₃ (27.7-33.1 %) and P (32.2-38.2%). Their ability though to attenuate sediments varies through a wide range (17.8-80.0 %). Dams are capable of reducing sediment loads and sediment associated P more than reducing soluble nutrient loads. Depending on the 50 percentile particle size of delivered sediment (d_{50}) which affects settling velocities, sedimentation in the dams or wetlands under the force of gravity would favour heavier particles. Dam1 had a d_{50} equivalent diameter of 71.4 μm (61.8 % sand, 24.3 % silt and 13.9 % clay) exhibited as 80.0 % attenuation rate. Dam2 on the other hand received lighter particles with an equivalent particle diameter, d_{50} , of 30.4 μm (35 % sand, 50 % silt and 15 % clay). Sediment consists of particles of all sizes, from fine clay particles to silt, sand, and gravel. The sediments reaching dam2 were mostly composed of silt hence the lower attenuation rate of 17.8 % (Figure 8.16).

The decline in nutrients after being routed through the wetland can be attributed to the hydrogeological and biochemical characteristics of wetlands. The ability of wetlands to retain water for prolonged periods of time promotes anaerobic conditions which facilitates the retention and loss of both N and P through mass adsorption and immobilisation (Knox *et al.*, 2008). N may also be lost through volatilisation. The migration of both N and P through the wetland was considered to be adequately simulated by the model and the total loads were also considered to be adequately reproduced (Figure 8.16). Following a rainfall event, the amount of sediment generated from upstream sources generally increases with an increase in runoff. The sharp decline in sediment between wetland entry and exit can be attributed to the settling effect of sediment when routed through the wetland. Subsequent to wetland routing, a similar reduction trend as observed for both runoff and sediment was also observed for nutrients. The *ACRU-NPS* model sediment retention capacities for wetlands ranged from 88.4-94.7 %, which compared well with 48-91 %, 88.4 % and 84 % for TSS in the US, Kenya and Nigeria respectively (Knox *et al.*, 2008; Adelegan and Agbede, 2011; Mburu *et al.*, 2013).

Riparian buffers perform several key roles in minimizing the impacts of agriculture on stream

water quality. According to McKergow et al. (2006) buffers can: (1) stabilize stream channel morphology, (2) protect streams from upland sources of pollution by physically filtering and trapping sediment, nutrient and chemicals in surface runoff, (3) provide suitable subsurface conditions for plant uptake and chemical transformations, such as denitrification, (4) displace sediment and nutrient-producing activities away from streams. Vegetated buffer strips can effectively control erosion by forming a physical barrier that slows the surface flow of sediment and debris, by stabilizing wetland edges and stream banks, and by promoting infiltration. The required width of a buffer size is determined by: (1) the type of vegetation present, (2) the extent and impact of the adjacent land use and (3) the functional value of the receiving wetland.

Gabor *et al.* (2004) found that the bulk of sediment removal occurs in the first few meters of the buffer zone with sediment removal of up to 75-97%. Buffer strips can effectively remove nutrients (NO_3^- and P) from surface water flow. The main mechanisms of NO_3^- removal are by vegetation uptake in the roots and anaerobic microbial denitrification in the saturated zone of the soil. Relatively narrow buffers (< 30 m) seem to be very effective in reducing N (35-96%) while buffer strips that contain both woody and herbaceous vegetation, grasses and cropped buffer systems can be effective in P retention (27-97%) (Gabor *et al.*, 2004). In the *ACRU-NPS* model N, P and sediment losses in buffer strips are associated with strip width. The strip width can be used as a boundary condition when modelling with wider ones expected to be more effective in reducing NPS pollutants. Buffer1 (10 m wide) received more nutrients and sediments from a larger upstream catchment area covered in both pasture (3.11 km²) and sugarcane (5.67 km²) compared to buffer2 (15 m wide) that had pasture (0.09 km²) (Figure 8.16). Both buffers were quite efficient in attenuating sediments passing through them. Nutrient loads (N and P) for both buffers were also significantly reduced. It is important to note that though there was no attenuation of discharges coming out of the buffer outlet, reductions of NPS pollutant loads was entirely dependent on strip width and not on their settlement. The retention capacities of Buffer1 for NO_3 , P and Sediments were 60.5 %, 60.5 % and 72.7 %, respectively. The buffer2 values were 70.2 %, 70.6 % and 82 % for NO_3 , P and Sediments, respectively.

8.2.3.2 (a) NPS pollutant loads through control features with different fertilizer application rates

In many areas of the world, nitrogenous fertilisers are routinely applied to sugarcane at rates of around 50-200 kg/ha/year, contributing (amongst other things) to the process of soil acidification (WWF, 2011). There is a direct economic incentive for farmers to reduce fertiliser inputs, as these represents significant costs and over-use of N fertiliser ultimately reduces sugar yield. Many sugar industries have consequently published recommendations on fertiliser use and incorporate these in guidance provided to their farmers. In the Mkabela Catchment crop fertilization is administered using primarily N and P-based fertilizers including compost farmyard manures. It has been noted specifically that farmers in the catchment apply divergent amounts of fertilizers. It was therefore prudent to run several scenarios by adjusting fertilizer application rates. This would eventually assist farmers in making the best management decisions on sustainable farming that would be economically and environmentally beneficial. Sustainability in this case does not necessarily imply reduced productivity and profits; indeed, measures to address environmental impacts can provide economic benefits for farmers or mills through cost savings from more efficient resource use.

Doubling of the fertilizer application rate (high) from the base rates resulted in higher NO_3 and P outputs from the control features (Figure 8.16). Because some of the excess fertilizer was taken up by the sugarcane, doubling of nutrient (NO_3 and P) loads at the control features outlet did not necessarily occur. Doubling of fertilizer application rate, as shown earlier, resulted in the highest crop yield increase in LS1 of 5 t/ha from base scenario. An economical benefit analysis however must be done to justify the extra income earned in comparison to pollution cost. Reducing base fertilizer application rates to half (low-1/2) resulted in lowered nutrient loads coming out of the control features. This seems to be a better option to implement for the following reasons: (1) no significant crop yield loss, (2) less fertilizer costs and (3) improved aquatic environment. Reducing base fertilizer application rate further to quarter (low-1/4) resulted in further reduction in crop yields with LS1 having the highest decrease of 6 t/ha. This is replicated in decreased amounts of pollutant loads coming out of the control features. Again embracing these options will entirely depend on the results of a cost-benefit analysis.

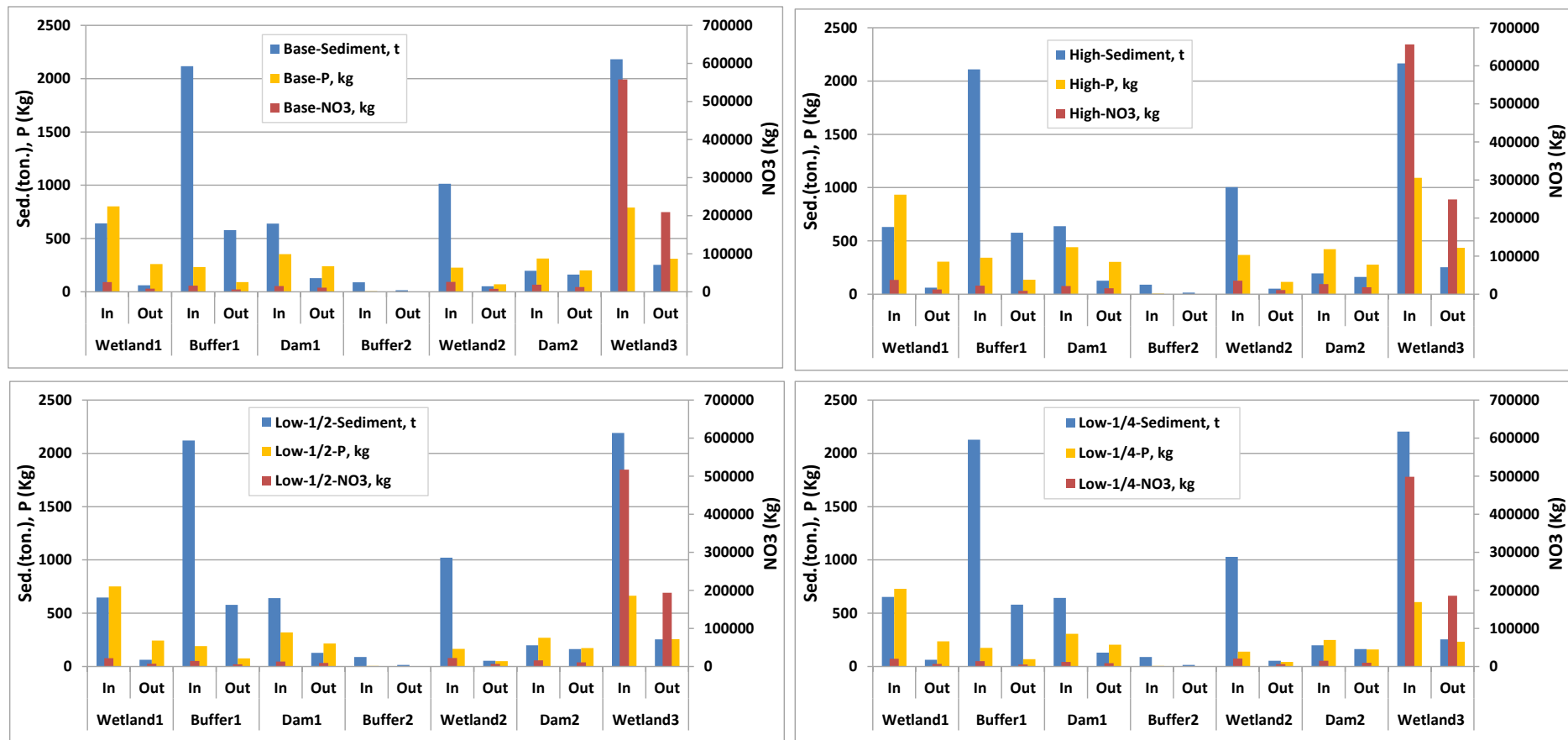


Figure 8.16: Total nutrient (NO₃ and P) and sediment loads from different fertilizer application rates routed out of wetlands, buffers and dams for the entire simulation period (2006-2012).

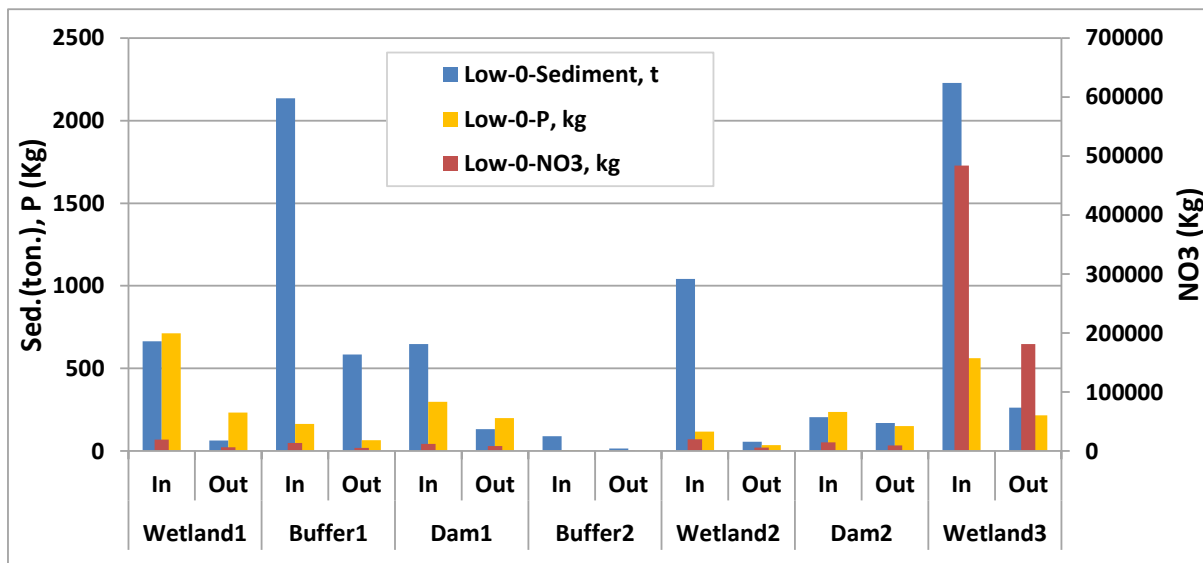


Figure 8.17: Total nutrient (NO₃ and P) and sediment loads for zero fertilizer routed out of wetlands, buffers and dams for the entire simulation period (2006-2012).

Using the zero fertilizer application option, the crop yields obtained are greatly reduced with LS1 having the highest drop of 11 t/ha. From the farmers' point of view, the benefits attained from having little NPS pollutant loads coming out of the catchment outlet with no fertilizer application may not make economic sense. This scenario produced the least amount of NPS pollutant loads at the control outlets but would not be viable to choose given that sugarcane crop yields were very poor or highly compromised (Figure 8.17). There was a slight increase in sediments received at the control features as seen in wetland3, ~48 tons, from base scenario case (Appendix I). This allowed more sediment to be generated during rainfall because of a decrease in crop density caused by a lack of fertilizer application (Figure 8.17).

8.2.3.2 (b) NPS pollutant loads through control features with different management scenarios

The different scenarios of management practices that were simulated are shown in Figure 8.18 and includes: (1) *No contours*: current land use, assuming no contours are used in the sugarcane estates; (2) *All sugar*: assuming all land area comprises sugarcane; (3) *Irrigation*: current land use, but with deficit irrigation applied to the sugarcane; (4) *No control features*: the base scenario with both artificial and natural structures (farm dams, buffers and wetlands) removed. All the above scenarios were run with the base fertilizer application rates.

Running the model with *no contours* resulted in more sediment reaching the control features which were eventually routed through them. These extra sediments came from sugarcane fields where soil conservation methods would normally be practised by contouring. Wetlands 1 and 2 received approximately 8 times more sediments from sugar1 and sugar3 fields, respectively. Buffer1 received approximately 3 times more sediments from sugar2 field while dam1, for which some sediment had been trapped in wetland1 and buffer1, received approximately 4 times more sediments than before. At the catchment outlet wetland3 received approximately 7 times more sediment from the entire upstream sub-catchments that included sediment from dam2 outlet.

Introduction of sugarcane in the entire catchment that involved replacing pasture, forest and vegetable fields with sugarcane resulted in varied responses of NPS pollutant loads at the control features. It is important to note that forest2 was not changed to sugarcane because of its steep slope of 13.5 %. Sugarcane currently grown on many steep slopes and hillsides has led to higher rates of soil erosion resulting from the increased rates of water runoff on sloping land. Though it is recommended that sugarcane should not be grown on slopes > 8 %, slopes of up to 20-30 % are planted, for example, in parts of the Caribbean and South Africa (WWF, 2011). In *all sugar* scenario (Figure 8.18), sediments entering buffer1 which had pasture originally (LP1) (3.11 km², slope 5.5 %) and now replaced with sugarcane, received 1.3 ton less sediments after the introduction of contours in the sugarcane field (Appendix I and J). On the contrary buffer2 received 80 ton less sediments from LP2 (0.09 km², slope 9.5 %) after introducing contours in sugarcane that replaced pasture (Appendix I and J). This information supports growing of sugarcane in gentle slopes. LP2 hillslope with smaller catchment and steep slope generated more sediments than LP1 hillslope that had larger catchment and gentle slope.

Sediment and nutrient (N and P) loads entering wetland1 were also reduced due to the introduction of sugarcane in place of forest1 (0.61 km²) and vegetables (1.06 km²). There was an overall reduction in sediment, NO₃ and P loads entering wetland1 by 82 ton, 4.7 ton and 0.3 ton, respectively (Appendix I and J). The introduction of contours in forest1 along with replacement of vegetable plot for sugarcane had a significant impact on reducing sediments. Sediment fingerprinting studies done by Miller *et al.* (2013) in the Mkabela Catchment suggests that silt- and clay-rich layers found within wetland and reservoir deposits of the upper and upper-mid sub-catchments were derived from the erosion of fine-grained, valley

bottom soils frequently utilized as vegetable fields. Hence most of the fine-grained sediments reaching wetland1 are most likely to be originating from the vegetable field.

Wetland3 received lesser nutrient loads at the catchment outlet even though forest2 was not converted to sugarcane. Appendix J shows wetland3 in the *all sugar* option received less pollutant loads by 1.5 ton and 7 ton for NO₃ and sediment respectively, from the base scenario. This may be due to the introduction of sugarcane hence implementation of soil conservation measures in fields that were originally with pastures and forests. This means less sediment is being received from the upstream land segments. NO₃⁻ that previously leached in the root zone of pastures would be utilized by the sugarcane crop that was introduced.

The irrigation required under standard conditions is the depth of water needed to meet water loss through evapotranspiration (ET) of a disease-free growing crop in a large field under non-restricting soil water and fertility and achieving full production potential under the given environment (Allen et al., 1998). Adopting *irrigation* increased NPS pollutant loads going into the control features which were eventually attenuated at their outlet after routing (Figure 8.18). Where irrigation is inefficient or rainfall is high, runoff is generally associated with loss of valuable soil from the field which often contains nutrients (N and P) and sediments. Erosion is a significant issue in areas under sugarcane particularly in tropical areas since erosion rates in tropical agro-ecosystems are usually greater than the rate of soil formation.

The physical loss of soil by erosion is influenced by a range of factors such as rainfall and irrigation, wind, temperature, soil type, cultivation disturbance and topography (WWF, 2011). Hence irrigated cane cultivation not done in a sustainable way threatens the biodiversity of natural wetlands and can be harmful to the livelihoods of communities that rely upon them. Sediments also occupy reservoir space reducing its lifespan or dams may require expensive dredging. Irrigation in the sugarcane fields resulted in final sediment and NO₃ load outputs from wetland3 to increase by an additional 312 tons for sediments and 38.5 tons for NO₃ during the 5 year-simulation period (Appendix I and J). Excess NO₃ reaching the wetland3 outlet was mainly from baseflow in the upstream catchment, while the sediment load increase was due to increased detachment and transportation of soil particles in response to increased flow volume and peak discharges.

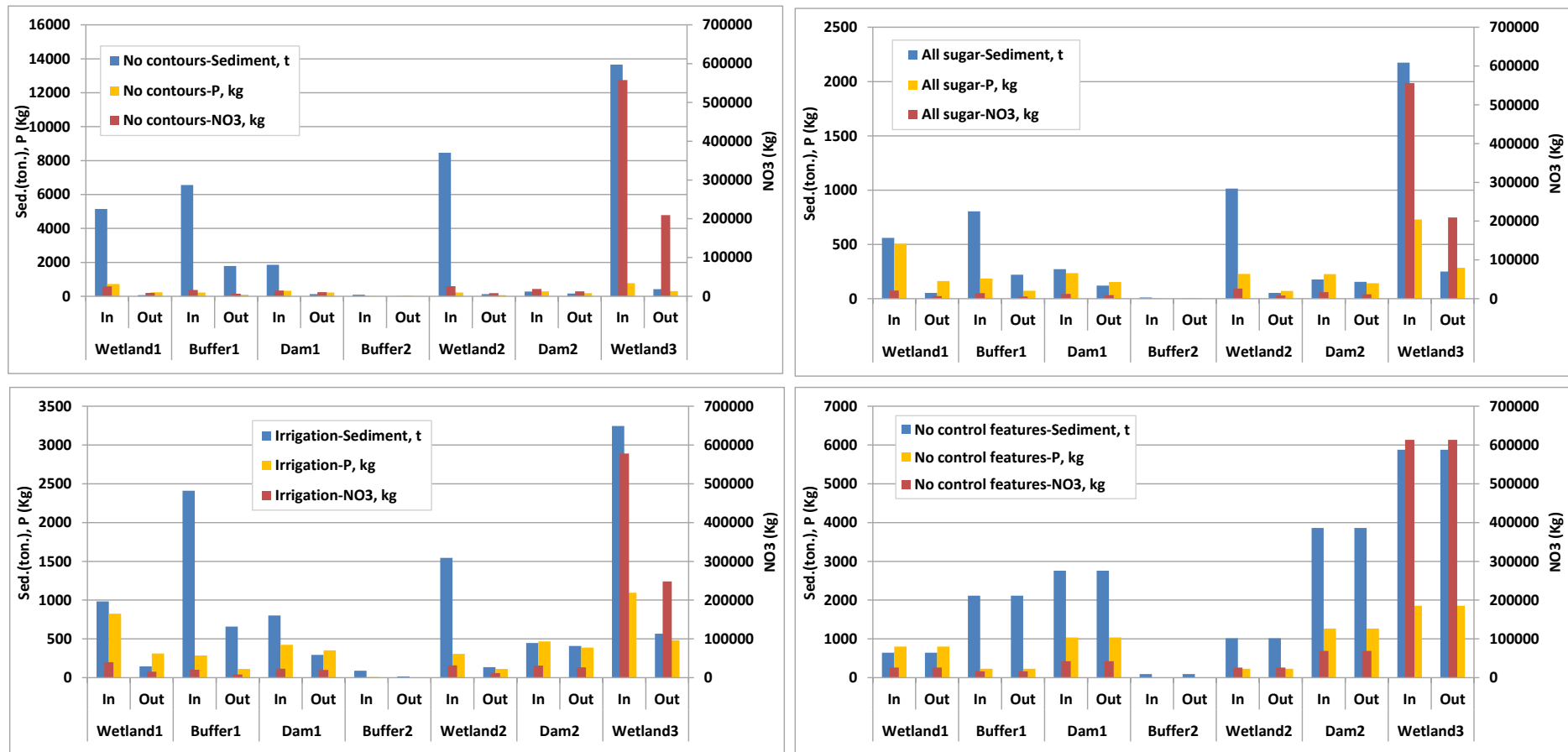


Figure 8.18: Total nutrient (NO₃ and P) and sediment loads for different management scenarios routed out of wetlands, buffers and dams for the entire simulation period (2006-2012).

During irrigation, the full sugarcane production potential under differing soil types (Av, Gc and Cf) was considered. The actual water requirement or actual evapotranspiration (AET) for sugarcane crop was dependent on the soil type and crop growth stage. Irrigation requirement (IR) for a crop was obtained by subtracting effective rainfall (ERFL) from AET (Equation 8.1).

$$IR = AET - ERFL \quad (8.1)$$

where $ERFL = RFL - SIMSQ$

$$SIMSQ = QUICKF + RUN$$

ERFL is dependent on soil type, soil moisture conditions and slope which characterises the different hillslopes in the Mkabela Catchment. ERFL is the rainfall that is effectively used by a crop where losses due to surface runoff/stormflow (QUICKF) and deep percolation/baseflow (RUN) have been accounted for. Simulated runoff (SIMSQ) in the *ACRU-NPS* model is composed of both stormflow and baseflow. Daily irrigation requirement (IR) was added to daily rainfall (RFL) obtained from the meteorological station before running the *ACRU-NPS* as a way of implementing irrigation.

No control features scenario involves removal of wetlands, dams and buffers in the catchment. The hydrological functions of wetlands include storage and eventual release of surface water, recharge of local and regional groundwater supplies, reduction in peak floodwater flows, de-synchronization of flood peaks and erosion prevention. Position in the landscape, location of the water table, soil permeability, slope and moisture conditions all influence the ability of wetlands to attenuate floodwaters (Gabor *et al.*, 2004). Wetlands are complex systems and several characteristics contribute to their roles as nutrient sinks. They retain nutrients in buried sediments, convert inorganic nutrients to organic biomass, and their shallow water depth maximizes water-soil contact and therefore microbial processing of nutrients and other material in the overlying waters (Gabor *et al.*, 2004). Wetlands can be effective NO₃ sinks in agricultural landscapes where up to 80 % removal can be achieved (Kirby, 2002). Phosphorus retention in wetlands can also be significant (up to 94 % removal) and is accomplished through adsorption onto particles, precipitation with metals and incorporation into living biomass (Kirby, 2002). Wetlands can also reduce the impacts of sedimentation on water quality within watersheds.

Hydrology is a primary determinant of the sediment-retention capacity of a wetland and controls the source, amount, and spatial and temporal distribution of sediment inputs (Gabor *et al.*, 2004). Percent of wetland area and position are important for reducing sediment loads of water passing through the system. Wetland drainage, however, reduces the natural capability of a watershed to attenuate runoff and associated NPS pollutants during flood conditions. The construction of a drainage ditch through a previously unchanneled wetland in the Mkabela Catchment in the 1990's altered the hydrologic connectivity of the catchment (Miller *et al.*, 2013). This allowed accelerated movement of water, nutrients and transport of sediments from the headwaters to the lower basin where much of sediments was deposited within the downstream riparian wetlands. This means that most of the NPS pollutant loads generated from the sugarcane and vegetable farms that would have been attenuated at the controls ended up in the river system. The NPS pollutants received from the upstream sub-catchments were easily cascaded downstream in the river and most of it reached the catchment outlet. The increased valley connectivity through constructed ditch, synonymous with wetland removal, therefore partly negated the positive benefits of controlling sediment/nutrient exports from the catchment by means of upland based, best management practices (Miller *et al.*, 2013).

The removal of control features means that beneficial influence of wetlands, buffers and dams to ameliorate the environment cannot be realised (Figure 8.18, *no control features*). The opportunity to reconcile the needs of the environment and people with the long-term development of sugar industry would therefore not be achieved. Hence absence of wetlands, dams and buffers would result in more pollution downstream. The total NPS pollutant loads coming out of wetland3 under the *no control features* scenario (Appendix J) were quite high compared to those under *base* scenario (Appendix I). This was represented by extra 5627 ton (sediments), 403.9 ton (NO₃) and 1.55 ton (P) from *no control features* scenario in excess of those loads generated under *base* scenario for the entire 5 year simulation.

CHAPTER NINE

9 CONCLUSIONS AND RECOMMENDATIONS

The nutrient (NO_3 and soluble-P) transport in the catchment mirrored the sediment migration through the channel system. The relationship between sediment and P was however poor. This suggests that much of the P transport from contributing hillslopes probably was in the dissolved phase and likely occurred through the subsurface during recession and low flow sequences. Further research is therefore recommended to observe and quantify subsurface controls of water and nutrient pathways, particular on hillslopes.

The first reservoir in the monitored network (Dam1) was effective in retaining event water from connecting with the downstream network for all but the most intense events. High intense events increases nutrient and sediment loads from the reservoir as a result of mixing and eventual release of resident nutrients and sediments. From the isotope analysis, certain events in Mkabela Catchment resulted in mixing in the dams and larger resultant outflow than inflow loads. These occurrences appeared to be a result of combinations of reservoir status, catchment antecedent conditions, rainfall depth and intensity. The nutrient loads between Bridge 1 and Bridge 2 stations reflected the bedrock control, where contributions from sugarcane hillslopes between these stations were not retained, even in the short wetland upstream of Bridge 2.

Stream discharge and consequent NPS pollutants from the two impounded tributaries was limited by the storage afforded in these impoundments. Isotope analyses showed that the headwaters, comprising 70 % of the catchment area, contributed as little as 29 % of the total catchment discharge, due to impoundments in this area. However, this contribution varied significantly for different events, reaching a maximum of 78 % of the catchment discharge. The geophysics in the Mkabela Catchment show that the dominant contribution mechanism for nutrients transfer across the landscape is in the subsurface flow, specifically lateral discharge in the intermediate layer between the sandy soil and bedrock. Event water, carrying high nutrient loads, dominated the responses at the field scale, while low flows reflected the groundwater concentrations of NO_3 and soluble-P.

The use of isotopes to define hydrological connectivity in the landscape and streams has enhanced our ability to interpret the movement of nutrients and sediments in agricultural catchments. It can be concluded that $\delta^{18}\text{O}$ and $\delta^2\text{H}$ isotopes of water were effective in assessing the contributions of different sources of water and that nutrient and sediment migration in the Mkabela Catchment was greatly influenced by hydrological connectivity. The water isotopes can be used to assess the contributions of different sources of water which impact the transport of nutrients and sediments in catchments and is recommended for improving NPS modelling.

The *ACRU-NPS* model was modified to include water and nitrogen stress algorithms for crop yield estimation and algorithms to simulate the effects of control features (wetlands, buffers and dams) on nutrient and sediment migration in the catchment. The *ACRU-NPS* model was successfully used to simulate NPS pollutants from sub-catchments for various land uses and for different control features in the stream network. Five simulation scenarios of pollution control and management measures were applied to the catchment. The analyses demonstrated that the use of the *ACRU-NPS* model played an important role in providing decision support during water quality management in the Mkabela Catchment. This however was not without some limitations. In fact one should be aware that in real scenarios sediment trap efficiency decreases when sediment deposition occurs in the reservoir. This decline in trap efficiencies through time should be included in the calculations of sediment yield as it is not done currently in the *ACRU-NPS* model.

The results illustrate the reduction in nutrient load caused by land management and natural and introduced flow path controls. Inclusion of sufficient scientific complexity into the model to allow for realistic predictions of NPS pollution loads through controls as well as crop yields has been a primary intention of this research. However, such a claim will have to be tested against different cropping and agricultural pollution control or mitigation systems. Nevertheless, the model can still serve as a decision management tool in addressing water quantity and quality problems. It can be used in designing of appropriate management strategies to control runoff and sediments from a catchment and water and fertilizer management in agricultural fields to minimize the NPS pollution losses with improved nutrient use efficiency of crops. Furthermore, the important role played by connectivity in the transfer of sediment and nutrient loads emanating from catchments has been realized. Stream network controls such as dams, wetlands and riparian buffers are important in attenuating

discharges for flood control as well as reducing detrimental effects of nutrient and sediment loads to downstream water pollution in rivers.

The crop yield component in the *ACRU-NPS* model could be developed further by introducing functions that relate soil depth (h), soil loss (ton) and input used (kg/ha of fertilizer). The volume lost due to erosion (m^3) may be determined by dividing the weight soil loss due to erosion (kg) by bulk density of the soil (kg/m^3). The soil depth (m) lost can be found by dividing soil volume lost (m^3) by area of crop under cultivation (m^2). The extent of soil fertility lost through erosion can then be found by relating organic matter (OM)/ organic carbon (OC) to the amount present in the soil. OM/OC lost could then be indirectly related to soil fertility lost and eventually the *ACRU-NPS* model may be used to predict crop yield loss due to soil erosion which is currently not done. This would eventually help in studying the soil loss-crop yield relationship. In the *ACRU-NPS* simulations the crop yields did not change with variation in soil loss/soil erosion.

Future modifications to *ACRU-NPS* model to allow use of detailed GIS mapping to identify the types of controls and connectivity features identified in this study is recommended. Modifications to model algorithms will also require features for simulating threshold responses in hillslope and streams to mimic the connectivity features identified. The techniques of hydrogeological delineation of typical hillslope response types should also be improved further and tested against hillslope monitoring of water and nutrient movement. Verification of simulated nutrient uptake and crop yield responses to water and nutrient stress and recovery through observation is also recommended.

REFERENCES

- ABEM 2005. A Nitro Consult Company, Bromma, Sweden. Lund Imaging System, Abem Instrument AB: Instruction Manual.
- Adelegan, J. A. and Agbede, O. A. 2011. The Future of Water, Sanitation and Hygiene: Innovation, Adaptation and Engagement in a Changing World. Wetland system: a cheaper and efficient treatment option for food processing waste in Africa. *Presentation at the 35th WEDC International Conference*. Loughborough, UK.
- Allen, R. G., Pereira, L. S., Raes, D. and Smith, M. 1998. *FAO Irrigation and Drainage Paper 56: Crop Evapotranspiration: Guidelines for computing crop water requirements*. FAO Publication, Rome, Italy.
- Amatya, D., Chescheir, G., Fernandez, G., Skaggs, R. and Gilliam, J. 1999. Export coefficient based lumped parameter water quality modelling. *Annual North Carolina Water Resources Research Conference (poster presentation), Raleigh, USA*.
- Ambrose, B. 2004. Variable active versus contributing areas or periods: a necessary distinction. *Hydrological Processes* 18(6): 1149-1155.
- Bereitschaft, B. J. F. 2007. Modeling nutrient attenuation by riparian buffer zones along headwater streams [Internet]. University of North Carolina, Greensboro, USA, 79 pp. Available from: <http://libres.uncg.edu/ir/uncg/listing.aspx?id=1087> [Accessed 10 October 2011].
- Beven, K. J. 1989. Changing ideas in hydrology: the case for physically based models. *Journal of Hydrology* 105(1-2): 157-172.
- Beven, K. J. 1993. Prophecy, reality and uncertainty in distributed parameter models. *Advances in Water Resources* 16: 41-51.
- Bhat, K. K. S., Flowers, T. H. and O'Callaghan, J. R. 1980. Nitrogen losses and surface runoff from landspreading of manures. *Proc. Euro Eco Comm Program of research on effluents from livestock, Wexford Ireland*. May 20-22: 222-246.
- Bingner, R. L., Murphee, C. E. and Mutchler, C. K. 1989. Comparison of sediment yield models on watershed in Mississippi. *Trans. ASABE* 32(2): 529-534.
- Bloeschl, G. 1997. Special edition: scale problems in hydrology. *Water Resources Research* 33(12).
- Bloeschl, G. 2001. Scaling in hydrology. *Hydrological Processes* 15(4): 709 - 711.

- Bouma, J., Droogers, P., Sonneveld, M. P. W., Ritsema, C. J., Hunink, J. E., Immerzeel, W. W. and Kauffman, S. 2011. Hydropedological insights when considering catchment classification. *Hydrol. Earth Syst. Sci.* 15: 1909-1919.
- Bracken, L. J. and Croke, J. 2007. The concept of hydrological connectivity and its contribution to understanding runoff-dominated geomorphic systems. *Hydrological Processes* 21(13): 1749-1763.
- Brierley, G., Fryirs, K. and Jain, V. 2006. Landscape connectivity: the geographic basis of geomorphic applications. *Area* 38(2): 165-174.
- Buttle, J. M. 1998. Fundamentals of small catchment hydrology. In Kendall, C. and McDonnell, J.J. (eds.). *Isotopes Tracers in Catchment Hydrology*, Elsevier: 1-49.
- Campbell, K. L., Kiker, G. A. and Clark, D. J. 2001. Development and testing of a nitrogen and phosphorous process model for South African water quality issues. ASAE Paper No. 012085, St. Joseph, MI, USA.
- Carpenter, S. R., Caraco, N. F., Corell, D. L., Howarth, R. W., Sharpley, A. N. and Smith, V. H. 1998. Non-point pollution of surface waters with phosphorous and nitrogen. *Ecological Applications* 8: 559-568.
- Chaplot, V., Saleh, A., Jaynes, D. B. and Arnold, J. 2004. Predicting water, sediment and NO₃-N loads under scenarios of land-use and management practises in a flat watershed. *Water, Air and Soil Pollution* 154: 271-293.
- Chapra, S. C. 1997. *Surface water-quality modeling*. WCB/McGraw-Hill, Boston, MA, USA.
- Craig, H. 1961. Isotopic variations in meteoric waters. *Science* 133: 1702-1703.
- Creed, I. F. and Band, L. E. 1998. Exploring functional similarity in the export of nitrate-N from forested catchments: A mechanistic modeling approach. *Water Resources Research* 34: 3079-3093.
- Deasy, C., Brazier, R., Heathwaite, L. and Hodgkinson, R. 2007. Quantifying agricultural phosphorus transfers at hillslope to catchment scales. *DJF Plant Science No.130*. Tjele, Faculty of Agricultural Sciences, University of Aarhus: 189-191.
- Detty, J. M. and McGuire, K. J. 2010. Topographic controls on shallow groundwater dynamics: implications of hydrologic connectivity between hillslopes and riparian zones in a till mantled catchment. *Hydrological Processes: Research Articles*. Published Online: Mar 24 2010.
- Di, H. J. and Cameron, K. C. 2000. Calculating nitrogen leaching losses and critical nitrogen application rates in dairy pasture systems using a semi-empirical model. *New Zealand Journal of Agricultural Research* 43(1): 139-148.

- Doorenbos, J. and Pruitt, W. O. 1977. Crop water requirements. *Irrigation and Drainage Paper No. 24, (rev.)* FAO, Rome, Italy.
- Fajardo, J. J., Bauder, J. W. and Cash, S. D. 2001. Managing nitrate and bacteria in runoff from livestock confinement areas with vegetative filter strips. *Journal of Soil and Water Conservation* 56(3): 185-191.
- Feng, X. Q., Zheng, G. X. and Xu, Y. J. 2013. Simulation of Hydrological Processes in the Zhalong Wetland Within a River Basin, Northeast China. *Hydrol. Earth Syst. Sci.* 17: 2797-2807.
- Fey, M. V. 2010. *Soils of South Africa*, Cambridge University Press, Cape Town.
- Freeman, M. C., Pringle, M. C. and Jackson, C. R. 2007. Hydrological connectivity and the contribution of stream headwaters to ecological integrity at regional scales. *Journal of the American Water Resources Association* 43(1): 5-14.
- Frey, M. P., Schneider, M. K., Dietzel, A., Reichert, P. and Stamm, C. 2009. Predicting critical source areas for diffuse herbicide losses to surface waters: Role of connectivity and boundary conditions. *Journal of Hydrology* 365(1-2): 23-26.
- Fryirs, K. A., Brierley, G. J., Preston, N. J. and Kasai, M. 2006. Buffers, barriers and blankets: The (dis)connectivity of catchment-scale sediment cascades. *Catena* 70(1): 49-67.
- Gabor, T. S., North, A. K., Ross, L. C. M., Murkin, H. R., Anderson, J. S. and Raven, M. 2004. The Importance of Wetlands and Upland Conservation Practises in Watershed Management: Functions and Values for Water Quality and Quantity. *Publication of Institute of Wetland and Waterfowl Research (IWWR)*. Canada.
- Gassman, P. W., Reyes, M. R., Green, C. H. and Arnold, J. G. 2007. The Soil and Water Assessment Tool: Historical Development, Applications and future Research Directions. *Center for Agricultural and Rural Development, Working Paper 07-WP 443*. Iowa State University, USA.
- Glover, J. 1972. Practical theoretical assessments of sugarcane yield potential in Natal. *Proceedings of the South African Sugar Technologists' Association* 46: 138-141.
- Griffiths, D. H. and Barker, R. D. 1993. Two-dimensional resistivity imaging and modelling in areas of complex geology. *Journal of Applied Geophysics*. 29: 211-226.
- Hatterman, F. F., Krysanova, V., Habeck, A. and Bronstert, A. 2006. Integrating wetlands and riparian zones in river basin modeling. *Ecological Modelling* 199(4): 379-392.

- Hayes, J. C., Barfield, B. J. and Barnhisel, R. I. 1979. Filtration of sediment by simulated vegetation. II. Unsteady flow with non-homogenous sediment. *Transactions of the American Society of Agricultural Engineers* 22: 1063-1067.
- Heathwaite, A. L. 2003. Making process-based knowledge useable at the operational level: a framework for modelling diffuse pollution from agricultural land. *Environmental Modelling & Software* 18(8-9): 753-760.
- Heathwaite, A. L., Sharpley, A. and Gburek, W. 2000. A conceptual approach for integrating phosphorus and nitrogen management at watershed scales. *Journal of Environmental Quality* 29: 158-166.
- Hewett, C. J. M., Quinn, P. F., Heathwaite, A. L., Doyle, A., Burke, S., Whitehead, P. G. and Lerner, D. N. 2009. A multi-scale framework for strategic management of diffuse pollution. *Environmental Modelling & Software* 24(1): 74-85.
- Higgins, J. M. and Kim, B. R. 1981. Phosphorous retention models for the Tennessee Valley Authority Reservoirs. *Water Resources Research* 17: 571-576.
- Hooke, J. 2003. Coarse sediment connectivity in river channel systems: a conceptual framework and methodology. *Geomorphology* 56(1-2): 79-94.
- Hornberger, G. M., Bencala, K. E. and McKnight, D. M. 1994. Hydrological controls on dissolved organic-carbon during snowmelt in the Snake River near Montezuma, Colorado. *Biogeochemistry* 25: 147-165.
- Howarth, R. W., Billen, G., Swaney, D., Townsend, A., Jaworski, N., Lajtha, K., Downing, J. A., Elmgren, R., Caraco, N. and Jordan, T. 1996. Regional nitrogen budgets and riverine N & P fluxes for the drainages to the North Atlantic Ocean: Natural and human influences. *Biogeochemistry* 35(1): 75-139.
- Howe, B. J. and Lorentz, S. A. 1995. Modelling sediment yield in the Mzinduzi basin using contributing area techniques. *Proceedings of the 7th South African National Hydrology Symposium*. IWR, Grahamstown, RSA.
- Inman-Bamber, N. G. 1994. Temperature and seasonal effects on canopy development and light interception of sugarcane. *Field Crops Research* 36: 41- 51.
- Jencso, K. G., McGlynn, B. L., Gooseff, M. N., Wondzell, S. M., Bencala, K. E. and Marshall, L. A. 2009. Hydrologic connectivity between landscapes and streams: Transferring reach-and plot-scale understanding to the catchment scale. *Water Resources Research* 45(4): 1-16.

- Jordan, T. E. and Weller, D. E. 1996. Human contributions to terrestrial nitrogen flux: assessing the sources and fates of anthropogenic fixed nitrogen. *BioScience* 46(9): 655-664.
- Kienzle, S. W. and Lorentz, S. A. 1993. Production of a soil erodibility map for the Henley dam catchment, Natal, using a GIS approach. *Proceedings, 6th South African National Hydrology Symposium*. University of Natal, Pietermaritzburg, Department of Agricultural Engineering, RSA.
- Kiker, G. A. and Clark, D. J. 2001. The development of a Java-based, object-oriented modeling system for simulation of southern African hydrology. *Presentation at the 2001 ASAE Annual International Meeting*. Sacramento, California, USA.
- Kirby, A. 2002. Wastewater treatment using constructed wetlands. *Canadian Water Resources Journal* 27: 263-272.
- Knisel, W. G. 1993. GLEAMS: Groundwater Loading Effects of Agricultural Management Systems. Version 2.10. *UGA-CPES-BAED Publication No. 5*.
- Knisel, W. G. and Davis, F. M. 1999. GLEAMS: Groundwater Loading Effects of Agricultural Management Systems. Version 3.0. *USDA-ARS Publication No. SEWRL-WGK/FMD-050199*, revised 081500: 191.
- Knox, A. K., Dahlgren, R. A., Tate, K. W. and Atwill, E. R. 2008. Efficacy of Natural Wetlands to Retain Nutrient, Sediment and Microbial Pollutants. *J. Environ. Qual.* 37: 1837-1846.
- Kollongei, K. J. and Lorentz, S. A. 2014. Connectivity Influences on Nutrient and Sediment Migration in the Wartburg Catchment, KwaZulu-Natal Province, South Africa. *J. Phys. Chem. Earth.* 67-69: 12-22
- Lane, S. N., Brookes, C. J., Heathwaite, A. L. and Reaney, S. 2006. Surveillant science: challenges for the management of rural environments emerging from the new generation diffuse pollution models. *Journal of Agricultural Economics* 57(2): 239-257.
- Le Roux, J. J., Sumner, P. D., Lorentz, S. A. and Germishuise, T. 2013. Connectivity Aspects in Sediment Migration Modelling Using the Soil and Water Assessment Tool. *Geosciences* 3(1): 1-12.
- Le Roux, P., Fraenkel, C. H., Bothma, C. B., Gutter, J. H. and Du Preez, C. C. 2006. *Soil Survey Report: Mkabela Catchment*. Report for Water Research Commission, Pretoria, RSA.

- Le Roux, P. A. L., Van Tol, J. J., Kuenene, B. T., Hensley, M., Lorentz, S. A., Van Huysteen, C. W., Hughes, D. A., Evison, E., Van Rensburg, L. D. and Kapangaziwiri, E. 2011. *Hydrogeological interpretation of the soils of selected catchments with the aim of improving efficiency of hydrological models*. WRC Proj. K5/1748. Water Research Commission, Pretoria, RSA.
- Lesschen, J. P., Schoorl, J. M. and Cammeraat, E. L. H. 2009. Modelling runoff and erosion for a semi-arid catchment using a multi-scale approach based on hydrological connectivity. *Geomorphology* 109: 174-183.
- LGR 2007. Los Gatos Research. DLT-100 Liquid-Water Isotope Analyzer Automated Injection: Manual 07 - C .
- Linsley, R. K., Kohler, M. A. and Paulhus, J. L. H. 1988. *Hydrology for Engineers, SI metric edition*, McGraw Hill Book Company Ltd, London.
- Lorentz, S., Freese, C., Orchard, C., Chaplot, V., Grellier, S., Pickles, J. and Kollongei, J. 2013. Collaborative Contribution to the Water Research Commission: The Use of Isotope Hydrology to Characterise and Assess Water Resources in South(ern) Africa. *Use of Isotopes in Catchment Hydrology, Vegetation Uptake and Non-Point Source Pollution Analyses*. WRC Report No. K5/1907. Water Research Commission, Pretoria, RSA.
- Lorentz, S., Miller, J., Lechler, P., Mackin, G., Lord, M., Kollongei, J., Pretorius, J., Ngeleka, K., Zondi, K. and Le Roux, J. 2011. *Definition of Process Zones and Connectivity in Catchment Scale NPS Processes*. WRC Research No. 1808/1/11. Water Research Commission, Pretoria, RSA.
- Lorentz, S. A., Kollongei, J., Snyman, N., Berry, S. R., Jackson, W., Ngaleka, K., Pretorius, J. J., Clark, D., Thornton-Dibb, S., Le Roux, J. J., Germishuys, T. and Gorgens, A. H. M. 2012. *Modelling Nutrient and Sediment Dynamics at the Catchment Scale*. WRC Research No. 1516/3/12. Water Research Commission, Pretoria, RSA.
- Lorentz, S. A. and Schulze, R. E. 1995. Sediment yield. In: ed. Schulze, R. E. *Hydrology and Agrohydrology: A Text to Accompany the ACRU 3.00 Agrohydrological Modelling System*. Water Research Commission, Report TT69/95, Pretoria, RSA.
- Marti, E. and Sabater, F. 1996. High variability in temporal and spatial nutrient retention in Mediterranean streams. *Ecology* 77: 854-869.
- Mburu, N., Tebitendwa, S. M., Van Bruggen, J. J. A., Rousseau, D. P. L. and Lens, P. N. L. 2013. Performance comparison and economics analysis of waste stabilization ponds and horizontal subsurface flow constructed wetlands treating domestic wastewater: A

- case study of the Juja sewage treatment works. *Journal of Environmental Management* 128: 220-225.
- McClain, M. E., Bilby, R. E. and Triska, F. J. 1998. Biogeochemistry of N, P, and S in Northwest Rivers: Natural distribution and responses to disturbance. In (eds.) Naiman, RJ and Bilby, RE. *River Ecology and Management: Lessons from the Pacific Coastal Ecoregion*, 347-372. Springer-Verlag, New York.
- McDonnell, J. J. 2003. Where does water go when it rains? Moving beyond the variable source area concept of rainfall-runoff response. *Hydrological Processes* 17(9): 1869 - 1875.
- McDowell, R. W., Biggs, B. J. F., Sharpley, A. N. and Nguyen, L. 2004. Connecting phosphorus loss from agricultural landscapes to surface water quality. *Chemistry and Ecology* 20(1): 1-40.
- McGlynn, B. L., McDonnell, J. J., Seibert, J. and Kendall, C. 2004. Scale effects on headwater catchment runoff timing, flow sources, and groundwater-streamflow relations. *Water Resour. Res* 40: 1-14.
- McGuire, K. J., Weiler, M. and McDonnell, J. J. 2007. Integrating tracer experiments with modeling to assess runoff processes and water transit times. *Advances in Water Resources* 30(4): 824-837.
- McKergow, L. A., Prosser, I. P., Weaver, D. M., Grayson, R. B. and Reed, A. E. G. 2006. Performance of grass and eucalyptus riparian buffers in a pasture catchment, Western Australia, part 2: water quality. *Hydrol. Process.* 20: 2327-2346.
- Medeiros, P. H. A., Güntner, A., Francke, T., Mamede, G. L. and De Araújo, J. C. 2010. Modelling spatio-temporal patterns of sediment yield and connectivity in a semi-arid catchment with the WASA-SED model. *Hydrological Sciences Journal* 55(4): 636-648.
- Miller, J. R., Mackin, G., Lechler, P., Lord, M. and Lorentz, S. 2013. Influence of basin connectivity on sediment source, transport, and storage within the Mkabela Basin, South Africa. *Hydrology and Earth System Sciences* 17(2): 761 - 781.
- Mishra, A. and Kar, S. 2012. Modeling hydrologic processes and NPS pollution in a small watershed in subhumid subtropics using SWAT. *J. of Hydrologic Engineering, ASCE.* 17(3): 445-454.
- Mishra, A., Kar, S. and Raghuwanshi, N. S. 2009. Modeling nonpoint source pollutant losses from a small watershed using HSPF model. *J. of Environmental Engineering, ASCE* 135(2): 92-100.

- Moberly, P. K. and Meyer, J. H. 1984. Soils: A management factor in sugarcane production in the South African sugar industry. *Proceedings of The South African Sugar Technologists' Association*.(June): 193.
- Molloy, R. and Ellis, D. 2002. Don't just measure impacts, predict the changes we can achieve. *Proceedings of Coast to Coast 2002 National Conference*, 295-298. Tweed Heads, Australia.
- Montgomery, D. R. and Buffington, J. M. 1998. Channel processes, classification, and response. *River Ecology and Management*. Springer-Verlag, New York: 13-42.
- Mucina, L. and Rutherford, M. C. 2006. *The Vegetation of South Africa, Lesotho and Swaziland*. Pretoria, South African National Biodiversity Institute.
- Müller, E. N., Wainwright, J. and Parsons, A. J. 2007. Impact of connectivity on the modeling of overland flow within semiarid shrubland environments. *Water Resour. Res.* 43(9): W09412.
- Munn, N. L. and Meyer, J. H. 1990. Habitat-specific solute retention in two small streams: an intersite comparison. *Ecology* 71: 2069-2082.
- Nash, D., Halliwell, D., Cox, J., Haygarth, P. M. and Jarvis, S. C. 2002. Hydrological mobilization of pollutants at the field/slope scale. In: eds. Haygarth, PM and Jarvis, SC. *Agriculture, Hydrology and Water Quality*, 225-242. CABI Publishing, Wallingford UK.
- Nash, J. E. and Sutcliffe, J. V. 1970. River flow forecasting through conceptual models. Part 1: A discussion of principles. *J. Hydrol.* 10(3): 282 - 290.
- Neitsch, S. L., Arnold, J. G., Kiniry, J. R. and Williams, J. R. 2005. *Soil and Water Assessment Tool—Theoretical Documentation—Version 2005*. Grassland, Soil & Water Research Laboratory, Agricultural Research Service and Blackland Research Center, Texas Agricultural Experiment Station, Temple, TX, USA.
- Newham, L. T. H. and Drewry, J. J. 2006. *Modelling Catchment-scale Nutrient Generation*. Technical Report 28/5. CSIRO Land and Water, Canberra, Australia.
- NRC 1993. *Soil and Water Conservation: An Agenda for Agriculture*. Committee on Long-Range Soil and Water Conservation, National Research Council. National Academy Press, Washington, D.C., US.
- NWA 1998. The National Water Act. 1998. RSA Government Gazette No. 36 of 1998 : 26 August 1998, No. 19182. Cape Town, RSA.

- Ocampo, C. J., Sivapalan, M. and Oldham, C. 2006. Hydrological connectivity of upland-riparian zones in agricultural catchments: Implications for runoff generation and nitrate transport. *Journal of Hydrology* 331(3-4): 643-658.
- OECD 2012. *Water Quality and Agriculture: Meeting the Policy Challenge*. OECD studies on Water. Organization For Economic Co-operation and Development (OECD) Publishing, Paris, France.
- Panuska, J. C. and Robertson, D. M. 1999. Estimating phosphorous concentration following alum treatment using apparent settling velocity. *Lakes and Reservoirs Management*. 15: 28-38.
- Payraudeau, S., Junker, P., Imfeld, G. and Gregoire, C. 2009. Characterizing hydrological connectivity to identify critical source areas for pesticides losses. *Proceedings of the 18th IMACS World Congress. Modelling and Simulation Society*, Canberra, Australia.
- Pohlert, T., Huisman, J. A., Breuer, L. and Frede, H. G. 2005. Modelling of point and non-point source pollution of nitrate with SWAT in the river Dill, Germany. *Advances in Geosciences*, 5: 7-12.
- Pringle, M. C. 2001. Hydrological connectivity and the management of biological reserves: a global perspective. *Ecological Applications* 11: 981-998.
- Quinn, P. 2002. Models and monitoring: scaling-up cause-and-effect relationships in nutrient pollution to the catchment scale. In : eds. Steenvoorden, J, Claessen, F and Willems, J. *Proceedings of an International Symposium on Agricultural Effects on Ground and Surface Waters : Research at the Edge of Science and Society*, 397-403. IAHS PUBLICATION, Wallingford, UK.
- Quinn, P. 2004. Scale appropriate modelling: representing cause-and-effect relationships in nitrate pollution at the catchment scale for the purpose of catchment scale planning. *Journal of Hydrology* 291(3-4): 197-217.
- Rankinen, K., Tattari, S. and Rekolainen, S. 2001. Modelling of vegetative filter strips in catchment scale erosion control. *Agricultural and Food Science in Finland* 10: 99-112.
- Refsgaard, J. C. and Butts, M. B. 1999. Determination of grid scale parameters in catchment modelling by upscaling local scale parameters. *Proceedings of International Workshop of EurAgEng's Field of Interest on Soil and Water*, 650-665. K.U. Leuven, Belgium.

- Riddell, E. S., Lorentz, S. A. and Kotze, D. C. 2010. A geophysical analysis of hydrogeomorphic controls within a headwater wetland in a granitic landscape, through ERI and IP. *Hydrol. Earth Syst. Sci.* 14: 1697-1713.
- Rossouw, J. N. and Gorgens, A. H. M. 2005. *Knowledge Review of Modelling Non-Point Source Pollution in Agriculture from Field to Catchment Scale*. Report No.1467/1/05. Water Research Commission, Pretoria, RSA.
- Salomons, W. and Stol, B. 1995. *Soil pollution and its mitigation: impact of land use changes on soil storage of pollutants*. Nonpoint pollution and Urban Stormwater Management (V. Novotny, ed.), Technomic Publishing, Lancaster, PA, USA.
- Sardar, S., Ilyas, S. U., Malik, S. R. and Javaid, K. 2006. Compost fertilizer production from Sugarcane Press Mud (SPM). *International Journal of Microbiology Research* 1(2): 20 - 27.
- SASA 2012. [Internet]. *South African Sugar Association (SASA). SOUTH AFRICAN SUGAR INDUSTRY DIRECTORY 2011/2012. Facts and Figures* <http://www.sasa.org.za/files/Industry%20Directory%202011-2012.pdf> [Accessed 1 November 2012].
- Schulze, R. E. 1975. Catchment evapotranspiration in the Natal Drakensberg. Unpublished PhD thesis, Department of Geography, University of Natal, Pietermaritzburg, RSA.
- Schulze, R. E. 1995. *Hydrology and Agrohydrology: A Text to Accompany the ACRU 3.00 Agrohydrological Modelling System*. Water Research Commission, Report TT69/95, Pretoria, RSA.
- Shaffer, M. J. 1995. Fate and transport of nitrogen, what models can and cannot do. *Working Paper No. 11, Agricultural Research Service, USDA, Colorado, USA*.
- Sharpley, A. N. and Williams, J. R. 1990. EPIC-Erosion/productivity impact calculator: Model documentation. *USDA-ARS, Tech Bulletin No 1768*: 235.
- Simons, D. B. and Sentürk, F. 1992. *Sediment Transport Technology: Water and Sediment Dynamics*. *Water Resources Publications*. Denver, CO, USA.
- Simpson, H. J. and Herczeg, A. 1991. Salinity and evaporation in the River Murray basin, Australia. *Journal of Hydrology* 124: 1- 27.
- Sivapalan, M. 2003. Process complexity at hillslope scale, process simplicity at the watershed scale: is there a connection? *Hydrological Processes* 17(5): 1037-1041.
- Sklash, M. G. and Farvolden, R. N. 1979. The role of groundwater in storm runoff. *Journal of Hydrology* 43: 45-65.

- Smithers, J. C. and Schulze, R. E. 1995. *ACRU Agrohydrological Modelling System : User Manual Version 3.00*. Water Research Commission, Report TT70/95, Pretoria, RSA.
- Stieglitz, M., Shaman, J., McNamara, J., Engel, V., Shanley, J. and Kling, G. W. 2003. An approach to understanding hydrologic connectivity on the hillslope and the implications for nutrient transport. *Global Biogeochemical Cycles* 17(4): 16-11,16-15.
- Tetzlaff, D., Soulsby, C. and Christian, B. 2010. Hydrological connectivity and microbiological fluxes in montane catchments: the role of seasonality and climatic variability. *Hydrological Processes* 24(9): 1231-1235.
- Turner, M. G., Romme, W. H., Gardner, R. H., O'Neill, R. V. and Kratz, T. K. 1993. A revised concept of landscape equilibrium: disturbance and stability on scaled landscapes. *Landscape Ecology* 8(3): 213-227.
- Valett, H. M., Morrice, J. A., Dahm, C. N. and Campana, M. E. 1996. Parent lithology, surface-groundwater exchange and nitrate retention in headwater streams. *Limnology and Oceanography* 41(2): 333-345.
- Van de Giesen, N. C., Stomph, T. J. and De Ridder, N. 2000. Scale effects of Hortonian overland flow and rainfall-runoff dynamics in a West African catena landscape. *Hydrological Processes* 14(1): 165-175.
- Van Liew, M. W. and Garbrecht, J. 2003. Hydrologic simulation of the little Washita River experimental watershed using SWAT. *J. Am. Water Resour. Assoc.* 39(2): 413 -426.
- Van Tol, J. J., Le Roux, P. A. L. and Lorentz, S. A. 2012. From genetic soil horizons to hydro-pedological functional units. *Proceedings of the 16th SANCIAHS symposium, 1st - 3rd October 2012*. University of Pretoria, Pretoria, RSA.
- Van Tol, J. J., Le Roux, P. A. L., Lorentz, S. A. and Hensley, M. 2013. Hydro-pedological classification of South African hillslopes. *Vadose Zone J.* doi:10.2136/vzj2013.01.0007.
- Van Zyl, A. J. 2007. A knowledge gap analysis on multi-scale predictive ability for agriculturally derived sediments under South African conditions. *Water Science & Technology* 55(3): 107-114.
- Verstraeten, G. and Poesen, J. 2000. Estimating trap efficiency of small reservoirs and ponds: methods and implications for the assessment of sediment yield. *Progress in Physical Geography* 24(2): 219.
- Ward, J. V., Tockner, K., Arscott, D. B. and Claret, C. 2002. Riverine landscape diversity. *Freshwater Biology* 47(4): 517-539.

- Wassmann, P. and Olli, K. 2004. Drainage basin nutrient inputs and eutrophication: an integrated approach [Internet]. Norwegian College of Fishery Sciences, University of Tromsø, Norway. Available from: www.ut.ee/~olli/eutr/ [Accessed 18 October 2009].
- Weissteiner, C. J., Bouraoui, F. and Aloe, A. 2013. Reduction of nitrogen and phosphorous loads to European rivers by riparian buffer zones. *Knowledge and Management of Aquatic Ecosystems* 408(08).
- Wenninger, J., Uhlenbrook, S., Lorentz, S. and Leibundgut, C. 2008. Identification of runoff generation processes using combined hydrometric, tracer and geophysical methods in a headwater catchment in South Africa. *Hydrological Sciences* 53(1): 65-80.
- Western, A. W., Blöschl, G. and Grayson, R. B. 2001. Toward capturing hydrologically significant connectivity in spatial patterns. *Water Resources Research* 37(1): 83-97.
- Williams, J. R. 1975. Sediment yield prediction with universal equation using runoff energy factor. In: *Present and Prospective Technology for Predicting Sediment Yields and Sources*, USDA, ARS, 40: 244-252.
- WRC 2002. *State of Rivers Report: The uMngeni River and Neighbouring Rivers and Streams*. WRC Report No. TT 200/02. Water Research Commission, Pretoria, RSA.
- WWF 2011. [Internet]. *Sugar and the Environment: Encouraging Better Management Practices in sugar production*. WWF Global Freshwater Programme, Zeist, Netherlands. Available from: www.panda.org/freshwater [Accessed 1 January 2014].

APPENDICES

A. COMPUTER PROGRAM FOR THE ISCO SAMPLER AT FLUME 1

'CR200 Series: Mkabela Upper flume

'Declare Variables and Units

Const deltaHS = .10 'Set depth (m) for change in sampling flow volume calculation

Const Vlf = 300 'Set low flow volume threshold

Const Vhf = 100 'Set high flow volume threshold

Const deltaT = 5 'Set time interval for depth of flow reading

Const a = 0 'parameter for depth of flow to discharge conversion

Const b = 0.004 'parameter for depth of flow to discharge conversion

Const c = 0.59 'parameter for depth of flow to discharge conversion

Const d = 0.012 'parameter for depth of flow to discharge conversion

Const e = 0.71 'parameter for depth of flow to discharge conversion

Const deltaHR = 0.002 'Set elevation change (mm) for recording Q

Public Batt_Volt

Public Ns 'Number of samples taken by ISCO

Public x 'variable

Public Qi 'FLOW

Public Hi 'current flow height

Public Hix 'The flow height at the last saved flow PUBLIC Hi " The flow at the current flow

Public V 'cumulative flow since last sample

Public Hi1 'The previous flow height measured

Dim FRun_14

Dim Old_15

Dim Change_16

Public CS450Data(2)

Public Observed 'This is a user input in the numeric table and is the measured water depth with a ruler in metres

Public Offset 'Calculated based on observed level

Alias CS450Data(1)=Lv1_m

Alias CS450Data(2)=Temp_C

Units Batt_Volt=Volts

Units Hi=mm

Units Qi=cumec

```

'Define Data Tables
DataTable (Flow,True,1000)
  Minimum(1,Batt_Volt,False,False)
  Sample (1,Qi)          'saves Qi the current flow to memory
  Sample (1,x)           'saves x the number of periods between data stored
    Sample(1,Lvl_m)      'level measured by sensor without offset
    Sample(1,Temp_C)
    Sample(1,Observed)   'observed measure using a ruler of water height
  Sample (1,Hi)         'the current depth with offset taken into account
    Sample(1,Offset)
EndTable

```

```

DataTable (ISCO,True,1000)
  Sample (1,Ns)         'saves sample number the current flow to memory
  Sample (1,Hi)         'saved the current depth to memory
  Sample (1,Hi1)        'save previous depth
  Sample (1,Qi)
  Sample (1,V)
EndTable

```

```

'Main Program
BeginProg
  Hix=0
  Hi1=0
  V=0
  Scan(deltaT,sec)     'This does the time interval between each depth of flow reading
  'Default Datalogger Battery Voltage measurement Batt_Volt:
  Battery(Batt_Volt)
  'CS450/CS455 Pressure Transducer measurements Hi (mm) and Temp_C
  SDI12Recorder(Lvl_m,"0M1!",1,0)
  Lvl_m=Lvl_m*0.70307
  -----
  'Offset calculation
    If FRun_14=0 Then
      Observed=0
      FRun_14=1
    EndIf
    Change_16=Observed-Old_15
    If Change_16=0 Then
      Hi=Lvl_m+Offset
    Else

```



```

        Offset=Observed-Lvl_m
        Hi=Lvl_m+Offset
        Old_15=Observed
    EndIf

```

```

-----
Qi = a +b*(Hi)+c*(Hi^2)+d*(Hi^3)+e*(Hi^4)
If ABS(Hi - Hix) > deltaHR Then    'if the flow - last saved flow > deltaHR
    'Call Data Tables and Store Data
    CallTable(Flow)
    x = 0        'reset x variable
    Hix = Hi    ' Set Hix to Hi at the last saved data
Else
    x = x + 1    'Increase X
EndIf

V = V + (Qi * deltaT)    'The volume (cu.m) is = the current volume + ( flow * time)

```

```

-----
'Decide if flow is high or low volume sampling
'Test for high flow conditions
'If measured height (m) > 0.1 and cumulative volume > 100 cumecs then
If Hi > deltaHS AND V > Vhf Then
    'Number of samples
    Ns = Ns +1
    CallTable(ISCO)
    'ISCO samples
    SWBatt (1)
    Delay (1,sec)
    SWBatt (0 )
    V = 0
EndIf

'send pulse to ISCO,
'set port PSW high
' Delay 1 Second
'set port Psw low
'reset flow to 0
'record that a sample was taken

'test for low flow conditions

```

```

'If measured height (m) < 0.1 and cumulative volume > 300 cumecs then
If Hi < deltaHS AND V > VIf Then
  Ns = Ns +1
  CallTable(ISCO)
  SWBatt (1)
  Delay (1,sec)
  SWBatt (0)
  V = 0
EndIf

"send pulse to ISCO, set port C2 high
" Delay 1 Second
"set port C2 low
" reset flow to 0
"record that a sample was taken
-----
  Hi1 = Hi      'records level as previous level
NextScan
EndProg

```

B. *ACRU-NPS* SOIL AND NUTRIENT VARIABLE INPUT DATA

Soil Input Model Parameters	Avalon (Av)		Westleigh (We)		Cartref (Cf)		Glencoe (Gc)		Hutton (Hu)	
	A1	B1	A1	B1	A1	B1	A1	B1	A1	B1
Organic Matter (OM) (%)	1.20	0.67	1.55	0.86	1.03	0.52	0.86	0.69	1.2	0.86
Bulk Density (BD) (g/cc)	1.65	1.65	1.64	1.65	1.52	1.66	1.65	1.7	1.4	1.5
Base Saturation (BSAT) (%)	62	83	37	50	68	61	86	45	36	24
CaCo3 (CACO) (%)	-	-	-	-	-	-	-	-	-	-
pH (PH)	4.5	5.83	5.0	5.2	5.3	5.6	6.1	6	4.4	5.1
Clay content (CL) (%)	11	18.67	21	23	9.7	17	10.8	8.4	42.1	54
Silt content (SLT) (%)	22.7	24.29	28.7	30.2	30.1	32.9	17.4	17.8	27.7	21.1
Nutrient Input Model Parameters (kg/ha)	Avalon (Av)		Westleigh (We)		Cartref (Cf)		Glencoe (Gc)		Hutton (Hu)	
	A1	B1	A1	B1	A1	B1	A1	B1	A1	B1
Stable N (STN)	1100.3	653.08	1437.8	492.5	1191.1	559.1	503.3	199.2	3826.9	582
Active N (ACN)	529.4	234.60	650.1	329.9	461.1	160.5	483.9	290.9	703.1	239.9
Stable P (STP)	717.8	180.37	175.78	170.44	201.7	190.42	209.45	837.79	256.84	165.49
Active P (ACP)	179.45	45.09	43.95	42.61	50.4	47.6	42.5	170	64.21	41.37
Organic humus P (OHP)	1042.3	1040.67	905.2	1041.3	1571.9	1740.8	1046.6	1097.2	822.9	1076.1
Ammonium -N (AMMN)	3.3	3.3	2.9	3.3	3.34	3.3	3.3	3.5	2.6	3.4
Nitrate - N (NITN)	16.5	16.43	14.3	16.45	24.8	27.5	16.5	17.3	13	17
Labile P (LABP)	35.18	15.50	10.21	9.79	16	12.3	25.56	15.96	8.38	10.66
Sugarcane										
Residue Biomass (PLBMAS)	9595	9595	9595	9595	9595	9595	9595	9595	9595	9595
Fresh Organic N (PLRSN)	37	37	37	37	37	37	37	37	37	37
Fresh Organic P (PLRSP)	10	10	10	10	10	10	10	10	10	10
Pasture										
Residue Biomass (PLBMAS)	936	936	936	936	936	936	936	936	936	936
Fresh Organic N (PLRSN)	79.4	79.4	79.4	79.4	79.4	79.4	79.4	79.4	79.4	79.4
Fresh Organic P (PLRSP)	12.75	12.75	12.75	12.75	12.75	12.75	12.75	12.75	12.75	12.75
Vegetables (Cabbages)										
Residue Biomass (PLBMAS)	8493.81	8493.81	8493.81	8493.81	8493.81	8493.81	8493.81	8493.81	8493.81	8493.81
Fresh Organic N (PLRSN)	79.4	79.4	79.4	79.4	79.4	79.4	79.4	79.4	79.4	79.4
Fresh Organic P (PLRSP)	12.75	12.75	12.75	12.75	12.75	12.75	12.75	12.75	12.75	12.75
Forest (Pinus/Wattle)										
Residue Biomass (PLBMAS)	1692	1692	1692	1692	1692	1692	1692	1692	1692	1692
Fresh Organic N (PLRSN)	79.4	79.4	79.4	79.4	79.4	79.4	79.4	79.4	79.4	79.4
Fresh Organic P (PLRSP)	12.75	12.75	12.75	12.75	12.75	12.75	12.75	12.75	12.75	12.75

Notes

1. Bulk density (BD) (g/cc), Base saturation (BSAT %), pH, clay content (CL %) and silt content (SLT %) were obtained from soil report (Le Roux et al, 2006) after the soil survey done in Mkabela. No data was available for CaCo₃ % from soil profile test analyses (probably no calcareous soils in Mkabela).
2. No profile tests were done in Cartref and Hutton hillslopes - the missing parameters were obtained in the following order;
 - a) " Soils of Kwazulu-Natal and Mpumalanga: Recognition of natural soil bodies" (PhD of David Turner, 2000) (University of Pretoria)
 - b) The next most dominant soil type in the hillslope (from available profile tests).
3. Organic Matter % estimated from " Soil Organic Matter Data: What do they mean?" (Miles et al., 2008) & GLEAMS/ACRU-NP Manual
 $OM \% = OC \% * 1.72$
4. Estimation of Labile-P (mg/kg) (Derived equations for SA soils) (Van der Laan et al., 2009)
Highly weathered soils: $0.059BP2 + 4.4$
Slightly weathered soils: $0.24BP2 + 5.9$
Highly weathered (acid tropical) soils: $0.17BP2 + 6.14$
5. Active P = Labile P / [PAI/ (1 -PAI)] (mg/kg) (Van der Laan et al., 2009) & ACRU-NP/GLEAMS MANUAL
Highly weathered soils: $PAI = 0.46 - 0.0916 * \ln(\text{Clay \%})$
Slightly weathered soils: $PAI = 0.0054 * \text{BaseSat\%} + 0.116 * \text{pH}(\text{H}_2\text{O}) - 0.73$
6. Stable P = 4*Active P (mg/kg) (Van der Laan et al., 2009) & ACRU-NP/GLEAMS MANUAL
7. Organic P = 633 mg/kg (USA average for soils used for sugarcane cultivation for long periods) (Castillo et al., 2008)
8. NH₄-N = 2 mg/kg of soil (GLEAMS MANUAL). Not an input to the nutrient component but is included as one of the active pools. It is estimated internally in the model as 2 mg/kg of soil. The nitrification of NH₄-N is a zero-order process and therefore it is very transient with LITTLE SENSITIVITY.
9. NO₃-N = 10 mg/kg of soil (GLEAMS MANUAL). If left blank in the parameter file, the model estimates it as 10 mg/kg of soil in all horizons. Because of the dynamic nature, transformations will rather quickly modify the values to more nearly represent ACTUAL CONDITIONS.
10. Active-N (kg/ha) = BD (g/cc) * OM (%) * Thickness of Horizon (cm) * $10^3 * 9.3 * 10^{-5}$ (GLEAMS/ ACRU-NP MANUAL)
 $= BD * OM * \text{Thickness of Horizon} * 9.3$
11. Rainfall P & N concentrations (summer in Everglades USA)
RNCONC = 0.02 mg/l
RPCONC = 0.028 mg/l
12. Estimating WP and FC from laboratory analysis of stable soils (Hutch, 1984) in ACRU manual
 $WP = 0.0602 + 0.00322 \text{ Clay \%} + 0.00308 \text{ Silt \%} - 0.0260 \text{ BD}$
 $FC = 0.0558 + 0.00365 \text{ Clay \%} + 0.00554 \text{ Silt \%} + 0.0303 \text{ BD}$
PO = From ACRU Manual Table 5.6.1 when soil texture class is known (Schulze, 1995) except for cartref (Table 5.4.1)
13. Potential Yield (Kg/ha/yr) and plant biomass (kg/ha/yr); Potential yields for sugarcane and cabbages were obtained from the department of Agriculture, KwaZulu-Natal Province. 10 % of potential yield was used to determine biomass trash for sugarcane and cabbages (Yadav et al, 2003-India).The basic density of the wattle tree log is 564kg/m³ (RIRDC, 1997) and its potential harvested yield is 15-25m³/ha (CTA Wageningen, 2005). This gives a harvested potential yield of wattle as 11280 kg/ha assuming an average wattle log yield of 20m³/ha.

C. *ACRU-NPS* MONTHLY MEANS OF CROP COEFFICIENTS (CAY), CANOPY INTERCEPTION LOSSES (VEGINT), ROOT MASS DISTRIBUTION IN THE TOPSOIL (ROOTA) , COEFFICIENT OF INITIAL ABSTRACTIONS (COIAM) AND % SURFACE COVER (PCSUCO)

Land use	Variable	Monthly Values											
		Jan.	Feb.	Mar.	Apr.	May	Jun.	Jul.	Aug.	Sep.	Oct.	Nov.	Dec.
Sugarcane	CAY	0.90	0.92	0.90	0.91	0.88	0.82	0.78	0.85	0.82	0.81	0.81	0.85
	VEGINT	1.80	1.80	1.80	1.80	1.80	1.80	1.80	1.80	1.80	1.80	1.80	1.80
	ROOTA	0.75	0.75	0.75	0.75	0.75	0.75	0.75	0.75	0.75	0.75	0.75	0.75
	COIAM	0.35	0.35	0.35	0.35	0.30	0.30	0.30	0.30	0.35	0.35	0.35	0.35
	PCSUCO	100	100	100	100	100	100	100	100	100	100	100	100
Cabbage	CAY	0.80	0.70	0.30	0.30	0.20	0.20	0.20	0.20	0.20	0.20	0.35	0.60
	VEGINT	0.50	0.50	0.50	0.50	0.50	0.50	0.50	0.50	0.75	1.00	0.75	0.50
	ROOTA	0.95	0.95	0.95	0.95	0.95	0.95	0.95	0.95	0.95	0.95	0.95	0.95
	COIAM	0.30	0.30	0.30	0.30	0.30	0.30	0.30	0.30	0.30	0.30	0.30	0.30
	PCSUCO	73.4	73.4	73.4	73.4	73.4	73.4	73.4	73.4	73.4	73.4	73.4	73.4
Pasture	CAY	0.55	0.55	0.55	0.55	0.35	0.20	0.20	0.20	0.35	0.45	0.55	0.55
	VEGINT	0.70	0.70	0.70	0.70	0.70	0.70	0.70	0.70	0.70	0.70	0.70	0.70
	ROOTA	0.95	0.95	0.95	0.95	0.95	1.00	1.00	1.00	0.95	0.95	0.95	0.95
	COIAM	0.15	0.15	0.15	0.25	0.30	0.30	0.30	0.30	0.30	0.30	0.20	0.15
	PCSUCO	64.0	64.0	64.0	64.0	64.0	64.0	64.0	64.0	64.0	64.0	64.0	64.0
Pinus	CAY	0.85	0.85	0.85	0.85	0.85	0.85	0.85	0.85	0.85	0.85	0.85	0.85
	VEGINT	3.50	3.50	3.50	3.50	3.50	3.50	3.50	3.50	3.50	3.50	3.50	3.50
	ROOTA	0.66	0.66	0.66	0.66	0.66	0.66	0.66	0.66	0.66	0.66	0.66	0.66
	COIAM	0.35	0.35	0.35	0.35	0.35	0.35	0.35	0.35	0.35	0.35	0.35	0.35
	PCSUCO	100	100	100	100	100	100	100	100	100	100	100	100
Wattle	CAY	0.90	0.90	0.90	0.88	0.85	0.86	0.89	0.90	0.92	0.92	0.90	0.90
	VEGINT	2.00	2.00	2.00	2.00	1.90	1.85	1.85	1.85	1.90	1.95	2.00	2.00
	ROOTA	0.83	0.83	0.83	0.83	0.83	0.83	0.83	0.83	0.83	0.83	0.83	0.83
	COIAM	0.25	0.25	0.25	0.30	0.30	0.30	0.30	0.30	0.30	0.30	0.25	0.25
	PCSUCO	100	100	100	100	100	100	100	100	100	100	100	100

D. *ACRU-NPS* PARAMETERS USED TO ESTIMATE SEDIMENT YIELD WITH THE MUSLE EQUATION

Parameter	Description	LS1	LS2	LS3	LS4	LV	LP1	LP2	LF1	LF2
SOIFC1	Max soil erodibility factor (K).	0.35	0.35	0.35	0.35	0.35	0.35	0.35	0.35	0.35
SOIFC2	Min soil erodibility factor (K).	0.35	0.35	0.35	0.35	0.35	0.35	0.35	0.35	0.35
ELFACT	Slope length and steepness (LS). A value of null will default the slope to the average catchment slope	0.65	1.97	1.97	1.97	0.27	1.07	1.97	1.07	3.06
PFACT	Support practice factor (P). PFACT = 1: no conservation practice	0.1	0.12	0.12	0.12	0.12	1.0	1.0	1.0	1.0
ICOVRD	Option which indicates that no daily values are available for cover factors (C), and that monthly factors (COVER (i)) will be utilized.	0	0	0	0	0	0	0	0	0
SEDIST	The fraction of the event based sediment yield from the catchment that reaches the outlet on the day of the event.	0.45	0.45	0.45	0.45	0.45	0.45	0.45	0.45	0.45
ALPHA	Runoff erosivity constant (α_{sv}).	8.934	8.934	8.934	8.934	8.934	8.934	8.934	8.934	8.934
BETA	Runoff erosivity constant (β_{sv}).	0.56	0.56	0.56	0.56	0.56	0.56	0.56	0.56	0.56

E. OBSERVED H-FLUME DATA FOR SELECTED EVENTS (JAN' 09 TO JAN' 12) FROM THE FIELD

Flume1 Event	Date	Rain mm	Runoff		Concentration (mg/l)			Load (kg)		
			mm	%	NO3	P	SS	NO3	P	SS
1	10-Jan-09	27	0.8	3.1	14.33	0.59	15	2.04	0.08	2.13
2	28-Feb-09	51	2.6	5.2	13.90	1.00	133	6.22	0.47	59.80
3	26-Jan-10	40	1.5	3.8	14.33	0.39	96	3.67	0.10	24.70
4	17-Feb-10	31	1.7	5.5	10.5	1.30	50	3.08	0.39	14.71
5	10-Nov-10	43	10.9	25.1	6.9	0.20	98	12.6	0.30	180.4
6	03-Dec-10	25	3.2	13.0	15.1	0.30	193	8.28	0.14	106.0
7	23-Jan-11	34	5.7	17.0	14.3	1.80	87	13.9	1.74	84.22
8	26-Jul-11	45	20.2	44.9	8.14	0.25	235	33.7	1.03	972.6
9	15-Aug-11	22	2.9	12.9	8.10	0.36	75	3.95	0.17	36.37
10	24-Nov-11	21	0.7	3.3	17.30	0.40	90	2.09	0.04	10.92
11	28-Dec-11	20	1.1	5.5	15.20	0.40	305	2.82	0.08	56.59
12	24-Jan-12	28	1.3	4.7	2.21	0.10	50	0.50	0.02	11.25

Flume2 Event	Date	Rain mm	Runoff		Concentration (mg/l)			Load (kg)		
			mm	%	NO ₃	P	SS	NO ₃	P	SS
1	10-Jan-09	27	1.4	5.2	24.39	0.80	40	19.85	0.65	33
2	28-Feb-09	51	12.6	24.8	12.10	0.20	250	88.59	1.46	1830
3	26-Jan-10	40	7.1	18.0	11.00	0.21	210	45.57	0.85	869
4	17-Feb-10	31	1.6	5.0	35.0	0.20	75	32.10	0.18	68.78
5	10-Nov-10	43	10.8	25.0	31.4	0.17	230	197.41	1.05	1445.6
6	03-Dec-10	25	5.8	23.5	23.0	0.08	170	77.77	0.27	574.18
7	23-Jan-11	34	3.9	11.4	57.2	0.40	450	128.05	0.89	1006.8
8	26-Jul-11	45	21.9	48.7	37.4	0.10	120	475.24	1.27	1525
9	15-Aug-11	22	2.8	12.8	37.4	0.52	280	61.39	0.85	459.59
10	24-Nov-11	21	2.3	10.9	23.0	0.10	100	31.04	0.13	135
11	28-Dec-11	20	2.1	10.9	40.0	0.21	260	49.62	0.26	323
12	24-Jan-12	28	1.4	4.9	2.21	0.08	50	1.79	0.07	40

F. STATISTICAL TESTS FOR OBSERVED (O_i) vs. SIMULATED (S_i) RUNOFF AND NPS POLLUTANTS FOR FLUME 2 FROM SIGMA PLOT

STUDENT -T TEST	Runoff (mm)		NO ₃ (kg/ha)		P (kg/ha)		Sed. (kg/ha)	
	O _i	S _i	O _i	S _i	O _i	S _i	O _i	S _i
Mean	0.40	0.40	1.36	1.31	0.015	0.014	11.84	11.76
Median	0.11	0.20	0.68	0.69	0.015	0.010	8.41	7.26
Std. Dev.	1.05	1.09	1.91	1.75	0.011	0.011	9.98	10.64
Std. Err	0.07	0.08	0.45	0.41	0.002	0.003	2.35	2.51
95% Conf.	0.15	0.15	0.95	0.87	0.005	0.006	4.96	5.29
99% Conf.	0.19	0.20	1.30	1.20	0.007	0.008	6.82	7.27
Size	200.00	200.00	18.00	18.00	18.00	18.00	18.00	18.00
Total	80.98	80.97	24.56	23.62	0.273	0.256	213.04	211.63
Min	0.00	0.05	0.03	0.06	0.001	0.002	0.56	0.21
Max	10.15	10.08	8.19	7.35	0.036	0.038	31.56	36.59
Min. Pos.	0.02	0.05	0.03	0.06	0.001	0.002	0.56	0.21
Missing	0.00	0.00	0.00	0.00	0.000	0.000	0.00	0.00
Other	0.00	0.00	0.00	0.00	0.000	0.000	0.00	0.00
t _c	-0.000005	-	-0.005	-	-0.014	-	-0.001	-
t _c -critical	1.97	-	1.97	-	1.97	-	1.97	-
NSE	0.87	-	0.96	-	0.90	-	0.95	-
R ²	0.94	-	0.98	-	0.95	-	0.98	-
RMSE	0.37	mm	0.44	kg/ha	0.006	kg/ha	3.35	kg/ha
D _v	0.01	%	3.82	%	6.21	%	0.66	%
Ratio	99.99	%	96.18	%	93.79	%	99.34	%

G. SIMULATED SUGARCANE CROP YIELDS (T/HA) FOR LANDSEGMENTS FOR DIFFERENT SOIL TYPES AND MANAGEMENT SCENARIOS

Land segment/soil	Season	Zero	QuarterBase	HalfBase	Base	DoubleBase	Irrigation
LS1(Av)	2006/2008	58	60	61	62	66	91
	2008/2009	51	56	57	62	69	66
	2009/2011	56	64	69	73	76	88
Average		55	60	62	66	71	82
LS2(Cf & Gc)	2006/2008	58	59	60	62	65	84
	2008/2009	50	55	56	60	66	68
	2009/2011	53	61	65	67	72	85
Average		54	58	61	63	68	79
LS3, LS4 (Cf)	2006/2008	62	63	63	64	66	85
	2008/2009	54	59	60	63	68	69
	2009/2011	55	62	66	68	73	84
Average		57	61	63	65	69	79

H. TOTAL LOADS THROUGH CONTROLS FROM *ACRU-NPS* MODEL SIMULATIONS WITH BASE SCENARIO (2006 -2012)

Control	Wetland1		Buffer1		Dam1		Buffer2		Wetland2		Dam2		Wetland3	
	In	Out	In	Out	In	Out	In	Out	In	Out	In	Out	In	Out
Sediment, t														
Sum	641.7	62.4	2115.6	578.1	640.5	128.12	90.5	16.3	1014.7	53.4	197.8	162.6	2181.1	254.0
Avg.	0.31	0.03	1.01	0.28	0.31	0.06	0.04	0.01	0.49	0.03	0.09	0.08	1.04	0.12
Max	25.5	0.09	87.4	23.9	23.98	0.67	3.74	0.68	55.77	0.41	1.55	0.51	86.5	0.76
Min	0	0.01	0	0	0.01	0	0	0	0	0	0	0	0.22	0.01
% Retained	-	90.3	-	72.7	-	80.0	-	82	-	94.7	-	17.8	-	88.4
NO₃, kg														
Sum	25820.2	8579.3	16520.2	6525.5	15104.8	10924.5	168.7	50.2	26238.9	8034.0	19008.7	12709.4	557491.1	209586.7
Avg.	12.34	4.1	7.87	3.1	7.22	5.2	0.08	0.024	12.54	3.8	9.09	6.1	266.5	100.2
Max	6843.7	56.0	3894.05	1538.2	1542.7	185.9	17.75	5.3	7309.0	59.4	215.6	112.7	59903.5	617.4
Min	0	0	0	0	0	0	0	0	0	0	0.09	0	0.02	0.3
% Retained	-	66.8	-	60.5	-	27.7	-	70.2	-	69.4	-	33.1	-	62.4
P, kg														
Sum	802.1	261.7	232.15	91.7	353.4	239.7	6.47	1.90	227.4	71.0	312.6	202.3	790.5	310.5
Avg.	0.38	0.12	0.11	0.044	0.17	0.10	0.003	0.001	0.11	0.03	0.15	0.06	0.38	0.10
Max	80.08	0.78	35.65	14.10	14.26	2.5	1.05	0.30	58.3	0.5	2.74	1.26	103.7	0.8
Min	0	0	0	0	0	0	0	0	0	0	0	0	0	0
% Retained	-	67.4	-	60.5	-	32.2	-	70.6	-	68.8	-	38.2	-	60.7
Q _{max} , m ³ /d	104505	2637	70278	70278	72442	33251	834	833	62280	2208	35855	25488	200958	9565
% Attenu.	-	97.5	-	0	-	54.1	-	0.1	-	96.5	-	28.9	-	95.2

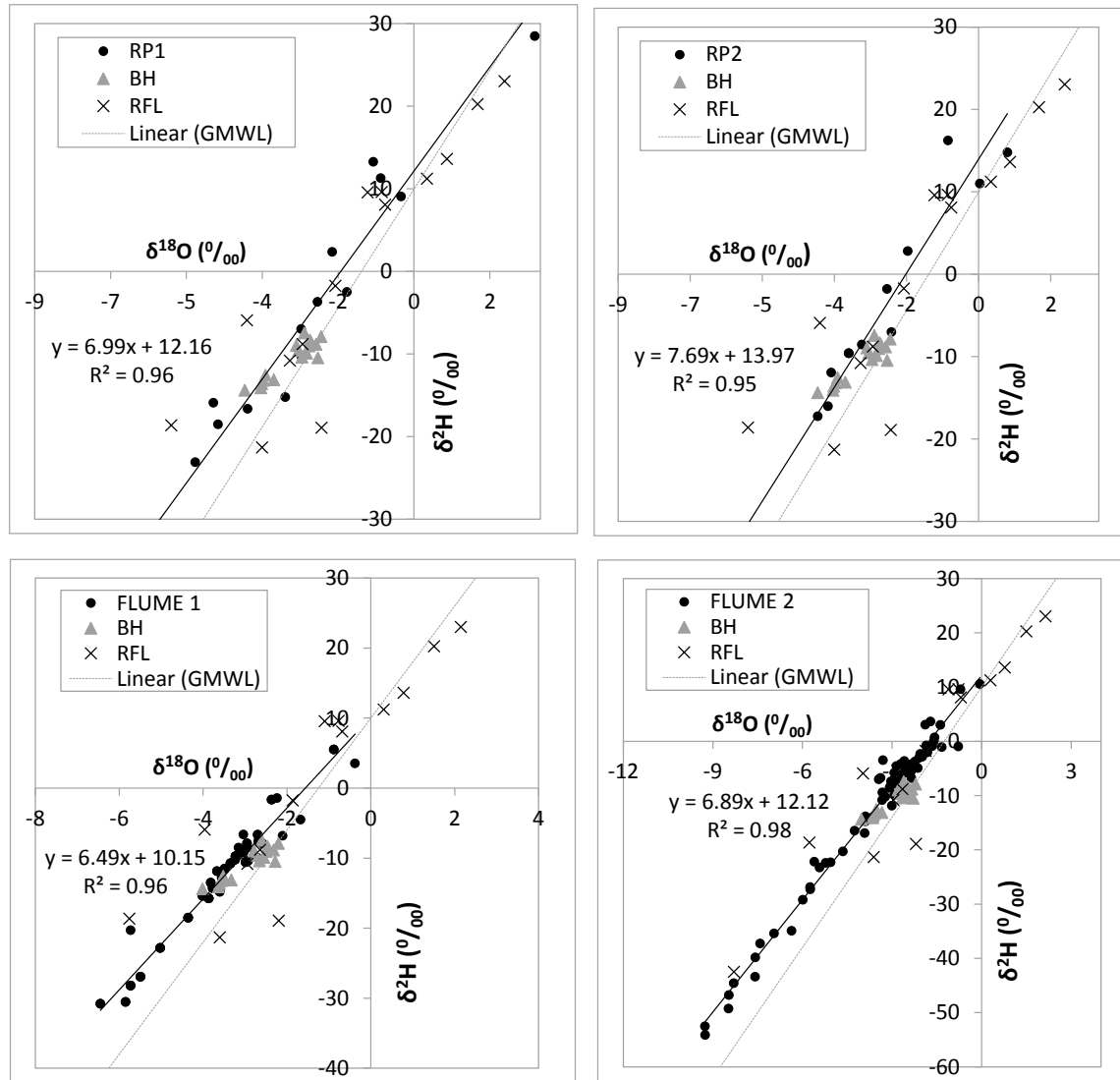
I. TOTAL LOADS FROM *ACRU-NPS* SIMULATIONS WITH DIFFERENT FERTILIZER APPLICATION RATES (2006 -2012)

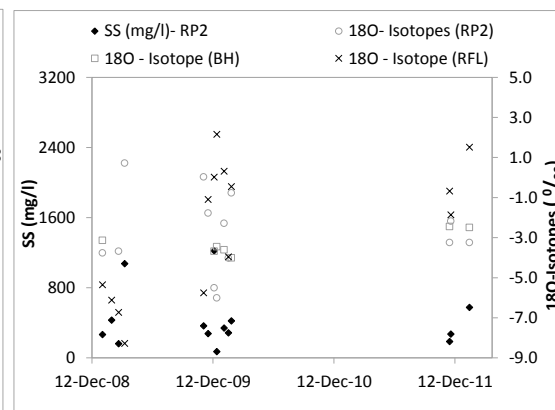
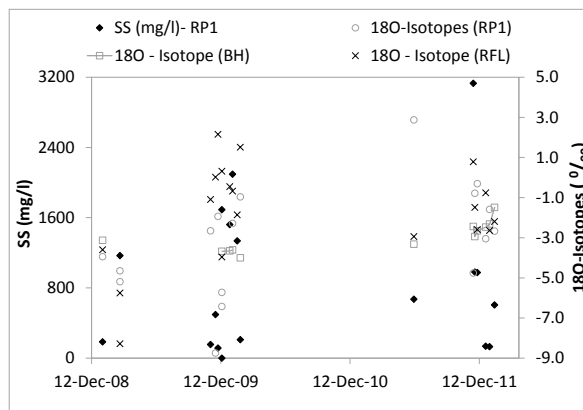
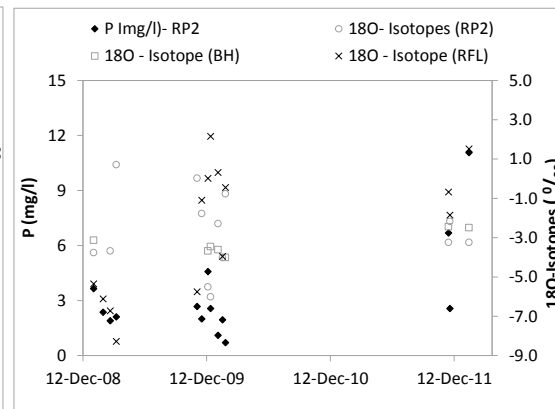
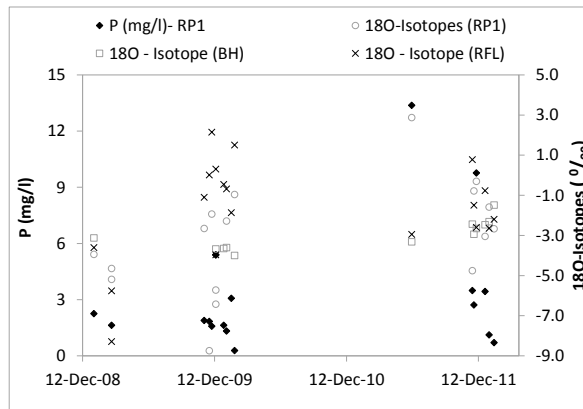
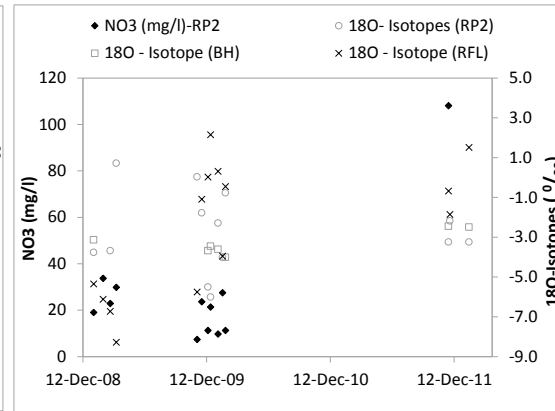
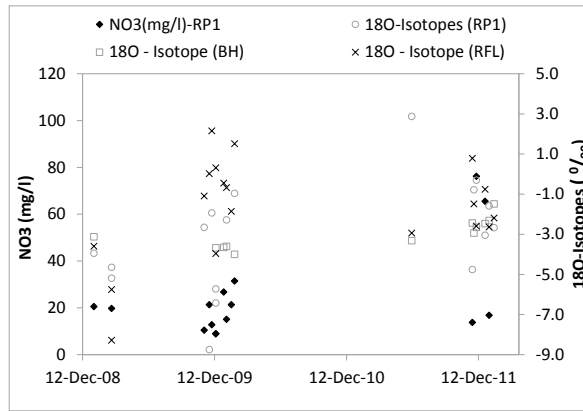
Control	Wetland1		Buffer1		Dam1		Buffer2		Wetland2		Dam2		Wetland3	
	In	Out	In	Out	In	Out	In	Out	In	Out	In	Out	In	Out
Base-Sediment, t	642	62	2116	578	641	128	91	16	1015	53	198	163	2181	254
Base-NO ₃ , kg	25820	8579	16520	6526	15105	10925	169	50	26239	8034	19009	12709	557491	209587
Base-P, kg	802	262	232	92	353	240	6	2	227	71	313	202	791	311
High-Sediment, t	631	62	2110	577	638	127	91	16	1005	53	197	162	2164	253
High-NO ₃ , kg	37461	12532	22506	8890	21421	15683	169	50	35676	11145	26877	18151	656043	249233
High-P, kg	934	305	343	135	441	304	6	2	369	116	422	278	1093	436
Low-1/2-Sediment, t	648	63	2121	580	643	129	91	16	1022	54	199	164	2191	255
Low-1/2-NO ₃ , kg	22133	7335	14722	5815	13150	9446	169	50	22686	6866	16363	10874	517254	193613
Low-1/2-P, kg	752	245	193	76	321	216	6	2	167	52	269	173	664	258
Low-1/4-Sediment, t	654	63	2127	581	644	130	91	16	1028	54	200	165	2203	256
Low-1/4-NO ₃ , kg	20472	6779	14003	5531	12310	8826	169	50	21110	6349	15225	10107	498375	186220
Low-1/4-P, kg	729	238	176	69	307	206	6	2	139	43	250	160	604	233
Low-0-Sediment, t	665	64	2136	584	648	133	91	16	1041	56	205	170	2229	263
Low-0-NO ₃ , kg	19464	6448	13798	5450	11898	8543	169	50	20044	6030	14623	9758	483902	181203
Low-0-P, kg	713	233	165	65	298	199	6	2	118	36	237	152	563	216

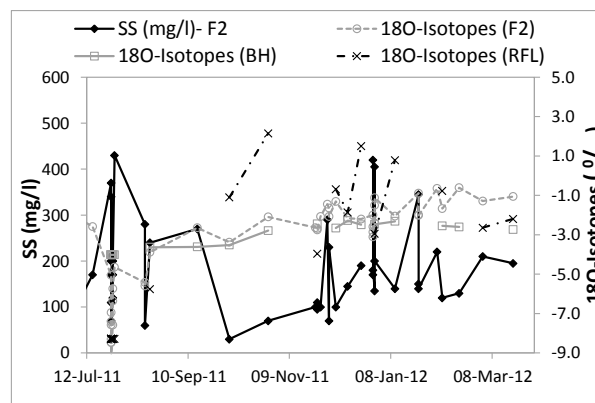
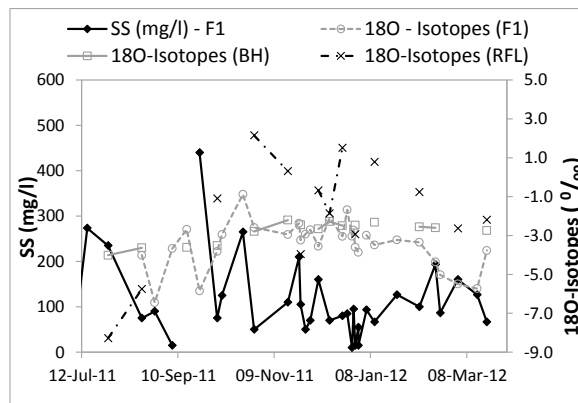
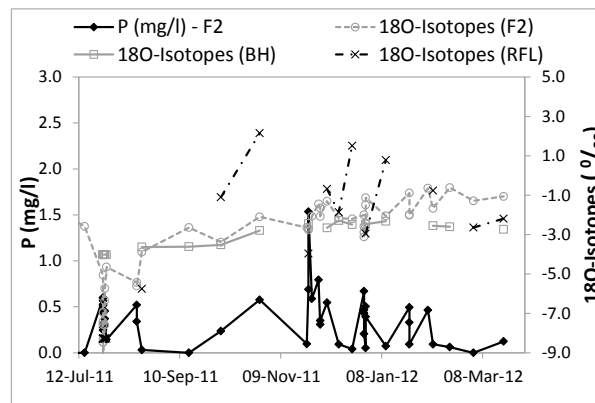
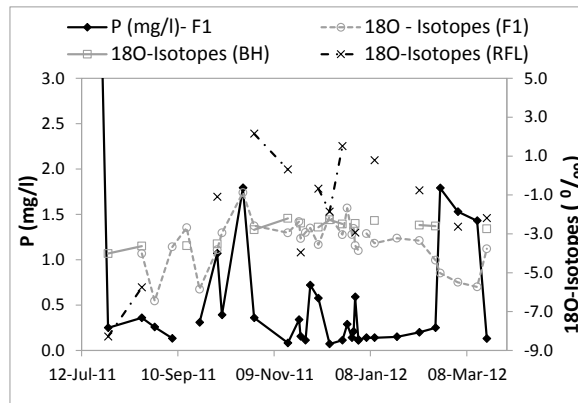
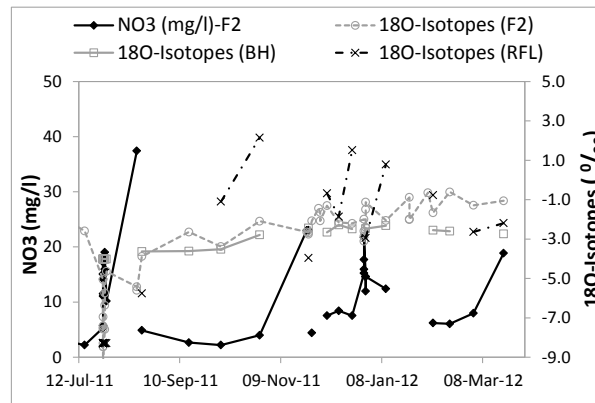
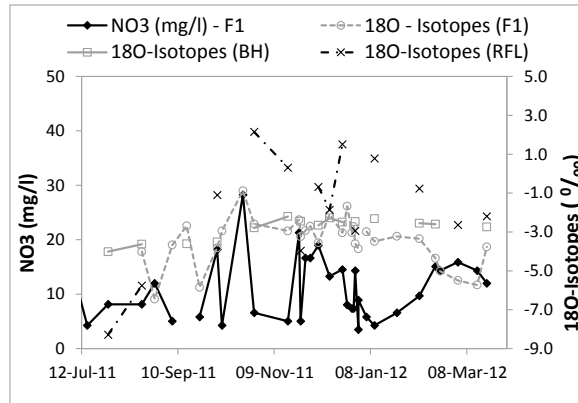
J. TOTAL LOADS FROM *ACRU-NPS* SIMULATIONS WITH DIFFERENT MANAGEMENT SCENARIOS (2006 -2012)

Control	Wetland1		Buffer1		Dam1		Buffer2		Wetland2		Dam2		Wetland3	
	In	Out	In	Out	In	Out	In	Out	In	Out	In	Out	In	Out
No contours-Sediment, t	5147	70	6555	1791	1862	128	91	16	8460	130	274	163	13654	418
No contours-NO ₃ , kg	25578	8512	16524	6527	15039	10889	169	50	26248	8037	18976	12692	557508	209594
No contours-P, kg	718	236	222	88	324	222	6	2	226	71	294	191	771	303
All sugar-Sediment, t	560	52	805	220	272	121	11	2	1015	53	176	155	2174	250
All sugar-NO ₃ , kg	21115	6786	14415	5694	12480	8955	110	33	26239	8034	17021	11202	555984	209582
All sugar-P, kg	505	162	186	74	235	153	4	1	227	71	226	142	730	285
Irrigation-Sediment, t	983	144	2410	659	803	294	91	16	1546	136	446	409	3245	566
Irrigation-NO ₃ , kg	39754	15087	20260	8003	23089	19720	169	50	31702	11595	31365	26582	578287	248068
Irrigation-P, kg	826	312	285	113	424	352	6	2	307	114	468	388	1096	483
No control features-Sediment, t	642	642	2116	2116	2757	2757	91	91	1015	1015	3863	3863	5881	5881
No control features -NO ₃ , kg	25820	25820	16520	16520	42340	42340	169	169	26239	26239	68748	68748	613530	613530
No control features-P, kg	802	802	232	232	1034	1034	6	6	227	227	1268	1268	1856	1856

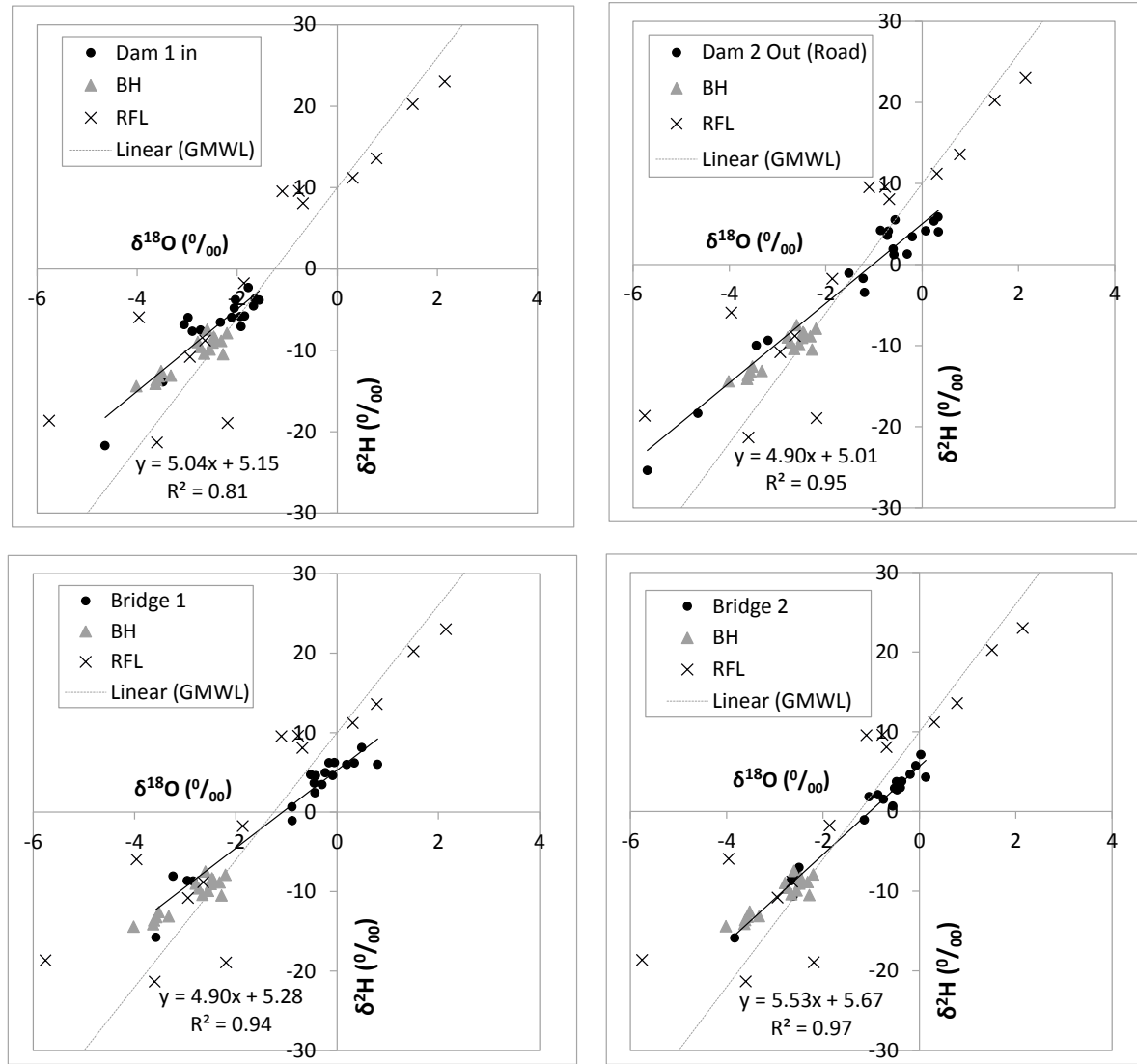
K. FIELD SCALE NUTRIENTS (NO₃ & P), SUSPENDED SOLIDS (SS) AND ISOTOPE PROCESSES IN RUNOFF PLOTS AND FLUMES

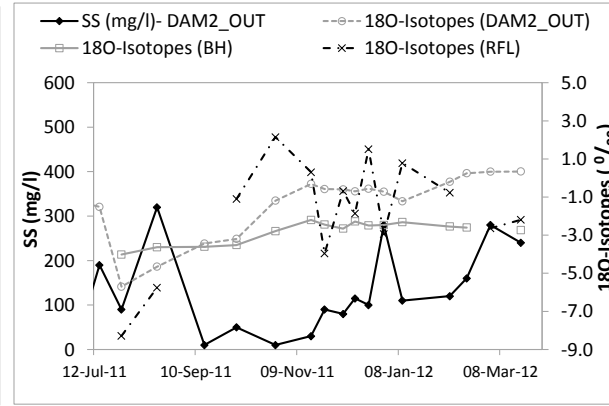
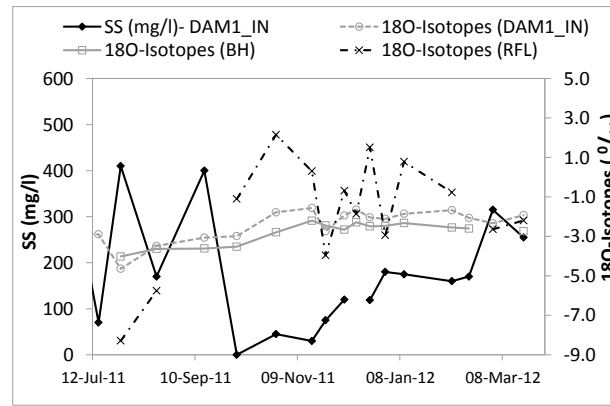
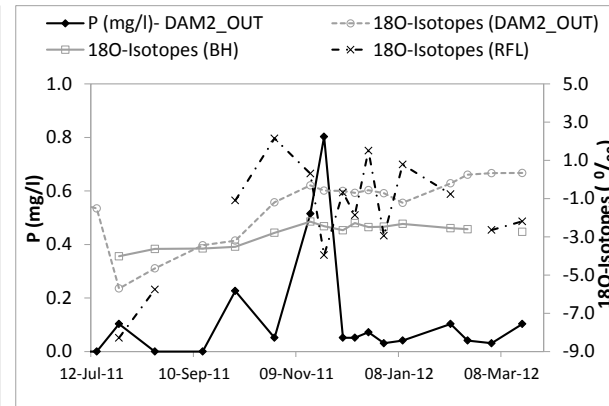
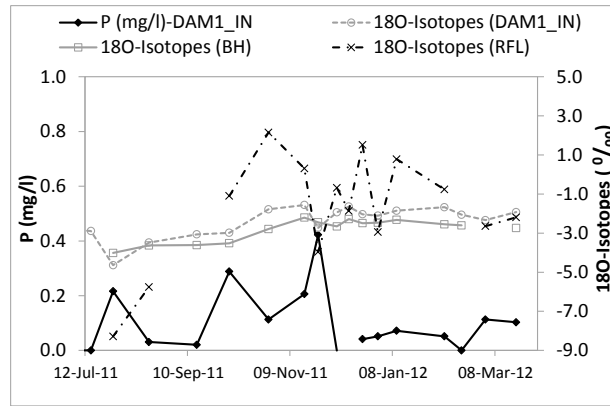
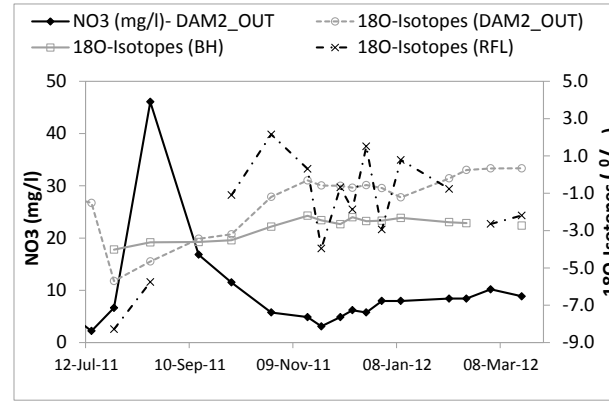
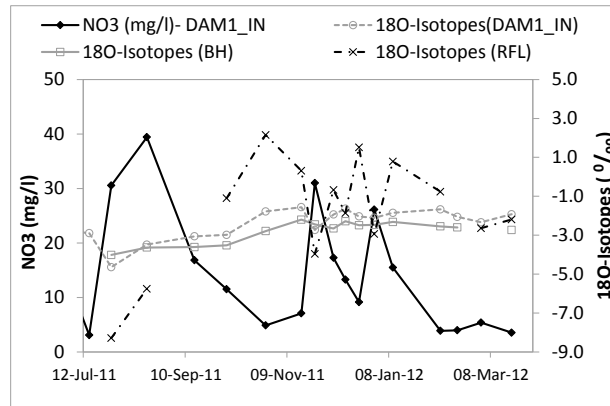


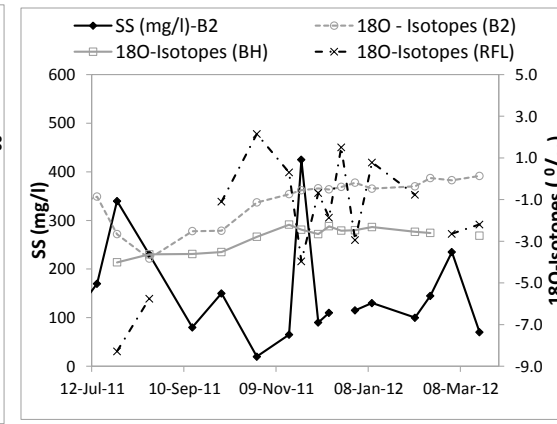
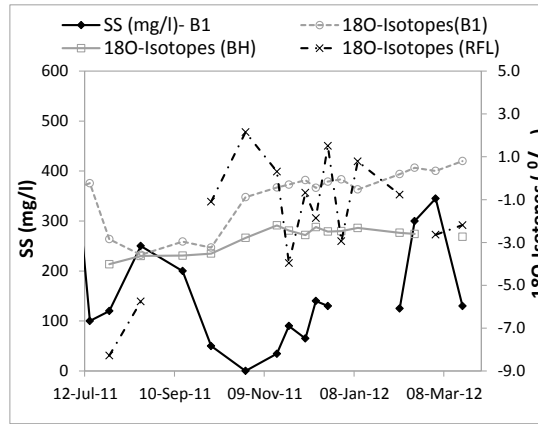
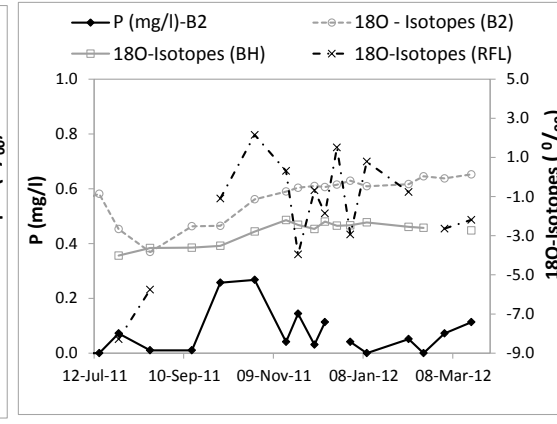
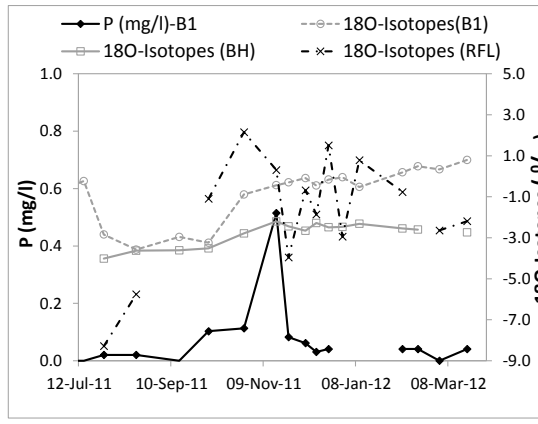
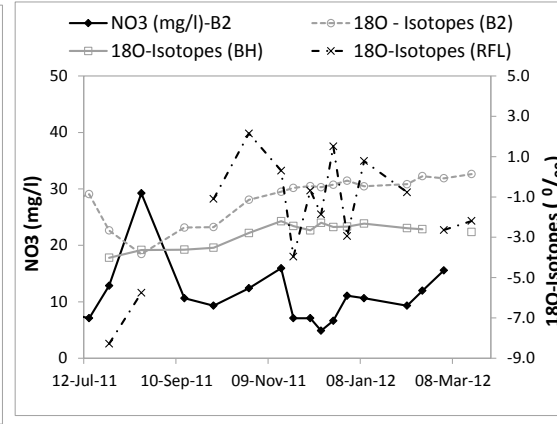
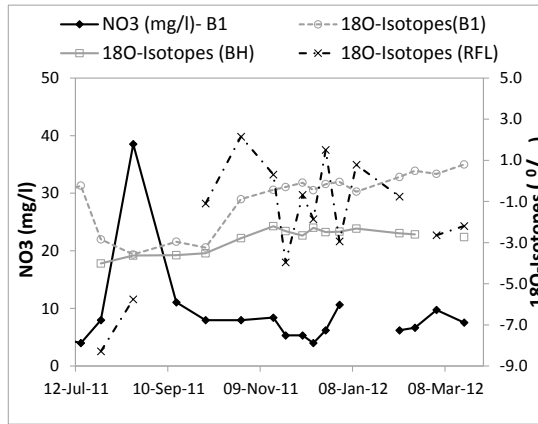




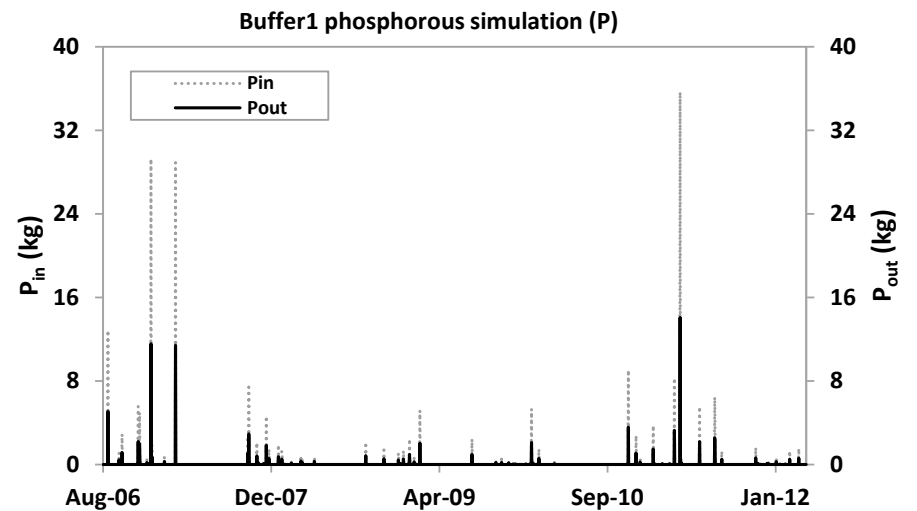
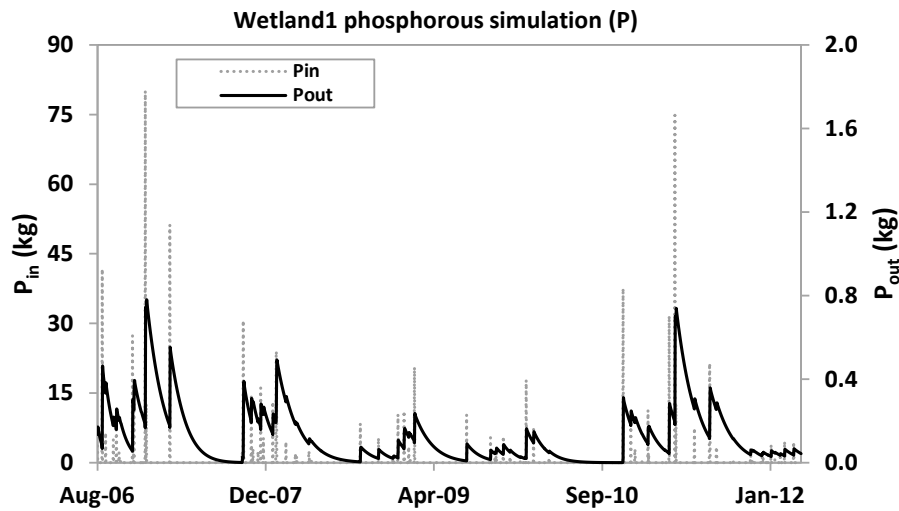
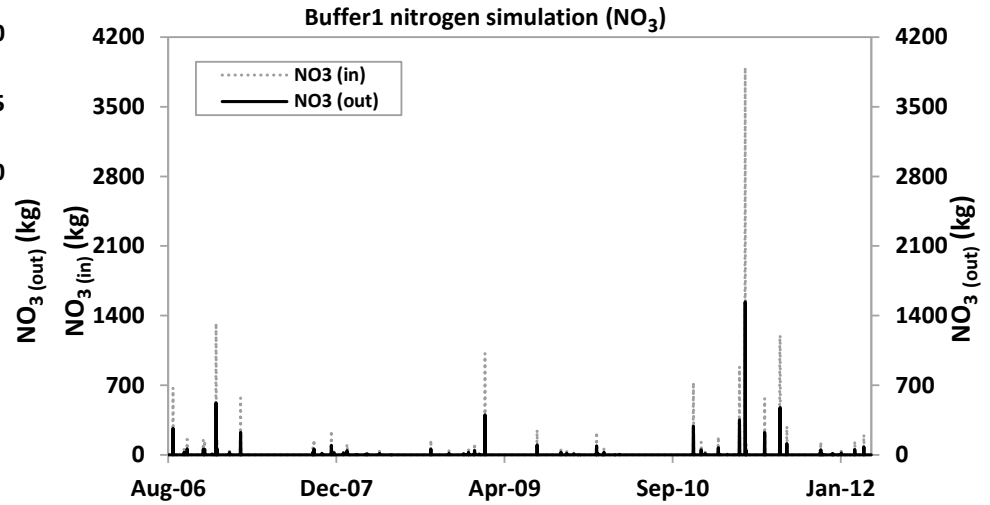
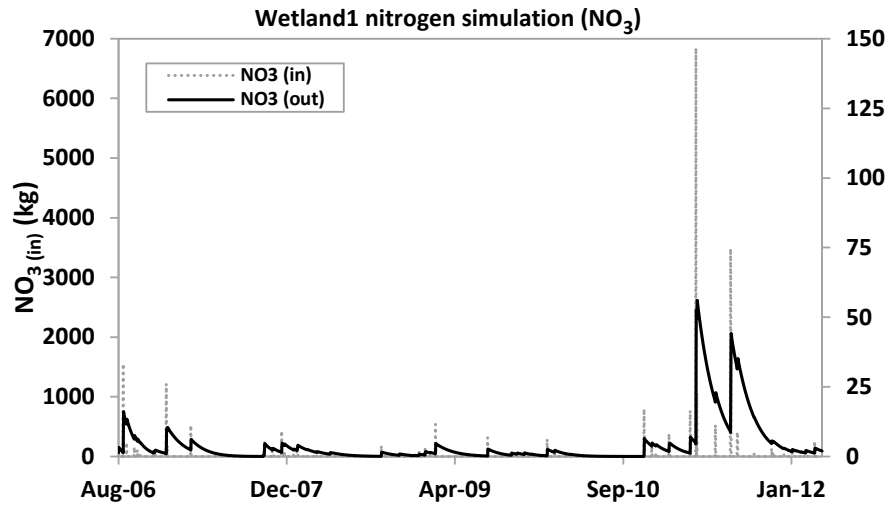
L. CATCHMENT SCALE NUTRIENTS (NO₃ & P), SUSPENDED SOLIDS (SS) AND ISOTOPE PROCESSES IN DAMS AND BRIDGES

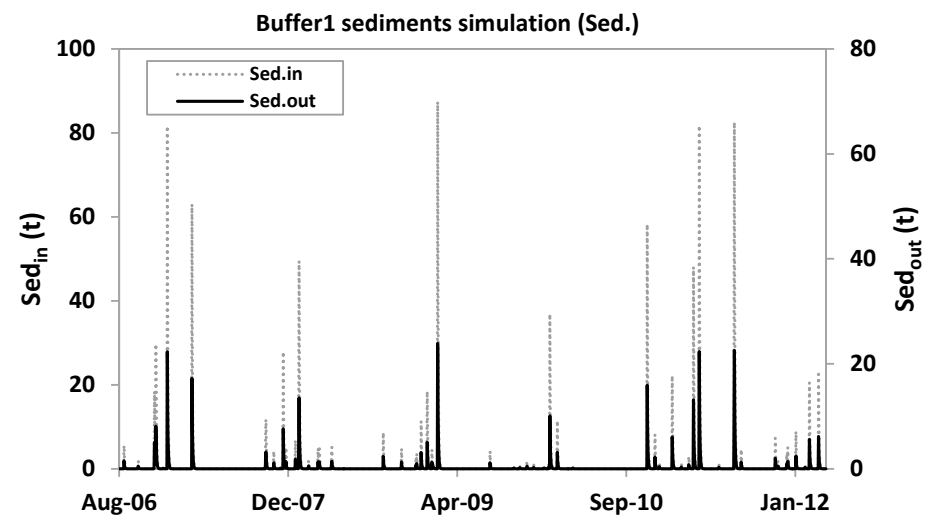
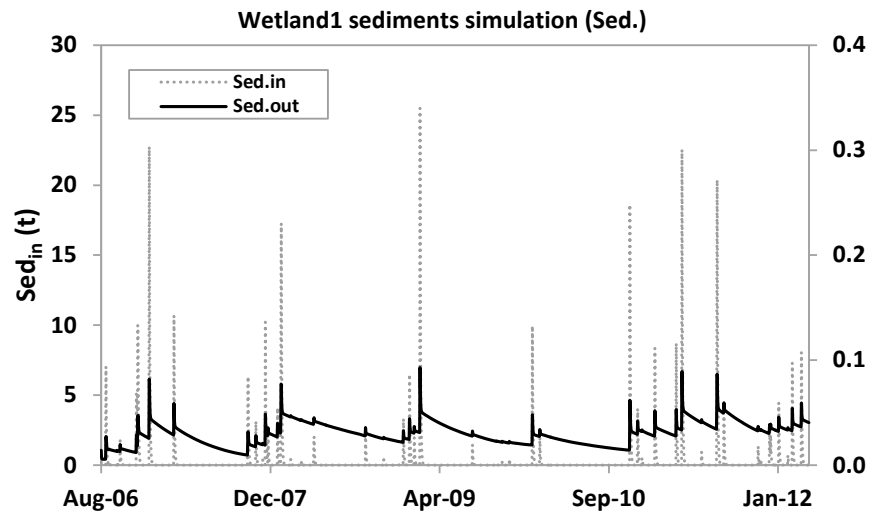


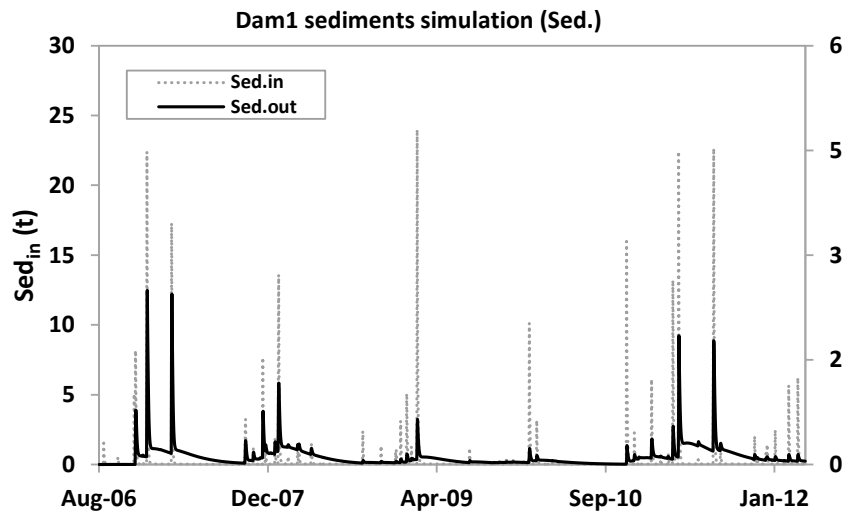
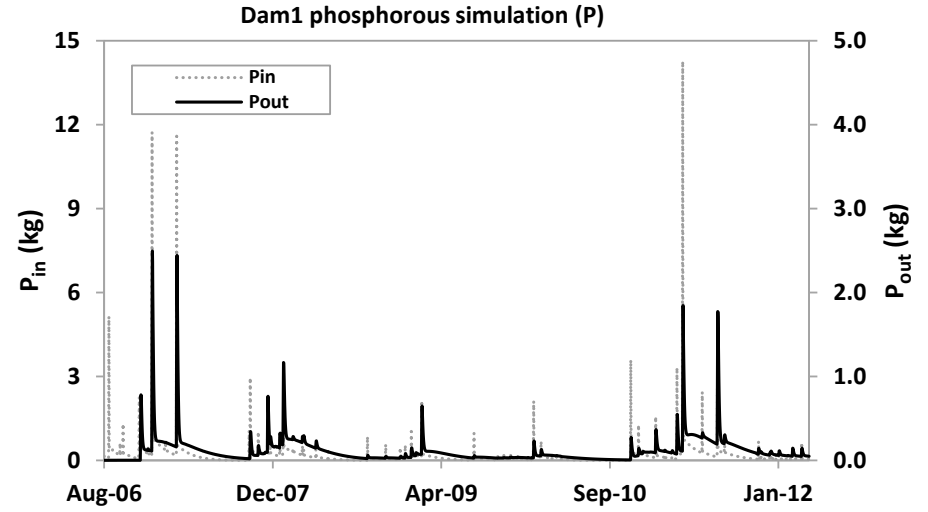
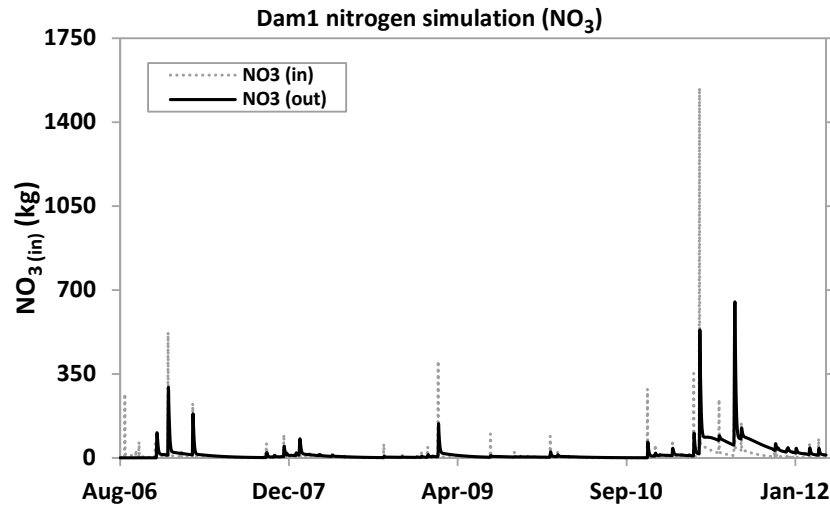


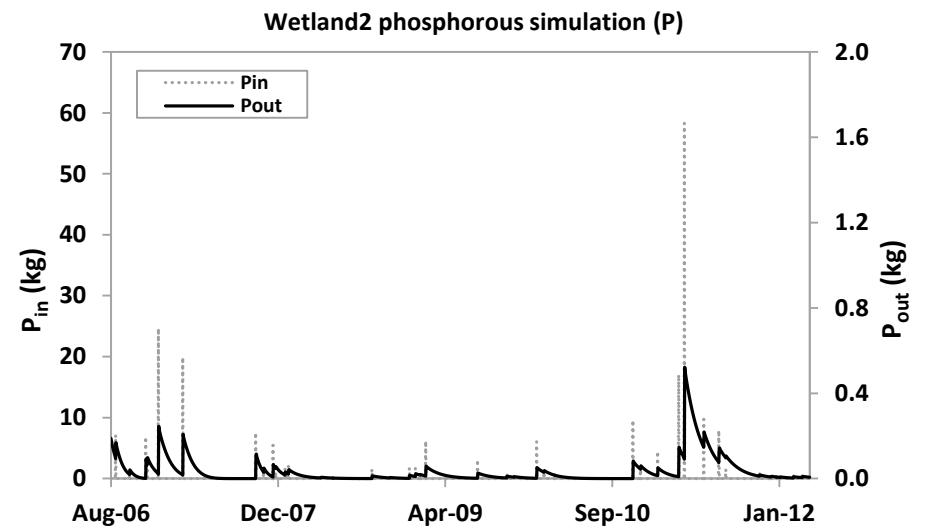
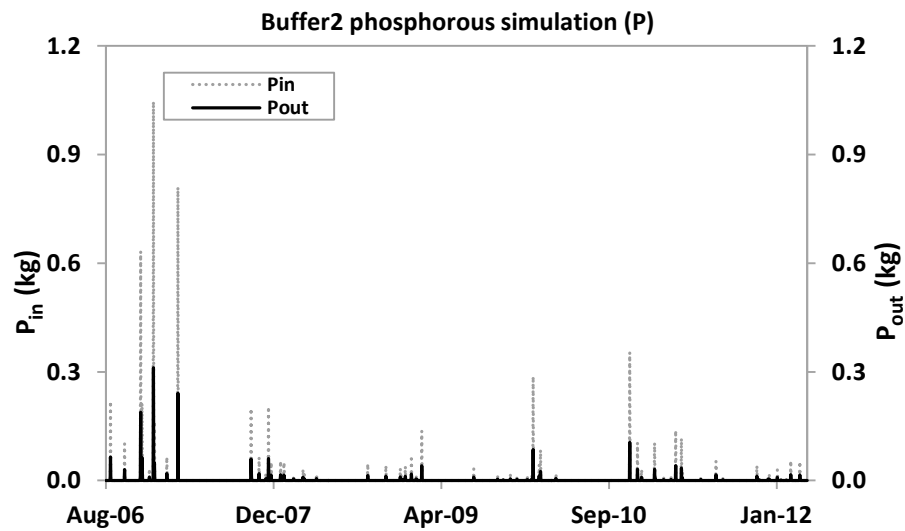
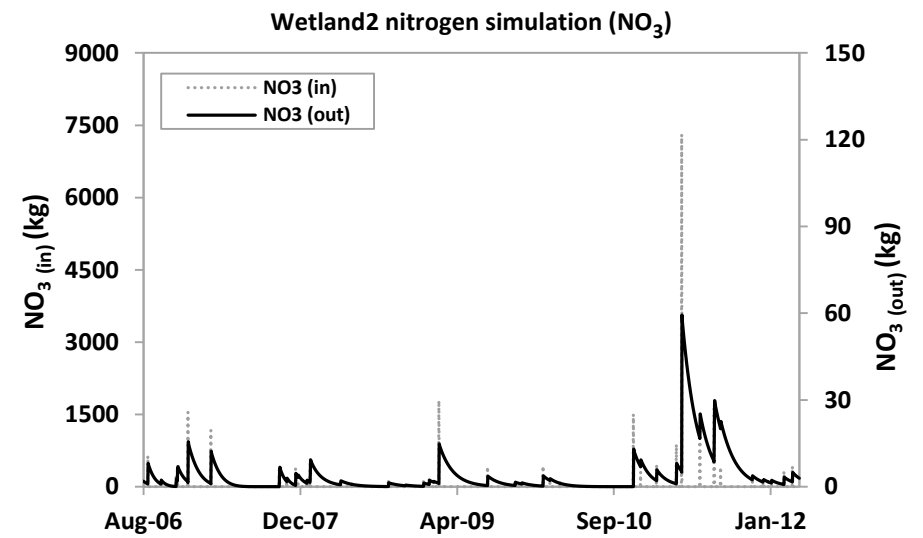
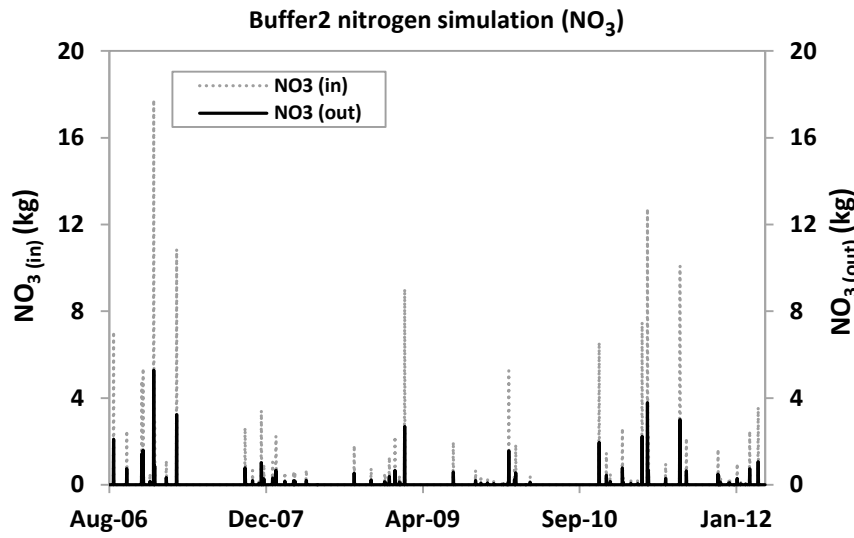


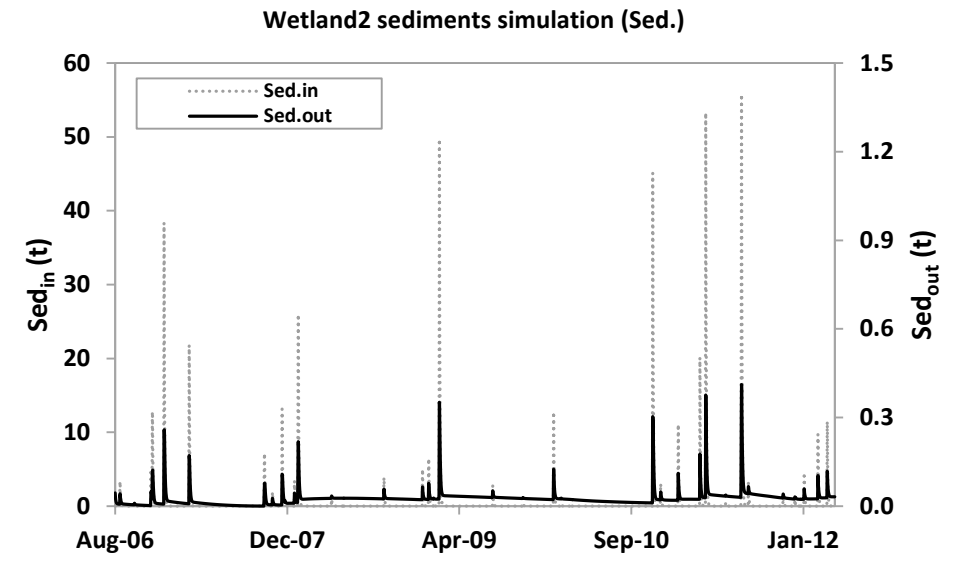
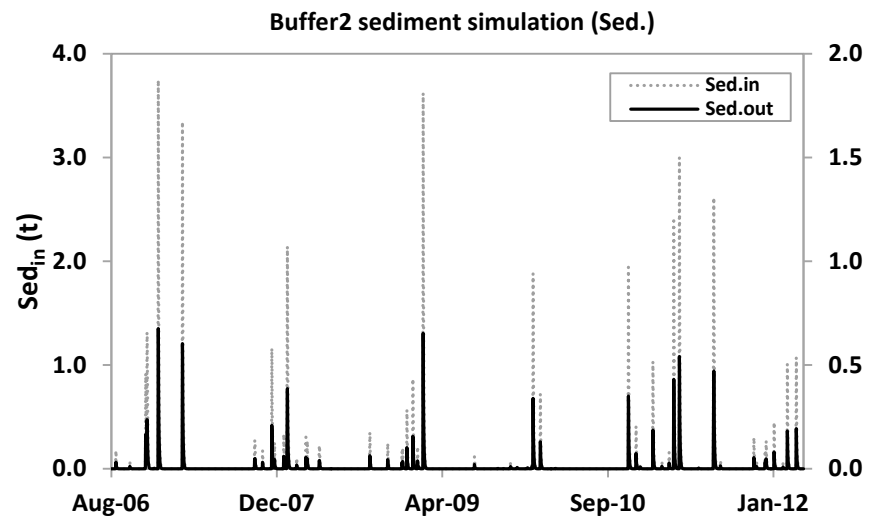
M. *ACRU-NPS* MODEL DAILY OUTPUT FOR NO₃, P AND SEDIMENTS ENTERING AND LEAVING WETLANDS, BUFFERS AND DAMS FOR BASE SCENARIO

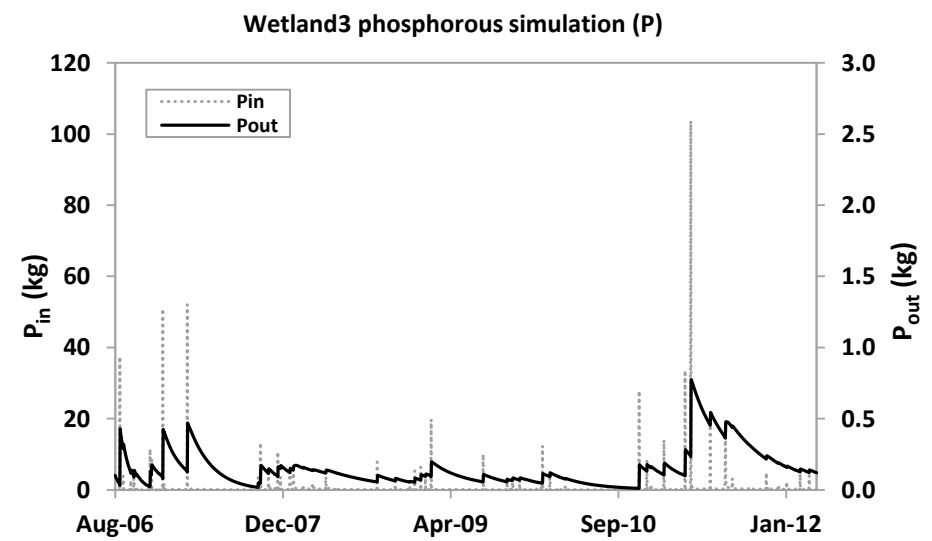
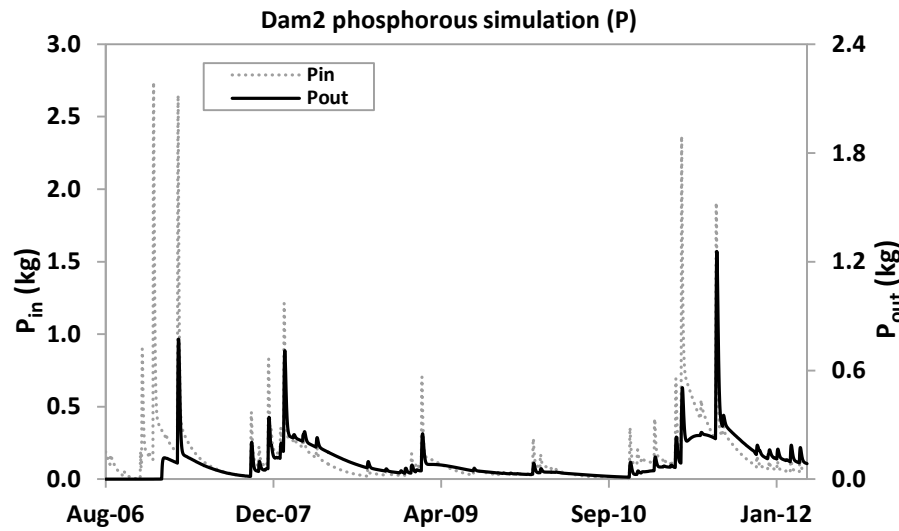
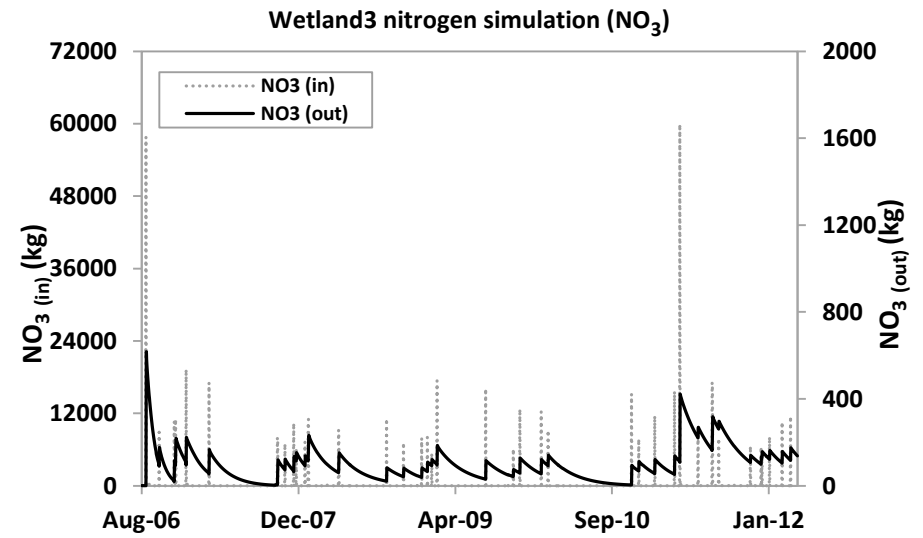
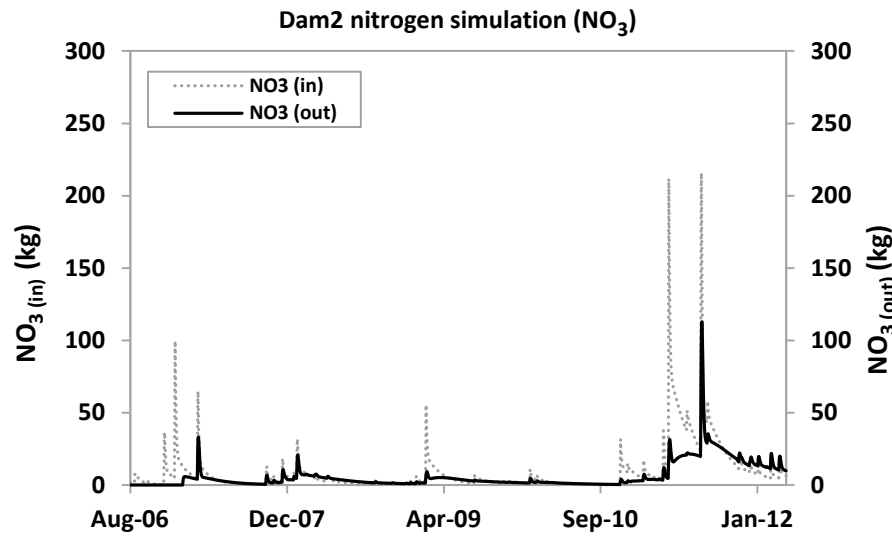




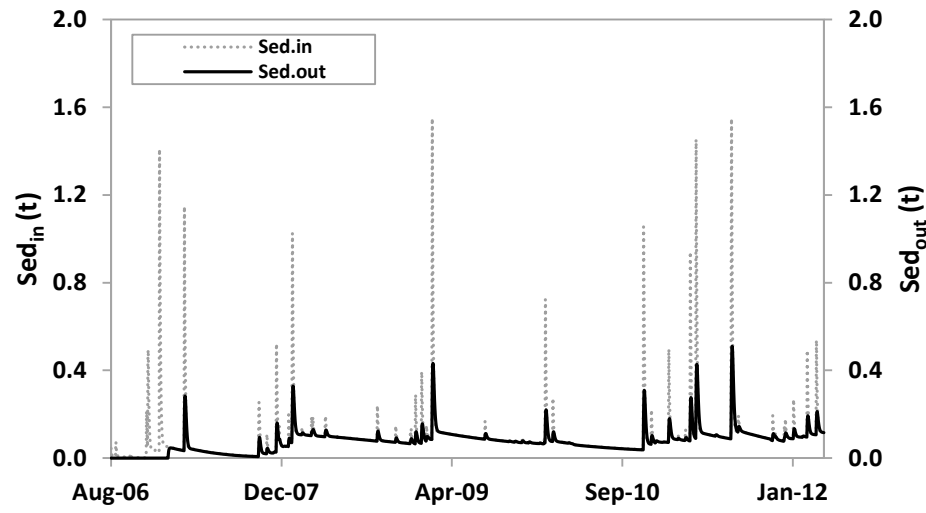








Dam2 sediments simulation (Sed.)



Wetland3 sediments simulation (Sed.)

